Role of Norepinephrine in Olfactory Learning:

in Young Age, in Adulthood, and in Alzheimer's disease

By © Abhinaba Ghosh

A thesis submitted to the School of Graduate Studies in partial fulfilment of the requirements for the degree of Ph.D.

Faculty of Medicine

Memorial University of Newfoundland

February, 2021

St. John's Newfoundland and Labrador Canada

Abstract

The objective of this dissertation is to elucidate the noradrenergic modulation of olfactory learning and memory, specifically, how it varies throughout developmental phases and in the context of disease. To that end, I have addressed three distinct but interrelated aspects.

First, I characterized how locus coeruleus (LC)-mediated norepinephrine (NE) modulates L-type calcium channels (LTCCs) in neonatal odor preference learning. Long term potentiation (LTP) is dependent on calcium influx. In chapter 2, I show that β adrenoceptor (AR) enhances LTCC-mediated calcium influx within the critical period and is responsible for olfactory preference learning.

Second, I studied how phasic and tonic firing patterns of LC differentially modulate olfactory discrimination learning and valence learning. Through optogenetic stimulation of rat LC neurons in 10-Hz phasic or 10-Hz tonic patterns, I show in chapter 3 that enhanced acquisition of similar odor discrimination occurs via phasic-stimulation through a LC-ventral tegmental area-piriform cortex-dopamine circuitry. 25-Hz tonic photostimulation induces conditioned odor aversion, but 10-Hz phasic stimulation produces an odor preference suggestive of a positive valence. 10-Hz phasic stimulation recruits more basolateral amygdala (BLA) cells that project to nucleus accumbens, while 25-Hz tonic stimulation preferentially activates BLA cells projecting to the central amygdala (CeA).

Finally, I studied LC-degeneration in an Alzheimer's disease (AD) pretangle tau model in rats. Braak's staging of AD suggests that the first brain pathology is the appearance of

hyperphosphorylated soluble tau in LC. It is not well understood if LC hyperphosphorylated tau initiates the pathology and causes the cognitive deficits in early stages. In a rat model I express pseudo-hyperphosphorylated human tau in LC through viral vector-dependent delivery of the appropriate transgene and test the hypothesis that LC pretangle human tau can cause preclinical AD (chapter 4). At 7 but not 4 months post-infusion, difficult odor discrimination learning is impaired in rats which received the infusion in young adulthood. This deficit is associated with low density of LC axons in the piriform cortex, and the pathology is aggravated in older rats. Altogether, this new animal model establishes the plausibility of Braak's hypothesis that AD can originate with pretangle tau expression in LC.

General Summary

Locus coeruleus (LC) is a small area in the brainstem that sends norepinephrine, a neurochemical related to adrenaline, throughout the brain. Norepinephrine performs critical roles in a wide array of functions including arousal, fight or flight response, learning, and regulation of immunological defense mechanisms throughout the lifespan. Different dynamics of norepinephrine release depend on the activity patterns of LC neurons, determining brain states and functions. Some activity patterns are associated with attention and task performance, whereas others are related to anxiety and stress. An exciting area of research being emphasized in recent years is to understand how these discrete patterns can exert individual functions. In this dissertation I have explored how norepinephrine modulates learning ability during the neonatal period. Using a rodent model of early life learning, I show that norepinephrine performs a critical role in facilitating learning but changes abruptly within a window of a few days during neonatal development. Furthermore, using advanced optogenetic stimulation techniques I explore how distinct activity patterns of LC neurons differentially modulate learning ability and valence in adulthood. Interestingly, LC is also the first spot in the brain that develops abnormal pretangle hyperphosphorylated tau (htau) which is thought to progress to neurofibrillary tangles in Alzheimer's disease. Research shows that htau in the LC is prevalent in the population; it can appear as early as the first year of life, and by the age of 40 years everyone is likely to have htau in LC. The pathogenic role of htau was, however, unclear from the current literature. During my PhD, I have established a rat model to study this problem by expressing htau genes in rats' LC. My research identified sensitive behavioral and imaging tests to accurately predict htau-dependent cognitive decline long before its appearance. This model will be useful to test various preventive and curative measures for Alzheimer's disease.

I dedicate my dissertation to the eternal scientific journey of understanding the nature and outsmarting it for the benefit of humans.

Acknowledgement

We did it together…

I would like to thank NSERC and CIHR, Memorial University: Faculty of Medicine and International student resource centre, Dean M. Ian Bowmer, Dr. Howard Strong's family, Dr. Bruce and Bernice Sells' family, and Aging Research Centre- NL for funding research work and donating generously for awards and fellowships for graduate students.

My graduate study is approaching its end. The experience has been overwhelmingly enriching, as I thought before I started walking this path. The "science", as usual, has been fascinating with lots of surprises and grand revelations. Here I acknowledge the "people", without whom the science would have been incomplete. My degree is not worth more than the beautiful experience I have had with these people around me in past four years.

I gratefully remember how my parents, parents-in-law and other near and dear family members including my in-laws, have supported me all through my journey. My sincerest thanks to the animal care facility staff, research support staff, non-academic support staff, Jimmy, Larry, and Sandra. I would also like to thank Dr. Ali Gheidi, Dr. Amin Shakhawat, Samantha Carew, and all other present and past members of the Yuan lab, who have helped and supported me all along. It was an immense pleasure knowing and working with such great colleagues.

I humbly acknowledge the contributions by my co-authors- Dr. Bandhan Mukherjee, Sarah Torraville, Faghihe Massaeli, Kyron Power, Tamunotonye Omoluabi, Julia Pritchett, Tayebeh Sepahvand, Vanessa Strong and Camila Reinhardt. Without their active contributions my journey would remain unfruitful.

I always wanted to be a part of a research environment where rigorous scientific discussions will take place frequently and young trainees will be exposed to different aspects of neuroscience research. I am grateful to the faculties and the students in the department for creating and maintaining such enriching environment. I have learned a lot from the present and past faculties including Dr. John McLean, Dr. Karen Mearow, Dr. Matthew Parsons, Dr. Michiru Hirasawa, Dr. Craig Moore and others. Discussing history and philosophy of modern science with Dr. Reza Tabrizchi helped me develop my own perspective in this journey. My sincerest thanks to my supervisory committee member Dr. Jacqueline Vanderluit; I have learned a lot from her. Her trouble shooting suggestions, unique teaching style and kind attitude to help have helped me a lot.

I am grateful to Dr. Susan Walling and Dr. Carolyn Harley for continuously supporting me and teaching me different aspects of my research field all along my journey. Discussing science with them never gets old. I have learned a lot from them in the past and the learning is still continuing.

My co-supervisor Dr. Xihua Chen has been extremely supportive during my PhD studies. His unending patience, highly effective teaching skill and guidance, unique ability to see and to show the big picture changed the way I approach science and life.

I do not have enough words to express my gratitude to my supervisor Dr. Qi Yuan. She has helped and guided me all through my journey beyond just supervising the research. Having a supportive supervisor can make all the difference in a young trainee's progress. She paid minute attention to every single team member's every single problem. She has patiently spent a lot of

time, often her personal time, to train me, to help me, and to listen to my problems- be it personal or scientific. I have always admired her knowledge, discipline, diligence, perseverance, and passion for science. Even close to the end of my training, I keep learning from her every day. I am fortunate to have reached the milestones I aimed for at the start of my program. This would have been impossible without her kind support, care and active guidance.

I hope to teach the lessons I learned during my graduate study and practice science in the truest sense of it.

Co-authorship statement

I, Abhinaba Ghosh, hold a first author status for the version of the manuscripts incorporated in this dissertation as chapters 2-4. Each manuscript is co-authored by my supervisors and colleagues. Author contribution in each manuscript is elaborated below.

Chapter 2

Ghosh A, Mukherjee B, Chen X, Yuan Q.

β-AR activation enhances L-type calcium channel currents in anterior piriform cortex pyramidal cells of neonatal mice: implication for odor learning. Learning & Memory. 2017 Mar 1;24(3):132-5.

As the first author, I (AG) contributed in the experimental design, conducted majority of the experiments, analyzed data and wrote parts of the manuscript. Research question was developed by QY and XC. BM contributed in the behavioral experiments and QY conducted a subset of recordings in figure 2B-D. Manuscript was edited by AG, XC and QY.

Chapter 3

Ghosh A, Massaeli F, Power KD, Omoluabi T, Torraville SE, Pritchett JB, Sepahvand T, Strong V, Reinhardt C, Chen X, Martin GM, Harley CW, Yuan Q.

Locus coeruleus activation patterns differentially modulate learning and valence in rats

Submitted, in revision. (A version available in bioRxiv, https://www.biorxiv.org/content/10.1101/2020.04.17.047126v1.full)

As the first author, I (AG) contributed in the experimental design, conducted majority of the experiments, analyzed data and wrote parts of the manuscript. Research question was developed by QY. In vivo recording was carried out by VS and FM (Fig 1B-D). I conducted experiments in figure 2 with SET. FM conducted experiments in 3B and E. I conducted experiments in 3C,D,F,G,H and 5 with TO and JBP. CTB surgeries in figure 7 were carried out by KDP. I conducted following IHC experiments and analysis with KDP. A subset of the BLA surgeries in fig 6 were carried out by TS and a subset of the LC infusion and optical fiber implantation surgeries were carried out by CR and KDP. XC, GMM and CWH helped improve the experimental design. Manuscript was edited by AG, CWH and QY.

Chapter 4

Ghosh A, Torraville S, Mukherjee B, Walling SG, Martin GM, Harley CW, Yuan Q.
An experimental model of Braak's pretangle proposal for the origin of Alzheimer's Disease: the role of locus coeruleus in early symptom development. Alzheimer's Research & Therapy. 2019 July;11(1):59.

As the first author, I (AG) conducted majority of the experiments, analyzed data and wrote parts of the manuscript. Research question was developed by CWH and QY. QY designed the experiments. I performed LC infusion surgeries. I conducted IHC experiments with SET, with help from SGW, BM and QY. I carried out behavioral experiments with help from SET. Initial behavioral experiments were assisted by BM. GMM assisted in statistical analysis. AG, GMM, CWH and QY wrote the manuscript.

Table of Contents

Abstract ii

General Summary iv

Acknowledgement vi

Co-authorship statement x

List of Tables xvii

List of Figures xviii

List of Abbreviations xx

List of Appendices xxvi

Chapter 1: Introduction 1

1.1 Overview 1
1.2 Brief anatomy and physiology of the noradrenergic system 3
1.2.1 Noradrenergic nuclei in the brainstem 3
1.2.2 Cellular and molecular organisation within LC 4
1.2.3 Functional diversity of the inputs to LC 5
1.2.4 Functional diversity of the outputs of LC 7
1.2.5 Modular activation 9
1.2.6 LC spiking patterns and optogenetics 10
1.3 Noradrenergic modulation of learning and memory: behavioral models and cellular-molecular-network mechanisms 12
1.3.1 Hippocampus-dependent learning 12
1.3.2 Amygdala-dependent learning 15
1.3.3 Olfactory learning 18
1.3.3.1 In adults 18
1.3.3.1.1 Odorant detection 18
1.3.3.1.2 Perceptual learning 19

1.3.3.1.3 Encoding olfactory memory 20
1.3.3.1.4 Duration of olfactory memory 20
1.3.3.1.5 Odor specificity 21
1.3.3.1.6 Go-no go olfactory paradigm 21
1.3.3.1.7 Concise overview of the mechanistic role of NE in olfactory learning 23
1.3.3.2 In neonates 24
1.3.4 Noradrenergic modulation of calcium influx through LTCC 26
1.4 Olfactory deficit in Alzheimer's Disease 28
1.5 Role of Locus Coeruleus in Alzheimer's disease 32
1.5.1 LC as the origin of tau-pathology in Alzheimer's disease 32
1.5.2 Noradrenergic deficit in Alzheimer's disease 35
1.5.2.1 Structural imaging 35
1.5.2.2 Functional imaging 35
1.5.2.3 Biochemical tests 36
1.5.2.4 Genetic changes 37
1.5.2.5 Postmortem findings 37
1.5.2.6 Animal studies 38
1.6 What is missing? 40
Chapter 2: β-AR activation enhances L-type calcium channel currents in anterior piriform cortex pyramidal cells of neonatal mice: implication for odor learning 42
2.1 Introduction 42
2.2 Methods 44
2.3 Results 47
2.4 Discussion 53
Chapter 3: Locus coeruleus activation patterns differentially modulate learning and valence in rats 55
3.1 Introduction 55
3.2 Methods 56
3.2.1 Animals and Ethics Statement 56
3.2.2 Viral Transduction 57

3.2.3 Stereotaxic Surgery 57
3.2.4 *In vivo* Electrophysiology 59
3.2.5 Behavioural Tests 60
3.2.5.1 Light Stimulation for Behavioural Experiments 60
3.2.5.2 Drug Infusion 61
3.2.5.3 General Behavioural Experiments 62
3.2.5.3.1 Open Field Maze 62
3.2.5.3.2 Elevated Plus Maze 62
3.2.5.4 Olfactory Behavioural Experiments 62
3.2.5.4.1 Odorants 62
3.2.5.4.2 Odor Discrimination Learning 63
3.2.5.4.3 Odor Valence Tests 64
3.2.5.5 cFos and Npas4 Induction Experiments 65
3.2.6 Immunohistochemistry and Histology 66
3.2.7 Statistical Analysis 68
3.3 Results 69
3.3.1 Validation of light activation of locus coeruleus neurons 69
3.3.2 Different patterns of LC activation show distinct general behavioural effects 72
3.3.3 LC phasic patterns enhance similar odor discrimination learning 76
3.3.4 LC-Ventral tegmental area (VTA)-PC dopamine circuitry mediates the facilitating effect in similar odor discrimination learning 80
3.3.5 LC phasic and tonic patterns promote differential odor valence learning 84
3.3.6 LC phasic and tonic patterns engage differential basolateral amygdala (BLA) circuitry in odor valence learning 88
3.4 Discussion 95
3.5 Conclusions 98
3.6 Supplementary figures 100
3.6.1 Supplementary figure 1 100
3.6.2 Supplementary figure 2 101
3.6.3 Supplementary figure 3 102
3.6.4 Supplementary figure 4 103

Chapter 4: An experimental model of Braak's pretangle proposal for the origin of Alzheimer's disease: the role of locus coeruleus in early symptom development 104

4.1 Introduction 104
4.2 Methods 108
4.2.1 Ethics statement and subjects 108
4.2.2 Experimental design and statistical analysis 109
4.2.3 Behavioral testing 110
4.2.3.1 Odor discrimination learning 110
4.2.3.2 Acute odor habituation/dishabituation test 111
4.2.4 Histology and immunohistochemistry 112
4.2.4.1 Thioflavin-S staining 115
4.2.4.2 Imaging analysis and quantification 115
4.3 Result 116
4.3.1 HtauE14 uptake in the LC and spread 116
4.3.2 HtauE14 in young adult LC: 3–4 months post-infusion 121
4.3.3 HtauE14 in young adult LC: 7–8 months post-infusion 124
4.3.4 HtauE14 in LC of 14–16-month-old rats: 5–7 months post-infusion 130
4.4 Discussion 132
4.5 Conclusion 142
4.6 Additional files 143
4.6.1 Additional file 1 143
4.6.2 Additional file 2 144
4.6.3 Additional file 3 145
4.6.4 Additional file 4 146
4.6.5 Additional file 5 147
4.6.6 Additional file 6 148
Chapter 5: Discussion 149

5.1 Summary of major findings and impacts 149
5.1.1 Mechanisms of noradrenergic modulation in learning 149
5.1.1.1 Noradrenergic support of the plasticity machinery 149
5.1.1.2 Norepinephrine's role in pattern separation 151

5.1.1.3 Variable norepinephrine-release and locus coeruleus spiking pattern difference influencing learning 153
5.1.2 Locus coeruleus-norepinephrine system in Alzheimer's disease 155
5.1.2.1 Establishment of a pretangle tau model 155
5.1.2.2 Advantages and limitations of the model 156
5.1.2.3 Therapeutic implications 157
5.2 Future directions 158
5.2.1 Mechanistic studies underlying differential effects of locus coeruleus spiking patterns 158
5.2.2 Role of locus coeruleus spiking patterns in Alzheimer's disease progression 159
5.2.3 Using the pretangle tau model to study intervention and epigenetic mechanism of Alzheimer's disease 160
References 162

Appendices 195

Ethics Approval 195

List of Tables

Table 3.1 List of Odorants……63

Table 4.1 List of Antibodies……...114

List of Figures

Figure 1.1 Major inputs and outputs of LC……6

Figure 2.1 L-type calcium currents (LTCCs) in mouse pups of P7 – 11 and P14 above. 48

Figure 2.2 Effects of b-adrenoceptor activation on whole-cell Ca2+ currents. 49

Figure 2.3 The interaction of β-adrenoceptors and LTCCs in early odor preference learning in mice. 51

Figure 3.1 Validation of the light activation of the locus coeruleus (LC) neurons 70

Figure 3.2 10-Hz phasic LC activation promotes exploration while 25-Hz tonic activation results in increased freezing and decreased mobility 75

Figure 3.3 LC phasic patterns, but not tonic pattern, enhance similar odor discrimination learning 79

Figure 3.4 LC phasic activation engages VTA dopamine release to facilitate DOD 82

Figure 3.5 Twenty five-Hz tonic LC activation leads to conditioned odor aversion while 10-Hz phasic pattern results in odor preference 86

Figure 3.6 Basolateral amygdala adrenoceptors mediate the conditioned preference and aversion in COPT 90

Figure 3.7 Ten-Hz phasic and 25-Hz tonic LC activation engage positive and negative projecting circuitry respectively in the BLA 93

Figure 4.1 HtauE14 uptake in the LC and spread. 118

Figure 4.2 No odor discrimination deficiency or LC degeneration in young 6-month-old rats infused with htauE14 at 2–3 months old 120

Figure 4.3 Impairment in go/no-go odor discrimination learning in 10-month-old rats infused with htauE14 at 2–3 months old. 123

Figure 4.4 LC axonal degeneration in 11-month-old rats infused with htauE14 at 2–3 months old.……126

Figure 4.5 Deficiency in odor discrimination and LC degeneration in 17–20-month-old rats infused with htauE14 at 12–14 months old. 129

Figure 4.6 HtauE14 release and uptake by neurons and microglia in an old AD rat. 131

List of Abbreviations

2-DG	2-deoxyglucose
4EBP-2	4E binding protein-2
AAV	Adeno-associated virus
aCSF	artificial Cerebro Spinal Fluid
AD	Alzheimer's Disease
AHP	Afterhyperpolarisation
AMPA	α-amino-3-hydroxy-5-methyl-4-isoxazolepropionic acid
AMPAR	α-amino-3-hydroxy-5-methyl-4-isoxazolepropionic acid receptor
AP	Action Potential
aPC	anterior Piriform Cortex
APP	Amyloid precursor protein
APV	(2R)-amino-5-phosphonovaleric acid
AR	Adrenoceptor
AT8	Anti-tau 8
BLA	Basolateral amygdala
BOLD	Blood oxygenation level dependent
CaMK	Calmodulin Kinase
cAMP	cyclic Adenosine Monophosphate
CeA	Central Amygdala
COPT	Conditioned odor preference test
CREB	cAMP Response Element-Binding Protein
CRF	Corticotrophin releasing factor

CS	Conditioned Stimulus
CTB	Cholera toxin B
DAB	Diaminobenzidine tetrahydrochloride
DBH	Dopamine beta-hydroxylase
DIO	Double inverted open reading frame
DG	Dentate Gyrus
DMN	Default mode network
EC	Entorhinal cortex
eIF4E	eukaryotic initiation factor
EPL	External Plexiform Layer
EPSC	Excitatory Post Synaptic Current
EPSP	Excitatory Post Synaptic Potential
GABA	Gamma Amino Butyric Acid
GC	Granule Cell
GCL	Granule Cell Layer
GFP	Green fluorescence protein
GL	Glomerular Layer
HT7	Human tau 7
Htau	Human pseudophosphorylated tau
Iba-1	Ionized calcium-binding adaptor molecule 1
IPL	Internal Plexiform Layer
IPSC	Inhibitory Post Synaptic Current
JG	Juxtaglomerular Cells

LC	Locus Coeruleus
LC-NE	LC-noradrenergic
LDT	Laterodorsal tegmental nuclei
LH	Lateral Hypothalamus
LH/PF	Lateral Hypothalamic/ Perifornical area
LLP	Long Lasting Potentiation
LOT	Lateral Olfactory Tract
LTCC	L-type calcium channel
LTD	Long Term Depression
LTP	Long Term Potentiation
MC	Mitral Cell
MCI	Mild cognitive impairment
MCL	Mitral Cell Layer
MDT	Mediodorsal nucleus of thalamus
mEPSC	miniature Excitatory Post Synaptic Current
mGluR	metabotropic Glutamate Receptor
mIPSC	miniature Inhibitory Post Synaptic Current
MMSE	Mini Mental State Examination
MRI	Magnetic Resonance Imaging
M/T	Mitral/Tufted
mV	millivolt
NAc	Nucleus accumbens
NBQX	2,3-dihydroxy-6-nitro-7-sulfamoyl-benzo[f]quinoxaline-2,3-dione

NMDA	N-methyl-D-aspartate
NMDAR	N-methyl-D-aspartate receptor
NE	Norepinephrine
NET	Norepinephrine transporter
NeuN	Neuronal nuclei
NFT	Neurofibrillary tangle
OB	Olfactory Bulb
OD	Optical density
OFC	Orbitofrontal cortex
ONL	Olfactory Nerve Layer
ORN	Olfactory Receptor Neurons
O/S+	Odor with Stroking
O/S-	Odor without Stroking
OT	Olfactory Tubercle
P8	Postnatal day 8
pA	Picoampere
PAG	Periaqueductal grey
PBS	Phosphate buffered saline
PFA	Paraformaldehyde
PFC	Prefrontal cortex
PC	Piriform cortex
pCREB	Phosphorylated CREB
PG	Periglomerular

PKA	Protein Kinase A
PKC	Protein Kinase C
PNDs	Postnatal Days
PP	Peppermint
PPT	Pedunculopontine tegmental nucleus
REM	Rapid Eye Movement
RMP	Resting Membrane Potential
ROD	Relative optical density
ROPT	Real time odor preference test
RVLM	Rostroventrolateral medulla
s.c.	Subcutaneous
SD	Sprague-Dawley
SA	Short Axon
SAN	Salience network
sAHP	slow After Hyper Polarisation
SEM	Standard Error of Mean
SEL	Subependymal layer
SorLA	sorting-related receptor with A repeat
TBS	Theta Burst Stimulation
TH	Tyrosine hydroxylase
TPH	Tryptophan hydroxylase
TMN	Tuberomamillary nucleus
UCS	Unconditioned Stimuli

VLPO	Ventrolateral preoptic nuclei
VTA	Ventral tegmental area

List of Appendices

Ethics Approval…….....195

Chapter 1: Introduction

1.1 Overview

Since the discovery of the LC neurons (Dahlström & Fuxe, 1964), scientists are relentlessly trying to understand its role in basic physiology, in synaptic plasticity and learning, and in disease processes. With advent of newer technologies and new knowledge in neuroscience, experts are readdressing the same broad questions at different depths periodically over several decades. Some answers stand strongly time-tested, while others added newer dimensions to our understanding.

The most prominent functions of LC include its role in attention and arousal. During sleep LC spiking decreases while it increases by the presentation of salient stimuli across sensory modalities (Aston-Jones & Bloom, 1981; Foote, Aston-Jones, & Bloom, 1980). LC response pattern is associated with the reward value (Bouret & Richmond, 2015) and the effort required to achieve the reward (Varazzani, San-Galli, Gilardeau, & Bouret, 2015). Novelty and relevance of the stimuli are also represented by LC response (Bari, Chokshi, & Schmidt, 2020). Altered LC activity-related change in NE release dynamics can impact downstream systems resulting in different behavioral outcomes (McBurney-Lin, Lu, Zuo, & Yang, 2019)

About half a century ago, Kety hypothesized that LC-NE facilitates associative learning between stimulus and outcome (Harley, 1987; Kety, 1970). This has received a lot of support through numerous reports over the years. But the finer details of the system, such as, NE concentration and LC pattern association or their implications in different types of task performance, have not been well understood. Aston-Jones and Cohen proposed an adaptive gain hypothesis highlighting a

switch between phasic and tonic spiking causing the switch between exploitation and exploration (Aston-Jones & Cohen, 2005). Research is still in progress to understand different roles of LC spiking patterns in modulating behavioral outcome.

NE-mediated excitation, inhibition and synaptic plasticity mechanisms have been explored widely. Depending on the AR type, downstream signaling cascades can vary widely. Also depending on the brain area, AR subtypes can play key roles in exerting synaptic plasticity. In general, α_1 (G_q-coupled) and β (G_s-coupled) ARs cause excitatory effect whereas, α_2 (G_i-coupled) ARs cause inhibitory effect. The overall effect in a given network depends on whether these AR expressions are on glutamatergic or GABAergic neurons and their connectivity patterns.

Rodent pups show an ability to form preference to a neutral stimulus if co-presented with a maternal cue. This associative form of learning has a critical period and does not happen beyond the second week of postnatal life. LC-NE has a known facilitating effect on this neonatal olfactory learning paradigm and underlying synaptic plasticity (Ghosh, Carew, Chen, & Yuan, 2017; McLean, Harley, Darby-King, & Yuan, 1999; Sullivan, Stackenwalt, Nasr, Lemon, & Wilson, 2000; Yuan, Shakhawat, & Harley, 2014), although several finer details addressing other important components of the plasticity machinery— such as, interaction with calcium channels— are not well understood.

Noradrenergic deficit is present in several types of brain-related diseases, including Alzheimer's disease. Analyzing thousands of post-mortem human brains from subjects aged 1-100 years, Braak and colleagues provided a comprehensive staging system of AD, centering on the expression of a pathological hyperphosphorylated tau protein throughout the brain. They showed that the very first

appearance of this protein is in LC, from where it spreads to other areas of the brain in a slow but progressive manner. Although this staging system gained popularity, a critical question has been repeatedly raised – does LC-expression of abnormal tau proteins indeed initiate AD pathophysiology and cognitive deficits?

Based on this preamble, four years back, I embarked on a journey to understand the role of LC-NE in neonatal and adult olfactory learning as well as in AD. I have documented my findings and interpretation in this dissertation.

1.2 Brief anatomy and physiology of the noradrenergic system

1.2.1 Noradrenergic nuclei in the brainstem

The pontomedullary area of the brain has several noradrenergic nuclei clustered in it. They are characterized by the common biochemical feature of norepinephrine production. The earliest identification of this cell group happened about half a century back (Dahlström & Fuxe, 1964). Although the cell bodies are clustered in the brainstem, their axonal projections reach almost everywhere in the brain including, but not limited to, cerebral cortex, hippocampus, thalamus, hypothalamus, midbrain, brainstem, and spinal cord. These target areas can receive noradrenergic innervation from one or more of the nuclei (Nieuwenhuys, 1985). The noradrenergic nuclei are named as A1-A7, subdivided among rostral, central, and caudal areas (Szabadi, 2013) and somewhat well preserved across several species including rodents (Schofield & Everitt, 1981), carnivores (Ishikawa, Shimada, & Tanaka, 1975; Poitras & Parent, 1978) and primates

(Nieuwenhuys, 1985). Among these seven nuclei, rostral nucleus A6 or Locus Coeruleus is of specific importance. It is the biggest noradrenergic nucleus in the brain, characterized by a grey-blue spot in each hemisphere, on the floor of the fourth ventricle- thus contributing to the Latin name locus coeruleus. Interestingly, the color arises from a pigment molecule neuromelanin which is a basis of Magnetic Resonance Imaging (MRI) based LC imaging technique in humans (Shibata et al., 2006).

1.2.2 Cellular and molecular organisation within LC

The noradrenergic neurons within the LC have two predominant morphological types- fusiform and multipolar. Fusiform neurons are smaller in size, approximately 20 μm diameter. The multipolar neurons are about 35 μm diameter. Besides these two cell types, there are some other types of cells, including- posterior pole cells, small round cells, and medium sized multipolar cells (also known as core cells) (Loughlin, Foote, & Grzanna, 1986). Ventral LC contains more multipolar cells whereas a higher proportion of fusiform cells are found in the dorsal LC (Grzanna & Molliver, 1980; Loughlin et al., 1986; Swanson, 1976). There is also a unique association of cellular morphology and distribution within LC depending on the projection target. Hippocampus and cortex projecting cells are fusiform, whereas, large sized multipolar cells in the ventral LC project caudally to spinal cord and cerebellum. Large multipolar cells residing in the anterior segment of LC project heavily to the hypothalamus (Loughlin et al., 1986). Diverse LC afferents are further elaborated in a later section.

1.2.3 Functional diversity of the inputs to LC

Afferent connections to LC can be both excitatory and inhibitory in nature (see figure 1.1). Axons from neocortex, amygdala, hypothalamus, brainstem and spinal cord reach LC and activate/deactivate it in function specific manner. This diversity is achieved by pathway specific selection of neurotransmitters and neuromodulators. Neocortical input is excitatory and glutametargic in nature (Szabadi, 2013), whereas corticotrophin releasing factor (CRF) is instrumental for excitatory amygdalar input to LC (McCall et al., 2015; Bockstaele, Pieribone, & Aston-Jones, 1989). In contrast, hypothalamus has mixed input to LC. The sleep-promoting venterolateral preoptic area sends GABAergic inhibitory input to LC (Cedarbaum & Aghajanian, 1978; Steininger, Gong, Mcginty, & Szymusiak, 2001). On the other hand, wakefulness-promoting lateral hypothalamus (LH) and tuberomamillary nucleus (TMN) excite LC by orexinergic inputs (Date et al., 1999; Cid-Pellitero; España, Reis, Valentino, & Berridge, 2005) and histaminergic inputs functional via H1 receptor (Korotkova, Sergeeva, Ponomarenko, & Haas, 2005; H. S. Lee, Lee, & Waterhouse, 2005), respectively.

Among the midbrain and pontine areas, ventral tegmental area (VTA), periaqueductal grey (PAG), pedunculopontine tegmental / laterodorsal tegmental nuclei (PPT/LDT) and dorsal raphe (DR) requires mentioning. Mixed direct and indirect evidence suggests that they all have an excitatory effect on the LC, albeit through different neuromodulators, such as dopamine for VTA (Beckstead, Domesick, & Nauta, 1979; Deutch, Goldstein, & Roth, 1986; Ornstein et al., 1987) and PAG (Bajic & Proudfit, 1999; Lu, Jhou, & Saper, 2006; Niepel et al., 2013); serotonin for DR (M.-A. Kim, Lee, Lee, & Waterhouse, 2004); and acetylcholine for PPT/LDT (Egan & North, 1985; Jones, 1990; Jones & Yang, 1985).

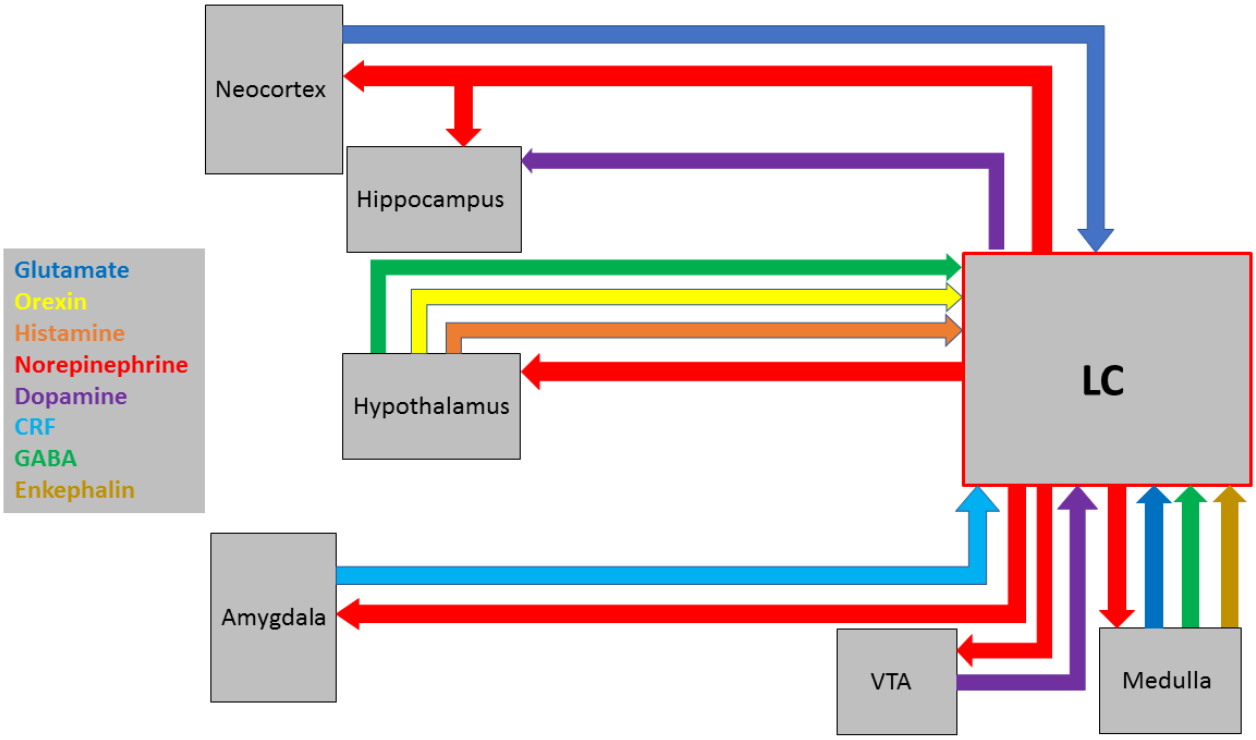

Figure 1.1 **Major inputs and outputs of LC**

Major inputs and outputs of LC are presented here.
VTA= ventral tegmental area

The medullary input to LC can also be either excitatory or inhibitory in nature. Rostroventrolateral medulla (RVLM) has glutamatergic projection to LC which is excitatory in nature (Ennis & Aston-Jones, 1986, 1988; Bockstaele & Aston-Jones, 1995). Inhibitory projections include GABAergic and enkephalinergic axons (Drolet, Bockstaele, & Aston-Jones, 1992). Nucleus prepositus hypoglossi has a role in rapid eye movement (REM) sleep modulation through a possible direct inhibitory effect on LC through GABAergic neurons (Ennis & Aston-Jones, 1989a, 1989b; Kaur, Saxena, & Mallick, 2001).

1.2.4 Functional diversity of the outputs of LC

Efferent fibers from LC innervate the whole brain extensively with large variations across regions. LC outputs can have excitatory or inhibitory effect on the target region depending on the receptor subtype expressed. We will broadly divide the areas among forebrain, limbic system, thalamus, hypothalamus, brainstem, cerebellum and spinal cord for the convenience of description.

The dorsal noradrenergic bundle, which carries axon fibers from LC, innervates the forebrain extensively (Gatter & Powell, 1977; Nieuwenhuys, 1985). LC has an excitatory effect on the neocortical area owing to the robust expression of α_1 (Jones & Yang, 1985; Papay et al., 2006) and β (Wanaka et al., 1989) ARs there. α_{1A}(Day, Campeau, Watson Jr, & Akil, 1997; Domyancic & Morilak, 1997), α_{1B} and α_{1D} (Day et al., 1997) subtypes are present there. Inhibitory α_2-ARs are present as well, mostly belonging to α_{2A} subtype (Blake, Tillery, & Reynolds, 1998) and are present in the inhibitory neurons (Andrews & Lavin, 2006). LC activity is closely associated with cortical activity and contributes to arousal-related states.

The basal forebrain containing medial septal area, preoptic area and substantia innominate, receive LC efferents (España & Berridge, 2006). The cholinergic neurons stay active during wakefulness (Manns, Alonso, & Jones, 2000b) and the GABAergic neurons stay active during sleep (Manns, Alonso, & Jones, 2000a). Interestingly, NE released in this area excite cholinergic neurons by α_1 and β_1-ARs (Craig W Berridge & Waterhouse, 2003). On the other hand, same NE inhibits the GABAergic neurons by α_2-ARs (Manns, Lee, Modirrousta, Hou, & Jones, 2003). Thus, despite having an expression of both excitatory and inhibitory ARs, the general effect of LC activation on basal forebrain remains excitatory in nature resulting in wakefulness.

The noradrenergic modulation of amygdalar activity is strongly related to anxiety and fear learning. α_{1A} (Manns et al., 2003), α_{2A} (Scheinin et al., 1994), β_1 (Ghiasvand, Rezayof, Ahmadi, & Zarrindast, 2011) and β_2 (Qu, Guo, & Li, 2008) ARs have been identified in the amygdala. Evidences suggest that β-AR can modulate anxiety (McCall et al., 2017; Silberman, Ariwodola, Chappell, Yorgason, & Weiner, 2010) and fear conditioning (Farb, Chang, & LeDoux, 2010).

Hippocampus receives LC innervation. NE from LC acts on the hippocampus by α_{1A} (Day et al., 1997), α_{1D} (Williams, Nguyen, & Morilak, 1997), α_{2A} (Scheinin et al., 1994) and β (Wanaka et al., 1989) ARs. Involvement of hippocampus in noradrenergic modulation of learning and memory has been elaborated in a later section.

Thalamus receives axons from LC as well. α_{1B} (Day et al., 1997), α_{2B} (Scheinin et al., 1994) and β_1-AR (Paschalis et al., 2009) have been identified in the thalamus. Noradrenergic modulation of

thalamic function is known to facilitate wakefulness (McCormick, Pape, & Williamson, 1991) and also alters sensory perception of pain (Zhang, Guo, Qiao, & Dafny, 1998).

Hypothalamus has several nuclei. Two particularly important hypothalamic nuclei modulating arousal are ventrolateral preoptic nuclei (VLPO) and lateral hypothalamic/ perifornical area (LH/PF). While inhibitory GABAergic neurons in VLPO receives LC-NE mediated inhibition by α_2-ARs and thereby facilitate wakefulness (Nelson et al., 2002) orexinergic LH neurons receive similar inhibition by α_{2A} AR, especially in a sleep-deprived state (Uschakov et al., 2011; Yamanaka, Muraki, Tsujino, Goto, & Sakurai, 2003). The latter may have a protective effect on LC preventing its overactivation during wakefulness (Szabadi, 2013).

Noradrenergic modulation of the brainstem function is exerted through sympathetic premotor nuclei (RVLM, caudal Raphe), parasympathetic preganglionic nuclei (Edinger-Westphal nuclei, salivatory nuclei, vagal nuclei), motor nuclei (for cranial nerves III,V,VII and XII) and sensory nuclei (for cranial nerves V and VIII) via different ARs. Cerebellar motor function relies on the norepinephrine (Szabadi, 2013). Noradrenergic modulation of cerebellum is mediated through α_{1A} (Day et al., 1997), α_{2A} (Scheinin et al., 1994) and β_1-AR (Paschalis et al., 2009). In the spinal cord, NE modulates nociception at the dorsal horn (Szabadi, 2013).

1.2.5 Modular activation

Earlier view of the role of LC suggested generalized control of behavioral states through change of its spiking pattern. Example of LC neuron spiking patterns can be found in fig 2 and 4, in Aston-

Jones and Cohen, 2005. It implied change in the brain-wide noradrenergic release dynamics through widespread arborisation of LC (Aston-Jones & Cohen, 2005; Aston-Jones & Waterhouse, 2016). But this view started changing with the discovery of differential cortical projection profile of subgroups of LC neurons (Chandler, Gao, & Waterhouse, 2014). For example, this was further strengthened by studies involving combinatorial approach of anatomical tracing-physiological recording-behavioral testing. One study discovered that different LC cell-clusters are responsible for facilitation and extinction of aversive learning. This was due to activation of LC-amygdala connection and LC-medial prefrontal cortex connection, respectively (Uematsu et al., 2017). LC neurons are known to spike in different modes. While phasic pattern is associated with increased attention and reward function, high tonic pattern is observed in stressful situations (Aston-Jones & Bloom, 1981; Aston-Jones & Cohen, 2005). Further evidence for modular activation of LC came from a relatively recent article combining tracing with physiological recording of LC spiking. They observed largely unsynchronised spiking across paired recordings of LC neurons in both phasic and tonic modes. Interestingly, they also provide evidence for non-topographic distribution of ensembles within LC, which surprisingly have similar forebrain target for efferent projections (Totah, Logothetis, & Eschenko, 2019). Thus, a complex functional and modular-organizational diversity in LC neuronal population is gradually becoming apparent.

1.2.6 LC spiking patterns and optogenetics

LC neurons spike spontaneously at a low frequency. Although *ex vivo* slice electrophysiology has shown that not all the neurons spike spontaneously (Jedema & Grace, 2004), the majority follow this pattern. Their spontaneous spiking frequency is less than 6 Hz (Jedema & Grace, 2004; Sanchez-Padilla et al., 2014; Williams, North, Shefner, Nishi, & Egan, 1984). *In vivo* LC

electrophysiology shows 1-3 Hz baseline spiking frequency in wakefulness with reduction in spiking during sleep (Aston-Jones & Bloom, 1981; Hobson, McCarley, & Wyzinski, 1975). LC neurons have two distinct spiking patterns- phasic and tonic (Aston-Jones & Cohen, 2005; C. W. Berridge, 2008). Phasic mode is described by brief bursts of action potentials at 8-10 Hz (Aston-Jones & Bloom, 1981; McCall et al., 2015), followed by a period of inactivity. This phasic activity has been associated with the presentation of novel or salient stimulus, focused attention and task-orientation (Aston-Jones & Bloom, 1981; Aston-Jones & Cohen, 2005; Carter et al., 2010; Dayan & Yu, 2006; Ramos & Arnsten, 2007). On the other hand, tonic pattern of spiking is regular in nature and reports suggest 3-8 Hz of spiking frequency (Carter et al., 2010; Curtis, Leiser, Snyder, & Valentino, 2012; McCall et al., 2015). It should be noted that low tonic spiking of 1-3 Hz is important for wakefulness and arousal (Carter et al., 2010) but high tonic pattern has been associated with stressful situations and agitation. Phasic mode is associated with baseline moderate tonic spiking, and it is proposed to optimize task performance (Aston-Jones & Cohen, 2005).

Experimental effort in studying LC activation patterns in relation to behavior and physiology has been facilitated by optogenetics. Opsins— light sensitive ion channels— from algae were expressed in LC neurons through viral vector mediated gene delivery in a Cre-recombinase-dependent manner. It rendered specificity to noradrenergic population. The excitatory opsin is a cation channel (channelrhodopsin) whereas the inhibitory one is a chloride pump (halorhodopsin) (Carter et al., 2010). Photostimulation was carried out through implanted optical fiber cannula, in specific wavelengths, as required by the opsins- 473 nm, i.e, blue light for channelrhodopsin and 593 nm, i.e, yellow light, for halorhodopsin. Photostimulation resulted in induced activation or inhibition of LC with a high temporal precision (Carter et al., 2010). This opened an avenue to reliably test the differential roles of phasic and tonic stimulation patterns, adopted by several studies later. Different

phasic patterns induced by optogenetic stimulations utilized a wide range of frequencies like 10 Hz (Carter et al., 2010; McCall et al., 2015), 12 Hz (Vazey, Moorman, & Aston-Jones, 2018), 20 Hz (Kempadoo, Mosharov, Choi, Sulzer, & Kandel, 2016) and 25 Hz (Takeuchi et al., 2016). Examples of different tonic frequencies include 3Hz (Carter et al., 2010; Vazey et al., 2018), 5 Hz (McCall et al., 2017) and 10 Hz (Carter et al., 2010).

1.3 Noradrenergic modulation of learning and memory: behavioral models and cellular-molecular-network mechanisms

1.3.1 Hippocampus-dependent learning

Hippocampal formation receives its input from entorhinal cortex (EC) at the dentate gyrus (DG) via perforant pathway. Then DG synapses on cornu ammonis3 (CA3) region via mossy fibers. Further, CA3 synapses on CA1 region via Schaffer collateral. LC innervates hippocampus and modulates learning and memory. Following LC stimulation, hippocampus-dependent learning has been facilitated, presumably due to NE release. Local NE administration in the dorsal hippocampus facilitates longevity of extinction memory (Chai et al., 2014). Glucocorticoid dependent hippocampal impairment of spatial memory retrieval in a water maze is also sensitive to a β-AR dependent mechanism (Roozendaal, Hahn, Nathan, Dominique, & McGaugh, 2004). Pharmacological antagonism of the β-AR prevents novel spatial learning (Hansen & Manahan-Vaughan, 2015). Hippocampus dependent inhibitory avoidance memory consolidation is also dependent on astrocytic β_2-AR. β_2-AR promotes astrocytic lactate release which is critical for long term memory (Gao et al., 2016).

Acquisition of avoidance learning can release NE in the DG. The NE level returns to normal after extinction. This avoidance learning can be modulated by α_1-AR, pharmacological inhibition of which resulted in an enhancement of learning (Lv et al., 2016). NE release in DG from LC is important for spatial learning too (Devauges & Sara, 1991; Sara & Devauges, 1988).

Acquisition of the memory of a novel context is dependent on the LC input to CA3, but not CA1 or DG. Optogenetic inhibition of this input prevents such learning as well as disrupts stable representation of a context in CA3 and downstream CA1 neurons (Wagatsuma et al., 2018).

In the CA1 area, LC electrical stimulation increased NE and facilitated a single-episode spatial memory. This was proven to be β-AR dependent (Lemon, Aydin-Abidin, Funke, & Manahan-Vaughan, 2009).

NE can modulate different forms of hippocampal synaptic plasticity, such as, LTP and LTD. LTP is a long-term potentiation of synaptic strength after high frequency stimulation. On the other hand, LTD is long-term weakening of synaptic strength. NE depletion reduces DG-LTP. Novel spatial experience facilitates LTP at perforant path-DG synapses in a β-AR dependent mechanism (Hansen & Manahan-Vaughan, 2015). NE binding to β-AR and subsequent adenylyl cyclase activation is causal to the plasticity (Sarvey, Burgard, & Decker, 1989; Stanton & Sarvey, 1985). Even in absence of high frequency stimulation, NE can induce long lasting potentiation (LLP) in DG which is similar to LTP. Both forms of plasticity are critically dependent on protein synthesis and NMDAR activity (Sarvey et al., 1989). α_1-AR mediated DG-LTP (Lv et al., 2016) can be due to an increased NMDAR conductance resulting in augmented glutamatergic neurotransmission (Sirviö &

MacDonald, 1999). Early phase LTP can be modulated by cyclic Adenosine Mono Phosphate-Protein Kinase A (cAMP-PKA) cascade preventing dephosphorylation of NMDAR (Thomas, Moody, Makhinson, & O'Dell, 1996). For late phase LTP, β-AR activation mediated cAMP-signaling may facilitate calcium influx in the cell via NMDAR and/or voltage gated calcium channels (Chay, Zamparo, Koschinski, Zaccolo, & Blackwell, 2016; Sarvey et al., 1989).

PKA can modulate both early and late phase of mossy fiber LTP (Huang et al., 2014). β-AR activation is important for both early phase and late phase mossy fiber LTP, the latter being a protein-synthesis dependent mechanism (Huang & Kandel, 1996). Gs-Gi alteration capability of β-ARs, and subsequent Gi inhibition to adenylyl cyclase, can engage different kinases important for synaptic plasticity (Chay et al., 2016).

Slice electrophysiology data shows that CA3-CA1 synapses can undergo LTD upon NE application and this plasticity is α_1-AR mediated (Scheiderer, Dobrunz, & McMahon, 2004). Schaffer collateral-CA1 stimulation with LC electrical stimulation induced LTD and temporary reduction of theta oscillation (Lemon et al., 2009).

From a molecular perspective, β-ARs mediate synaptic plasticity by two major ways. First, by inhibiting protein phosphatase-1 by phosphorylated inhibitor-1 (secondary to PKA activation). This helps phosphorylating NMDAR, CaMKII, β_2-AR, thereby maintaining their function directly contributing to the formation of LTP. Second, by facilitating the translation machinery to promote maintenance of LTP (O'Dell, Connor, Guglietta, & Nguyen, 2015). Adrenergic receptor activation triggers ERK and mTOR signaling and eventually phosphorylates 4E binding protein-2 (4EBP-2) (Gelinas et al., 2007; Klann, Antion, Banko, & Hou, 2004). This results in release and activation of

eukaryotic initiation factor (eIF4E) from the inhibition of 4EBP-2 promoting protein synthesis (Banko et al., 2005).

1.3.2 Amygdala-dependent learning

LC axons heavily innervate amygdalar nuclei. Stress is associated with high tonic spiking of the LC neurons. Stressor mediated LC activation leads to increased NE in the amygdala (Gallvez, Mesches, & McGaugh, 1996; Quirarte, Galvez, Roozendaal, & McGaugh, 1998). This results in a heightened activation in the subnuclei of the amygdala, such as BLA, indexed by cFos expression. It reduces when LC is inactivated by pharmacological intervention. In a gain of function approach, α_2-AR antagonist administration, which can increase NE release, increases BLA cFos activation (Singewald, Salchner, & Sharp, 2003). On the other hand, α_2-AR agonist administration, which decreases NE release, reduces BLA cFos activation and affects fear conditioning (Davies et al., 2004).

The manipulation of the LC-NE system will alter the amygdala-dependent learning. Depending on the experiment, results can vary within a wide range. For example, toxin mediated lesion of the noradrenergic bundle can affect fear learning (Cole & Robbins, 1987; Selden, Robbins, & Everitt, 1990), or increase aversion (Selden, Everitt, & Robbins, 1991) , or remain ineffective (Mason & Fibiger, 1979). β-AR in BLA is critical for fear memory acquisition. Specific antagonist infusion in BLA before training affects fear conditioning (Bush, Caparosa, Gekker, & LeDoux, 2010; Díaz-Mataix et al., 2017). Optogenetic activation of LC projections to BLA in a high tonic pattern induces anxiety and fear conditioning in mice through β-AR (McCall et al., 2017) α_1-AR antagonist

infusion in BLA improves aversive learning as well as strengthens LTP in lateral amygdala (Lazzaro, Hou, Cunha, LeDoux, & Cain, 2010). It is important to note that NE is effective in multi trial stronger protocols than in single trial weaker conditioning protocols (Díaz-Mataix et al., 2017; Giustino & Maren, 2018).

NE can modulate fear memory expression too. Local clonidine infusion in lateral amygdala reduces NE neurotransmission by activating α_2-AR and decreases fear memory expression in startle response measurement (Schulz, Fendt, & Schnitzler, 2002). In line with this, BLA slice recording shows that NE's ability to enhance glutamatergic neurotransmission (via β-AR) remains unaltered after fear conditioning. But its ability to enhance GABAergic neurotransmission (via α_1 and β_3-AR) reduces following fear conditioning (Skelly, Ariwodola, & Weiner, 2017)

NE has no reported role in cued fear memory consolidation (Lee, Berger, Stiedl, Spiess, & Kim, 2001). Local administration of propranolol in BLA did not affect auditory fear memory consolidation either (Bush et al., 2010). This is in contrast with contextual fear memory consolidation. Enhancing noradrenergic neurotransmission with α_2-AR antagonist enhances contextual fear memory consolidation (Gazarini, Stern, Piornedo, Takahashi, & Bertoglio, 2015; Gazarini, Stern, Carobrez, & Bertoglio, 2013). BLA specific NE application echoed the same (LaLumiere, Buen, & McGaugh, 2003). Reactivated memory undergoes an unstable state that requires protein synthesis dependent reconsolidation for stabilization. Evidence suggests that enhancing NE by clonidine administration facilitates reconsolidation (Gamache, Pitman, & Nader, 2012). Furthermore, this process is β-AR mediated, as propranolol administration prevents

reconsolidation of cued and contextual fear memories (Debiec & LeDoux, 2004; Pitman et al., 2011; Przybyslawski, Roullet, & Sara, 1999; Schneider et al., 2014).

Extinction of cued fear memory is also NE-dependent, but the relationship can be bidirectional. Decreased NE level can delay extinction (Cain, Blouin, & Barad, 2004; Tsaltas, Gray, & Fillenz, 1984) but pharmacological intervention increasing NE facilitates extinction (Cain et al., 2004). On the other hand, extinction training placed close to fear conditioning, can be affected due to stress related higher NE levels. Both systemic and local infusion of propranolol in BLA facilitates extinction learning which would otherwise be impaired (Fitzgerald, Giustino, Seemann, & Maren, 2015; Giustino et al., 2017). Similar evidence exists for contextual fear memory extinction. NE infusion in BLA facilitates extinction learning (Berlau & McGaugh, 2006). Given the importance of hippocampus in contextual learning, it remains as a possibility that α_2-AR engaging concentrations of NE in BLA are able to alter hippocampal plasticity and favor extinction learning (Giustino & Maren, 2018).

Mechanistically, β-AR activation increases NMDAR mediated excitatory postsynaptic potential (EPSP) in BLA pyramidal neurons. This increase in excitation is secondary to cAMP signaling and P-type calcium channel opening (Gean, Huang, Lin, & Tsai, 1992). This is in agreement with β_1 and β_2-AR mediated enhancement of LTP (Abraham et al., 2008). NE (Tully, Li, Tsvetkov, & Bolshakov, 2007) or β-AR (Pu, Krugers, & Joëls, 2009) mediated LTP facilitation occurs even for subthreshold stimuli. On the other hand, α_2-AR activation inhibits LTP (DeBock et al., 2003).

Reduction in noradrenergic modulation of inhibitory neurotransmission in BLA is associated with fear conditioning (Skelly et al., 2017; Skelly, Snyder, & Silberman, 2020). Local feedback

interneurons in BLA express α_1-AR. NE depolarizes those neurons (Kaneko 2008) and increase inhibitory tone on the BLA pyramidal neurons. This is further supported by NE mediated increase in spontaneous IPSC frequency in BLA pyramidal neurons, suggesting a presynaptic effect (Braga, Aroniadou-Anderjaska, Xie, & Li, 2003). Coming to a full circle, blocking α_1-AR in BLA facilitates LTP and fear learning (Lazzaro et al., 2010). On the other hand, pericapsular inhibitory neurons receive input from cortical areas and sends feedforward inhibition onto the BLA pyramidal neurons (Marowsky, Yanagawa, Obata, & Vogt, 2005). β_1-AR mediates the postsynaptic enhancement of GABAergic neurotransmission onto pyramidal neurons in a cAMP-dependent mechanism, as evident from slice electrophysiology (Silberman et al., 2010; Silberman, Ariwodola, & Weiner, 2012). It is important to note that β_3-AR shows similar trend with a distinct feature of selective action only at feedforward inhibitory synapses (Silberman et al., 2012).

1.3.3 Olfactory learning

1.3.3.1 In adults

1.3.3.1.1 Odorant detection

Detection of an odorant is the first step in olfactory information processing. Typically, detection threshold is explored by scientists in order to understand the sensitivity of the detection process with respect to the odorant concentration. Serially diluted odorants are presented across multiple test sessions and sniffing time is recorded. This is based on the principle that the subject will sniff

for longer duration, compared to mineral oil, if an odor is detected (Escanilla, Arrellanos, Karnow, Ennis, & Linster, 2010).

NE is known to reduce odor detection threshold by improving the signal to noise ratio, thus facilitating peri-threshold odor detection. Research suggests NE can increase the signal by increasing spiking of the principal neurons (Linster, Nai, & Ennis, 2011). Alternatively, it can reduce the noise of spontaneous activity by increasing inhibitory neurotransmission (Nai, Dong, Hayar, Linster, & Ennis, 2009; Nai, Dong, Linster, & Ennis, 2010). It is also important to note that noradrenergic modulation can change motivation-based odorant detection. In a reward-associated motivation-based odor detection paradigm, blockade of NE in the olfactory bulb impairs low-concentration odorant detection (Escanilla, Alperin, Youssef, Ennis, & Linster, 2012). Interestingly, toxin mediated NE depletion in OB does not affect odor detection threshold in a motivation-dependent paradigm (Doty, Ferguson-Segall, Lucki, & Kreider, 1988) Finally, noradrenergic modulation of odor input mediated neuronal activity in OB was possible when the odor was associated with an unconditioned stimulus, shock (Gray, Freeman, & Skinner, 1986). This underscores differential noradrenergic modulation of odor information processing in both spontaneous and motivation-associated tasks.

1.3.3.1.2 Perceptual learning

Perceptual learning is a relatively simpler form of learning through odor exposure only. It utilizes odor recognition (identifying previously encoded odor) or odor habituation principles (multiple encoding of the same odor followed by a recall and/or test session) (Linster & Escanilla, 2019).

Interestingly, perceptual learning is critically dependent upon adult born neurons and NE in OB (Moreno et al., 2012; Moreno et al., 2009). Briefly, in a cross-habituation olfactory task, authors show that perceptual learning is NE-dependent and NE-induced facilitation of learning is neurogenesis dependent. They also showed noradrenergic fibers innervate newly born neurons which are responsive to the bath application of NE in slice electrophysiology experiments. Altogether, they infer that successful perceptual learning is dependent on NE and adult-born neurons.

1.3.3.1.3 Encoding olfactory memory

Memory encoding is the neural activity correlate of a sensory input that is retrievable for future recall. In its simplest form, encoding of olfactory memory can be examined in a habituation task by estimating investigation time. Chemical ablation of LC resulted in an acquisition deficit, retrievable by local bulbar infusion of NE (Guerin, Peace, Didier, Linster, & Cleland, 2008). In a more complicated model using similar odor pairs and reward-association, odor encoding coupled with odor discrimination was dependent on α and β-ARs in OB (Doucette, Milder, & Diego Restrepo, 2007; Mandairon et al., 2008) and in PC (Shakhawat et al., 2015). Lastly, LC electrical stimulation facilitated odor encoding even in absence of a reward-association (Shea, Katz, & Mooney, 2008).

1.3.3.1.4 Duration of olfactory memory

It is debatable how NE modulate duration of olfactory memory. On one hand, global NE depletion reduces memory duration, but global NE increase enhances it (Veyrac, Nguyen, Marien, Didier, &

Jourdan, 2007). On the other hand, a bulbar infusion study showed that NE dose dependently alters memory duration. Lower and higher doses reduce the memory duration, whereas medium dose is ineffective (Manella, Alperin, & Linster, 2013).

1.3.3.1.5 Odor specificity

Specificity of an encoded odor memory can be tested in odor recognition, odor habituation, odor-reward association, and olfactory discrimination-based go-no go paradigms. Except for the last one, all paradigms utilize a comparison of investigation time between encoded and other novel odors. NE has been shown to be critical for the specificity of the encoded memory in many different paradigms (Doucette et al., 2007; Escanilla et al., 2010; Mandairon et al., 2008) utilizing similar odor pairs, possible mechanism being a change of neural representation of the odors. This has been demonstrated further in a PC-based reward-associated go-no go odor discrimination paradigm (Shakhawat et al., 2015).

1.3.3.1.6 Go-no go olfactory paradigm

The olfactory bulb is the first relay station of the olfactory information processing. Mitral cells (MC) and tufted cells receive input from the olfactory sensory neurons and carry this information to other brain areas through their axons. Inhibitory granule cells (GC) can modify this flow of information locally at the olfactory bulb.

A go-no go paradigm operates on the principle that the subject makes a decision and act (go) or do not act (no go) based on the learning. Normally subjects are kept either food or water deprived at a fraction of their daily requirement. In food retrieval paradigm, digging method is used fairly commonly (Berger-Sweeney, Libbey, Arters, Junagadhwalla, & Hohmann, 1998). For water deprived models, computer controlled olfactometers can operate semi-automatically. Briefly, water deprived rodents are habituated in the olfactometer for licking and receive 30 ul of water reward on each lick. Afterwards, the positively reinforced odor is introduced. On every insertion of the snout to the odor port, odor is delivered before water reward is released. Next, the subject learns to lick the water-port in quick succession (six times in one second) in order to retrieve the reward upon delivery of the positively reinforced odor. Subject can choose to lick (go) or to not lick (no-go) depending on positive or negative odor delivery. Brief time-out periods between snout insertions ensure motivated subjects during the entirety of the experiment. Percentage of correct choices is measured automatically in the computer.

Shakhawat et al. 2015 has shown that α and β-ARs in the PC are critical for successful discrimination learning of similar but not dissimilar odor pairs in the olfactometer. Successful discrimination led to more distinct neural representations of the similar odors as indexed by immediate early gene activation in a fluorescent *in situ* hybridization technique.

1.3.3.1.7 Concise overview of the mechanistic role of NE in olfactory learning

In the olfactory bulb, NE increases MC spiking and GC spiking through α_1-AR activation (Hayar, Heyward, Heinbockel, Shipley, & Ennis, 2001; Mouly, Elaagouby, & Ravel, 1995; Nai et al., 2010) . In presence of a peri-threshold sensory stimulation, NE mediated increase in spiking of MCs can give rise to higher signal to noise ratio. On the other hand, NE action on the inhibitory GC cells can reduce spontaneous MC spiking following LC stimulation (Jiang 1996), thus potentially contributing to noise reduction. Another mechanism requires mention that the presynaptic inhibition of MC mediated GC activation results into a disinhibitory excitation of MC by NE (Trombley & Shepherd, 1992). NE concentration dependent AR engagement can also play a role in shaping the overall effect of NE. At lower concentrations α_2-AR is more activated, thus leading to an overall MC excitation by disinhibitory mechanism, whereas, at higher concentration when α_1-AR is engaged, GC activation mediated MC inhibition will be predominant (Nai et al., 2009; Nai et al., 2010).

Similar to OB, PC is also under the influence of NE for olfactory information processing. LC electrical stimulation increases PC spiking (Bouret & Sara, 2002). On the other hand, NE application reduces excitatory neurotransmission between principal neurons, thus providing a window for enhanced signal to noise ratio for incoming PC input (Hasselmo, Linster, Patil, Ma, & Cekic, 1997). Overall, it is speculated that cortical NE modulation influences associative learning and synaptic plasticity (Linster, 2019). Besides, olfactory learning induced excitability in PC is caused by reduction in after-hyperpolarisation (AHP) (Barkai, 2005). NE works as a “brake” and

prevents the reduction in AHP, thereby prevents hyperexcitation in the network (Brosh, Rosenblum, & Barkai, 2006; Saar & Barkai, 2009).

1.3.3.2 In neonates

Early odor preference learning occurs in neonates through a critical time window. The young pups learn to associate neutral olfactory input (conditioned stimulus) with maternal cues (unconditioned stimulus) and forms a preference towards it. A wide range of unconditioned stimuli can be utilized, such as- paintbrush stroking or other somatosensory input (McLean, Darby-King, Sullivan, & King, 1993; Moore & Power, 1992; Pedersen, Morishima, Finster, Arthur, & Covino, 1982; Sullivan & Leon, 1986), tail pinch (Sullivan & Leon, 1986), low amplitude foot shock (Camp & Rudy, 1988; Roth & Sullivan, 2001, 2003), saliva (Sullivan & Leon, 1986) or milk (Johanson & Hall, 1979; Johanson & Teicher, 1980) from the mother. Depending on the strength of the training, the duration of the memory can vary as well (Fontaine, Harley, & Yuan, 2013). Interestingly, beyond second week of rodent-life, this learning does not take place. Role of LC-NE is widely accepted as a crucial factor for this learning to happen. It has been shown that NE (Sullivan, Zyzak, Skierkowski, & Wilson, 1992) or the β-AR agonist (Sullivan et al., 2000) or α_1-AR agonist (Harley, Darby-King, McCann, & McLean, 2006) itself can function as the unconditioned stimulus in OB (Sullivan et al., 1992) or PC (Morrison, Fontaine, Harley, & Yuan, 2013) and replace the maternal cue.

As for the mechanism, several research teams have identified important roles of NE in this learning. In the OB, α_2-AR mediates disinhibition of MC, that can be important for gamma oscillation in

MC-GC network (Pandipati & Schoppa, 2012). In the piriform cortex, β-AR activation increases theta burst induced LTP in piriform cortex (Morrison et al., 2013). From a signaling cascade perspective, cAMP-PKA-pCREB pathway is recruited by the AR activation leading to memory formation. Successful training leads to pCREB activation in MC layer (McLean et al., 1999). This underscores a convergence of NE-cAMP-PKA and calcium-calmodulin systems in CREB phosphorylation (Yuan, Harley, Darby-King, Neve, & McLean, 2003). Drug enhancing cAMP action successfully alters a suboptimal isoprotenerol (β-AR agonist) infusion to an effective dose for learning (McLean, Darby-King, & Harley, 2005). This is in line with a cAMP peak occurring 10 min post-training (Cui, Smith, Darby-King, Harley, & McLean, 2007). Interestingly, PKA has similar temporal profile and PKA agonist itself can act as an unconditioned stimulus (Grimes, Harley, Darby-King, & McLean, 2012).

Related to these mechanisms, alteration in noradrenergic dynamics or function is likely to underlie the termination of the critical period. Indeed, several research works have found different aspects of noradrenergic neurotransmission or its downstream effects to change according to the critical period. α_2 autoreceptor function increases in the LC after the critical period, leading to a reduction in LC spiking (Nakamura, Kimura, & Sakaguchi, 1987).In the OB, strong gamma oscillations from MC-GC network decreases after the critical period; a potential explanation is the decreased α_2-AR signaling leading to reduced inhibition of the inhibitory GC (Pandipati & Schoppa, 2012). Post-critical period, noradrenergic effect increases inhibitory neurotransmission and decreases excitatory neurotransmission in the piriform cortex (Ghosh, Purchase, Chen, & Yuan, 2015). Altogether, a noradrenergic dependence of neonatal olfactory learning is evident from these findings.

1.3.4 Noradrenergic modulation of calcium influx through LTCC

NE binding to α_1, α_2 and β-AR initiates Gq, Gi and Gs mediated molecular cascades respectively. NE functioning through G protein coupled ARs is critical for several forms of learning and synaptic plasticity, as elaborated in the previous section. The calcium influx plays a huge role in this matter, making calcium channels one of our focus areas in this dissertation. Evidence suggests that NE can modulate LTCC mediated calcium influx via β-AR mediated Gs-PKA pathways (Ghosh et al., 2017). Blockade of LTCC by antagonist infusion in OB can prevent NE's action as UCS. LTCC agonist Bay K-8644 is able to rescue learning impairment caused by NMDAR antagonist administration. But this rescue of learning lacks input-specificity (Mukherjee & Yuan, 2016a). Congruent to these findings, NE mediated LTP is also dependent on LTCC activity in OB slices (Zhang et al., 2010). Periglomerular cells (PGCs) in the OB express LTCC. Administration of agonist BAY K 8644 initiates GABA release from them, resulting in inhibition of MCs (Murphy, Darcy, & Isaacson, 2005). β-AR agonist can suppress PGC activity (Jerome, Hou, & Yuan, 2012; Yuan, 2009) leading to calcium influx through MC-LTCC. Thus a strong association of NE, LTCC and odor learning seems to be robust. But, how do the different kinases related to different G-proteins modulate LTCC?

cAMP-PKA pathway is favored by Gs activation and inhibited by Gi activation. Different first messengers (ligands of GPCRs) can activate Gs and increase second messenger cAMP production, followed by enhanced PKA activity. PKA is known to make modifications at the C- terminus of the LTCC (CaV 1.2). This has been established in various systems (De Jongh et al., 1996; Fuller, Emrick, Sadilek, Scheuer, & Catterall, 2010; Gao et al., 1997; Hall et al., 2007; Murphy et al., 2014). Reports document that PKA can increase LTCC activity (Bray & Mynlieff, 2011; Dittmer,

Dell'Acqua, & Sather, 2014; Yang et al., 2001; Young, Huang, Lin, Shen, & Gean, 2001; Zanatta et al., 2012) or decrease it (Hoddah, Marcantoni, Comunanza, Carabelli, & Carbone, 2009). In one report, Gi decreased PKA activity, which in turn decreased LTCC function (Seseña, Vega, & Soto, 2014).

β-ARs' modulation of LTCC function and underlying contribution of PKA are widely explored in neurons and other excitable cells. Activation of β-AR can inhibit calcium-dependent inactivation of high voltage gated calcium channels which includes LTCC. Data suggest that A-Kinase anchor protein guides PKA mediated phosphorylation of LTCC, thereby inhibiting calcium-dependent inactivation of the channel (Rankovic et al., 2011).

LTCC in hippocampal cells undergo PKA-mediated serine 1928 phosphorylation to have increased function. A long term potentiating effect of theta stimulation required increase in CaV1.2 activity. This was dependent upon serine 1928 phosphorylation by β_2-AR-cAMP-PKA pathway, but not β_1-AR. On the other hand, in cardiomyocytes, β_1-AR mediated enhancement of LTCC function is PKA-regulated but independent of serine 1928 (Qian et al., 2017). In the spines of CA1 pyramidal neurons, β_2-AR-PKA increases calcium influx through LTCC (Hoogland & Saggau, 2004). β_1 and β_2-AR can also oppose each other's action on LTCC. For example, in adrenal chromaffin cells, β_1-PKA augments LTCC function but β2 mediated decrease is by Gi/Go (Cesetti, Hernandez-Guijo, Baldelli, Carabelli, & Carbone, 2003).

Gq protein activation enhances protein kinase C (PKC) function. PKC can enhance LTCC function in the heart (Weiss & Dascal, 2015), in the retina (Farrell, Raymond, Foote, Brecha, & Barnes, 2010; Liu, Weng, Yang, & Zhong, 2015), in the prefrontal cortex (Xia et al., 2009), and in the

hippocampus (Bray & Mynlieff, 2011; Karls & Mynlieff, 2015; Topolnik, Chamberland, Pelletier, Ran, & Lacaille, 2009; Zhang et al., 2010). On the other hand, few reports demonstrated inhibition of LTCC function by PKC (Farrell, Rankin, Brecha, & Barnes, 2014; Zhang et al., 2010).

Overall, rich and complex findings in the literature indicate robust noradrenergic modulation of calcium influx through LTCC, mediated by the action of the kinases. However precise role of it can vary from one system to another.

1.4 Olfactory deficit in Alzheimer's Disease

Loss of olfactory function is an early yet extremely prevalent symptom in Alzheimer's disease. Presence of olfactory dysfunction has been identified relatively earlier in the disease progression, even at a stage of mild cognitive impairment (MCI), and has served well as a sensitive predictor of progression to AD from MCI (Zou, Lu, Zhang, & Zhou, 2016). However, an aging-related deficit in olfactory function is not uncommon either. As different studies have identified, a strong correlation of prevalence of olfactory deficit with increased age of the study population is quite evident, often extending over 60% for higher age brackets (Doty et al., 1984; Murphy, Jernigan, & Fennema-Notestine, 2003). Age related olfactory dysfunction is more prevalent in males than females and has been partially attributed to a difference in the cell population in the olfactory bulb. Total cell number, number of neuronal cells and number of non-neuronal cells are significantly higher in female olfactory bulbs compared to that of males (Oliveira-Pinto et al., 2014). Despite the similarities, aging and AD are likely to take different routes of pathogenesis for olfactory dysfunction. Ossification in the cribriform plate and cumulative olfactory sensory neuron damage

are likely the primary cause of aging related olfactory dysfunction. On the other hand, two major histopathological hallmarks of AD are intracellular formation of neurofibrillary tangle (NFT) and extracellular formation of β-amyloid plaque. For AD, tauopathy and amyloidosis in different brain structures are of critical importance to understand the cause of olfactory deficit (Zou et al., 2016).

Over the years several evaluation tools have been used to assess olfactory deficits- Pocket Smell Test, Sniffin' Sticks Odor Identification Test, Cross Cultural Smell Identification Test, Brief Smell Identification Test and University of Pennsylvania Smell Identification. These tests are used to investigate odor identification, recognition, discrimination, and perception threshold. Different studies have identified olfactory deficits in multiple domains. Deficit in olfactory recognition has been associated with early AD and higher threshold has been identified in late stage of AD. Moreover, olfactory recognition ability but not threshold is correlated with Mini Mental State Examination (MMSE) score reflecting general cognitive ability (Serby, Larson, & Kalkstein, 1991). Some studies found olfactory threshold increase in early AD (Djordjevic, Jones-Gotman, De Sousa, & Chertkow, 2008) while others did not (Kareken et al., 2001; Larsson et al., 1999). Discrepancy among different reports may arise from different methods obtained by different groups. It is important to note that olfactory deficits are also prevalent in other neurodegenerative diseases with variable rates, but subtle differences may exist. For example, olfactory dysfunction in AD is generally more severe than in Parkinson's disease (PD), but particularly olfactory detection threshold is more affected in the latter (Rahayel, Frasnelli, & Joubert, 2012).

Support from the imaging studies provides brain-wide structural and functional basis of olfactory dysfunction. Reduction in hippocampal volume has been associated with deficit in olfactory ability

in AD patients (Kjelvik et al., 2014; Murphy et al., 2003). fMRI studies reveal a difference in blood oxygenation level dependent (BOLD) signal in olfactory dysfunction in AD patients. Intensity and distribution area of the BOLD signal in the olfactory cortex was positively correlated with odor intensity in the AD patients but not in healthy controls (Wang et al., 2010). Fluorodeoxyglucose-PET scan in early stage AD patients revealed that while odor recognition is associated with superior parietal lobule, occipitotemporal gyrus and inferior frontal gyrus, odor discrimination ability was associated with one activity cluster in the left postcentral cortex. On the other hand, odor detection threshold level was related to activity in the right thalamus and cerebellum (Förster et al., 2010).

Progressive accumulation of hyperphosphorylated tau proteins in forms of fibrils and tangles have been observed in the olfactory bulb. Interestingly β-amyloidosis was restricted in the glomerular layer (Bathini, Brai, & Auber, 2019; Bathini, Mottas, Jaquet, Brai, & Alberi, 2019). Increase in dopaminergic periglomerular neurons (Mundinano et al., 2011), change in centrifugal innervation, and possible imbalance of excitation-inhibition (Bathini, Brai, et al., 2019) are also probable causes of olfactory dysfunction in AD.

The olfactory tract undergoes structural change and may lose over 50% of myelinated axons in AD (Bathini, Mottas, et al., 2019; D. Davies, Brooks, & Lewis, 1993). Splitting of the olfactory tract occurs at the olfactory tubercle before it reaches to the piriform and other areas. NFT accumulation occurred in this area as well (Hyman, Hoesen, Damasio, & Barnes, 1984).

In the piriform cortex (PC) multiple mechanisms can contribute to functional impairment. Loss of synapses in the PC has been identified in AD (Giannakopoulos, Gold, Gunten, Hof, & Bouras, 2009). Calretinin and somatostatin positive GABAergic interneurons continue to reduce in number,

while the number of parvalbumin positive neurons keeps increasing (Saiz-Sanchez, Rosa-Prieto, Ubeda-Banon, & Martinez-Marcos, 2015). In Tg2576 transgenic rodent model of AD, odor memory impairment occurred in absence of odor perception deficit.

The amygdala has important roles in processing valence information associated with odors. Abundant tauopathy including neuronal loss is a common finding in this area with progressive AD (Arriagada, Growdon, Hedley-Whyte, & Hyman, 1992) even at an early stage (Poulin et al., 2011)

The EC has important role in fine discrimination ability of similar odors. Tauopathy in layer II may interfere with this function in AD (Stranahan & Mattson, 2010). The possibility of an amyloidosis-independent pathophysiological mechanisms of olfactory discrimination deficit has been addressed before (Wilson et al., 2014).

Thalamic degeneration is common in AD (Vasavada et al., 2017; Yi et al., 2016). The mediodorsal nucleus of thalamus (MDT), which is critical in olfactory learning (Kawagoe et al., 2007; Zelano, Mohanty, & Gottfried, 2011), is subject to extensive tauopathy in AD (H. Braak & Braak, 1991; Paskavitz, Lippa, Hamos, Pulaski-Salo, & Drachman, 1995).

The orbitofrontal cortex (OFC) critically processes olfactory information. A medio-lateral division represents odor-associated positive and negative valences, respectively (Gottfried, Deichmann, Winston, & Dolan, 2002). The rostral-caudal division differentiates higher order and lower order olfactory processing, respectively (Gottfried & Zald, 2005). Layer III and V of OFC is affected in AD by NFTs, but β-amyloidosis is relatively sparse (Gordon et al., 2018; Van Hoesen, Parvizi, & Chu, 2000).

Several studies have attempted to assess the predictive value of olfactory dysfunction tests in the prognosis of MCI and AD. These studies spanned 2-4 years and assessed to what degree olfactory deficit is associated with worsening of symptoms within this time span. Overall results suggest a strong positive correlation of the progression of the disease with olfactory deficit scores (Conti et al., 2013; Devanand et al., 2008; Lojkowska et al., 2011). Although 6% of early AD patients complain about olfactory deficits, 90% of them develop it at a later stage of the disease (Devanand et al., 2000). It is of paramount importance to pay attention to the early stage of olfactory deficit, its pathophysiology and prognostic value as clinical biomarker. It is easily overlooked but can serve as a reliable screening test.

1.5 Role of Locus Coeruleus in Alzheimer's disease

1.5.1 LC as the origin of tau-pathology in Alzheimer's disease

Alzheimer's disease is a progressive neurodegenerative disorder of the nervous system, primarily characterised by loss of memory. It is believed to have decades long prodromal stage before clinical symptoms surface. Hyperphosphorylated tau protein, that progressively converts to an insoluble stage and makes NFT, is an intracellular pathological hallmark of the disease. Another hallmark is the extracellular β-amyloid inclusions. Different schools of thoughts emphasize the causal and correlational roles of these hallmarks in the AD pathogenesis differently.

Tau is a microtubule-associated protein which is required for microtubule-assembly. Phosphorylation of tau protein at different amino acids is critical for its physiological function.

Hyperphosphorylation of tau is believed to be the start of the pathological form, which, in its initial stage, is soluble in nature. This is known as the pretangle stage. Progressive entanglement makes it insoluble at one point and finally creates intracellular NFTs, giving rise to the tangle stage.

Braak and colleagues conducted post-mortem immunohistochemical study in 2332 brains over a large range for age, 1-100 years. Gallyas silver method was used to identify argyrophilic NFTs and AT8 staining was used to identify abnormal hyperphosphorylation at serine 202 and threonine 205 residue. Their study helped characterize a comprehensive staging method for AD pathology and its progression as elaborated below (H. Braak, Thal, Ghebremedhin, & Del Tredici, 2011).

Pretangle stage a

Intraneuronal change was first observed in the brain-stem nuclei, most commonly in LC. The lesions were distal to the axon initial segment but within proximal part of the axons. Reportedly these lesions appeared without any precursor or intermediate form and was most common in the younger age groups.

Pretangle stage b

At this stage hyperphosphorylated tau spread to somatodendritic segments of the LC neurons. Smooth contour of the soma changed to spike-shaped protrusions along the boundary. More AT8+ material appeared in the distal segment of the axons.

Pretangle stage c

AT8+ material spread further, outside of LC, to non-thalamic cortical projecting nuclei (for eg. Raphe nucleus). Pretangle stages a-c are devoid of cortical involvement and mostly occurred in younger age groups.

Pretangle stages 1a and 1b

Besides the subcortical pathology, cortical features appear in stage 1a, starting at medial part of the temporal lobe in the transentorhinal region, likely confined to the axons projecting to this area. It is important to note that none of the lesions were devoid of subcortical counterpart.

In 1b, AT8+ material appeared in the somatodendritic compartment of the pyramidal cells in the cerebral cortex, mostly in the transentorhinal region and that too in the cortical projecting cells.

Neurofibrillary stages I-VI

Besides the AT8+ material, stage I had intraneuronal Gallyas+ lesions indicating NFT. They were mostly confined in transentorhinal region and were small in numbers. In stage II, additional lesions were observable in the entorhinal region proper and hippocampus. Stage III was characterised by additional intraneuronal material in the basal neocortical area of the temporal lobe. Stage IV displayed lesions in the basal frontal and insular cortices in addition to the aforementioned lesions

in previous stages. In stage V, higher order sensory association areas in the neocortex along with the prefrontal cortex were involved. Stage VI included further spread to first order sensory association areas, primary fields, premotor and primary motor areas. It is important to note that NF stages V-VI occurred at higher prevalence in elder age groups and also were most commonly associated with β-amyloid staining.

1.5.2 Noradrenergic deficit in Alzheimer's disease

1.5.2.1 Structural imaging

Although conventional MRI cannot distinguish LC, fast spin-echo T1 weighted imaging can do so due to the paramagnetic property of the neuromelanin which is present in the LC and also in other monoaminergic nuclei. Reduced signal from LC has been identified in MCI patients irrespective of their progression to AD (Takahashi et al., 2015).

1.5.2.2 Functional imaging

Analyzing functional connectivity from low frequency BOLD signal in resting state fMRI, positive and negative connectivity of LC to the rest of the brain can be delineated. Compared to healthy controls, AD patients are known to have a disruption spot at LC in functional connectivity study (Zhao, Rangaprakash, Venkataraman, Liang, & Deshpande, 2017). While the positive connectivity outlines area that may be activated by environmental stimuli, the negative connectivity partakes in the default mode network (DMN). LC plays an important role in reducing the DMN and facilitating

saliency and executive systems (Peterson & Li, 2018). Decreased DMN connectivity is indicative of disease severity in AD patients (Petrella, Sheldon, Prince, Calhoun, & Doraiswamy, 2011) and is considered a robust finding in this disease. Interestingly this applies in MCI (Badhwar et al., 2017) as well as in asymptomatic subjects in the risk groups (Quiroz et al., 2015). The salience network (SAN) is critical for multimodal integration of sensory, autonomic and visceral information for efficient decision-making and goal-directed behavior. SAN has critical importance in regulating DMN network too. Results showed that SAN hyperconnectivity exists in AD patients (Badhwar et al., 2017) and in risk groups (Goveas et al., 2013). Reduced resting state connectivity between LC and left parahippocampal gyrus is correlated with poor memory scores in MCI patients (Jacobs et al., 2015).

1.5.2.3 Biochemical tests

High performance liquid chromatography of cerebrospinal fluid samples from AD patients had lower level of NE (Martignoni et al., 1992)But other studies had antemortem assessment of NE metabolite 3-methoxy-4-hydroxyphenylglycol (MHPG) from the brain sample collected during diagnostic craniotomy. MHPG:NE ratio was found high in AD patients indicating increased NE turnover (Palmer 1987). Increased NE in CSF has been correlated with cognitive dysfunction in AD (Tohgi, Ueno, Abe, Takahashi, & Nozaki, 1992).

1.5.2.4 Genetic changes

Population specific polymorphism of dopamine β hydroxylase (DβH) gene could act as a risk factor for AD (Combarros et al., 2010; Komatsu et al., 2014). Interaction of amyloid precursor protein (APP) with sorting-related receptor with A repeat (SorLA) is prevented by α_{2A}-AR signaling and thereby promotes amyloidogenesis. Reduced SorLA in AD patients (Scherzer et al., 2004) and polymorphism in SorLA gene associated with AD (Pottier et al., 2012) indicates a potential noradrenergic dysfunction contributing to AD pathology. This is further supported by the finding that α_{2A}-AR is upregulated in AD and in its risk factor containing population (Gannon et al., 2015). Polymorphism of β_2-AR is associated with AD onset and vulnerability and could be linked to cAMP signaling mediated increased APP production (Bullido et al., 2004; Yu et al., 2008).

1.5.2.5 Postmortem findings

Loss of noradrenergic neurons from LC is a robust finding in Alzheimer's disease (Förstl, Levy, Burns, Luthert, & Cairns, 1994; Iversen et al., 1983; Mann, Lincoln, Yates, Stamp, & Toper, 1980; Matthews et al., 2002; Zarow, Lyness, Mortimer, & Chui, 2003). Unbiased stereology from postmortem human brains shows that LC volume decreases by approximately 8% with every stage of progression in Braak's staging method described above (Theofilas et al., 2017). Another postmortem study of AD brains with NET-specific radioligand showed a reduction in the LC and in the thalamus. This also correlated with the progression of the disease pathology in Braak staging (Gulyás et al., 2010). In parallel, other studies have identified significant decrease in NET binding sites in AD brains (Gulyás et al., 2010; Tejani-Butt, Yang, & Zaffar, 1993).

Despite neuronal loss from LC, some studies reported sprouting of axons and dendrites of remaining neurons, as measured by presynaptic α_2-ARs. Interestingly, postsynaptic α_1-AR had a trend of overexpression in prefrontal cortex (PFC) layers I/II despite a reduction of α_{1A}-AR mRNA. On the other hand, postsynaptic α_{2C}-AR mRNA was reduced specifically in layer II of the PFC. Moreover, α_{1D}-AR and α_{2C}-AR mRNA were decreased in the hippocampus of dementia patients while α_{1A}-AR and α_{2A}-AR mRNA were unchanged (Szot et al., 2006, 2007). Earlier studies identified reduction in α_1-AR density in PFC (R. N. Kalaria, 1989) and hippocampus (Shimohama, Taniguchi, Fujiwara, & Kameyama, 1986). While β_1-AR density is similar between AD and controls (Lemmer, Langer, Ohm, & Bohl, 1993), increase in the PFC β_2-AR of AD patients have been reported (R. Kalaria et al., 1989).

Utilizing HPLC (Matthews et al., 2002; Nazarali & Reynolds, 1992) and fluorescence based detection methods (Reinikainen et al., 1988), studies have shown that NE level decreases across the brain correlating with the degree of cognitive dysfunction (Matthews et al., 2002). But high MHPG:NE ratio from post-mortem brain samples argue for compensatory increase in NE turnover and thereby increased metabolism (Hoogendijk et al., 1999).

1.5.2.6 Animal studies

Several animal studies have been conducted on specific rodent models of AD. Some of the frequently used models include Tg2576 mouse model (overexpresses a mutant form of amyloid

precursor protein APP), TgCRND8 mouse model (express human APP gene coupled with double mutations linked to Swedish and Indiana familial AD mutation), APP/PS1 transgenic mouse model (carries APP transgene with Swedish mutation and Presinilin1 mutation) and TgF344 rat model (carries human APP transgene with Swedish mutation and mutated Presinilin1).

In aged rats it has been shown that neophobia and impairment of spatial memory is related to noradrenergic neuromodulation in the cortex (Collier, Greene, Felten, Stevens, & Collier, 2004). Related studies have been conducted in transgenic rodent models of AD. Tg2676 mice have neurodegeneration in LC along with olfactory deficit (Guérin, Sacquet, Mandairon, Jourdan, & Didier, 2009). TgCRND8 mice show behavioral deficit and is correlated with low NE at the tissue level (Francis et al., 2012). APP/PS1 transgenic mice have profound LC degeneration which worsens odor discrimination and memory of an odor (Rey et al., 2012). Noradrenergic innervation is critical for β amyloid clearing as evident from different studies in transgenic models (Klann et al., 2004; Pugh et al., 2007; Rey et al., 2012). NE precursor treatment has shown improved learning in the Morris water maze in such a model (Kalinin et al., 2007). NE can possibly act on microglial ARs to promote β-amyloid clearing (Hammerschmidt et al., 2013; Heneka et al., 2010). APP/PS1 transgenic mice shows improved cognitive function upon administration of α_2 receptor antagonists idazoxan or fluparoxan (Chen et al., 2014; Scullion, Kendall, Marsden, Sunter, & Pardon, 2011). Action of these drugs could be mediated through SorLA activity. TgF344-AD rat model that contains mutant APP and presenilin-1, has a noradrenergic deficit in hippocampal formation. Chemogenetic activation of LC by designer drugs in these rats ameliorates their cognitive deficit (Rorabaugh et al., 2017).

1.6 What is missing?

The following three chapters (2-4) address three different sets of questions, unanswered so far by the current literature.

1) Previous results suggest that NE promotes excitation in the neonatal piriform cortex through β-ARs within the critical period (Ghosh et al., 2015). This enhancement of excitation is largely presynaptic in nature. Does NE exert its effect postsynaptically as well? Long lasting type calcium channel (LTCC) mediated calcium influx is known to be critical for LTP (Moosmang et al., 2005). In neuronal tissue, β-AR mediated upregulation of LTCC is well explored as well (Hoogland & Saggau, 2004). These converge on a critical question – does β-AR modulate LTCC function in neonatal piriform cortex? If yes, does it determine the critical period of early odor preference learning? We explored these questions in chapter 2 through behavioral and slice electrophysiology experiments.

2) As mentioned before, LC neurons are known to spike in phasic and tonic modes with different physiological and behavioral implications. Although some research had been carried out in the past exploring different aspects of LC-modulated learning, role of LC spiking patterns in reward-based olfactory discrimination learning and olfactory associative valence learning has not been addressed systematically. NE in the piriform cortex is critical for pattern-separation dependent difficult discrimination learning of two similar odor pairs (Shakhawat et al., 2015). Do phasic and tonic spiking modes modulate this olfactory discrimination learning differentially? Also, do these two patterns of LC spiking carry different intrinsic valences? We addressed these questions in chapter 3

through optogenetic modulation of rat behavior in different behavioral paradigms along with pharmacological intervention and quantitative immunohistochemistry.

3) Precise location of the first occurrence of AD pathology in the brain has been searched for several decades. Examining thousands of postmortem brains ranging ages 1-100 years, Braak and colleagues provided a framework of the disease staging and proposed that hyperphosphorylated tau protein, an intracellular pathological feature of AD, first appears in LC neurons. One criticism of this idea is that hyperphosphorylated tau can be associated with other disease processes. Also, it was impossible to speculate whether the young subjects with hyperphosphorylated tau in LC would develop AD in later life. In other words, does expression of hyperphophorylated tau protein in LC induce pathological changes and cognitive deficits similar to Alzheimer's disease? We addressed this question in a rat model, by delivering transgene through viral vector and thereby expressing psudophosphorylated (a proxy for hyperphosphorylated) tau in LC. This is elaborated in chapter 4.

2 Chapter 2: β-AR activation enhances L-type calcium channel currents in anterior piriform cortex pyramidal cells of neonatal mice: implication for odor learning

This chapter is a version of the article Ghosh et al., 2017, published in Learning & Memory. 2017 Mar 1;24(3):132-5; [doi:10.1101/lm.044818.116] http://learnmem.cshlp.org/content/24/3/132.full

2.1 Introduction

L-type calcium channels (LTCCs) are expressed in the heart (Hess, Lansman, Nilius, & Tsien, 1986) and brain (Hell et al., 1993). In neurons, LTCC-mediated calcium influx is critical for long-term potentiation (Grover & Teyler, 1990; Kapur, Yeckel, Gray, & Johnston, 1998; Moosmang et al., 2005; Weisskopf, Bauer, & LeDoux, 1999), the putative cellular mechanism for learning. Blockade of LTCC leads to deficits in different learning paradigms including passive avoidance learning (Lashgari, Motamedi, Asl, Shahidi, & Komaki, 2006), spatial memory (Moosmang et al., 2005), fear extinction (Davis & Bauer, 2012), and olfactory associative

learning (Jerome et al., 2012; Zhang et al., 2010). Upregulation of LTCC Cav1.2 subunit activity by β-AR signaling plays an important role in regulating Ca^{2+} influx into myocytes (Reuter, 1983; Yue, Herzig, & Marban, 1990) and neurons (Gray & Johnston, 1987; Hoogland & Saggau, 2004; Kavalali, Hwang, & Plummer, 1997). However, few studies have looked at the functional role of β-AR modulation of LTCCs in learning.

Early odor preference learning is a type of classical conditioning in which a tactile stimulus mimicking maternal care (e.g., brush stroking) serves as the unconditioned stimulus (US), and a novel odor serves as the conditioned stimulus (CS). The pairing of the US and CS lead to an approach response to the CS odor, lasting hours to days depending on the training paradigms (Yuan et al., 2014). Tactile stimulation triggers norepinephrine release onto the olfactory bulb and anterior piriform cortex (aPC) and activates the cAMP/PKA pathway via β-ARs (Ghosh et al., 2015; Grimes et al., 2012; McLean et al., 2005; Morrison et al., 2013). Early odor preference learning occurs in a sensitive post-natal period and terminates around post-natal day (PD) 10 (Sullivan et al., 2000) when a tactile stimulus no longer triggers sufficient norepinephrine release (Nakamura et al., 1987). NMDA receptors (NMDARs) and LTCCs activated upon exposure to an odor critically mediate calcium-dependent kinase activities (Jerome et al., 2012; Lethbridge, Hou, Harley, & Yuan, 2012; Morrison et al., 2013). The convergence of the US and CS pathways leads to CREB phosphorylation and CREB-dependent transcription critical for odor learning (McLean et al., 1999; Yuan et al., 2014). Here we investigated whether β-ARs directly modulate LTCCs in aPC pyramidal cells as seen in heart (Yue et al., 1990) and hippocampal neurons (Gray & Johnston, 1987; Hoogland & Saggau, 2004; Kavalali et al., 1997). We compared the proportions of the LTCC currents and β-AR modulations in pups

within and beyond the sensitive period. The interaction of β-ARs and LTCCs in early odor preference learning was studied with pharmacological manipulations in the aPC during training.

2.2 Methods

All experimental procedures were approved by the Animal Care Committee at Memorial University and adhered to Canadian Council on Animal Care guidelines. C57B1/6J mice (Charles River) were bred on site. Dams were maintained under a 12-h light-dark cycle with ad libitum food and water. Day of birth was considered PD0.

We used whole-cell patch clamp recording to study aPC pyramidal cell calcium currents. Mouse pups of either sex from P7 – 10 or P14 above (P14 – 20) age groups were anesthetized with isoflurane and decapitated. Brains were extracted quickly and put in ice cold high-sucrose solution containing (in mM): 83 NaCl, 2.5 KCl, 3.3 $MgSO_4$, 1 NaH_2PO_4, 26.2 $NaHCO_3$, 22 glucose, 72 sucrose, 0.5 $CaCl_2$, bubbled with 95% O_2 and 5% CO_2. Para-sagittal slices of 300 µm thickness were cut in Leica vibratome (VT 1000P) and incubated in sucrose solution at 35◦C for 30 min and then left at room temperature. Slices were transferred to a recording chamber perfused with warm (30◦C–32◦C) Barium artificial CSF (aCSF) containing (in mM): 110 NaCl, 2.5 KCl, 1.3 $MgCl_2$, 1 NaH_2PO_4, 26.2 $NaHCO_3$, 22 glucose, 2.5 $BaCl_2$, tetrodotoxin (0.5 *m*M; Tocris) with a flow rate of 2– 3 mL/min. Slices were viewed with Olympus BX51WI upright microscope in differential interference contrast. Whole-cell Ca^{2+} currents were recorded selectively from layer II pyramidal neurons with 3– 6 MΩ glass

micropipette pulled in a Flaming/Brown puller (P-97, Stutter Instrument Co.). To distinguish from semilunar cells, pyramidal cells were selected by somatic morphology under differential interference contrast (DIC; oval shaped vs. semilunar shaped), depth in the layer II (deeper vs. superficial) (Suzuki & Bekkers, 2006). In a previous report (Ghosh et al., 2015), we used the same criterion of cell selection and posthoc biocytin reconstruction demonstrated that the majority of cells recorded were pyramidal cells. Intrapipette solution contained (in mM): 130 D-gluconic acid, 130 CsOH, 5 NaCl, 10 HEPES, 12 phosphocreatine, 3 MgATP, 0.2 NaGTP, and 0.2 EGTA. Cells included in the data set had an initial access resistance < 20 MΩ with < 25% change throughout the duration of recording.

Cells were held at -70 mV in voltage-clamp mode, and depolarizing currents were injected into the cell through a recording pipette for 150 msec during each step. Steps ranged from -60 to 10 mV with 5 mV increase in each step. It is been reported that nifedipine-sensitive LTCCs in the piriform cortex demonstrates slow kinetics and half activation at 0 mV (Magistretti, Brevi, & De Curtis, 1999). Ca^{2+} current was measured during the 0 mV step at its steady state at 146 msec. Control traces were recorded 10 min after establishing the whole-cell configuration. Drugs (LTCC antagonist nifedipine, 10 *m*M; *β*-AR agonist isoproterenol, 10 *m*M; PKA inhibitor H89, 10 *m*M; Sigma) were added to the aCSF for 10 min and then washed with aCSF for 30 min. Cadmium chloride (100 *m*M, Sigma) was added to the bath at the end of the experiments. Leak subtraction was done by subtracting cadmium traces from corresponding control, drug, and wash traces as shown in example traces. Multiclamp 700B amplifier and pClamp10 software was used for data acquisition. Signals were filtered at 2 kHz and digitized at 10 kHz sampling frequency. Clampfit 10.6 was used for data analysis.

Behavioral study was done at 27°C with previously established protocols (Ghosh et al., 2015; Morrison et al., 2013). Briefly, intracranial infusion surgery and odor training were carried out on P7 pups. Pups were anesthetized via hypothermia (under ice) and placed in a stereotaxic apparatus. After an incision of the skin, two small holes were drilled. Of note, 0.5 µL of drug (isoproterenol 500 µM, dissolved in saline; nifedipine 100 µM dissolved in 1% ethanol + saline; isoproterenol + nifedipine; isoproterenol + H89 100 µM dissolved in saline; isoproterenol + APV 100 µM dissolved in saline) or vehicle (1% ethanol + saline) was infused bilaterally in specific coordinates for aPC (1.8 mm anterior and 2 mm bilateral, 3.5 mm ventral with respect to the bregma) at the rate of 0.25 µL/min through cannulas attached to the infusion tubing. The infusion tubing was attached to a Hamilton syringe driven by a precision pump (Fusion 400, Chemyx Inc.). One minute after infusion, cannulas were gently withdrawn, skin was sutured, and pups were left for 30 min on warm bedding for recovery before odor training.

Pups were placed on peppermint-scented bedding (0.3 mL peppermint extract in 500 mL bedding) for 10 min and were returned to the dam afterward. Twenty-four hours after the training, pups were placed in a two-choice testing apparatus consisting of a stainless steel box (30 × 20 × 18 cm) with mesh bottom kept over two training boxes—one with peppermint-scented bedding and the other with non-scented normal bedding. Time spent over either side was recorded in five 1-min trials with 1 min rest in between trials. Time spent over peppermint bedding was measured as percentage of total trial time. The aPC location was verified with methylene blue (2%) in the pilot experiments (n = 6), and infusion tracks were checked in pups following testing.

2.3 Results

Figure 2.1 A and B shows the whole-cell calcium currents and nifedipine-sensitive LTCCs in two age groups (P7 – 10 vs. >P14). Whole-cell Ca^{2+} currents were reduced in the presence of nifedipine, suggesting an LTCC-mediated component. The LTCC component was significantly bigger in P7 – 10 pups (49.5%± 4.09% of the control, n = 11, example current traces in one animal are shown in *upper* panel and the $I – V$ curve is shown in the *lower* panel) than in P14 above pups (27.2%± 6.05%, n= 8, t = 3.18, P = 0.006; the comparison of the two age groups is shown in C). The larger portion of the LTCC current in P7–10 pups correlates with a highly plastic period in which LTCC-dependent early odor preference learning occurs (Jerome et al., 2012; Mukherjee & Yuan, 2016a).

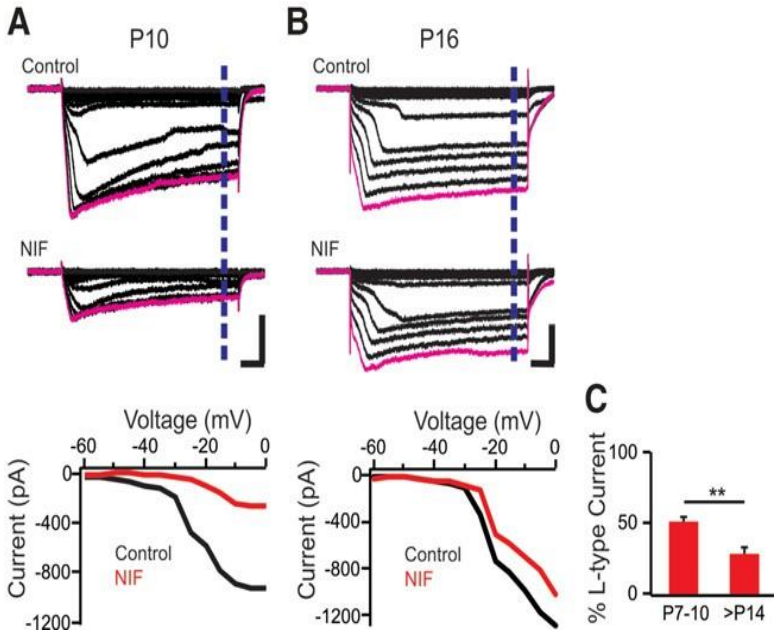

Figure 2.1 **L-type calcium currents (LTCCs) in mouse pups of P7 – 11 and P14 above**.

(A) Example traces of whole-cell currents in a P10 mouse pup under control condition and during nifedipine (NIF) application (upper panel) and I – V relationship (lower panel). (B) Example traces of whole-cell currents in a P16 mouse pup under control condition and during nifedipine (NIF) application (upper panel) and I – V relationship (lower panel). Scale bars: 25 msec and 500 pA. Dotted lines indicate the time point for calcium current measurement. (C) Percentage of LTCC currents in P7 – 11 and P14 above mice. (∗) $P < 0.05$.

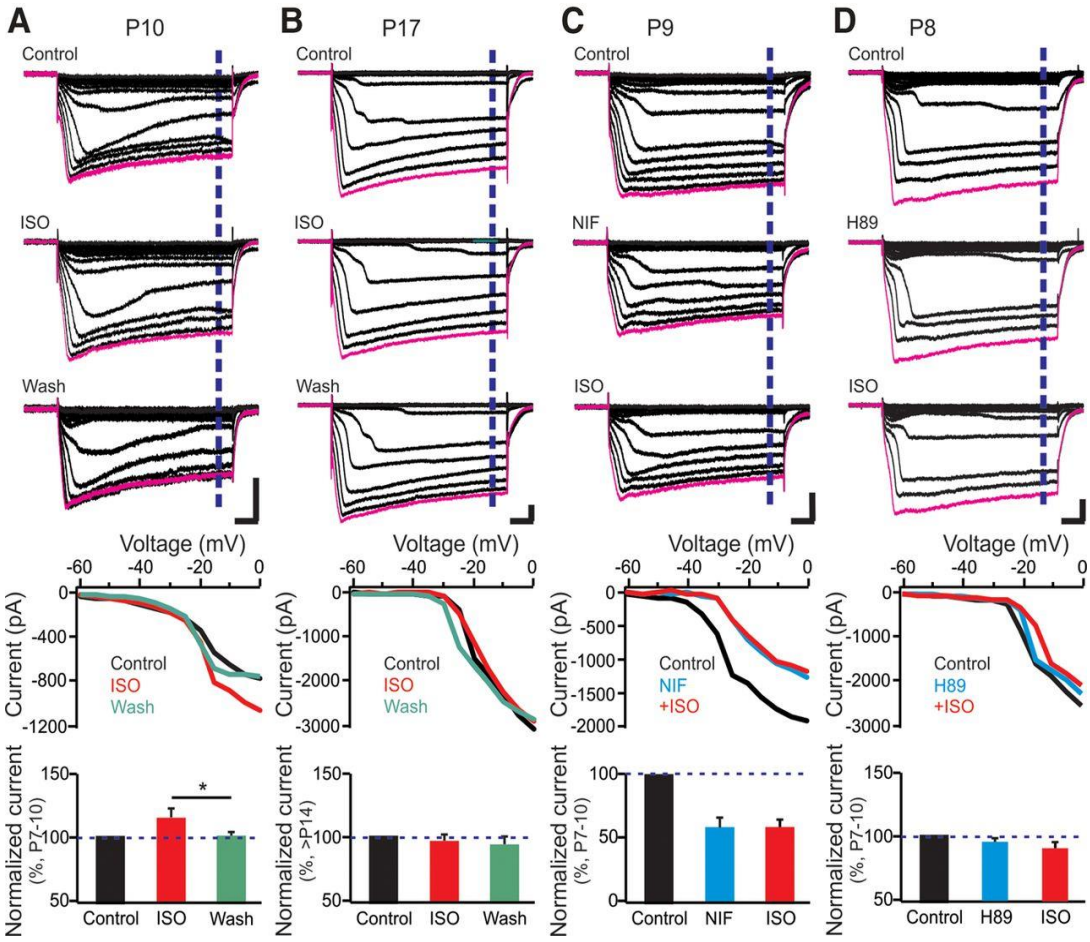

Figure 2.2 **Effects of b-adrenoceptor activation on whole-cell Ca2+ currents.**

(A) Example traces of whole-cell currents in a P10 mouse pup under control condition, during isoproterenol (ISO) application and wash (upper panel), I – V relationship (middle panel), and normalized current plots (lower panel). (B) Example traces of whole-cell currents in a P17 mouse under control condition, during isoproterenol (ISO) application and wash (upper panel), I – V relationship (middle panel), and normalized current plots (lower panel). (C) Example traces of whole-cell currents in a P9 mouse pup under control condition during nifedipine (NIF) and NIF ISO applications (upper panel), I – V relationship (middle panel), and normalized current plots (lower panel). (D) Example traces of whole-cell currents in a P8 mouse pup under control condition during nifedipine (NIF) and NIF+ISO applications (upper panel), I – V relationship (middle panel), and normalized current plots (lower panel).

(∗)P<0.05. Scale bars: 25 msec and 500 pA.

Figure 2.2 A and B demonstrated effects of isoproterenol on the whole-cell calcium currents in the two age groups. β-AR activation by isoproterenol moderately increased whole-cell Ca^{2+} current in P7–10 mice (115% ± 7% normalized to the control, compared with the wash 101% ± 3%, $n = 8$, $t = 2.51$, $P = 0.04$, paired *t*-test; *Figure 2.2*A). However, isoproterenol was ineffective in older pups (96% ± 5% normalized to the control, compared with the wash 94% ± 6%, $n = 7$, $t = 0.44$, $P = 0.68$, paired *t*-test; *Figure 2.2*B). In subsequent experiments, we tested whether isoproterenol enhanced LTCCs in the younger age group. Nifedipine application prior to isoproterenol abolished the effect of isoproterenol on whole-cell Ca^{2+} currents in P7–10 pups (normalized to control, nifedipine: 52% ± 6%, nifedipine + isoproterenol: 53% ± 4%, $n = 5$, $t = 0.23$, $P = 0.83$, paired *t*-test; *Figure 2.2*C). This result suggests that β-AR activation enhances LTCC-mediated currents in young pups during the sensitive period. Finally, isoproterenol enhancement of whole-cell Ca^{2+} current was also dependent on the cAMP/PKA activation. PKA inhibitor H89 preincubation prevented isoproterenol mediated increase in Ca^{2+} currents (normalized to the control: 96% ± 3% in H89, 91% ± 5% in isoproterenol, $n = 5$, $t = 1.34$, $P = 0.25$, paired *t*-test; *Figure 2.2*D).

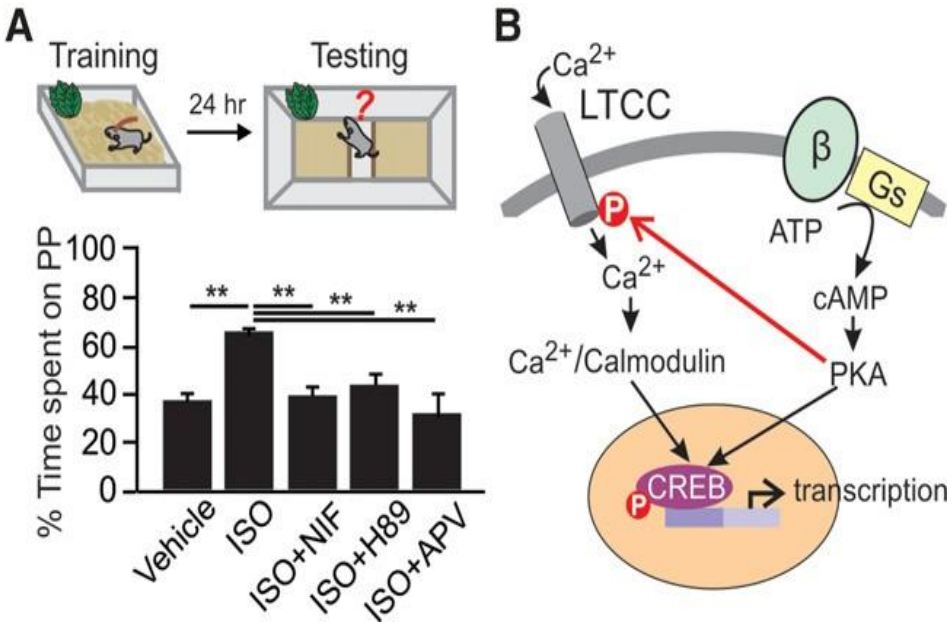

Figure 2.3 **The interaction of β-adrenoceptors and LTCCs in early odor preference learning in mice**.

(A) Percentage of time spent over peppermint-scented bedding in vehicle, ISO or NIF ISO infused groups. (∗∗) $P < 0.01$. (B) A proposed model for β-adrenoceptor interaction with LTCCs in anterior piriform cortex of pyramidal neurons. b-adrenoceptor activation serves as unconditioned stimulus to activate cAMP/PKA pathway. PKA translocates to the nucleus to phosphorylate CREB, and phosphorylate LTCCs in the membrane to enhance LTCC-mediated calcium signaling, which converges with cAMP/PKA pathway on CREB phosphorylation.

We then investigated interaction of the β-ARs and LTCCs in learning during the sensitive period. Previous research has shown that aPC ARs are critical for early odor preference learning in rodents (Ghosh et al., 2015; Morrison et al., 2013). Blocking β-ARs with propranolol systemic injection prevented odor preference learning in mice induced by pairing peppermint odor with stroking (Ghosh et al., 2015). In Figure 2.3, we show different behavioral outputs (percentage of time spent over peppermint-scented bedding during the testing) in pups with aPC drug or vehicle infusions. Training and testing schematic is shown in the upper panel of Figure 2.3A. Direct activation of β-ARs in the aPC induced odor preference learning when paired with odor alone. One-way ANOVA demonstrated significant group effects ($F_{(4,22)} = 11.82$, $P < 0.01$, Figure 2.3A). Post hoc Fisher Test showed that the isoproterenol-infused group spent significantly more time in peppermint (65.6% ± 1%, $n = 6$) compared with the saline infused group (37.2% ± 2.6%, $n = 6$, $t = 5.50$, $P < 0.01$). The isoproterenol effect was reversed by co-infusion of H89 (43.9% ± 2.6%, $n = 6$, $t = 4.21$, $P < 0.01$). Co-infusion of nifedipine prevented early odor preference learning (39.3 ± 3.21, $n = 5$, $t = 7.8$, $P < 0.01$). These results suggest that LTCC-mediated calcium signaling is critical. β-AR augmentation of the LTCC currents likely promotes LTCC-mediated plasticity and learning through cAMP/PKA signaling (proposed pathways and interactions shown in Figure 2.3B). β-AR-dependent LTCC activation at olfactory bulb synapses is also critical for odor associative learning (Jerome et al., 2012; Zhang et al., 2010). One caveat is that in vivo drug infusion affects more cell types than pyramidal cells in the aPC.

2.4 Discussion

Detailed characterizations of whole-cell calcium currents in the piriform cortex have revealed diverse kinetics of the calcium currents among pyramidal cells (Magistretti et al., 1999; Suzuki & Bekkers, 2006), similar to what we have observed in this study. These studies demonstrate various calcium channels in piriform cortex neurons including at least L-, N-, and T-type channels recorded at the soma. In this study, we focused on the nifedipine-sensitive LTCCs and its regulation by β-AR activations given their roles in odor learning. LTCCs contribute to ~50% of the total voltage-gated Ca^{2+} current in pyramidal cells in the hippocampus and visual cortex (Mintz, Adams, & Bean, 1992).Their roles in plasticity and learning are proposed to be bridging neuronal excitation to transcription of Ca^{2+}-regulated genes (Bading, Ginty, & Greenberg, 1993; Deisseroth, Heist, & Tsien, 1998; Dolmetsch, Pajvani, Fife, Spotts, & Greenberg, 2001; Impey et al., 1996). In the hippocampus, LTCCs mediate protein synthesis sensitive, NMDAR-independent late phase LTP and spatial learning (Grover & Teyler, 1990; Moosmang et al., 2005). However, in the aPC, we have shown that LTCC activation is dependent on NMDAR activation and both channels play critical but distinct roles in the early odor preference learning (Mukherjee & Yuan, 2016a). Here either D-APV or nifedipine blocked isoproterenol induced learning (Figure 2.3A), consistent with the learning requirement on both NMDARs and LTCCs. Between the two isotypes CaV1.2 and CaV1.3, CaV1.2 has been identified as a major player since CaV1.2 knock out (Moosmang et al., 2005) but not CaV1.3 knockout (Clark et al., 2003) mice have deficiency in synaptic plasticity or learning. CaV1.2 channels contain PKA binding site (Davare et al., 2001). PKA activation by cAMP enhances LTCC current in the hippocampus (Hoogland & Saggau, 2004; Kavalali et al., 1997), likely through phosphorylation of LTCCs. Our result showing PKA-dependent enhancement

of calcium currents by β-ARs in neonatal aPC is consistent with these reports.

An intriguing result from this study is the age-dependent changes of both LTCC component and β-AR modulation. LTCC component in the aPC pyramidal cell is larger (~50%) in the sensitive period mice (P7–10) compared with those beyond the sensitive period (~27%, P14–20). A reduced proportion of LTCC currents parallel age-dependent down-regulation of NMDARs (Franks & Isaacson, 2005) that has been attributed to reduced plasticity in older rats in the aPC (Poo & Isaacson, 2011). Altered AR expressions and functions with age can also contribute to changes in plasticity (Ghosh et al., 2015; Pandipati & Schoppa, 2012). For example, we have shown previously that β-AR activation enhances excitatory inputs and reduces inhibitory inputs in the aPC only in mice within the sensitive period (Ghosh et al., 2015). Here we provide further evidence for postsynaptic correlates of β-AR roles in synaptic plasticity and odor learning through LTCCs. The lack of modulation of LTCCs by β-ARs in older mice may relate to reduced expression of either LTCCs or β-ARs with age.

3 Chapter 3: Locus coeruleus activation patterns differentially modulate learning and valence in rats

This chapter is a version of the preprint manuscript Ghosh et al., 2020, currently in revision following peer review. A version of it is available in bioRxiv, https://www.biorxiv.org/content/10.1101/2020.04.17.047126v1.full

3.1 Introduction

Locus coeruleus (LC) adrenergic neurons fire in both phasic and tonic modes. However, differential behavioural modulation by these contrasting patterns has not been widely studied. Phasic and tonic LC patterns induce waking in mice arguing for similar arousal effects. In sensory coding, tonic patterns enhance thalamic feature selectivity and encoding in rats (Rodenkirch, Liu, Schriver, & Wang, 2019), while phasic LC activation accelerates spatial learning and promotes its consolidation in mice (Kempadoo et al., 2016; Takeuchi et al., 2016). Phasic, not tonic, LC activation enhances salience when phase-locked with sensory stimuli in mice (Vazey et al., 2018).

Here we compare phasic and tonic LC activation on difficult odor discrimination (DOD) learning using similar odor pairs in adult rats. Discrimination of similar odors requires norepinephrine (NE) in the piriform cortex (PC) (Shakhawat et al., 2015) and the olfactory bulb (Doucette, Milder, & Restrepo, 2007; Mandairon et al., 2008). Increased olfactory bulb NE lowers thresholds for odor discrimination (Escanilla et al., 2010) and is associated with higher signal to noise ratios (de Almeida, Reiner, Ennis, & Linster, 2015). Blockade of NE input retards DOD learning (Mandairon

et al., 2008; Shakhawat et al., 2015). In adult rats, a short burst of 40 Hz electrical stimulation of the LC sharpens odor representation in the PC (Bouret & Sara, 2002). It is not known, however, whether phasic and tonic LC activations differentially affect odor processing and odor discrimination learning.

We also compare the two patterns on valence. In mice, tonic patterns promote aversions and anxiety (McCall et al., 2015). A conditioned place aversion and increased anxiety-like behavior in rats has been demonstrated by chemogenetically increasing tonic firing of PFC-projecting LC neurons (Hirschberg, Li, Randall, Kremer, & Pickering, 2017) and BLA-projecting LC neurons (Llorca-Torralba et al., 2019). While phasic LC activation is regarded as learning-promoting, whether it, itself, carries valence is unclear. In neonatal rat odor preference learning, LC-NE activation serves as an unconditioned reward (Yuan et al., 2014). Phasic LC firing to tactile stimuli in neonates mediates preference learning. Tactile stimulation fails to activate LC after the early sensitive period and no longer induces odor preferences (Moriceau & Sullivan, 2004). Here we test the valence values of LC patterns in adult rats using real-time and conditioned odor preference tests. Our results reveal novel features of heterogeneity of release effects within LC projection sites in mediating differential behavioral outcomes induced by differing LC activation patterns.

3.2 Methods

3.2.1 Animals and Ethics Statement

TH-CRE homozygous male breeders (Sage laboratories, Boyertown, PA) were bred with Sprague-

Dawley (SD) female breeder rats (Charles River, Saint-Constant, Canada) for TH-CRE heterozygous offspring that were used in this study. Rats of both sexes were housed in 12 h light/dark cycle and had *ad libitum* access to food and water unless during food deprivation for experiments. During food deprivation, each rat was given 20 g of regular rat chow/day and was monitored for body-weight and health status on weekly basis. All experimental protocols followed the guidelines of Canadian Council of Animal Care and were approved by Memorial University animal care committee.

3.2.2 Viral Transduction

An adeno-associated virus (AAVdj or AAV8) served as a vector to carry the genetic construct of channelrhodopsin 2 (ChR2) with reporter gene for fluorescent proteins (EYFP or mCherry) under a double-floxed inverted open reading frame (DIO). Experimental constructs were AAVdj-EF1a-DIO-hChR2(H134R)-mCherry or AAV8-Ef1a-DIO-eChR2 (H134R)-EYFP. The control construct was AAVdj-EF1a-DIO-mCherry. All AAVs were provided by Deisseroth Laboratory at Stanford University.

3.2.3 Stereotaxic Surgery

Three to ten months old adult TH-Cre rats received bilateral virus infusions (5e12/ml) in the LC under isofluorane anesthesia in a stereotaxic frame. Each hemisphere received two infusions, each of 0.7 µl (fluorescent beads: virus = 2:5) at the rate of 0.5 µl/min. The cannula was lowered at a 20° angle to avoid the transverse sinus. Infusion coordinates were 11.8-12.2 mm posterior, 1.2 and 1.4 mm bilateral, and 6.3 mm ventral with respect to bregma. At a minimum one month after infusion

surgery, rats underwent optical fiber cannula (ferrule attached, containing optical fiber; Doric Lenses, Quebec, Canada) implantation surgeries (11.8-12.2 mm posterior, 1.3 mm bilateral, and 6.3 mm ventral with respect to bregma), followed by a minimum of two weeks of recovery period before commencing behavioural tests.

For experiments requiring drug infusion, metal infusion cannulas were implanted in the BLA (AP: 2.5 mm posterior, ML: 4.9mm bilateral, DV: 7.8 mm) (Carew et al., 2018), or PC (AP: 1.8-2.0 mm anterior, ML: 4 mm bilateral, DV: 7.3-7.4 mm) (A. M. Shakhawat et al., 2015), or VTA (AP: 5.3 mm posterior, ML: 1mm bilateral , DV: 8.1 mm) (Nunes et al., 2019; Rodriguez-Manzo & Canseco-Alba, 2017) combined with LC optical fiber cannula implantation.

For experiments requiring CTB infusions, surgeries were combined with LC optical fiber cannula implantation and were allowed 10 days recovery before carrying out experiments. CTB-594 and CTB-488 (1% w/v in phosphate buffer; Invitrogen, Waltham, MA) were infused by separate 32g bevelled 1µl Hamilton syringes (Neuros 7001 KH) attached to a vertical infusion pump (Pump 11 Elite; Harvard Apparatus, Saint-Laurent, Canada) (Dong, Li, & Kirouac, 2017; J. G. McCall et al., 2017) in NAc (200 nl; AP: 1 mm anterior, ML: 1 mm bilateral, DV: 6.5 mm) and CeA (150 nl; AP: 2.1 mm posterior, ML: 4.2 mm bilateral, DV: 7.5 mm) respectively. Each infusion lasted 5 min, followed by a 5-min wait before withdrawing the syringe.

3.2.4 Electrophysiology

In vivo electrophysiology

Rats underwent *in vivo* electrophysiology experiment one month post-infusion. Rats were anaesthetized with 15% urethane at 10 ml/kg of body weight and placed in a stereotaxic frame. The surgical procedure was carried out following appropriate sterilization. A hole was drilled in the skull (12.3 mm posterior, 1.3 mm left lateral to bregma) and an optrode, assembled just before the experiment (400 µm glass optical fiber; Thorlabs Inc, Newton, NJ), bundled with 200/280 µm tungsten electrode; FHC, Bowdoin, ME), was lowered down at 20° angle to 6.1-6.9 mm ventral to brain surface until LC neurons were identified by slow spontaneous spiking and burst response to toe pinch (audio-monitor and oscilloscope response) (Quinlan et al., 2018). A glass optical fiber was connected to a laser diode fiber light source (Doric Lenses, Quebec, Canada) by a mono-fiberoptic patch cord (0.48 NA, 400/430 µm). Blue light of 450 nm at a power of 90 mW for 400 µm core and 0.48 nA optical fiber was applied. Light pattern was controlled from a Doric software. Data were acquired and analyzed by SciWorks (DataWave/A-M Systems, Sequim, WA). Signal was detected at a lowest threshold of 1.5X amplitude of the background. Autosort protocol was used to isolate similar cellular waveforms and cluster them in a cell-specific manner. Only clusters with LC-spike characteristics were further analyzed.

Slice electrophysiology

Rats were anesthetized with isoflurane drops in a glass jar followed by decapitation. Brains were quickly removed and placed in ice-cold aCSF containing (in mM): NaCl 124, KCl 2.5, NaH2PO4 1.2, NaHCO3 24, HEPES 5, Glucose 12.5, MgSO4 2, CaCl2 2. Coronal slices (350 µm) of the brain stem containing LC were cut in a vibratome (Leica VT-1200) and incubated in aCSF

for 30 min at 32°C then left at room temperature. Recording was conducted in an open bath chamber continuously perfused with warm (30–32°C) aCSF at the rate of 2–3 mL/min. Slices were visualized with an Olympus BX51WI upright microscope, equipped with a cooled-CCD camera system (Andor Clara, T.I.L.L. Photonics).

Extracellular loose patch recordings were obtained with glass pipettes filled with aCSF (2–3 MΩ) and positioned at the cell body of LC neuron. Light excitations (488 nm and 589 nm) were provided by a Lambda XL light source (Sutter Instrument). Multiclamp 700B amplifier and pClamp10 software were used for data acquisition (filtered with 2 kHz low pass filter) and digitization (10 kHz sampling frequency).

3.2.5 Behavioural Tests

3.2.5.1 Light Stimulation for Behavioural Experiments

Two to four weeks after optical cannula implantation surgery, rats underwent behavioural tests. Bilateral photostimulation at 450 nm – 90 mW was carried out by two Laser light sources (LDFLS_450; Doric Lenses, Quebec, Canada) through mono-fiberoptic patch cords. Current equivalence of the power was 150 mA. A total of 4 different photo stimulation patterns were used in the behavioural tests, namely: 10-Hz long phasic (10 sec every 30 sec); 10-Hz brief phasic (300 msec every 2 sec); 10-Hz tonic; and 25-Hz tonic. For general behavioral effects, odor discrimination and valence learning, all patterns were explored (Fig. 3.2, 3.3, 3.5, except 25-Hz tonic was excluded in odor discrimination learning due to the freezing and reduced mobility induced by this pattern). For studying the role of VTA and PC dopamine in odor discrimination learning (Fig. 3.4), 10-Hz brief phasic and 10-Hz tonic patterns were used. For

the effect of BLA adrenergic blockade in odor valence learning (Fig. 3.6), 10-Hz long phasic and 25-Hz tonic light were used. For cFos activation in BLA (Fig. 3.7), the 10-Hz brief phasic was compared with 25-Hz tonic light. Different patterns of stimulation were controlled from Doric software. Behavioural sessions were video-recorded by ANY-Maze software (Stoelting, Wood Dale, IL) and analyzed offline. Subsets of experiments were analyzed by persons who were blind to the experimental conditions.

3.2.5.2 Drug Infusion

Drugs or vehicle were infused 30 min before behavioral testing through a 10 µl Hamilton syringe and infusion pump. Lidocaine (4%; Sigma, Oakville, Canada) was infused in the VTA (0.3 µl/ hemisphere over 3 min with an additional 1-min wait before withdrawing the syringe) (Nunes et al., 2019). For PC and BLA infusions, 1 µl of drug or vehicle was infused per hemisphere over 2 min followed by 1 min wait before withdrawing the syringe. D1/5 receptor antagonist SCH 23390 (3.47 mM, Sigma, Oakville, Canada), α-adrenoceptor antagonist phentolamine hydrochloride (10 mM; Sigma, Oakville, Canada) and β-adrenoceptor antagonist alprenolol hydrochloride (120 mM; Tocris Bioscience, Bristol, UK) (K. A. Kempadoo, E. V. Mosharov, S. J. Choi, D. Sulzer, & E. R. Kandel, 2016; A. M. Shakhawat et al., 2015) were used for PC and BLA infusions.

3.2.5.3 General Behavioural Experiments

3.2.5.3.1 Open Field Maze

Rats explored an opaque plexiglass box (60 cm x 60 cm x 40.5 cm) with a black bottom for a 10 min daily session for four consecutive days while receiving no stimulation on day 1, 10-Hz long phasic stimulation on day 2, 10-Hz tonic stimulation on day 3 and 25-Hz tonic stimulation on day 4. Distance travelled, time spent rearing (both free and supported), and time spent freezing were recorded and analyzed. Freezing was counted as no body movement except breathing.

3.2.5.3.2 Elevated Plus Maze

Following a 15-min photo-stimulation in the home cage, rats were placed in the center of an elevated plus maze (EPM; 50 cm x 10 cm each arm, 38 cm wall on the closed arms, 11 cm x 11 cm central platform, 52 cm high from the ground, inside painted black) facing the open arm opposite to the experimenter. Rats spent 5 min in the EPM while the stimulation continued. Time spent in closed and open arms was recorded.

3.2.5.4 Olfactory Behavioural Experiments

3.2.5.4.1 Odorants

Odors used in the experiments were listed in Table 3.1.

Table 3.1 List of Odorants

Name of the test	Odor 1 (O1; **associated with photostimulation*)	Odor 2 (O2)
Dissimilar odor discrimination	Almond extract	Coconut extract
Similar odor discrimination	Heptanol and Octanol (40:60 mixture; 0.001%)	Heptanol and octanol (50:50 mixture; 0.001%)
Valence test (10 Hz long phasic)	Vanilla (2%)	Peppermint (2%)
Valence test (10 Hz tonic)	Orange (2%)	Propanoic acid (0.033%)
Valence test (25 Hz tonic)	Benzaldehyde (0.05%)	Isoamyl acetate (0.05%)

The odor concentrations for similar odor discrimination and valence tests were chosen either based on previous publication (Shakhawat et al., 2015) or estimated vapor pressure of 1 Pascal (Devore, Lee, & Linster, 2013).

3.2.5.4.2 Odor Discrimination Learning

Rats were food deprived for 4-7 days before the onset of the experiments and food deprivation continued during the course of the experiment. Five days of habituation for context (box (60 cm x 60 cm x 40.5 cm), sponge and positive reinforcement (chocolate cereal)) were conducted first. Afterwards rats performed an odor discrimination task consisting of 10 trials/day, each trial being a

maximum of 3 min. Two sponges containing odor 1 (O1) and odor 2 (O2) respectively were presented randomly in two corners of the box. The O1 sponge had a 2 cm^2 hole at the top center, containing a retrievable chocolate cereal. To balance the smell of the chocolate cereal, a non-retrievable chocolate cereal was placed in a hidden hole in the O2 sponge. Between trials rats were confined to a "home corner" in the box with an L-shaped plexiglass barrier for 20 sec while sponge positions were changed. During trials rats were allowed to explore the box and sniff the sponges. Trials ended as soon as a nose poke was made inside the hole, irrespective of the odor identity. Response was considered correct if nose poke was in O1 sponge. Trials in which no nose-poke occurred within 3 min were excluded from analysis. Percentage of correct responses was counted as the number of correct responses over the number of total nose poke trials. Light stimulation was given only during trials, but not during intertrial intervals.

Dissimilar odor discrimination continued for a minimum of 7 days until rats reached two consecutive days of 80% success rate, followed by similar odor discrimination for 10 days.

3.2.5.4.3 Odor Valence Tests

For conditioned odor preference test (COPT), rats underwent a single 30 min session of habituation in a T-maze (long arm 183 cm x 19 cm, neutral arm 19 cm x 19 cm; 20.5 cm high wall) on day 1. On day 2, O1 and O2 sponges were placed in two opposing arms, with positions counter-balanced between morning and afternoon sessions. Time spent in the arms corresponding with O1 and O2 during a 10 min session was recorded. On day 3, rats were confined to the O1 arm for 10 min in the morning with light stimulation; and to the O2 arm in

the afternoon without light stimulation. The odors were switched in the arms on day 4 and the same conditioning as day 3 was repeated. Rats were trained for 1 trial or 3 trials (repeating procedures as in day 4-5 three times) and data were pooled. On the testing day, arm time was measured in morning and afternoon sessions with O1 and O2 sponges positioned in the exact same manner as day 2.

For real-time odor preference test (ROPT), a 122 cm-long arm was used. Day 1 habituation and day 2 baseline light response were conducted in the same manner as in COPT. On day 3, rats explored the maze freely for two 10 min sessions in the morning and afternoon. Light stimulation started upon rat entering the O1 arm and stopped upon rat leaving the O1 arm. Odor positions were switched between morning and afternoon sessions.

3.2.5.5 cFos and Npas4 Induction Experiments

For cFos induction in Fig. 4&6, rats were habituated to the experimental environment for two days. On the third and fourth days, rats were optically stimulated with either phasic or tonic patterns in their home cages, for 10 min/day, while being exposed to an odorized sponge (benzaldehyde 0.05%). Control rats were exposed to the odor only without light stimulation. Ninety min following the stimulation on the fourth day, rats were anesthetized, perfused, and brains were collected.

For Npas4 induction to validate light activation in Fig. 3.1, rats were habituated to the experimental environment for one day. Next day they were perfused 60 min following light stimulation in their home cage.

3.2.6 Immunohistochemistry and Histology

Rats underwent trans-cardiac perfusion with cold isotonic saline followed by 4% paraformaldehyde. Brains were extracted and kept in 4% paraformaldehyde. Brains were then sectioned using a vibratome (Leica VT 1000P; Leica Biosystems, Ontario, Canada) in 50 µm thick coronal slices and saved in a polyvinylpyrrolidone solution. For immunohistochemistry with Npas4 and DBH, slices were washed in PBS, and then incubated with primary antibodies.

Npas4 (1:500, Thermo Fisher Scientific, Waltham, MA) primary antibody mixed in phosphate buffer saline (PBS) with 2% normal goat serum and 0.2% Triton-X was applied for three nights at 4°C. Following a 3 x 10 min wash in PBS, a biotinylated anti-rabbit secondary antibody (1:1000; Vector laboratories, Burlingame, CA) was applied. After 2 hrs of secondary incubation and a 3 x 10 min wash, slices were incubated in an avidin-biotin complex for 1.5 hrs followed by a PBS wash. Slices were then placed in a solution containing 15 µl SG Grey chromogen (Vector laboratories, Burlingame, CA) with 24 µl peroxide per ml of PBS. After optimum color development, slices were washed in PBS, dried overnight, dehydrated in graded ethanol, and mounted with permount.

For DBH staining, after a primary antibody (1:500, EMD Millipore, Burlington, MA) incubation, slices were incubated with a fluorescence conjugated anti-mouse secondary antibody (1:1000; Invitrogen/Thermo Fisher Scientific, Waltham, MA) at room temperature for 2 hrs, followed by cover-slipping with Vectashield® antifade mounting medium (Vector laboratories, Burlingame, CA).

For cFos and TH co-labeling, 50 µm free floating sections from phasic and tonic stimulated rats, belonging to similar positions in antero-posterior axis of the brain as determined by unaided visual observation, were chosen in an unbiased manner. The sections were washed in Tris buffer (0.1M, pH 7.6) twice for 10 min each, followed by 10 min in Tris A (0.1%TritonX in Tris buffer) and Tris B (0.1% TritonX and 0.005% BSA in Tris buffer) before applying a blocking solution of 10% normal goat serum (Sigma-Aldrich, Oakville, Canada) for 1 hour. This was followed by a 10 min wash each in Tris A and Tris B before incubating in 1:2000 primary antibody solution prepared in Tris B at 4°C (TH, EMD Millipore, Burlington, MA; cFos, Cell Signaling, Danvers, MA). After two nights, sections were washed for 10 min each in Tris A and Tris B and incubated in a 1:1000 secondary antibody solution prepared in Tris B at 4°C (anti-rabbit Alexa 647, anti-mouse Alexa 488; Invitrogen/Thermo Fisher Scientific, Waltham, MA). This was followed by 10 min washes in Tris A, Tris D (0.1%Triton X and 0.005% BSA in 0.5M Tris buffer), and Tris buffer respectively. Finally, sections were mounted with antifade mounting medium.

Nissl staining was done by rehydrating the slides in graded ethanol, incubating in 0.5% cresyl violet for 8 min, washing in distilled water for 1 min and then dehydrating in graded ethanol. After a 5-min xylene step, slides were coverslipped with permount.

Image Acquisition and Analysis

Images were acquired by a Zeiss microscope (Toronto, Canada), an EVOS 5000 (Thermo Fisher Scientific, Waltham, MA) and a BX-51 (Olympus, Richmond Hill, Canada) for fluorescent and bright-field images. Images were acquired similarly for phasic and tonic

stimulated rats, keeping gain and exposure time the same throughout each experiment. Images were analyzed using ImageJ software. Images underwent background subtraction before manual cell counting. For LC activation success, the number of $Npas4^{+}$ cells was counted. For BLA and VTA activation, $cFos^{+}$ cells and double-labeled CTB cells were counted. Three to six images per animal were analyzed and values from both hemispheres were averaged. A subset of the images was analyzed blindly.

3.2.7 Statistical Analysis

One-way repeated ANOVAs were used in Fig. 3.1C to compare the frequency changes pre-, during-, and post-light stimulation, followed by *post-hoc* Tukey tests. Two group comparison in Fig. 3.1F was subjected to Student's t-tests (unpaired, two-tailed). Two-way mixed ANOVAs were used to compare the effects of different patterns of light on general behavior in Fig. 3.2A-C, followed by *post-hoc* Tukey tests. T-tests (unpaired, two-tailed) was used in Fig. 3.2D-E for closed arm and open arm times separately. Two-way mixed ANOVAs followed by linear trend analyses were used to determine statistical significance for the odor discrimination experiments, followed by *post-hoc* tests between the control and ChR2 groups in Fig. 3.3 and Fig. 3.4B&4C. One-way ANOVA followed by *post-hoc* Tukey tests were used in Fig. 3.4F-H. Two-way repeated ANOVAs were used to compare the two odor valences in ROPT and COPT in Fig. 3.5 and Fig. 3.6, followed by *post-hoc* Tukey tests. One-way ANOVA followed by *post-hoc* Tukey tests were used in in Fig. 3.7. Data are presented as Mean ± S.E.M in the graphs.

3.3 Results

3.3.1 Validation of light activation of locus coeruleus neurons

Three weeks following LC AAV infusion (for targeting see supplementary figure 1), we observed ChR2 uptake marked by the fluorescence reporter EYFP (Figure 3.1A) or mCherry. The transfection rate determined by the overlapping of ChR2 and dopamine β-hydroxylase (DBH) expressing cells was 73.7 ± 12.8% (n = 8). We conducted *in vivo* optrode LC recordings. Figure 3.1B1-2 shows an LC neuron activated by a 10-sec, 10-Hz light train (30-msec pulses, laser intensity 150 mA). Figure 3.1C1-C3 shows LC activation by 10-Hz trains with two light intensities and pulse widths. LC firing frequency changes were significantly induced by 10-sec, 10-Hz light at 30-msec duration, 150 mA ($F_{2,10} = 8.69$, $p = 0.006$, One-way repeated ANOVA; pre vs. during and during vs. post p=0.02 and p=0.007, respectively; Figure 3.1C1), or 10 Hz at 50-msec duration, 150 mA ($F_{2,10} = 25.42$, $p < 0.001$; pre vs. during and during vs. post p=0.0008 and p=0.0001, respectively; Figure 3.1C2), but not at 30-msec duration, 100 mA ($F_{2,6} = 2.48$, $p = 0.16$; Figure 3.1C3). The 30-msec, 150-mA light that effectively drove LC firing was used subsequently in recording (Figure 3.1D) and behavioural experiments. Increasing light frequency elevated LC firing in ~linear fashion in the frequency range <30 Hz (Fig. 3.1D), with a firing output up to 15 Hz. While average LC firing rates with 5- and 10-Hz light approximate activation rates, we found LC neurons were not individually driven at those rates *in vivo*. Similar outcomes were observed in mouse *in vivo* where average LC firing with light activation was made up of LC neuron responses of widely varying frequencies (McCall et al., 2015). *In vitro* cell-attached recording shows that responses follow 10 and 20 Hz blue light activation (Supplementary Fig. 2). The immediate early gene Npas4 revealed light-induced expression in LC ($t = 4.53$, $p < 0.001$; Figure 3.1E&F).

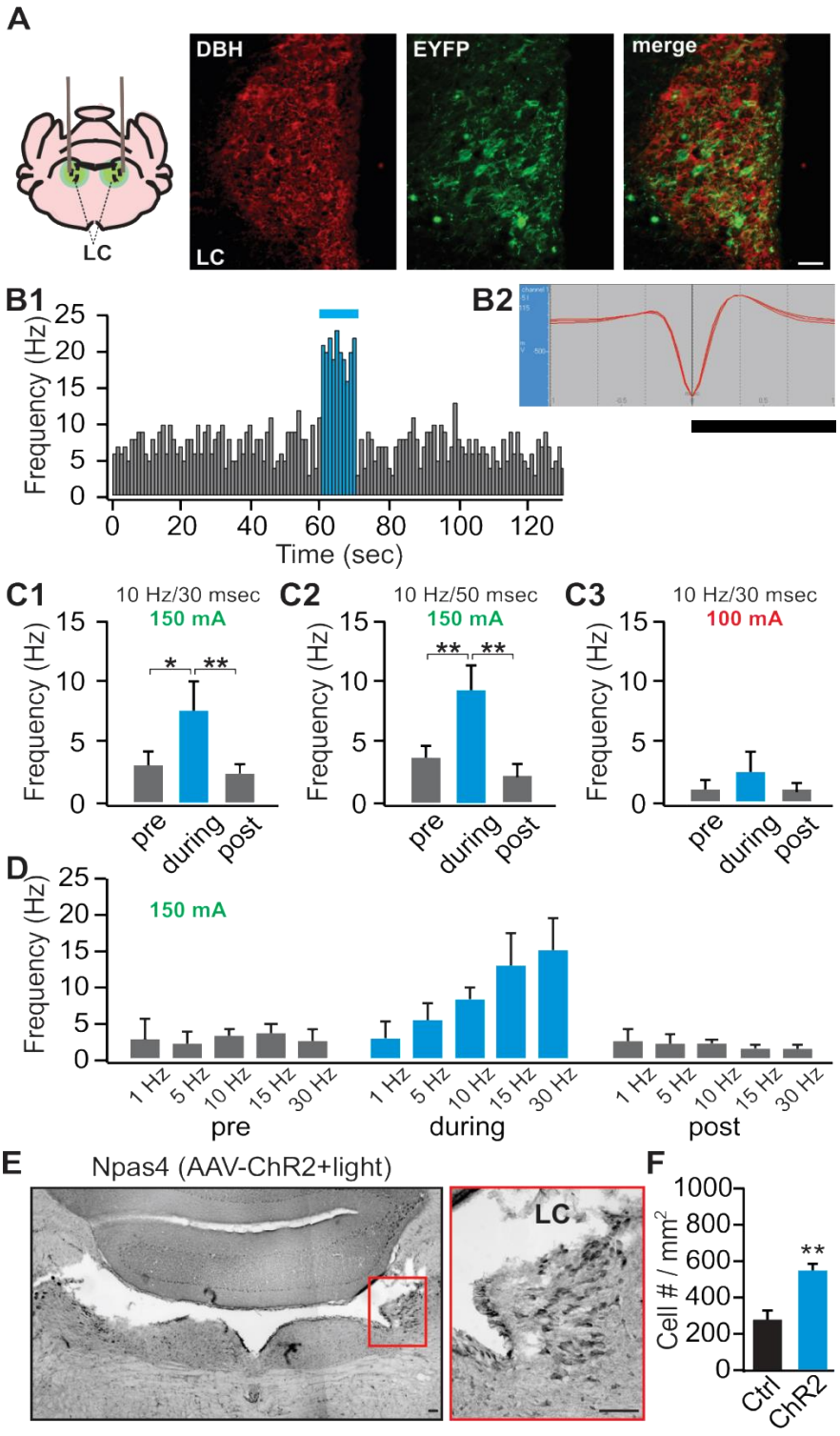
A
DBH
EYFP
merge
LC
LC
B1
B2
Frequency (Hz)
Time (sec)
C1
10 Hz/30 msec
150 mA
C2
10 Hz/50 msec
150 mA
C3
10 Hz/30 msec
100 mA
pre
during
post
D
150 mA
1 Hz
5 Hz
10 Hz
15 Hz
30 Hz
E
Npas4 (AAV-ChR2+light)
LC
F
Cell # / mm2
Ctrl
ChR2

Figure 3.1 **Validation of the light activation of the locus coeruleus (LC) neurons**

A. Co-localization of DBH (red) and EYFP (green) in the LC of a TH-CRE rat infused with an AAV8-Ef1a-DIO-eChR2(H134R)-EYFP. **B1.** An example of an *in vivo* recording from the LC, showing increased firing of a LC neuron to a 10-Hz, 10-sec light (30-msec duration, 150-mA intensity). **B2.** The waveform of the recorded cell. Scale bar 1msec. **C1-C3.** LC firing frequency changes induced by 10-sec, 10-Hz light at 30-msec duration, 150 mA (n = 6, **C1**), at 50-msec duration, 150 mA (n = 6, **C2**), or at 30-msec duration, 100 mA (n = 4, **C3**). **D.** LC responses to light activation with a range of frequencies at 150-mA intensity (n (1/5/10/15/30 Hz) = 2/3/12/6/6). **E.** An example of Npas4 staining of the LC following light stimulation. Right panel is the zoom in of the red square on the left panel. Scale bars, 50 μm. **F.** $Npas4^{+}$ cell counts in the control (n = 6) *vs.* ChR2 rats (n = 7). *$p < 0.05$; **$p < 0.01$.

3.3.2 Different patterns of LC activation show distinct general behavioural effects

First we investigated whether phasic and tonic LC activations have differential effects on locomotion, exploratory behavior and stress. We included four patterns including two phasic patterns: 10-Hz long phasic (10 sec every 30 sec), and 10 Hz brief phasic (300 msec every 2 sec). These patterns are consistent with recent studies in terms of frequency range and duration (Carter et al., 2010; Kempadoo et al., 2016; Vazey, Moorman, & Aston-Jones, 2018). The 10 Hz brief phasic pattern mimics physiological LC firing in response to environmental stimuli (Aston-Jones & Bloom, 1981; Nakamura, Kimura, & Sakaguchi, 1987). The two tonic patterns are 10-Hz tonic and 25-Hz tonic, corresponding to the LC output in the range of 10-15 Hz in our *in vivo* recording (Figure 3.1D).

The effects of these LC activation patterns on open field distance travelled, duration of rearing, and freezing were tested (Figure 3.2A-C). In the open field experiments, rats underwent a series of 10 min long tests in a fixed order: baseline without light activation, 10-Hz long phasic, 10-Hz tonic and 25-Hz tonic. Data generated by different light patterns were normalized to the same baseline parameters for comparisons. A subset of rats underwent baseline measurements followed by 10-Hz brief phasic light activation. Ten Hz phasic and tonic stimulated rats showed increased rearing while 25 Hz rats showed less mobility and increased freezing.

For distance traveled, the baseline in the ChR2 (24.70 ± 3.10 meters) and control groups (19.71 ± 4.30 meters) are similar ($t = 0.916$, $p = 0.376$). There is a significant effect of Light Pattern X

Group interaction ($F_{2, 24}$ = 8.831, p = 0.001; Figure 3.2A). The ChR2 group showed a reduction in distance traveled with 25-Hz light compared to the control group (t = 4.02, p = 0.002). For duration of rearing with various light patterns, there was a significant effect of Light Pattern X Group interaction ($F_{2, 24}$ = 13.617, p < 0.001). The ChR2 group showed increased rearing (Figure 3.2B) with the 10-Hz long phasic light compared to the control group (t = 6.449, p < 0.001), and the 10-Hz tonic light (t = 3.015, p = 0.043). Significant effects were also observed between the 10-Hz long phasic and 25-Hz tonic light (t = 7.908, p < 0.001), and between the 10-Hz tonic and 25-Hz tonic light (t = 4.847, p = 0.006) in the ChR2 groups. For the amount of freezing with various light patterns, there was a significant effect of Light Pattern X Group interaction ($F_{2, 22}$ = 15.759, p < 0.001; Figure 3.2C). The ChR2 group with 25-Hz tonic light showed increased freezing compared to the control group (t = 7.903, p < 0.001). Significant effects of light patterns were also observed in the ChR2 group, between the 25-Hz tonic and 10-Hz long phasic (t = 8.002, p < 0.001), and between the 25-Hz tonic and 10-Hz tonic (t = 6.749, p = 0.001) light activation. A separate test of the 10-Hz brief phasic light with a corresponding light control group showed increased duration of rearing (t = 2.232, p = 0.038; Supplementary Fig. 3), similar to that of the 10-Hz long phasic light.

Anxiety during tonic and phasic 10-Hz light patterns was measured in an elevated plus maze (EPM, Figure 3.2D & E), and no differences were observed in the light-activated and control groups. For 10 Hz tonic, there was no difference between the ChR2 and the control group in time spent in either the closed arms (t = 1.383; p = 0.188) or the open arms (t = 0.101, p = 0.921; Figure 3.2D). Similarly, neither the time spent in the closed arms (t = 1.439; p = 0.181), nor in the open arms (t = 0.838, p = 0.421), was significantly different between ChR2 and control groups with 10 Hz phasic light activation (Figure 3.2E).

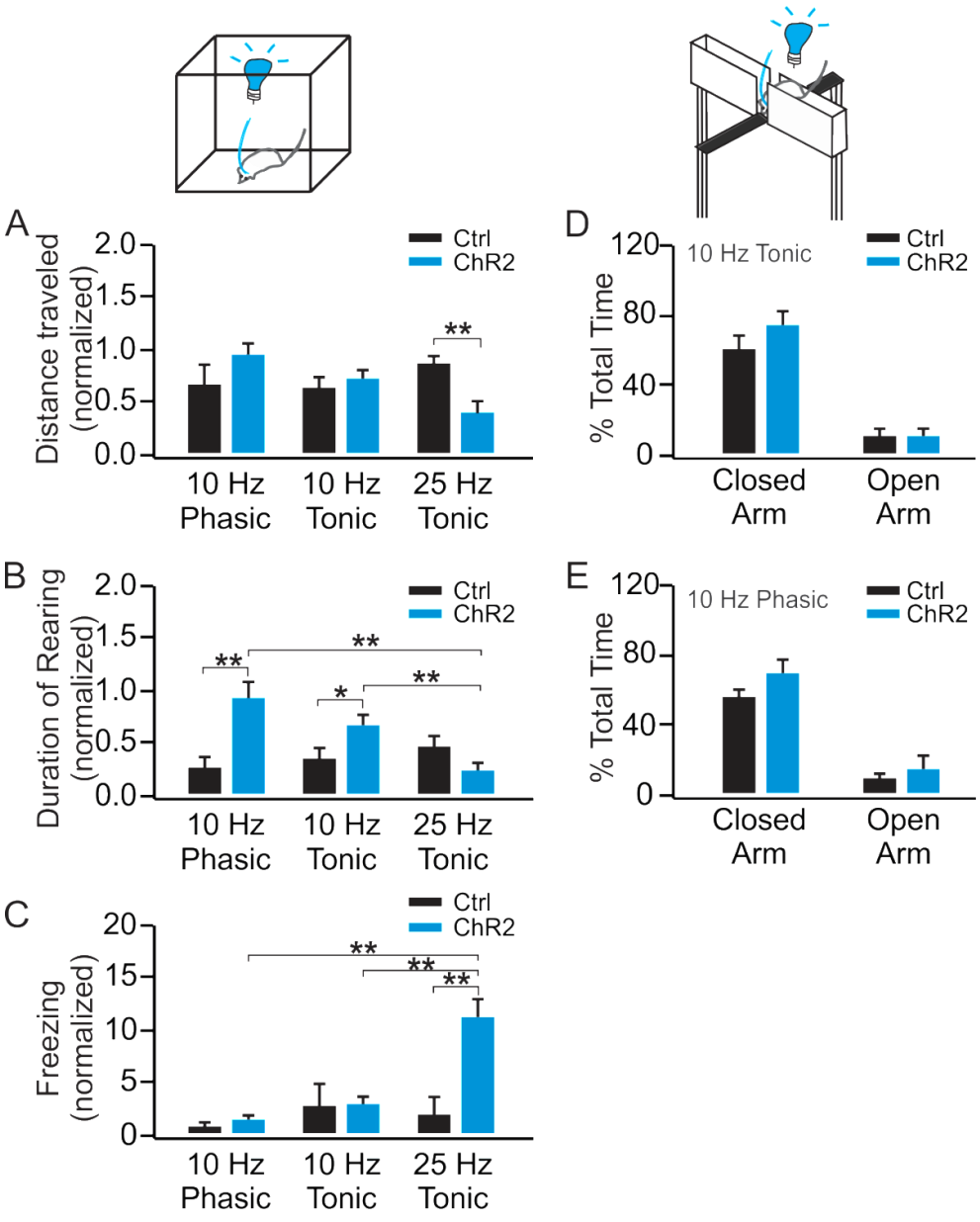
A
Distance traveled (normalized)
2.0
1.5
1.0
0.5
0.0
Ctrl
ChR2
**
10 Hz Phasic
10 Hz Tonic
25 Hz Tonic
B
Duration of Rearing (normalized)
2.0
1.5
1.0
0.5
0.0
Ctrl
ChR2
**
**
*
**
10 Hz Phasic
10 Hz Tonic
25 Hz Tonic
C
Freezing (normalized)
20
15
10
5
0
Ctrl
ChR2
**
**
**
10 Hz Phasic
10 Hz Tonic
25 Hz Tonic
D
% Total Time
120
80
40
0
10 Hz Tonic
Ctrl
ChR2
Closed Arm
Open Arm
E
% Total Time
120
80
40
0
10 Hz Phasic
Ctrl
ChR2
Closed Arm
Open Arm

Figure 3.2 **10-Hz phasic LC activation promotes exploration while 25-Hz tonic activation results in increased freezing and decreased mobility**

A. Distance traveled in the open field with various light patterns in the ChR2 (n = 7) and control (n = 7) rats, normalized to the baseline before the light stimulation. **B.** Duration of rearing with various light patterns in the ChR2 (n = 7) and control (n = 7) rats. **C.** Amount of freezing with various light patterns in the ChR2 (n = 6) and control rats (n = 7). **D.** Percentage time spent in open and close arms of the EPM with 10-Hz tonic light activation in the ChR2 (n = 7) and control (n = 9) rats. **E.** Percentage time spent in open and close arms of the EPM with 10-Hz long phasic light activation in the ChR2 (n = 6) and control (n = 6) rats. *$p < 0.05$; **$p < 0.01$.

3.3.3 LC phasic patterns enhance similar odor discrimination learning

Rats were trained to associate a food pellet with one odor from an odor pair (Figure 3.3A). After learning the simple odor discrimination (SOD) with a dissimilar odor pair (Figure 3.3 B, C &D), rats learned the DOD with a similar odor pair with LC activation (Figure 3.3E, F & G). Three light patterns were used during DOD training: 10-Hz 10-sec phasic (10 sec every 30 sec; Figure 3.3B & E), 10-Hz brief phasic (300 msec every 2 sec; Fig 3C & 3F) and 10-Hz tonic (Figure 3.3D & G). The 25 Hz tonic stimulation that induced significant freezing was not included in this learning paradigm. While both phasic patterns facilitated DOD learning, 10 Hz tonic light activation had no effect on DOD learning.

ChR2 and control rats showed similar learning in the initial SOD. There was a Day effect ($F_{6, 60}$ = 10.99, $p < 0.001$ for 10-Hz long phasic, Fig. 3B; $F_{6, 72} = 9.125$, $p < 0.001$ for 10-Hz brief phasic, Fig. 3C; $F_{6, 66} = 12.097$, $p < 0.001$ for 10-Hz tonic light, Fig 3D), but no Group X Day interaction or Group effect in all light patterns**.** However, both brief and long phasic LC activations accelerated DOD acquisition. For long phasic 10-Hz LC activation, there was a significant Day effect ($F_{9, 90}$ = 10.513, $p < 0.001$), a Day X Group interaction ($F_{9, 90} = 2.880$, $p = 0.005$), and a Group effect ($F_{1, 10}$ = 10.069, $p = 0.010$; Fig 3E). Better performance in the ChR2 group was observed on days 3-8 ($p < 0.05$ or $p < 0.01$). Similarly, for DOD training with 10-Hz brief phasic light, there was a significant Day effect ($F_{9, 108} = 11.774$, $p < 0.001$), a Day X Group interaction ($F_{9, 108} = 4.429$, $p < 0.001$), and a Group effect ($F_{1, 12} = 17.47$, $p = 0.001$; Fig 3.3E). Better correct response rates were observed from days 3-7 with this 10-Hz brief phasic light pattern ($p < 0.05$ or $p < 0.01$). In contrast, tonic 10-Hz LC activation did not alter acquisition. There was a significant effect of Day ($F_{9, 99} = 5.067$, $p < 0.001$), however, no effect of Day X Group interaction ($F_{9, 99} = 0.983$, $p = 0.459$), or Group ($F_{1, 11}$ =

0.033, p = 0.860). Linear trend analysis showed improvement with time in both ChR2 ($F_{1, 5}$ = 12.810, p = 0.016) and control groups ($F_{1, 6}$ = 61.491, p < 0.001; Fig 3.3F).

SOD learning was not affected by phasic 10-Hz LC activation (Fig 3.3H). There was a significant effect of Day ($F_{6, 66}$ = 10.713, p < 0.001), but no Group X Day interaction ($F_{6, 66}$ = 0.755, p = 0.608), or Group effect ($F_{1,11}$ = 0.527, p = 0.483). This underscores NE's role in discriminations that require pattern separation (Shakhawat et al., 2015; Shakhawat, Harley, & Yuan, 2014). Enhancement of subtle tactile discriminations by tonic 5-Hz LC activation (Rodenkirch, Liu, Schriver, & Wang, 2019) has also been reported in rats, a frequency not explored here.

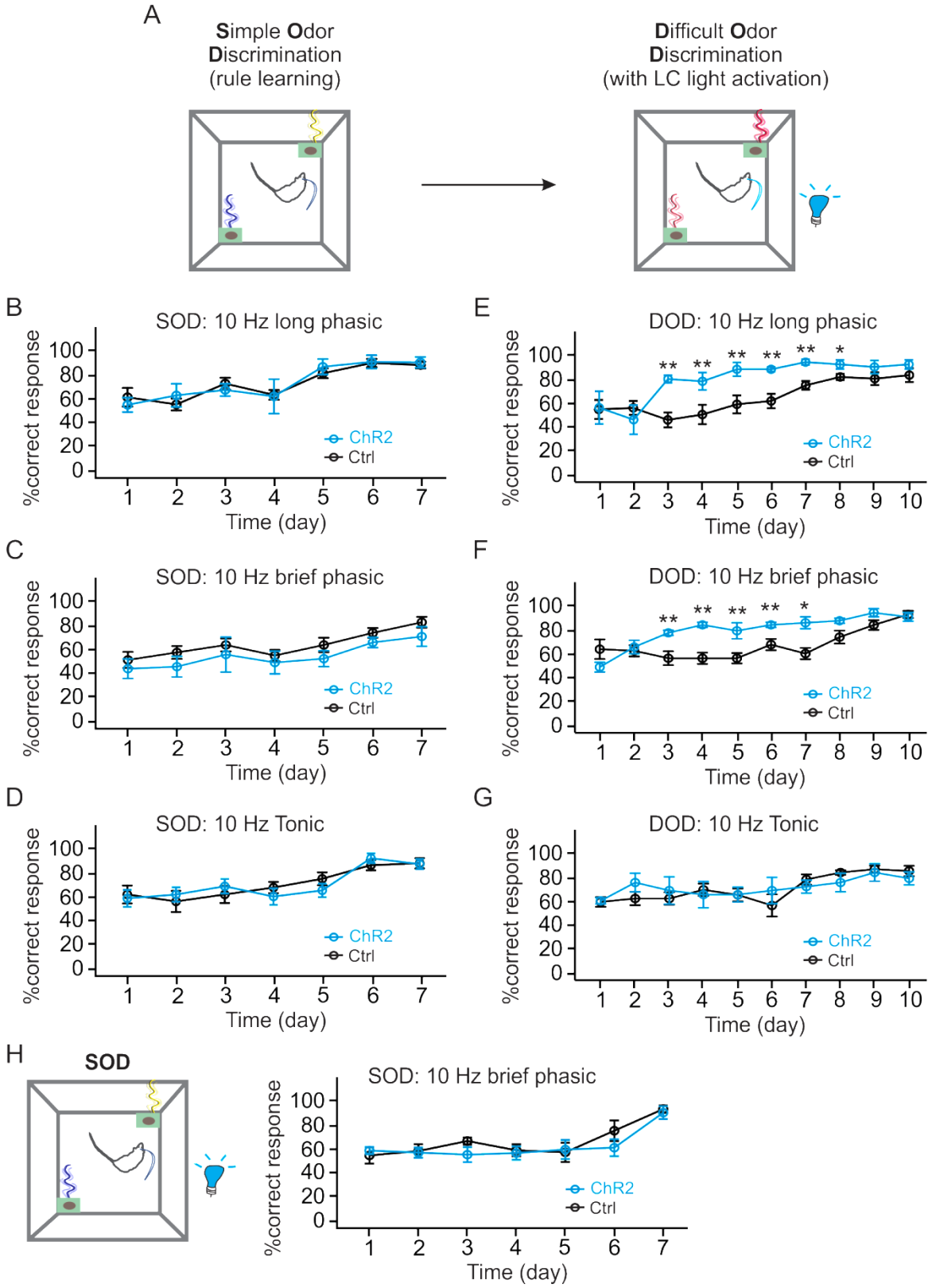
A
Simple Odor Discrimination (rule learning)
Difficult Odor Discrimination (with LC light activation)
B
SOD: 10 Hz long phasic
E
DOD: 10 Hz long phasic
C
SOD: 10 Hz brief phasic
F
DOD: 10 Hz brief phasic
D
SOD: 10 Hz Tonic
G
DOD: 10 Hz Tonic
%correct response
Time (day)
ChR2
Ctrl
H
SOD
SOD: 10 Hz brief phasic

Figure 3.3 **LC phasic patterns, but not tonic pattern, enhance similar odor discrimination learning**

A. Schematic of odor discrimination learning in rats. Simple odor discrimination (SOD) learning without light is followed by difficult odor discrimination (DOD) learning in the presence of various light patterns. **B.** SOD training in rats of the 10-Hz long phasic groups (n (ChR2/Control) = 5/7). **C.** SOD training in rats of the 10-Hz brief phasic groups (n (ChR2/Control) = 6/8). **D.** SOD training in rats of the 10-Hz tonic light groups (n (ChR2/Control) = 6/7). **E.** DOD training with 10-Hz long phasic light. **F.** DOD training with 10-Hz brief phasic light. **G.** DOD with 10-Hz tonic light. **H.** SOD training with 10-Hz brief phasic light (n (ChR2/Control) = 6/7). *$p < 0.05$; **$p < 0.01$.

3.3.4 LC-Ventral tegmental area (VTA)-PC dopamine circuitry mediates the facilitating effect in similar odor discrimination learning

Dopamine (DA) co-release from the LC terminals in the hippocampus has been shown to be critical in spatial learning (Kempadoo et al., 2016) and novelty-mediated memory consolidation (Takeuchi et al., 2016). We next tested the potential involvement of NE and DA in the PC upon LC 10-Hz brief phasic light activation in DOD (Fig. 3.4A). DOD was prevented when the adrenoceptor (AR) antagonists phentolamine and alprenolol were infused in the PC before training, however, D1/5 receptor (DR) antagonist SCH 23390 infusion selectively abolished LC phasic light induced learning facilitation (Fig. 3.4B), but not DOD acquisition. There was a significant Day effect ($F_{9, 207}$ = 15.98, $p < 0.001$), a Group X Day interaction ($F_{27, 207}$ = 5.196, $p < 0.001$), and a Group effect ($F_{3, 23}$ = 17.73, $p < 0.001$)**.** A significant difference in learning was observed between the D1/5 antagonist group and ChR2 vehicle group ($t = 8.624$, $p < 0.001$), and the AR antagonist group ($t = 8.091$, $p < 0.001$), and between the AR antagonist group and the ChR2 vehicle group ($t = 17.488$, $p < 0.001$).

These results argue that while NE is essential for pattern separation-dependent odor discrimination to occur, DA release in the PC during LC phasic light mediates the learning facilitating effect. There are two possible scenarios: either LC axon terminals co-release DA upon LC phasic activation (Kempadoo et al., 2016; Takeuchi et al., 2016), or VTA releases DA into the PC (Aransay, Rodriguez-Lopez, Garcia-Amado, Clasca, & Prensa, 2015; Datiche & Cattarelli, 1996) upon LC activation. To determine the source of DA released during odor discrimination learning, we infused lidocaine into the VTA to silence the VTA during DOD. Lidocaine infusion prevented the learning facilitation effects of the LC phasic light (Fig. 3.4C), but not the acquisition of DOD learning. There was a significant Day effect ($F_{9, 90}$ = 41.46, $p < 0.001$), a Group X Day interaction

($F_{9, 90} = 5.60$, $p < 0.001$), and a Group effect ($F_{1, 10} = 90.94$, $p < 0.001$)**.** Higher correct response rates of the ChR2 vehicle group relative to the ChR2 lidocaine group on days 4-7 were observed ($p < 0.01$). However, the performance of the two groups on the last three days (8-10) was comparable ($P > 0.05$).

Why does phasic LC activation promote DOD while tonic activation at the same frequency does not? In other words, does LC phasic activation engage DA neurons in the VTA more effectively than tonic activation? We next studied neuronal activation patterns in the VTA by phasic *vs* tonic LC activations. We measured cFos expression in the VTA following odor exposure only (no-light control), 10-Hz brief phasic or 10-Hz tonic LC activation paired with an odor (Fig. 3.4D). The phasic light increased overall cFos activation in the VTA, as well as the portion of activated TH^+ cells (Fig. 3.4E-G). Despite the similar numbers of TH^+ cells in the three groups ($F_{2,12} = 0.062$, $p = 0.940$), there were different activations of $cFos^+$ cells ($F_{2,12} = 11.633$, $p = 0.002$) and $TH^+/cFos^+$ cells ($F_{2,12} = 10.436$, $p = 0.002$; Fig. 3.4E and F). The phasic pattern activated significantly more $cFos^+$ cells in the VTA than the no-light control ($t = 4.649$, $p = 0.017$) and the tonic pattern ($t = 6.647$, $p = 0.001$), and had a larger number of $TH^+/cFos^+$ cells compared to the control ($t = 4.598$, $p = 0.017$) and the tonic activation ($t = 6.230$, $p = 0.002$). The percentage of $cFos^+$ cells in the total TH^+ population is significantly higher with the phasic pattern than with the no-light control and the tonic pattern ($F_{2,12} = 33.984$, $p < 0.001$; Fig. 3.4G). The percentage of $TH^+/cFos^+$ cells over total $cFos^+$ cells is also higher in the phasic group ($F_{2,12} = 4.938$, $p = 0.027$; Fig. 3.4H). These results argue that the 10-Hz LC phasic pattern engages VTA DA neurons whereas the 10-Hz tonic pattern does not. This may explain the learning facilitation effect of PC DA with phasic, but not tonic, LC activation.

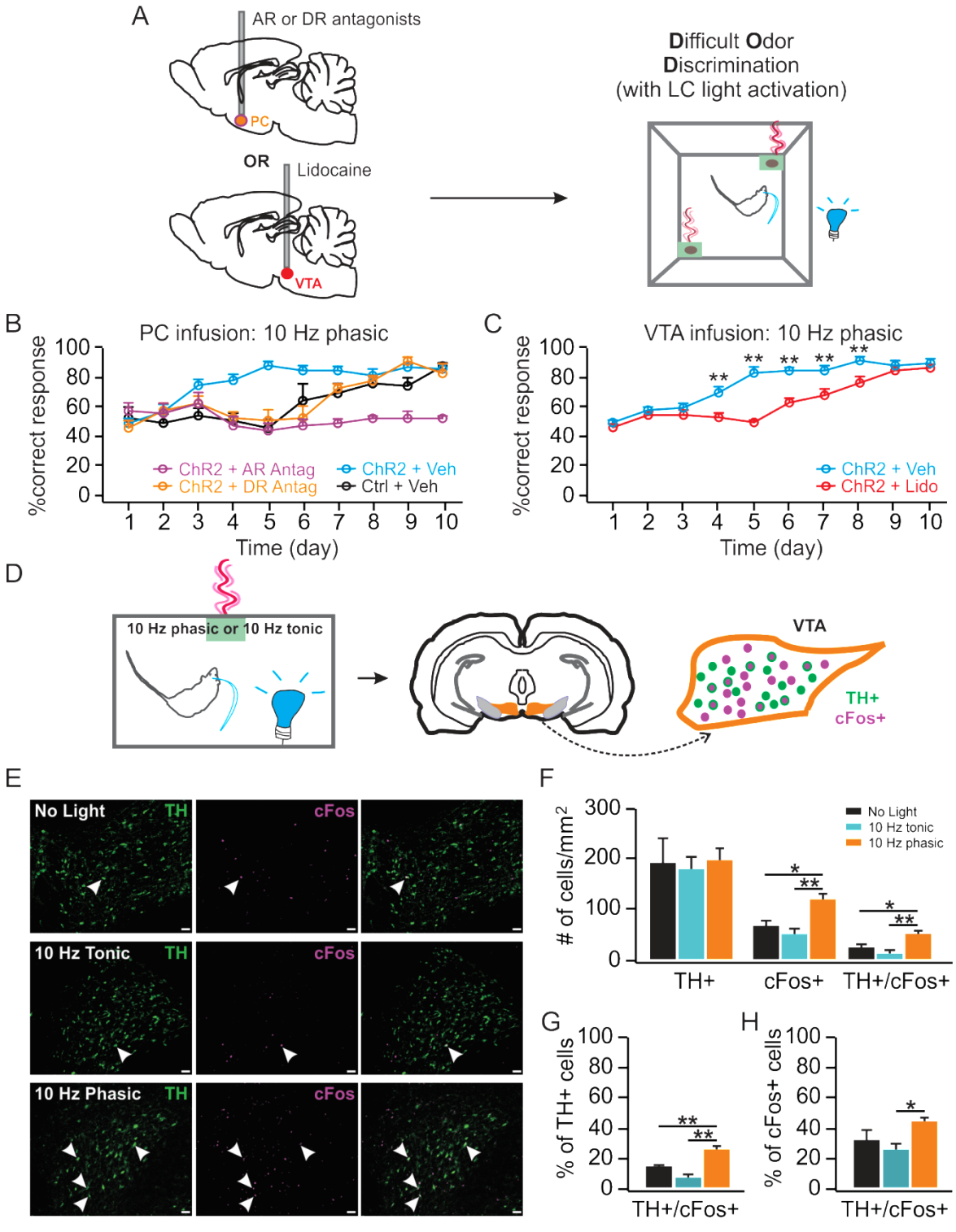
A
AR or DR antagonists
PC
OR
Lidocaine
VTA
Difficult Odor
Discrimination
(with LC light activation)
B
PC infusion: 10 Hz phasic
%correct response
Time (day)
ChR2 + AR Antag
ChR2 + DR Antag
ChR2 + Veh
Ctrl + Veh
C
VTA infusion: 10 Hz phasic
%correct response
Time (day)
ChR2 + Veh
ChR2 + Lido
D
10 Hz phasic or 10 Hz tonic
VTA
TH+
cFos+
E
No Light
TH
cFos
10 Hz Tonic
10 Hz Phasic
F
# of cells/mm2
No Light
10 Hz tonic
10 Hz phasic
TH+
cFos+
TH+/cFos+
G
% of TH+ cells
TH+/cFos+
H
% of cFos+ cells
TH+/cFos+

Figure 3.4 **LC phasic activation engages VTA dopamine release to facilitate DOD**

A. Schematic of DOD training with cannular infusion. **B.** DOD training with vehicle or drug infusions in the PC (n (ChR2 vehicle/Control vehicle/ChR2 AR block/ChR2 DR block) = 9/6/6/6). **C.** DOD training with vehicle or lidocaine infusions in the VTA (n (lidocaine/vehicle) = 6/6). **D.** Schematic of measuring cFos expression in the VTA with no-light control and different LC light patterns. **E.** Examples images of cFos and TH staining in the VTA with no-light control (upper panel), 10-Hz tonic (middle panels) and 10-Hz phasic light (lower panels). Arrows indicated example $TH^+/cFos^+$ cells. Scale bars, 50 μm. **F.** Total $cFos^+$, TH^+ and $TH^+/cFos^+$ cells activated in different groups (n (control/tonic/phasic) = 5/5/5). **G.** Percentage $TH^+/cFos^+$ cells over total TH^+ population. **H.** Percentage $TH^+/cFos^+$ cells over total $cFos^+$ population. AR: adrenoceptor; DR: dopaminergic receptor; *$p < 0.05$; **$p < 0.01$.

3.3.5 LC phasic and tonic patterns promote differential odor valence learning

Besides differentially modulating discrimination learning by different LC activation patterns, tonic LC activation is involved in stress and aversive learning (Hirschberg et al., 2017; Llorca-Torralba et al., 2019; McCall et al., 2017). However, the effect of phasic LC light on adult valence encoding is unknown. We next tested the intriguing possibility that tonic and phasic LC activations could differentially mediate valence learning. We employed a real time odor preference test (ROPT) and a conditioned odor preference test (COPT; Fig 3.5A). In the ROPT, rats were tested for the time spent in the two odor zones, first in the absence, then in the presence, of light activation associated with one odor (O1). Ten-Hz long phasic activation increased the time ChR2 rats spent in the light-paired odor zone (Fig. 3.5B). A significant Odor X Time interaction was observed in the ChR2 group ($F_{1,8} = 8.269$, $p = 0.021$), but not in the control group ($F_{1,7} = 0.080$, $p = 0.786$). ChR2 rats spent significantly more time in O1 during the 10-Hz phasic light, compared to the baseline ($t = 3.35$, $p = 0.045$). Ten-Hz brief phasic activation did not have a significant Odor X Time interaction in the ChR2 group ($F_{1,5} = 0.781$, $p = 0.417$), nor in the control group ($F_{1,7} = 0.429$, $p = 0.533$; Fig. 5C). However, there was a significant effect of Time in the ChR2 rats ($F_{1,5} = 12.490$, $p = 0.017$), and ChR2 rats spent more time in O1 during light stimulation compared to baseline ($t = 4.341$, $p = 0.028$; Fig. 5C). In contrast, 10-Hz tonic light had no significant effect in the ChR2 group ($F_{1,9} = 2.587$, $p = 0.142$; Fig. 3.5D).

In the COPT, rats were light-stimulated in the presence of one odor, O1. Time spent with O1 *vs*. a control odor O2, before and after conditioning was compared. There was a conditioned preference with both 10-Hz phasic patterns, but not 10-Hz tonic pairing. With 10-Hz long phasic light

conditioned with O1, a significant Odor X Time interaction was observed in the ChR2 group ($F_{1,10}$ = 8.213, p = 0.017), but not in the control group ($F_{1,11}$ = 0.034, p = 0.857; Fig. 3.5E). ChR2 rats spent significantly more time in O1 (t = 3.34, p = 0.040) and less time in O2 (t = 3.829, p = 0.022) after odor conditioning with the 10-Hz phasic light. Similarly, 10-Hz brief phasic activation also induced preference for the light-conditioned O1 in the ChR2 group ($F_{1,5}$ = 6.610, p = 0.049), but not the control group ($F_{1,6}$ = 0.001, p = 0.975; Fig. 3.5F). ChR2 rats spent more time in O1 following odor conditioning (t = 3.889, p = 0.040). However, the 10-Hz tonic light had no effect on odor preference ($F_{1,10}$ = 0.017, p = 0.899; Fig. 3.5G).

The immobility associated with the tonic 25-Hz light (Fig. 3.2C) excluded ROPT testing. In COPT, a conditioned avoidance was induced by the 25-Hz light-paired odor (Fig. 3.5H). A significant Odor X Time interaction was observed in the ChR2 group ($F_{1,7}$ = 14.811, p = 0.006). ChR2 rats spent significantly less time in the O1 arm after it was associated with the 25-Hz tonic light, compared to the baseline (t = 4.23, p = 0.020), while they spent more time in the control odor O2 (t = 5.169, p = 0.008). This replicates the conditioned place aversion seen with tonic 5-Hz activation in mice (McCall et al., 2015).

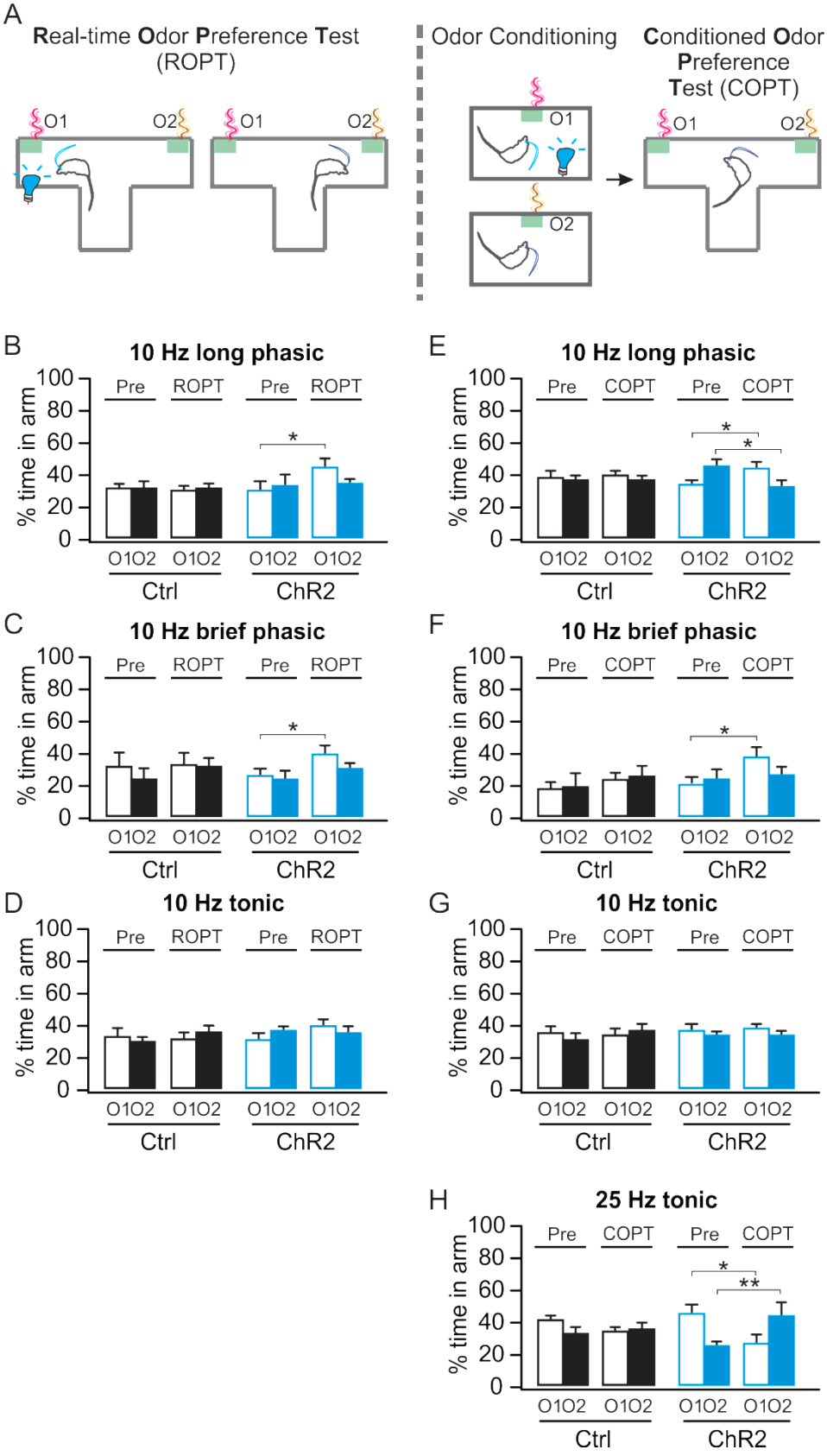
A
Real-time Odor Preference Test (ROPT)
Odor Conditioning
Conditioned Odor Preference Test (COPT)
O1
O2
B
10 Hz long phasic
C
10 Hz brief phasic
D
10 Hz tonic
E
10 Hz long phasic
F
10 Hz brief phasic
G
10 Hz tonic
H
25 Hz tonic
% time in arm
Pre
ROPT
COPT
O1O2
Ctrl
ChR2

Figure 3.5 **Twenty five-Hz tonic LC activation leads to conditioned odor aversion while 10-Hz phasic pattern results in odor preference**

A. Schematic of real-time odor preference test (ROPT) and conditioned odor preference test (COPT). **B.** Percentage time spent in each odors in ROPT, with 10-Hz long phasic light paired with O1 (n (ChR2/Control) = 9/8). **C.** Percentage time spent in each odors in ROPT with 10-Hz brief phasic light (n (ChR2/Control) = 6/8). **D.** Percentage time spent in each odor in ROPT with 10-Hz tonic light (n (ChR2/Control) = 10/7). **E.** Percentage time spent in each odor in COPT, with 10-Hz long phasic light conditioned with O1 (n (ChR2/Control) = 11/12). **F.** Percentage time spent in each odor in COPT, with 10-Hz brief phasic light (n (ChR2/Control) = 6/7). **G.** Percentage time spent in each odor in COPT with 10-Hz tonic light (n (ChR2/Control) = 11/10). **H**. COPT with 25-Hz tonic light (n (ChR2/Control) = 8/11). *$p < 0.05$; **$p < 0.01$.

3.3.6 LC phasic and tonic patterns engage differential basolateral amygdala (BLA) circuitry in odor valence learning

In mice, it has been shown that LC tonic activity promotes aversive behavior through BLA β-ARs (McCall et al., 2017). The BLA is a critical site for valence associative learning (O'Neill, Gore, & Salzman, 2018). BLA has been found to contain functionally distinct neuronal populations projecting to either negative- (central amygdala, CeA) or positive- (nucleus accumbens, NAc) valence encoding circuitry (Kim, Pignatelli, Xu, Itohara, & Tonegawa, 2016; Namburi, Al-Hasani, Calhoon, Bruchas, & Tye, 2016). It is plausible that the LC-BLA projection is involved in the odor valence encoding observed here with differential LC light activation patterns.

Here we first tested the involvement of BLA ARs in ROPT and COPT with either 10-Hz long phasic or tonic LC activation (Fig. 3.6A). Increased time in the light stimulated odor zone with 10-Hz phasic light in ROPT was not affected by AR blockade (Fig. 3.6B). Significant Time X Odor effects were observed in both vehicle-infused rats ($F_{1,6}$ = 6.947, p = 0.039) and AR antagonist infused rats ($F_{1,6}$ = 9.693, p = 0.021). Both vehicle (t = 3.730, p = 0.039) and AR antagonist groups (t = 4.088, p = 0.027) showed more time spent in the light-activated odor zone O1 during ROPT.

However, BLA α- and β-AR blockade with phentolamine and alprenolol prevented both LC 10-Hz phasic light induced odor preference (Fig. 3.6C) and LC 25-Hz tonic induced odor aversion in COPT (Fig. 3.6D). For COPT with the 10 Hz-phasic light, a significant effect of Time X Odor was observed for the vehicle group ($F_{1,7}$ = 7.220, p = 0.031), but not for the AR antagonist infused group ($F_{1,5}$ = 2.778, p = 0.156; Fig. 3.6C). The vehicle group spent significantly more time in the conditioned odor O1 during the COPT (t = 5.048; p = 0.009). For COPT with the 25-Hz tonic light,

the AR antagonist infused group showed no significant effects ($F_{1,4} = 3.297$, $p = 0.129$), while the vehicle group showed a significant effect of time ($F_{1,7} = 5.875$, $p = 0.046$; Fig. 3.6D). The vehicle group spent significantly more time in the conditioned odor O1 during the COPT ($t = 4.309$, $p = 0.019$).

Taken together, while BLA NE mediates conditioned valence learning dependent on differential patterns of LC activation, this circuitry is not involved in real-time preference in ROPT. Phasic light mediated enhanced exploration (Fig. 3.2B) may explain the acute ROPT effect of 10-Hz phasic light.

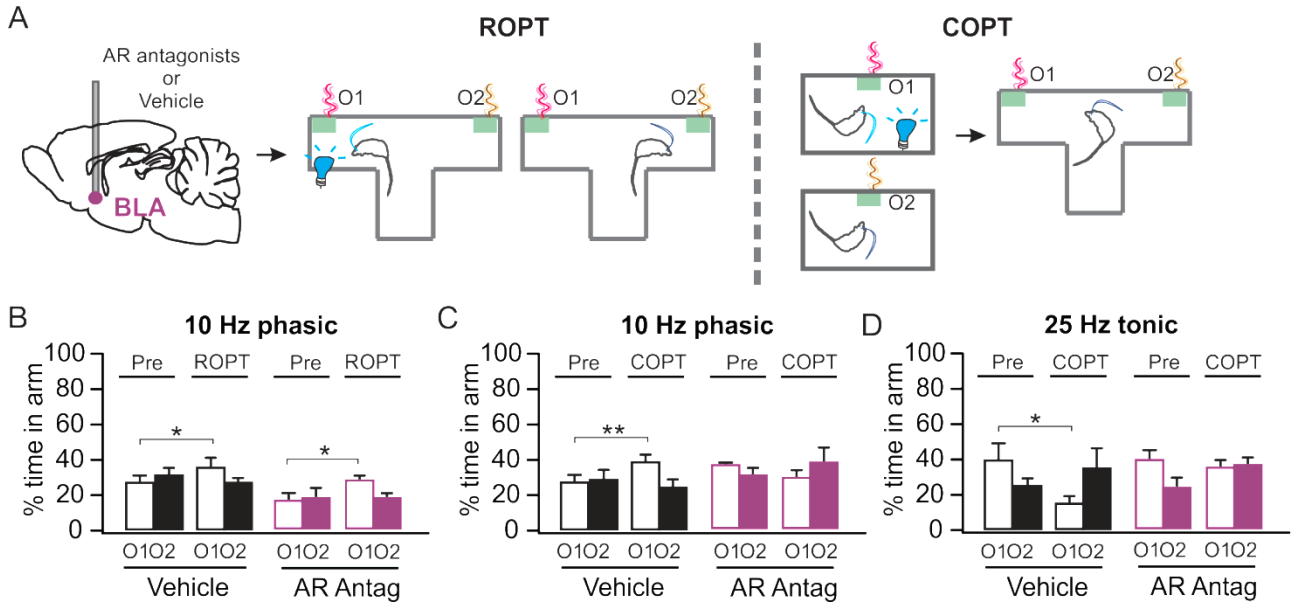

Figure 3.6 **Basolateral amygdala adrenoceptors mediate the conditioned preference and aversion in COPT**

A. Schematic of brain infusion, followed by real-time odor preference test (ROPT) and conditioned odor preference test (COPT). **B.** Percentage time spent in each odors in ROPT, with 10-Hz phasic light paired with O1 (n (Vehicle/AR block) = 7/7). **C.** Percentage time spent in each odor in COPT, with 10-Hz phasic light conditioned with O1 (n (Vehicle/AR block) = 8/6). **D**. COPT with 25-Hz tonic light (n (Vehicle/AR block) = 8/6). AR: adrenoceptor. *p < 0.05; **p < 0.01.

After establishing the requirement of BLA NE in LC light mediated valence learning in COPT, we next tested whether tonic and phasic activation of the LC biases activation of the BLA ensembles projecting to BLA-CeA aversive and BLA-NAc reward circuitry respectively. We infused retro-tracing dyes linked to Cholera Toxin B (CTB) in the central amygdala (CeA) and nucleus accumbens (NAc), and examined the overlap of CeA or NAc projecting neurons with $cFos^+$ cells in the BLA activated by odor only (no-light control), 10-Hz brief phasic or 25-Hz tonic LC lights (Fig. 3.7A and 7B). The CTB labeled CeA ($F_{2,7} = 2.028$, $p = 0.202$) and NAc ($F_{2,7} = 0.340$, $p = 0.723$) projecting cell numbers were comparable in the three groups (Fig. 3.7C). Intriguingly, although the two LC light patterns activated similar numbers of $cFos^+$ cells in the BLA compared to the control ($F_{2,7} = 0.888$, $p = 0.453$; Fig. 3.7C), the distribution patterns of $cFos^+$ cells were dramatically different (see example images in Fig 7B). The proportion of CeA^+ cells in $cFos^+$ cells was significantly higher in the 25-Hz tonic group ($F_{2,7} = 14.232$, $p = 0.003$; Fig. 3.7D) compared with either the non-light control ($t = 4.539$, $p = 0.008$) or the10-Hz phasic light ($t = 4.796$, $p = 0.006$). On the other hand, the proportion of NAc^+ cells in $cFos^+$ cells was significantly higher in the 10-Hz phasic light group ($F_{2,7} = 10.648$, $p = 0.008$; Fig. 3.7E) compared with either non-light controls ($t = 4.033$, $p = 0.015$) or the 25-Hz tonic light ($t = 4.052$, $p = 0.015$). The differential distributions of $cFos^+$ cells in different groups are displayed in the pie charts (Fig. 3.7F). In no-light controls, equal amount of $cFos^+$ cells (11%) were NAc and CeA projecting cells, whereas 37% are NAc projecting and 5% were CeA projecting with the 10-Hz phasic light, and 54% are CeA projecting and 9% were NAc projecting with the 10-Hz tonic light. A small portion of projecting cells (4.4%) expressed both CTBs, however, the activation of the double-CTB-labelled cells was very low (0.72%). Phasic and tonic modes of LC activations re-distributed neuronal ensembles activated by an odorant in the BLA. Selective activation of one valence encoding ensemble may inhibit the ensemble of the opposite valence in the BLA (P. Namburi et al., 2015). Taken together, the 10-Hz

LC phasic pattern preferentially activates NAc projecting neurons in the BLA, whereas the 25-Hz tonic LC activation preferentially engages CeA projecting neurons.

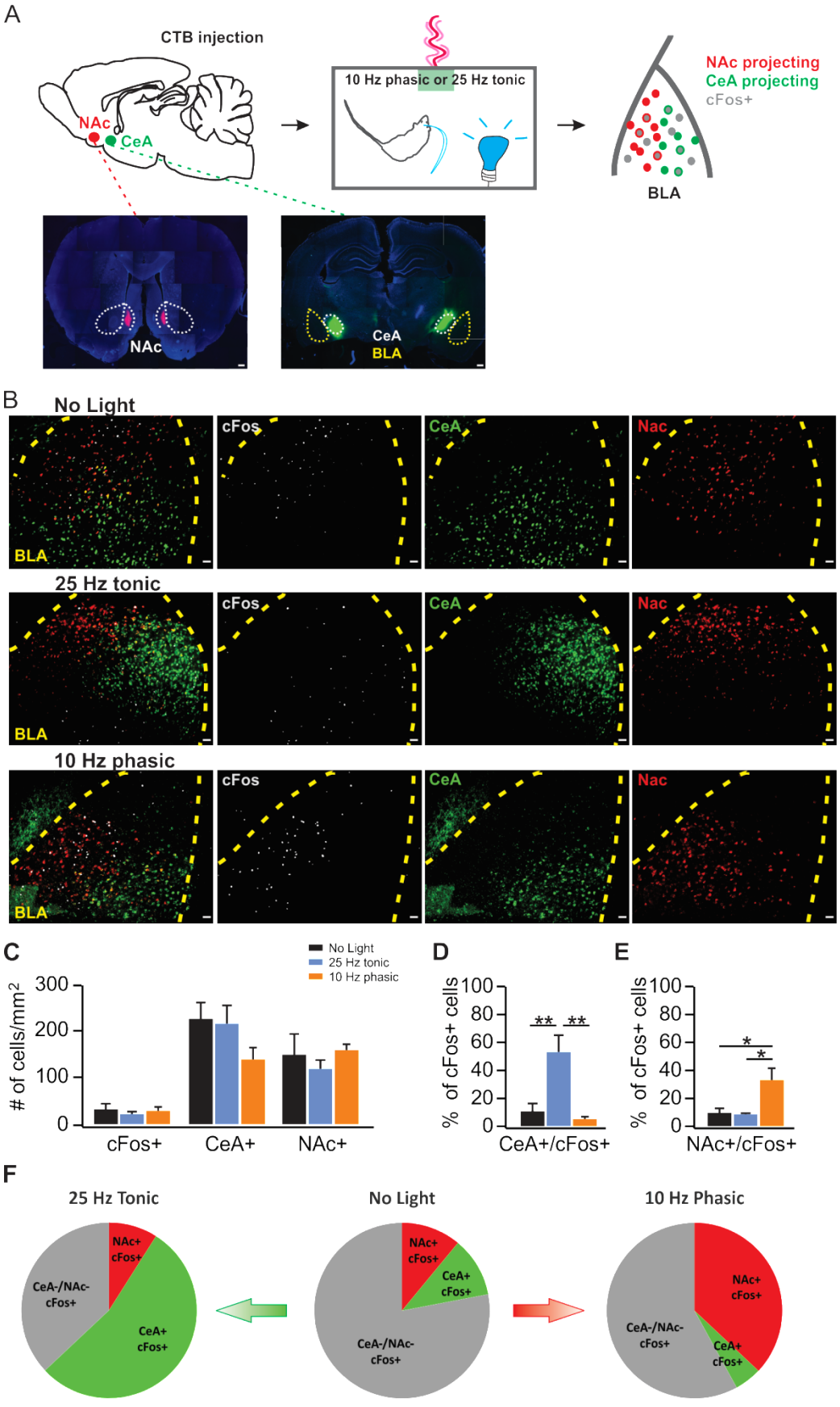
A
CTB injection
NAc
CeA
10 Hz phasic or 25 Hz tonic
NAc projecting
CeA projecting
cFos+
BLA
NAc
CeA
BLA
B
No Light
25 Hz tonic
10 Hz phasic
cFos
CeA
Nac
BLA
C
No Light
25 Hz tonic
10 Hz phasic
# of cells/mm2
300
200
100
0
cFos+
CeA+
NAc+
D
% of cFos+ cells
100
80
60
40
20
0
**
**
CeA+/cFos+
E
% of cFos+ cells
100
80
60
40
20
0
*
*
NAc+/cFos+
F
25 Hz Tonic
No Light
10 Hz Phasic
NAc+ cFos+
CeA+ cFos+
CeA-/NAc- cFos+

Figure 3.7 **Ten-Hz phasic and 25-Hz tonic LC activation engage positive and negative projecting circuitry respectively in the BLA**

A. Schematic of measuring cFos activation in the BLA with CTB labeling NAc and CeA projecting neurons. DAPI in blue. **B.** Examples images of cFos, CTB-488 (labeling CeA projecting neurons) and CTB-594 (labeling NAc projecting neurons) in the BLA in no-light control (upper panels), activated by 25-Hz tonic (middle panels) and 10-Hz phasic light (lower panels). Scale bars, 50 μm. **C.** Total $cFos^+$, CeA^+ and NAc^+ cells activated by tonic and phasic lights (n (control/tonic/phasic) = 4/3/3). **D.** Percentage $CeA^+/cFos^+$ cells over total $cFos^+$ population. **E.** Percentage $NAc^+/cFos^+$ cells over total $cFos^+$ population. *$p < 0.05$. **F.** Distributions of $cFos^+$ cells in the BLA in no light (middle), 25-Hz tonic light (left) and 10-Hz phasic light (right) conditions.

VTA projections to the NAc facilitate BLA-NAc circuitry in promoting a reward-seeking response to sensory cues (Ambroggi, Ishikawa, Fields, & Nicola, 2008; Yun, Wakabayashi, Fields, & Nicola, 2004). The 10-Hz phasic, but not 10-Hz tonic, LC activation, efficiently recruited VTA dopaminergic neurons in our study (Fig. 4 D-H) suggests that 10-Hz phasic LC activation likely engages NAc more efficiently compared to a tonic pattern. This is indeed the case when we compared the cfos activation in the VTA by 10-Hz phasic light vs. 25-Hz tonic light (Supplementary Fig. 4). More $cFos^+$ cells were observed with 10-Hz phasic LC activation and a bigger portion of NAc projecting neurons were involved.

3.4 Discussion

This work aimed to further our understanding of whether and how the LC produces activation mode-specific behavioural responses. We assessed how LC activation patterns differentially modulate general behaviour, odor discrimination learning and valence encoding. In general behaviour, our assessments revealed increased exploration with both 10-Hz phasic and tonic activation, expressed as increased rearing. With 25-Hz tonic activation there was reduced distance traveled and increased freezing. An increase in rearing has not been previously reported with LC activation, but hippocampal NE infusions increase open field rearing (Flicker & Geyer, 1982; Geyer & Masten, 1989) as seen here. Freezing with 25-Hz tonic LC activation is similar to the report of behavioural arrest with tonic LC activation (10-25 Hz) in mice (Carter et al., 2010). However, in the mice, 3-Hz tonic activation also increased distance traveled, while 10-Hz phasic activation decreased it. In rats, neither distance traveled in the open field nor anxiety in the EPM, was altered by phasic or tonic 10-Hz LC activation. The rat outcome also contrasts with mice that show increased anxiety to 5-10 Hz LC tonic activation as indexed by decreased center open field entries and increased closed arm time in an EPM (McCall et al., 2015). Anxiety differences between mice and rats with 10-Hz LC activation may relate to species differences or to total LC-NE release, which could be less in rat as fewer cells are likely to be recruited given LC size relative to the optic fiber. Behavioural inhibition in mice was linked to a decrease in NE release as indexed by micro-dialysis during 10 min of a 10-Hz LC light (Carter et al., 2010). Presynaptic NE exhaustion was proposed to explain the NE reduction, however, we have also documented inhibition of LC after 2 min of 10-Hz light activation (Quinlan et al., 2018). Nevertheless, high tonic patterns result in distress in both mice and rats, which likely serve as the negative signal in valence encoding.

A theory of LC-NE function based on monkey data (Aston-Jones & Cohen, 2005a) proposes that phasic firing facilitates performance and optimizes behavior during focused task performance (exploitation), while tonic firing interferes with phasic coding and facilitates exploration (Aston-Jones & Cohen, 2005a). Optogenetic studies mimicking these conditions, including the present study, are consistent with a role for phasic LC activation in enhancing task performance. The present LC effects argue for enhanced attention or plasticity with phasic LC activation accelerating pattern separation learning here, consistent with previous reports of accelerated spatial learning (Kempadoo et al., 2016) and perceptual learning (Glennon et al., 2019) with optogenetic phasic LC activation. Since these tasks were multi-trial, enhancement of plasticity-related proteins by phasic activation, previously shown to promote consolidation (Glennon et al., 2019), could also contribute to faster acquisition. The plasticity of LC neurons themselves, by pairing a phasic burst with a sensory stimulus, has also supported enhancement of sensory cortical representations (Martins & Froemke, 2015).

Here we show phasic LC activation accelerates learning even when not time-locked to stimuli or to decisions. It was assumed that phasic activation tightly linked to input mediated selective input modulation previously. A recent direct test of that hypothesis in anesthetized rats demonstrated transient NE effects temporally-locked to input-LC pairing (E. M. Vazey et al., 2018). However, the present outcomes, and earlier evidence (Kempadoo et al., 2016; Takeuchi et al., 2016), suggest there are additional consequences of phasic LC activation. Interestingly, these effects of LC phasic learning enhancement appear mediated by DA, not NE.

Hippocampal-dependent learning has been shown to involve LC co-released DA (Kempadoo et al.,

2016; Takeuchi et al., 2016). DA release from the LC axonal terminals in the dorsal hippocampus, but not NE, mediates spatial learning (Kempadoo et al., 2016) and novelty mediated learning enhancement (Takeuchi et al., 2016). Whether co-release of DA from LC axons exists in other structures is not known. Here we show that while DA mediates the facilitating effect of odor discrimination with 10-Hz phasic LC activation, the effect is mediated *via* VTA activation by the LC phasic light and release of DA, not by co-release of DA from LC varicosities. This highlights region-dependent mechanisms of LC release and modes of actions. In odor valence conditioning, however, the valence encoding appears to be directly mediated by NE release in the BLA. Noradrenergic antagonist infusion in the BLA prevented both LC 10-Hz phasic induced preference and 25-Hz tonic light induced avoidance.

Recent evidence suggests that functional heterogeneity within the LC itself is responsible for the distinct roles of the LC (Chandler et al., 2019; Schwarz & Luo, 2015; Schwarz et al., 2015; Uematsu, Tan, & Johansen, 2015). However, heterogeneity of release effects within LC projection sites may also plays a key role in LC functional diversity. Our results demonstrate that this is the case. We have shown that 10-Hz phasic LC activation preferentially engages VTA DA neurons compared to tonic light patterns. This appears to explain why 10-Hz phasic LC activation is more effective in promoting accelerated odor discrimination learning (through VTA-PC circuitry) and in activating the VTA-NAc circuitry involved in positive valence coding. It appears that the "pause" (the quiescent period between phasic bursts) associated with the phasic pattern is, in some way, essential for these effects. A similar conclusion is reached when examining DA's role in providing a teaching signal (Chang, Gardner, Conroy, Whitaker, & Schoenbaum, 2018). We have also demonstrated that phasic and tonic patterns, which lead to differential valence outcomes in our study, engage different neuronal ensembles in the BLA. The BLA, a projection site of the LC, has

been found to contain functionally distinct neuronal populations projecting to either negative- (CeA) or positive- (NAc) valence encoding circuitry (Kim et al., 2016; Namburi et al., 2016). We show that tonic and phasic activation of the LC biases activation towards neuronal ensembles in the BLA projecting to CeA and NAc circuitry respectively, thereby highlighting the role of downstream projection site heterogeneity in differential LC functions.

3.5 Conclusions

In summary, the present outcomes support Aston-Jones and Cohen's hypothesis (Aston-Jones & Cohen, 2005a) that LC phasic bursts promote optimized adaptation as proposed, but phasic patterns can also generate exploration. Frequency is critical for tonic effects with a report of discrimination benefits at 5 Hz in rats (C. Rodenkirch et al., 2019) and aversive valence at 5 Hz in mice (McCall et al., 2015). The present experiments reveal aversive valence at 25-Hz, but not 10-Hz tonic activation, in rats, and, for the first time, demonstrate positive valence with phasic optogenetic LC activation in adult rat. Positive valence effects with phasic LC electrical stimulation were reported in much earlier studies (Ritter & Stein, 1973), although the idea was not well supported due to criticisms regarding the specificity of the stimulation and the lack of establishment of conclusive causal relationships (Wise, 1978).

The several network mechanisms by which differing patterns and frequencies of LC activation achieve specific behavioural outcomes revealed in these experiments means that there is still a great deal of work remaining to understand LC's functional contributions. Differing receptor populations in target structures, differing concentrations of local NE release, the effects of co-release of

peptides and amino acids, and the conditions under which they occur are all open questions for future investigations. The physiological mechanisms illuminated in these experiments will need to be integrated with the recent structural evidence for greater specificity of LC subpopulation targeting than previously suspected (Chandler et al., 2019; Schwarz & Luo, 2015). The interaction of these more selective physiological and structural features of LC modulation of brain networks promises a broad array of insights to come with novel functional implications for both basic and clinical brain science.

3.6 Supplementary figures

3.6.1 Supplementary figure 1

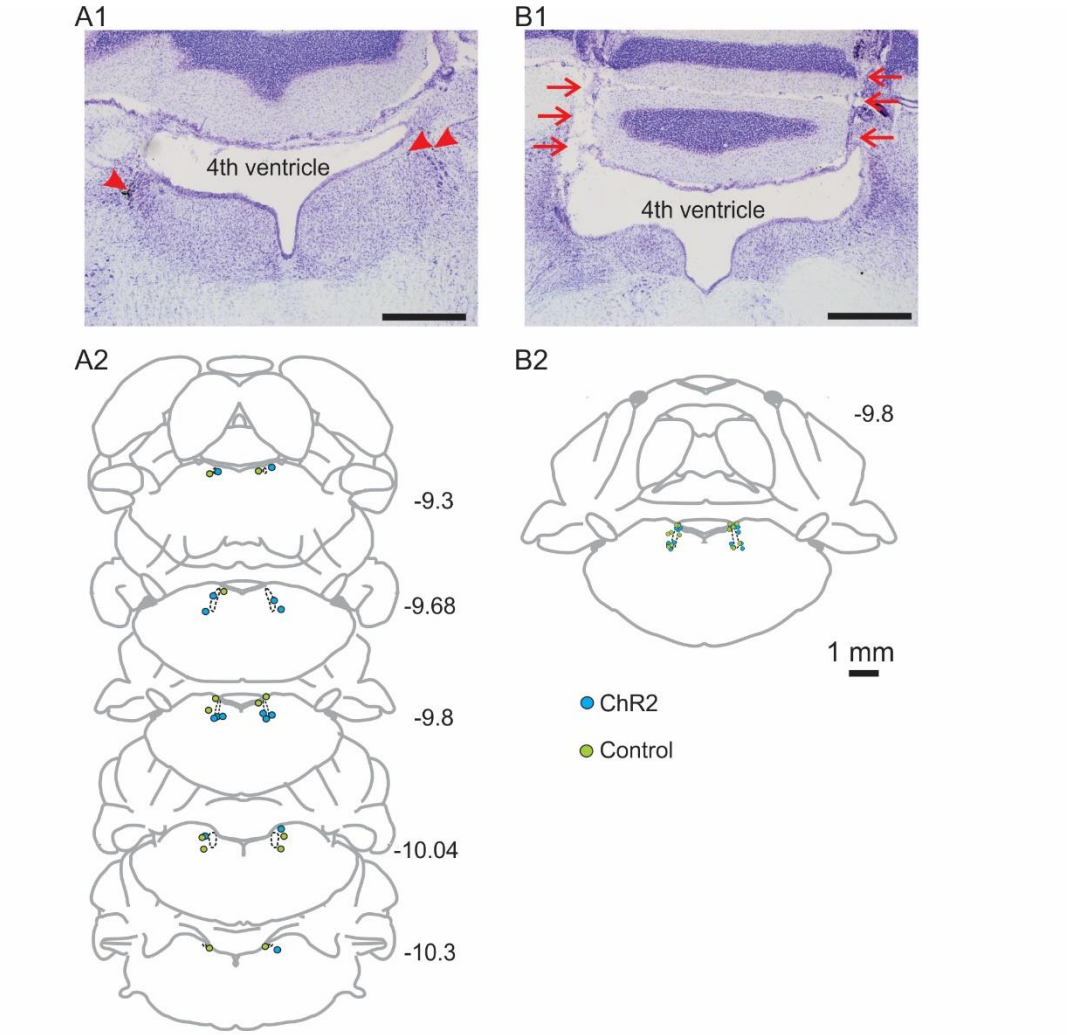

Supplementary Figure 1. LC targeting summary
A1. An example of blue beads infused into the LC. Arrow heads indicate visible blue beads. **A2.** Schematics showing the infusion sites from ChR2 and control rats at different coronal levels (ChR2: N = 8; Control: N = 8). **B1.** An example of cannula tracks (indicated by red arrows bilaterally). **B2.** Schematics showing the cannular sites from ChR2 and control rats at -9.8 level (ChR2: N = 8; Control: N = 8). Scale bars for A1 and B1, 500 μm.

3.6.2 Supplementary figure 2

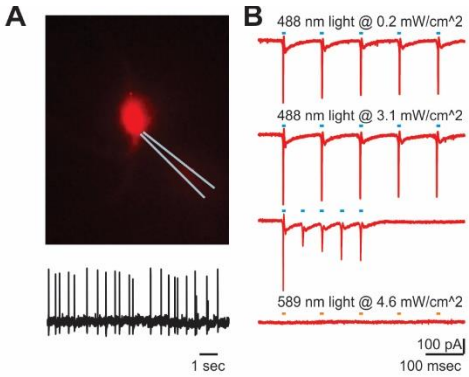

Supplementary Figure 2. *In vitro* LC light activation
A. Cell attached recording of a ChR2-mCherry expressing LC neuron showing spontaneous spiking at ~1.5 Hz. **B.** 488nm light (indicated by blue marks) induced currents at 10 Hz and 20 Hz (upper three traces) and no currents induced by 589 nm light (indicated by yellow marks).

3.6.3 Supplementary figure 3

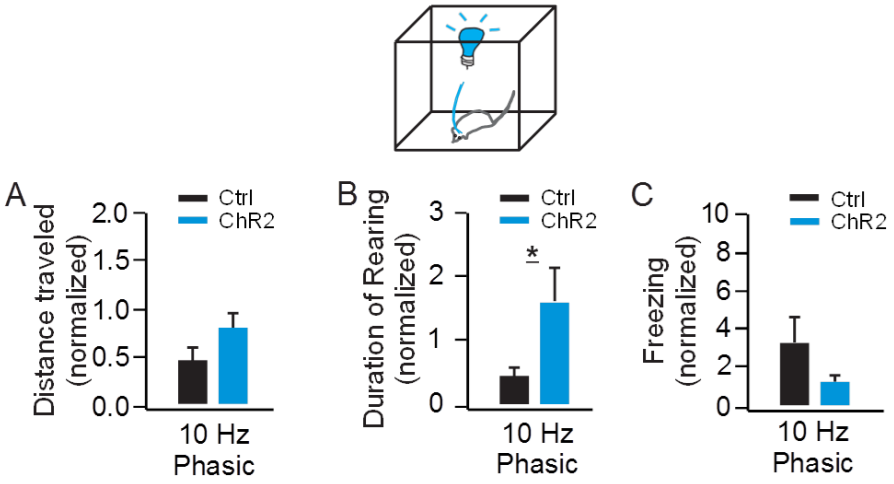

Supplementary Figure 3. Ten-Hz brief phasic LC activation (300 msec every 2 sec) increases exploration in rats
A. Distance traveled in the open field. **B.** Duration of rearing in the open field. **C.** Percentage freezing in the open field. *p < 0.05.

3.6.4 Supplementary figure 4

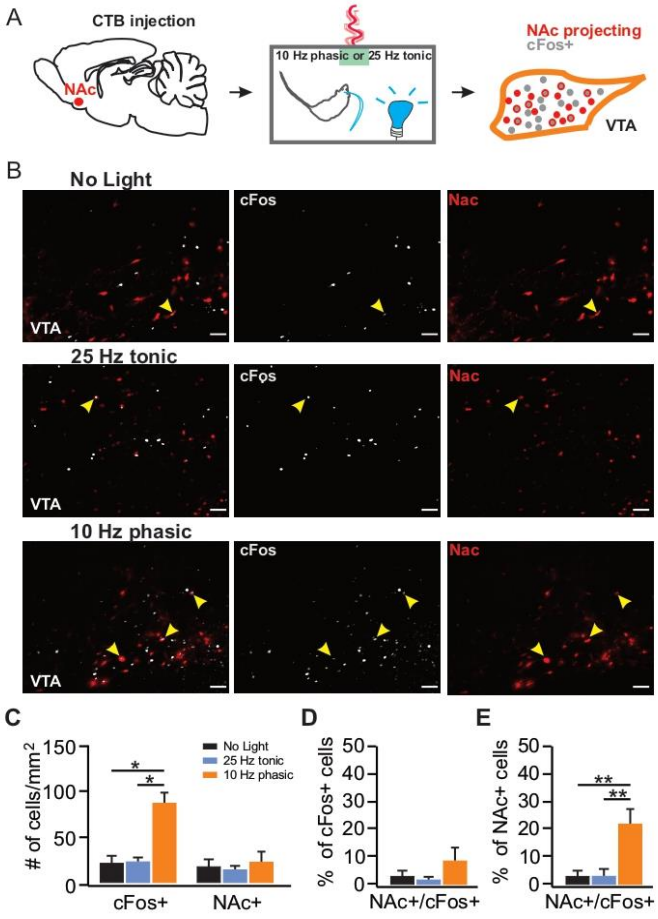

Supplementary Figure 4. Ten-Hz phasic LC activation engages NAc projecting neurons more efficiently than 25-hz tonic in the VTA
A. Schematic of measuring cFos activation in the VTA with CTB labeling NAc-projecting neurons. **B.** Examples images of cFos and CTB-594 (labeling NAc-projecting neurons) in no-light control (upper panels), activated by 25-Hz tonic (middle panels) and 10-Hz phasic light (lower panels). Scale bars, 50 μm. **C.** Total $cFos^+$ and NAc^+ cells activated in different groups (n (control/tonic/phasic) = 4/4/3). **D.** Percentage of $cFos^+$ cells that are NAc^+. **E.** Percentage of NAc^+ cells that are $cFos^+$. *$p < 0.05$. **$p < 0.01$

4 Chapter 4: An experimental model of Braak's pretangle proposal for the origin of Alzheimer's disease: the role of locus coeruleus in early symptom development

This chapter is a version of the article Ghosh et al., 2019, published in Alzheimer's Research & Therapy. 2019 July;11(1):59. [https://doi.org/10.1186/s13195-019-0511-2]

4.1 Introduction

In a survey of 2332 human brains aged from 1 to 100, Braak and colleagues reported that the first evidence of soluble abnormal or hyperphosphorylated tau, which appears later in association with the cortical tangles of Alzheimer's disease (AD), is in the locus coeruleus (LC) neurons of the brain stem (Braak et al., 2011). Importantly, this abnormal tau appears even at young ages. Five pretangle tau stages were identified in the human brain (Braak &

Tredici, 2011): (a) abnormal tau in LC axons, (b) in LC axons and the somatodendritic LC compartment, and (c) in the foregoing and other neuro- modulatory cell groups, such as the serotonergic raphe nuclei; (1a) along LC axons to their terminals in transentorhinal/entorhinal cortex; (1b) in the pyramidal cells of transentorhinal cortex. When Braak's AD diagnostic *insoluble* tau tangle stages (Braak I–VI) appear, the pretangle stages are still present (Braak & Tredici, 2015). Pretangle stages a–c only, pre- dominate at ages 10–20, 1a–1b appear mainly at ages 40– 50, while from age 60 onwards, Braak tangle stages I–II are more frequently observed, followed by symptomatic AD stages III–VI in the 80–100 age range. In these later stages, LC neurons themselves are lost (Theofilas et al., 2017). While Braak's model appears compelling, some investigators (Goudsmit, 2016) have assumed that, as pretangle stages are ubiquitous in the human brain, they are unlikely to be the driving source of AD and note, further, that there is no evidence that pre- tangles can generate AD phenomenology. Here, we use an animal model to ask if LC pretangles, in the absence of any amyloid, can generate functional and anatomical path- ology characteristic of preclinical AD descriptions. This outcome would support the hypothesis that LC pretangles are AD ground zero.

The work of Braak and others (Elobeid, Soininen, & Alafuzoff, 2012; Shin, Kitamoto, & Tateishi, 1991) demonstrates soluble tau pretangle expression in the LC neurons and, subsequently, in other subcortical nuclei (Stratmann et al., 2016) and in the entorhinal cortex. The earliest tangles reported are associated with the anterior olfactory nucleus and entorhinal cortex (Kovacs, Cairns, & Lantos, 2001; Price, Davis, Morris, & White, 1991). The anterior olfactory nucleus is a component of the human olfactory cortex (pre-piriform/piriform) (Crosby & Humphrey, 1941). Both the entorhinal cortex and the

anterior olfactory nucleus receive direct projections from the olfactory bulb (Price, 1990).

Our work on LC function in rats, and its critical role in highly challenging olfactory discrimination tasks (Amin MD. Shakhawat et al., 2015), led us to hypothesize that pretangle stages characterized, initially, by persistent hyperphosphorylated tau expression in the LC neurons may explain the early appearance of human odor identification deficits with aging (Doty et al., 1984) since Braak's data argues that all aging humans will have some hyperphosphorylated abnormal tau in the LC neurons. Worsening olfactory deficits are subsequently predictive of MCI development, when LC neurons are likely to begin to be lost, while yet greater olfactory identification impairment deficits predict AD itself (Conti et al., 2013; Devanand, 2016; Devanand et al., 2015; Josefsson, Larsson, Nordin, Adolfsson, & Olofsson, 2017; Lafaille-Magnan et al., 2017; Liang et al., 2016; MacDonald, Keller, Brewster, & Dixon, 2018; Palta et al., 2018; Quarmley et al., 2017; Risacher et al., 2017; Roalf et al., 2017; Roberts et al., 2016; Vassilaki et al., 2017; Woodward, Amrutkar, et al., 2017).

Importantly, olfactory identification deficits, as we hypothesize, have been shown to appear in a cognitively normal population prior to the appearance of episodic memory deficits. In a longitudinally studied population, the early identification deficits predicted the subsequent rate of episodic memory decline (Wilson et al., 2009). Decreases in human olfactory identification ability have been related to tau pathology (Wilson, Arnold, Schneider, Tang, & Bennett, 2007), to impairments in odor coding (Li, Howard, & Gottfried, 2010), and to hypometabolism in primary olfactory structures including the piriform cortex (Cerf-Ducastel

& Murphy, 2003; J. Wang et al., 2010). The identification of the precise mechanistic underpinning of early olfactory dysfunction may be critical for early intervention to prevent the development of AD.

In the present study, we generate an animal model to test the hypothesis that the expression of persistently phosphorylated tau in the LC neurons will lead initially to impairments in associative olfactory learning and memory. Our model is generated by infusing a human pseudophosphorylated tau (htau) gene into the LC. Pseudophosphorylation functionally mimics soluble persistently phosphorylated tau (Hoover et al., 2010). Although Braak used an antibody (AT8) to two tau phosphorylation sites to identify pretangle tau, a recent examination of human LC neurons displaying abnormal tau (Andres-Benito et al., 2017) used additional antibodies and reported another 5 persistently phosphorylated sites. These seven sites are all proline-directed serine/threonine sites. Normal tau has 87 phosphorylation sites available, but those identified with early AD are typically the proline-directed sites. Goedert proposed that "while normal brain tau is phosphorylated at only a few of the 17 serine/threonine-proline sites, (AD) tau is phosphorylated at a large number of these sites" (Goedert, 1993). The phosphorylation of AD-related soluble and insoluble tau survives death and fixation unlike the phosphorylation of normal tau; for this reason, we use the phrase "persistently phosphorylated." Persistent phosphorylation argues that the normal dephosphorylation mechanism is not effective for pretangle tau. Karen Ashe has provided a plasmid for human tau on Addgene with 14/17 proline-directed sites pseudophosphorylated (htauE14) that produces, functionally, persistent phosphorylation of those sites. Since persistent phosphorylation of proline-directed sites in LC pretangles is

characteristic, this led us to choose the Ashe plasmid for E14 tau for insertion in the LC neurons. Human LC pretangle neurons also show an increase in 4R isoforms (Kelly et al., 2017), which is the backbone of the Addgene E-14 tau (0N/4R).

Here, we inserted htauE14 in the LC to initiate the human soluble hyperphosphorylated pretangle stages in tyrosine hydroxylase (TH)-Cre rats. We subsequently tested these rats for their ability to perform simple and difficult odor discriminations. We also examined the spread of human tau along the LC axons, LC neuron density, and fiber density in the primary olfactory (piriform) cortex. We correlated behavioral deficiency with LC pathophysiology at different stages in rats.

4.2 Methods

4.2.1 Ethics statement and subjects

Experiments were conducted following the guidelines of the Canadian Council of Animal Care. Experimental protocols were approved by the Memorial University Institutional Animal Care Committee. TH-Cre male rats (Sage) were bred with Sprague-Dawley (SD) female rats to generate the heterozygous offspring used in the experiments. Forty-four TH-Cre and twelve SD rats of both sexes were used in this study. Rats were housed on a 12- h light/dark cycle with ad libitum access to water and dry food. Water deprivation started 5 days before the behavioral tests in an olfactometer. During that period, rats had access to either ad libitum water for an hour per day or a total volume of 25 ml water per day.

4.2.2 Experimental design and statistical analysis

We first characterized AAV uptake and htauE14 expressions in the LC and spread to the serotonergic raphe neurons in our TH-Cre rats. We then conducted three experiments. In the first experiment, rats were infused with htauE14 AAV or control GFP-only AAV at 2–3 months of age, trained in the odor discrimination learning task at 2– 3 month post-infusion (~ 5 month of age), and sacrificed for brain histology and immunohistochemistry following the behavioral task (~ 6 month of age). In the second experiment, rats were infused at 2–3 months of age and trained in the olfactory tasks 7–8 months later (~ 10 months of age), followed by brain processing (~ 11 months of age). A subset of rats underwent either behavioral training or immunohistochemistry, but not both at these time points. In the third experiment, rats were infused at 14–16 months of age and trained in the olfactory discrimination task 6 months later (~ 20–22 months of age). Brain histology and immunohistochemistry were conducted 5–7 months post-infusion. A cohort of non-infused rats was used as a control in different age groups as well.

Two-way mixed ANOVAs followed by linear trend analyses were used to determine statistical significance for the difficult odor discrimination experiment and the habituation/dishabituation experiment. One-way ANOVAs and post-hoc Tukey's tests were applied to the experiments with > 2 group comparisons. All two group comparisons were subjected to Student's *t* tests (unpaired, two-tailed). Data are presented as mean ± SEM.

The primary outcome measure was the number of trials to criterion for the difficult similar odor discrimination task. Based on our previous investigation of such learning with adrenergic receptor blockade in the piriform cortex in rats (Shakhawat et al., 2015), an *n* of 4 rats/group is sufficient to detect normal acquisition of a difficult odor discrimination with a power of 0.74. Accordingly, all odor learning experiments had group sizes of at least 4/group.

Viral transduction of LC neurons by stereotaxic surgery We used a human tau construct in which 14 proline-directed phosphorylation sites were substituted with glutamate to produce a pseudophosphorylated tau (htauE14) (Braak et al., 2011). Adeno-associated virus 9 (AAV9) was used as a vector (AAV9-rEF1a-DIO-EGFP-htauE14; $2.26E^{+13}$ vg/ ml, MIT). The EGFP-htauE14 expression cassette was placed under a double inverted open reading frame (DIO) for Cre-dependent expression. Control virus lacked htauE14 (AAV9-rEF1a-DIO-EGFP, $2.35E^{+13}$ vg/ml). Under isofluorane anesthesia, TH-Cre rats were placed in a stereo- taxic. One microliter of virus mixed with 0.4 μl fluorescent beads (0.1%) was infused in each LC through an infusion pump and a guide cannula which was placed in a parasagittal plane at an angle of 20° caudal to the coronal plane. LC coordinates were 11.8–12.2 mm posterior, 1.3 mm bilateral, and 6.3 mm ventral with respect to the bregma.

4.2.3 Behavioral testing

4.2.3.1 Odor discrimination learning

Rats underwent go-no go odor discrimination training in a four-channel Knosys

olfactometer as described previously (Shakhawat et al., 2015; Shakhawat, Harley, & Yuan, 2014). Initially, rats were trained to lick a water delivery port for a reward of a 30-µl drop/lick following 1% orange odor presentation (S^+). Duration of the trial was 2.5 s with the first 0.5 s for odor presentation. A minimum of 6 licks delivered the reward. The intertrial interval was 5 s. Each rat underwent approximately 100 trials per day for 3 days before moving on to the simple odor discrimination phase, in which a 2% peppermint odor (S^-), not associated with reward, was added. In blocks of 20 trials, S^+ and S^- odors were presented an equal number of times in a random order. Each rat went through 5–10 blocks of training each day, until they reached a learning criterion of 3 consecutive blocks with at least 70% correct. Following successful simple odor discrimination, rats underwent difficult odor discrimination training in which a pair of similar odors had to be discriminated in order to get water reward. 0.001% heptanol vs. 0.001% heptanol and octanol at a 1: 1 ratio were used as the difficult odor pair. Rats were trained until the learning criterion was reached or until a certain number of blocks were completed. Odorants were prepared freshly for each experiment in 10 ml of mineral oil solvent.

4.2.3.2 Acute odor habituation/dishabituation test

In a modified version of a detection test described by Escanilla et al. (Escanilla et al., 2010), rats were tested with similar odors presented on sponges (O1 = 0.001% heptanol; O2 = 0.001% heptanol and octanol at 1:1 ratio). Following a 5- min habituation period inside a semi-transparent plastic box (600 x 600 x 600 mm^3), rats were presented with an odor-free sponge at one corner of the box for another 5 min. After that, 7 trials of sponge presentation

took place, of which the first 3 contained mineral oil, second 3 contained O1, and the last one contained O2. Each trial lasted 50 s with 5 min intertrial intervals. Each sponge contained 60 μl of odorant or mineral oil. Rat's sniffing time within a radius of 1 cm around the sponge was videotaped and measured offline during O1 and O2.

4.2.4 Histology and immunohistochemistry

Rats were anesthetized by intraperitoneal injection of a 50-mg/kg pentobarbital solution followed by transcardiac perfusion of 0.9% saline and 4% paraformaldehyde (PFA) respectively. The brains were extracted and left in PFA overnight at 4 °C and then transferred to a 20% sucrose solution the next day. Thirty-micrometer slices were cut in a Leica cryostat and collected on gelatin-coated glass slides for further processing.

For Nissl staining, the slides were brought to room temperature, and rehydration was performed by dipping the slides in decreasing concentrations of ethanol (100%, 95%, and 70%) for 3 min each and deionized water for 1 min followed by an aqueous solution of 0.5% cresyl violate acetate (Sigma) for 8 min. After 1 min in deionized water, the slides were dehydrated in increasing concentrations of ethanol (70%, 95%, and 100%) for 3 min each. Afterwards, a quick clearing step was performed by dipping the slides in xylene for 1 min. The slides were then coverslipped using Permount (Fisher Scientific).

Immunohistochemistry was performed by incubating the slides inside a humidified chamber overnight at 4 °C in primary antibodies (see Table 4.1), which were dissolved in phosphate-

buffered saline (PBS) and mixed with 2% normal goat serum and 0.25% Triton X-100. For fluorescence staining, after a 30-min wash in PBS, the slides were incubated in suitable secondary antibody (see Table 4.1) for 1 h at room temperature followed by a 30-min wash in PBS and mounting with DAPI (visualized as blue in the images). For amplification, following overnight primary antibody incubation, the slides were washed in PBS for 30 min and incubated in a suitable biotinylated secondary antibody (see Table 4.1) for 1 h. After a 30-min wash in PBS, an avidin and biotinylated enzyme amplification step (A+B) was applied. In the end, color was developed by a diaminobenzidine tetrahydrochloride (DAB) reaction [50 mg DAB (Amresco) + 50 ml PBS + 50 ml water + 30 μl 30% H_2O_2]. Antigen retrieval was performed by heating the slides in 10 mM sodium citrate buffer containing 0.05% Tween (pH adjusted to 6.0) at 90 °C for 15 min before incubating with tryptophan hydroxylase (TPH), NeuN, and β_1-AR primary antibodies.

Table 4.1 List of Antibodies

Primary Antibody	Company/ Product number	Primary antibody		Secondary antibody (Fluorescence)		Secondary antibody (Biotinylation-amplification)	
		Host	Conc.	Company/Product	Conc.	Company/Product	Conc.
Iba-1	Wako/ 019-19741	Rabbit	1:1000	Invitrogen/ A31572	1:500	-	-
β_1-AR	Abcam/ ab3442	Rabbit	1:400	-	-	Vector/ BA 1000	1:500
NET	Invitrogen/MA5-24647	Mouse	1:500	Invitrogen/ A31570	1:500	-	-
DBH	Millipore/ MAB308	Mouse	1:500	Invitrogen/ A31570	1:500	-	-
TPH	Sigma/ T0678	Mouse	1:400	Invitrogen/ A31570	1:500	Vector/ BA 9200	1:500
NeuN	Millipore/ MAB 377	Mouse	1:100	Invitrogen/ A31570	1:500	-	-
HT7	Invitrogen/MN1000	Mouse	1:500	Invitrogen/ A31570	1:500	Vector/ BA 9200	1:1000
GFP	Thermofisher A11122	Rabbit	1:200	Invitrogen/ A27034	1:500	-	-

4.2.4.1 Thioflavin-S staining

Slides were quenched of GFP signal first by heating at 90 °C for 10 min. After 5 min of defatting in xylene, slides were rehydrated in serial dilutions of ethanol (100%, 95%, 70%, 50%; 3 min each) and water (2 × 3 min). Then slides were incubated for 8 min in a filtered 1% aqueous solution of Thioflavin-S (Sigma) in the dark at room temperature. Washes with ethanol (70%, 2x3min; 95%, 3 min) and water (3 exchanges) followed before mounting with aqueous mounting media (Sigma).

4.2.4.2 Imaging analysis and quantification

Bright-field and fluorescence images were acquired by Apotome 2 (Zeiss) and BX-51 (Olympus). Images were analyzed with ImageJ software. For LC fiber density, images were background subtracted and converted into binary images. Fiber length was calculated using the DiameterJ plugin. For LC cell counts and Iba-1^+ cell count in the piriform cortex, the population density of neurons (number of neurons per unit area) was calculated and averaged over 3–6 sections rostral to caudal in each rat. LC neurons were identified from the Nissl stains following Garcia-Cabezas et al. (Garcia-Cabezas, John, Barbas, & Zikopoulos, 2016). For β_1-AR density in the piriform cortex, a region of interest (ROI) was manually traced over the layer II pyramidal cells of the anterior piriform cortex ventral to the lateral olfactory tract. An optical density (OD) reading of the background was taken in layer Ia for comparison. The relative OD (ROD) was calculated using the following formula: ROD = |(OD of ROI −

OD of background)/OD of background|. RODs from 3 to 4 sections were averaged for each animal.

4.3 Result

4.3.1 HtauE14 uptake in the LC and spread

LC neurons co-expressed htauE14 within 1 week of infusion (Figure 4.1a1–a3) and htauE14 became mislocalized to the LC cell bodies and dendrites (b) similar to the pathology in pretangle AD (Braak et al., 2011) and the htauE14 mislocalization reported in hippocampal neurons (Hoover et al., 2010). The transfection rate indexed by GFP^+ cells over DBH^+ LC neurons is 83.0 ± 4.3% in htauE14 rats (n = 9). The targeting to LC is shown in Additional file 1. At 6 weeks, htauE14 spread along LC axons toward forebrain targets, and by 12 weeks, htauE14 reached its furthest target, the olfactory bulb and other cortical areas such as the hippocampus and the piriform cortex (Additional file 2). At the same time, the spread of the GFP signal to pontine midline neurons was observed (Figure 4.1c1, c2). Using an antibody HT7 which detects human tau, we confirmed human tau co-localized with GFP in the LC (Figure 4.1d1–d3) and HT7 could be seen with light microscopy in the LC (Figure 4.1e1, e2). HT7 was also observed to have spread to putative raphe midline neurons (Figure 4.1f1, f2) as seen in humans (Ehrenberg et al., 2017; Stratmann et al., 2016). The location of midline raphe neurons in rats is indicated by TPH staining (Additional file 3). We confirmed GFP co-localization in raphe neurons with TPH (Figure 4.1g1–g3).

We have attempted to index tau hyperphosphorylation with the AT8 antibody. However, staining was not observed (Additional file 4). Some phosphorylation site- specific antibodies

such as AT8 typically do not recognize sites that are pseudophosphorylated (Eidenmuller et al., 2000). Nevertheless, we could demonstrate that pseudophosphorylated human tau was expressed in our tissue by the HT7 antibody.

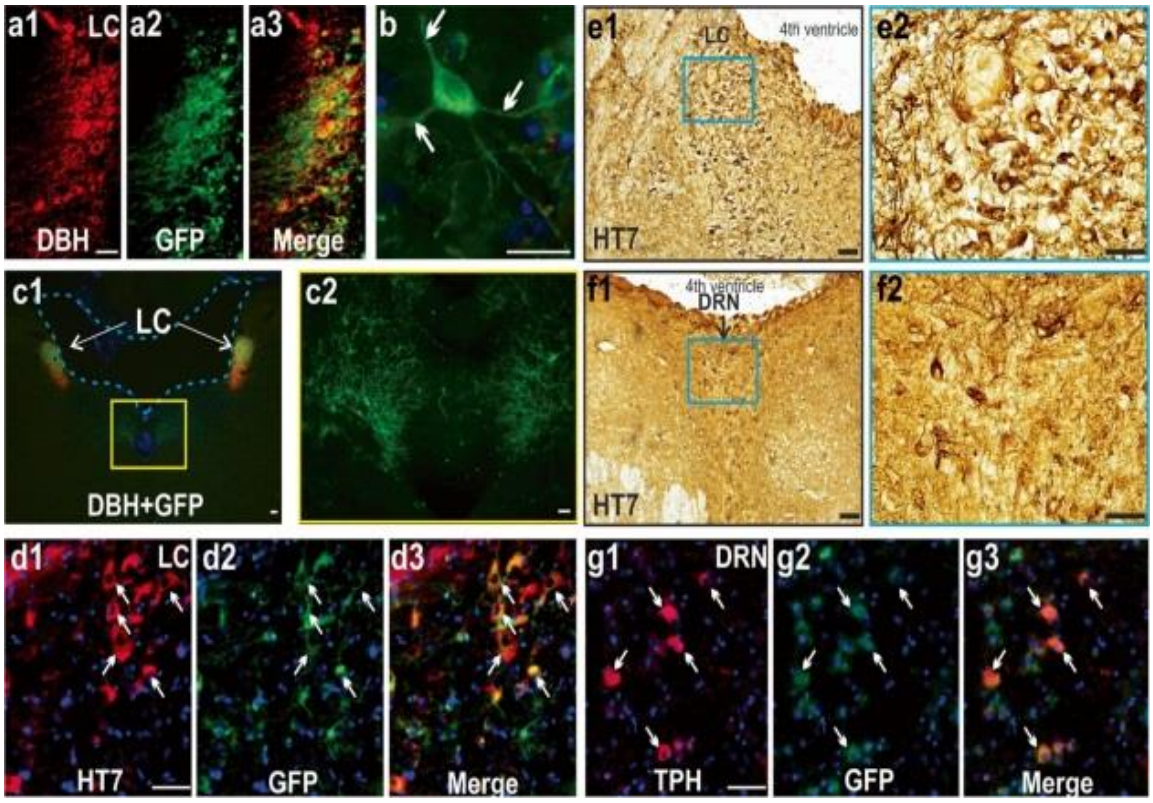

Figure 4.1 **HtauE14 uptake in the LC and spread**.

a1–a3 Expression of htauE14 (green) in DBH (red) LC neurons in a rat. b Somatodendritic mislocalization of htauE14 in an LC neuron (arrows). c1 Spread of htauE14 to the midline brain stem in an 8-month-old rat (12 weeks post-infusion). c2 Enlargement of GFP cells in c1 (yellow box). d1–d3 HT7 (red) expression in the LC in a 19-month-old rat (7 months post-infusion). Arrows indicate GFP and HT7 co-expressed cells. e1–e2 HT7 staining in the LC in the same rat as in d. f1–f2 Midline $HT7^{+}$ dorsal raphe neurons (DRN). g1–g3 Co-expression of GFP and TPH in cells (indicated by arrows) in the midline. Scale bar, 50 μm

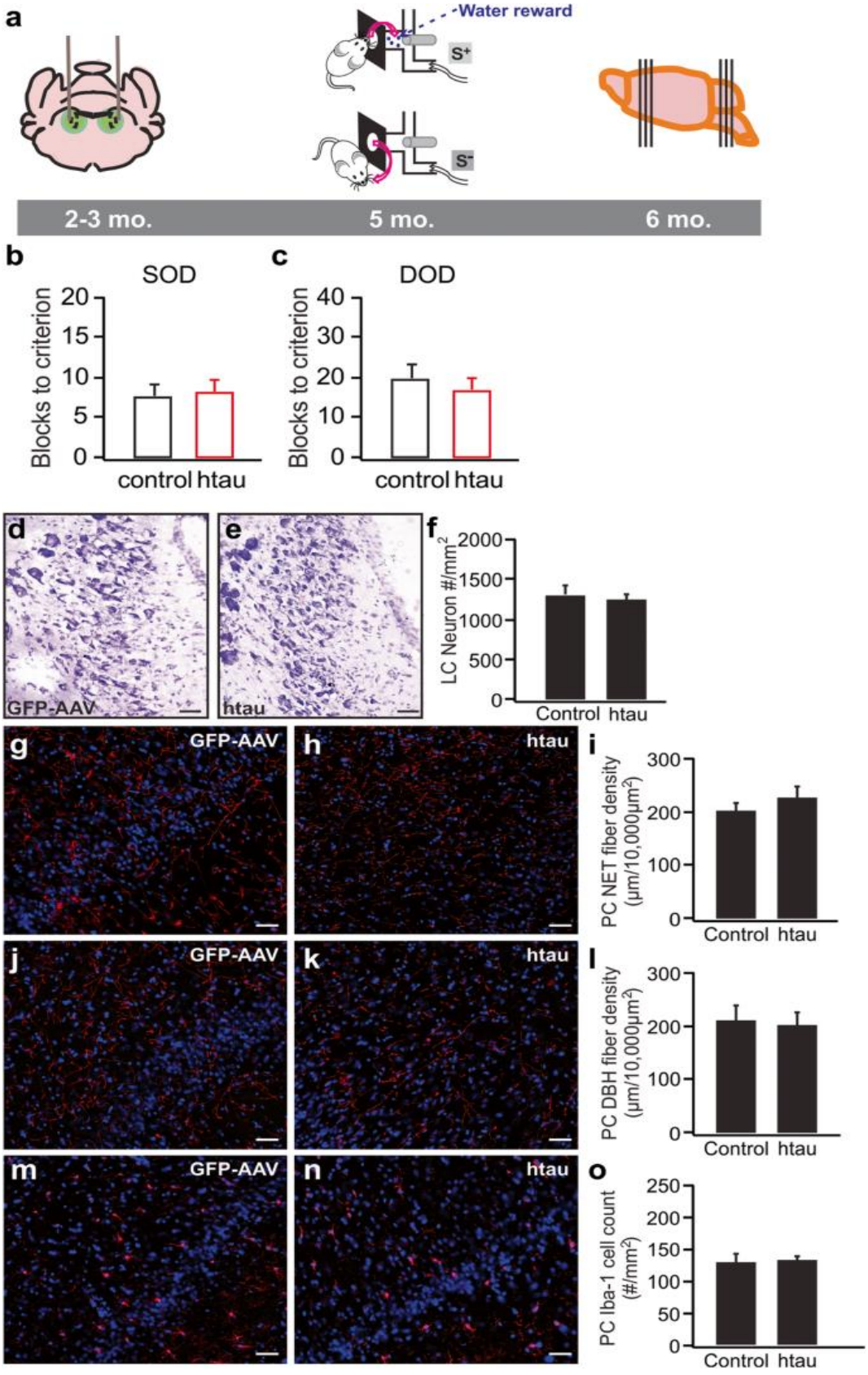
a
Water reward
S+
S-
2-3 mo.
5 mo.
6 mo.
b
SOD
Blocks to criterion
20
15
10
5
0
control htau
c
DOD
Blocks to criterion
40
30
20
10
0
control htau
d
GFP-AAV
e
htau
f
LC Neuron #/mm2
2000
1500
1000
500
0
Control htau
g
GFP-AAV
h
htau
i
PC NET fiber density (µm/10,000µm2)
300
200
100
0
Control htau
j
GFP-AAV
k
htau
l
PC DBH fiber density (µm/10,000µm2)
300
200
100
0
Control htau
m
GFP-AAV
n
htau
o
PC Iba-1 cell count (#/mm2)
250
200
150
100
50
0
Control htau

Figure 4.2 **No odor discrimination deficiency or LC degeneration in young 6-month-old rats infused with htauE14 at 2–3 months old**.

a Schematics of the time course of the AAV infusion, odor discrimination training, and histology. b Simple odor discrimination (SOD) training using dissimilar odors. c Difficult odor discrimination (DOD) training using similar odor pairs. (N: htau/control: 6/4). d–f LC cell counts in htauE14 and control rats. (N: htau/control: 5/5). g–i NET fibers (red) in the piriform cortex (PC). (N: htau/control: 6/5). j–l DBH fibers (red) in the PC. (N: htau/control: 6/5). m–o Iba-1 cell staining (red) in the PC. (N: htau/control: 6/5). Scale bars, 50 μm; DAPI in blue.

4.3.2 HtauE14 in young adult LC: 3–4 months post-infusion

In humans, AD-associated soluble persistently phosphorylated tau as indexed by the AT8 antibody first appears in the LC in a minority of individuals prepubertally (Braak & Tredici, 2011) but is observed nearly universally by 40 years of age (Braak et al., 2011; Braak & Tredici, 2015). Despite the prevalence of pretangle tau in LC, the early effects of this tauopathy in middle-aged humans are unknown. Our model mimics the early expression of soluble persistently phosphorylated tau in LC through the infusion of htauE14 in 2–3-month-old rats. We subsequently first examined physiological and cognitive changes in adult rats 5–6 months old (3–4 months post-infusion; Figure 4.2), a time point at which, besides abnormal tau expression in LC and its projection along LC axons to the olfactory cortex (piriform), transfer of abnormal tau to other midline brain stem cell groups have been observed. Both htauE14 rats and control rats were subjected to odor discrimination training 3 months post-infusion, and brain histology and immunohistochemistry were conducted at 4 months post-infusion, following the odor discrimination task (Figure 4.2a).

The htauE14 rats showed no deficiency in either dissimilar (no. of blocks to reach learning criterion 7.75 ± 1.25, $n = 4$ in control vs. 8.33 ± 1.28, $n = 6$ in htauE14, $t = 0.31$, $p = 0.76$; Figure 4.2b), or similar odor discrimination learning (no. of blocks to reach learning criterion 20.50 ± 2.60, $n = 4$ in control vs. 17.17 ± 2.48, $n = 6$ in htauE14, $t = 0.89$, $p = 0.40$; Figure 4.2c). In parallel, htauE14 rats showed no LC cell loss (htauE14 1276.2 ± 38.6/mm^2, $n = 5$ vs. control 1339.4 ± 86.8/mm^2, $n = 5$, $t = 0.67$, $p = 0.52$; Figure 4.2d–f), no difference in norepinephrine transporter (NET) fiber density in the piriform cortex (htauE14 227 ± 21.3

μm/10, 000 μm^2, n = 6 vs. control 204.6 ± 12.5 μm/10,000 μm^2, n = 5, t = 0.85, p = 0.41; Figure 4.2g–i), and no difference in DBH fiber density (htauE14 203.7 ± 21.9 μm/10,000 μm^2, n =6 vs. control 212.8 ± 26.2 μm/10,000 μm^2, n = 5, t = 0.27, p = 0.79; Figure 4.2j–l). Iba-1 staining was not different in the two groups (htauE14 132.2 ± 6.7 #/mm^2, n =6 vs. control 131.2 ± 12.8 #/mm^2, n = 5, t = 0.07, p = 0.94; Figure 4.2m–o).

Together, these results suggested that the initial pretangle stages are not linked to the difficulties in odor discrimination, consistent with the lack of olfactory identification deficits in humans in a preclinical stage, despite pretangle abnormal tau being present universally at age 40.

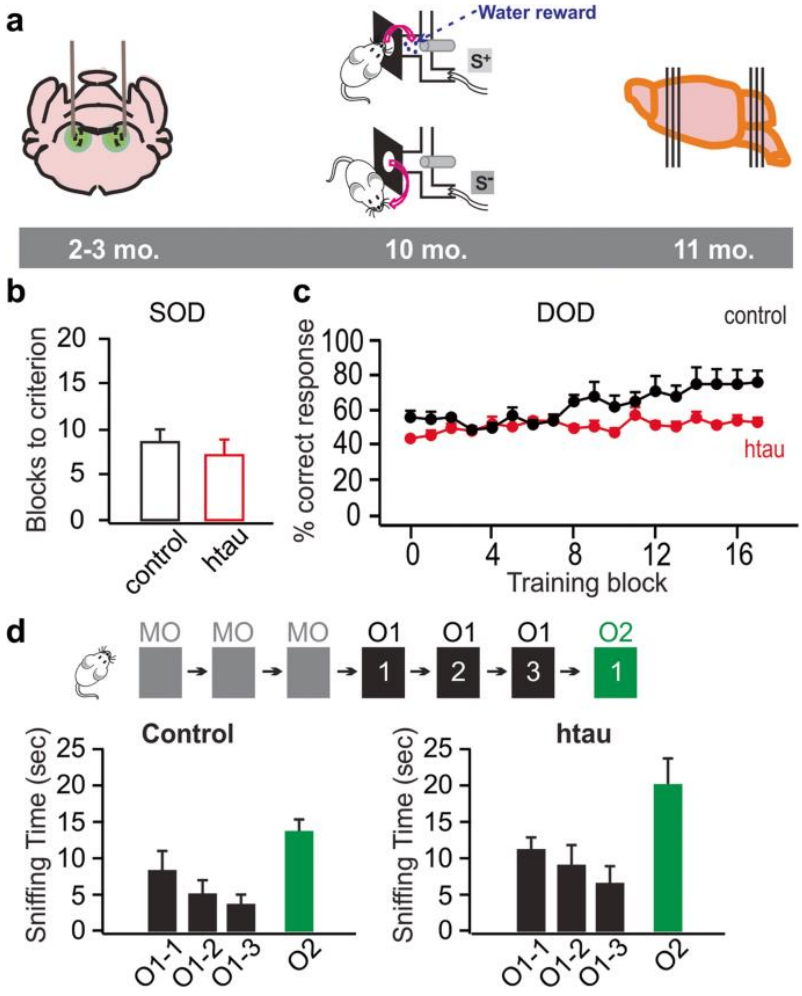

Figure 4.3 **Impairment in go/no-go odor discrimination learning in 10-month-old rats infused with htauE14 at 2–3 months old**.

a Schematics of the time course of the AAV infusion, odor discrimination training, and histology. b Simple odor discrimination (SOD) training using dissimilar odors. (N: htau/control: 7/7). c Difficult odor discrimination (DOD) training using similar odor pairs. (N: htau/control: 6/5). d Odor habituation/ dishabituation test. (N: htau/control: 6/7). MO, mineral oil. O1, odor 1. O2, odor 2

4.3.3 HtauE14 in young adult LC: 7–8 months post-infusion

We next examined rats that were 7–8 months post- infusion (Figure 4.3a). Unlike the earlier time point, by 7 months post-infusion, htauE14 rats did exhibit deficiency in difficult, similar odor discrimination learning. While there was no difference in simple, dissimilar odor discrimination learning (no. of blocks to reach learning criterion 8.6 ± 1.25, $n = 7$ in control vs. 7.1 ± 1.52, $n = 7$ in htauE14, $t = 0.72$, $p = 0.48$; Figure 4.3b), we observed a significant impairment in difficult similar odor discrimination learning in the htauE14 rats compared to the same aged GFP control rats (Figure 4.3c). A 2 (group) × 18 (block) ANOVA revealed that the htauE14 group performed more poorly than the control group in the difficult similar odor discrimination ($F_{1, 9} = 30.319$, $p < 0.001$). There was also a block effect ($F_{17, 153} = 6.309$) and a group × block interaction ($F_{17, 153} = 4.237$, $p < 0.001$). An analysis of the interaction revealed that the htauE14 group's performance did not change over the 18 blocks ($F_{17,102} = 1.145$, $p = 0.324$) while the control group did differ over blocks ($F_{17, 51} = 4.485$, $p < 0.001$). Subsequent linear trend analysis showed that the control group improved over blocks ($F_{1, 3} = 14.467$, $p = 0.032$). This absence of a change in the htauE14 rats and improvement in the control rats shows that htauE14 LC expression impaired the capacity of the rats to learn a difficult odor discrimination relative to controls. Another cohort of rats, comparable in age and post-infusion times, was tested with the difficult odors used for the previous discrimination task in an odor habituation/ dishabituation task ($n = 7$ control and $n = 6$ htauE14; Figure 4.3d). A 2 × 3 ANOVA (group × odor presentation) revealed a significant effect of odor presentation ($F_{(2, 22)} = 9.45$, $p < 0.001$) but no group × odor presentation interaction ($F_{(2, 22)} = 0.274$, $p = 0.763$) or group effect ($F_{(1, 11)} = 1.605$, $p = 0.231$). The odor presentation effect reflected a habituation to

the odor by both groups as indicated by a significant linear trend ($F_{(1, 11)} = 17.639$, $p < 0.001$). A 2 × 2 (group × last trial of odor 1 versus new odor 2) ANOVA revealed a significant difference between the odor 1 and new odor 2 ($F_{(1, 11)} = 22.418$, $p < 0.001$) and no group × odor interaction ($F_{(1, 11)} = 0.570$, $p = 0.466$) or group effect ($F_{(1,}11) = 4.114$, $p = 0.07$). This pattern of results argues that the rats that failed the difficult discrimination learning were likely to have been able to detect the odor differences.

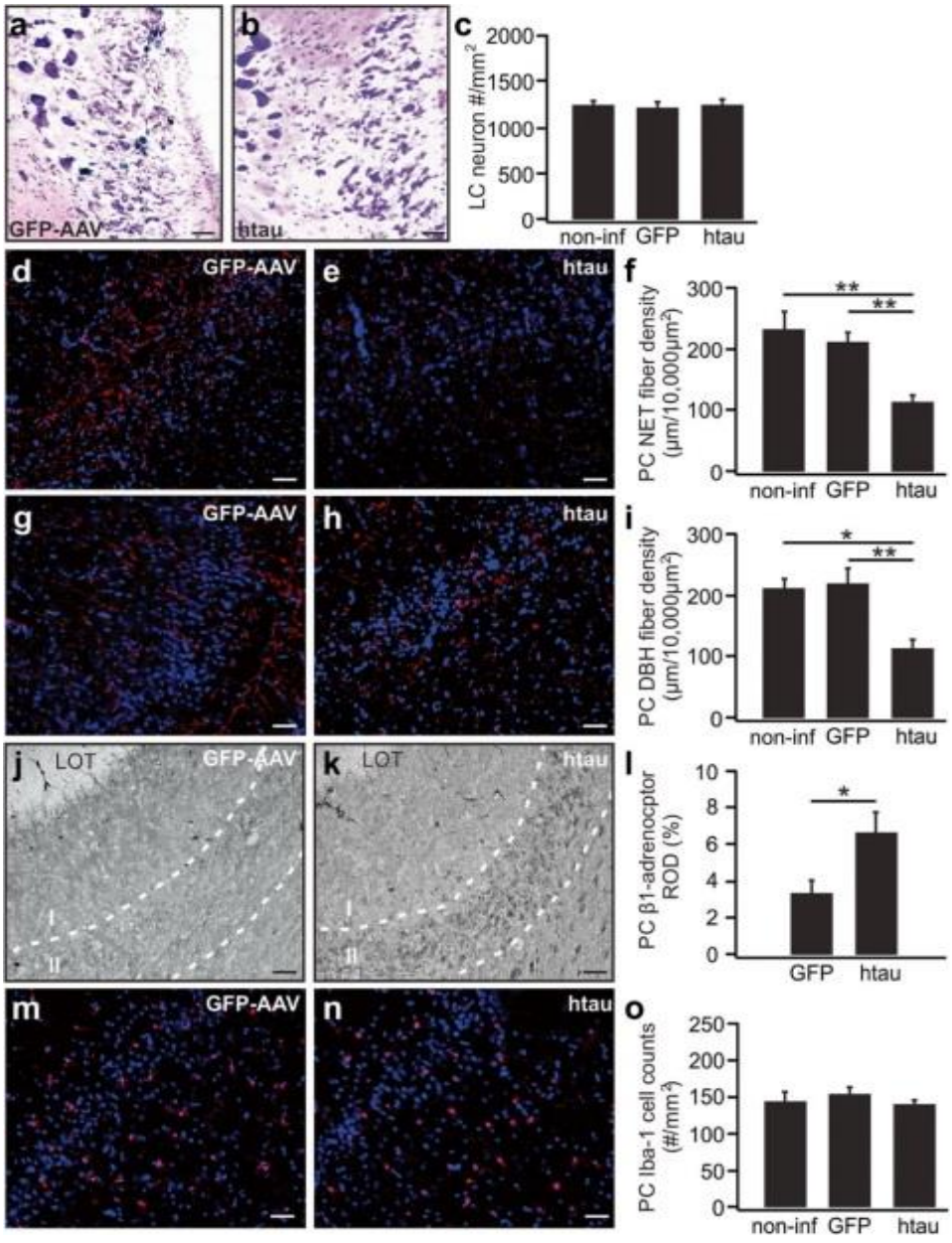

Figure 4.4 **LC axonal degeneration in 11-month-old rats infused with htauE14 at 2–3 months old**.

a–c LC cell counts in htauE14 and control rats. (N: htau/GFP/ non-infused: 7/6/6). d–f NET fibers (red) in the piriform cortex (PC) (N: htau/GFP/non-infused: 6/6/5). g–i DBH fibers (red) in the PC. (N: htau/GFP/non-infused: 6/5/5). j–l β_1-adrenoceptors in the PC. (N: htau/GFP: 4/4). m–o Iba-1 in the PC. (N: htau/GFP/non-infused: 6/5/6). LOT, lateral olfactory tract. Scale bars, 50 µm; DAPI in blue.

Nissl staining and cell counting of 11-month-old htauE14 and control rats (EGFP and non-infused) demonstrated no LC cell loss ($F_{(2, 16)} = 0.17$, $p = 0.84$; Figure 4.4a–c), but significant NET fiber loss in the piriform cortex of the htauE14 rats indexed by either NET fiber density ($F_{(2,14)} = 12.43$, $p = 7.9E{-}4$; Figure 4.4d–f) or DBH fiber density in the piriform cortex ($F_{(2, 13)} = 14.98$, $p = 4.2E{-}4$; Figure 4.4g–i). HtauE14 rats showed comparable levels of LC cell numbers (1277.7 ± 45.7/mm^2, $n = 7$) to either GFP control rats (1235.8 ± 55.8/mm^2, $n = 6$) or non-infused rats (1260.3 ± 52.3/mm^2, $n = 6$). On the other hand, the htauE14 group showed a significant reduction in the NET fibers (111 ±11.5 μm/10,000 μm^2, $n = 6$) compared to either GFP controls (212.2 ± 16.4 μm/10,000 μm^2, $n = 6$, $p = 7.5E{-}4$) or non-infused controls (233.2 ± 27.8 μm/10,000 μm^2, $n = 5$, $p = 0.001$). Similarly, DBH fiber density was significantly lower in the htauE14 rats (114.8 ± 10.8 μm/10,000 μm^2, $n = 6$) compared to either GFP controls (220.8 ± 21.9 μm/ 10,000 μm^2, $n = 5$, p = 0.001) or non-infused controls (213.2 ± 14.1 μm/10,000 μm^2, $n = 5$, $p = 0.002$). The LC axonal degeneration in the piriform cortex is accompanied by an upregulation of β_1-ARs (ROD 0.07 ± 0.01 (htauE14) vs. 0.03 ± 0.005 (GFP), $n = 4$, $t = 2.52$, $p = 0.045$; Figure 4.4j–l). However, Iba-1 staining of the microglia in the piriform cortex indicated no elevated microglia in the piriform cortex ($n = 6$ htauE14; $n = 5$ GFP; $n = 6$ non- infused control; $F_{(2, 14)} = 0.94$, $p = 0.41$; Figure 4.4m–o).

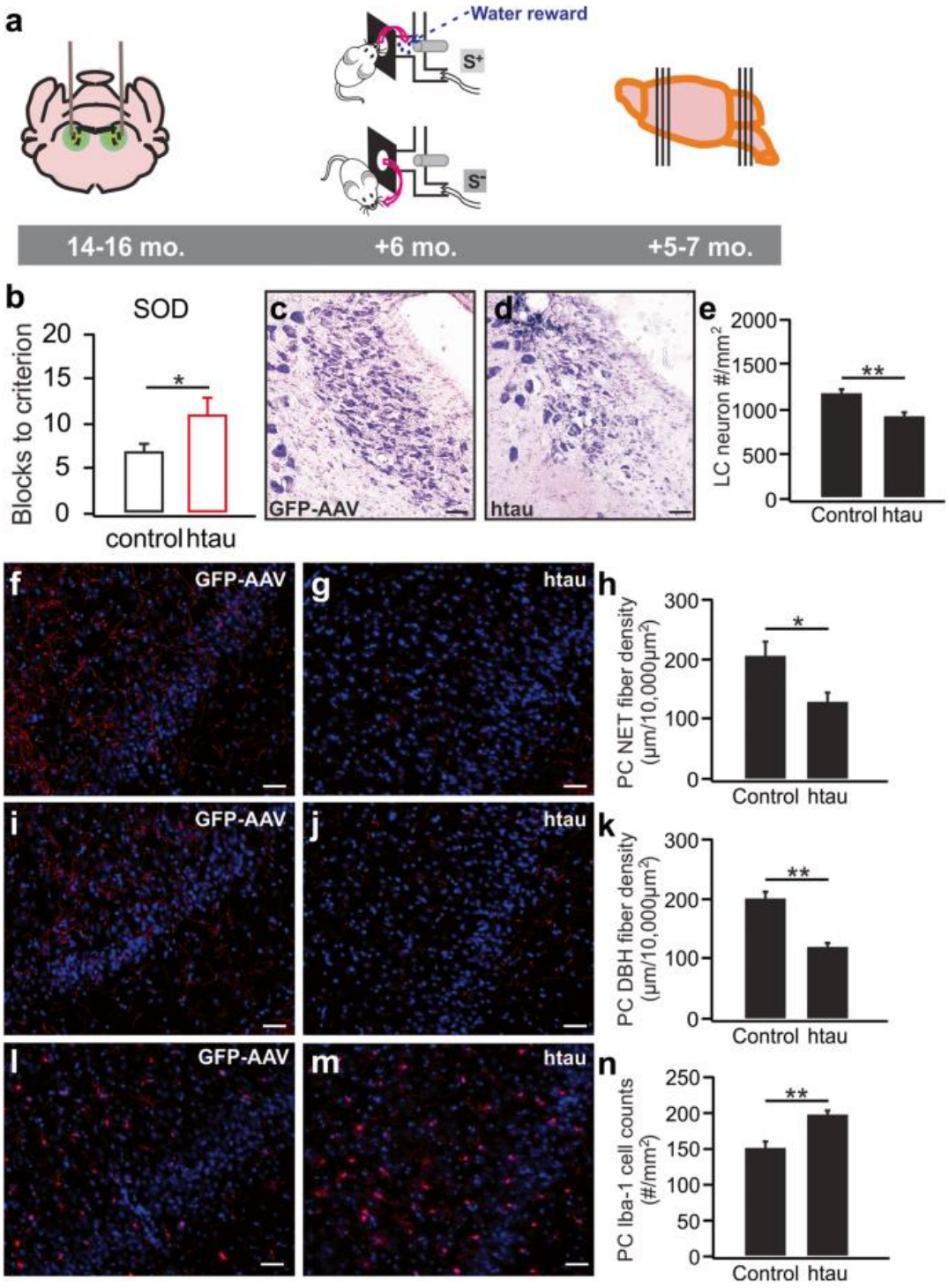
a
Water reward
S+
S-
14-16 mo.
+6 mo.
+5-7 mo.
b
SOD
Blocks to criterion
20
15
10
5
0
*
control
htau
c
GFP-AAV
d
htau
e
LC neuron #/mm2
2000
1500
1000
500
0
**
Control
htau
f
GFP-AAV
g
htau
h
PC NET fiber density (µm/10,000µm2)
300
200
100
0
*
Control
htau
i
GFP-AAV
j
htau
k
PC DBH fiber density (µm/10,000µm2)
300
200
100
0
**
Control
htau
l
GFP-AAV
m
htau
n
PC Iba-1 cell counts (#/mm2)
250
200
150
100
50
0
**
Control
htau

Figure 4.5 **Deficiency in odor discrimination and LC degeneration in 17−20-month-old rats infused with htauE14 at 12−14 months old**.

a Schematics of the time course of the AAV infusion, odor discrimination training, and histology. b Simple odor discrimination (SOD) training using dissimilar odors. (N: htau/GFP: 4/7). c−e LC cell counts in htauE14 and control rats. (N: htau/GFP: 6/5). f−h NET fibers (red) in the piriform cortex (PC). (N: htau/GFP: 6/6). i−k DBH fibers (red) in the PC. (N: htau/GFP: 6/6). l−n Iba-1 staining in the PC. (N: htau/GFP: 6/6). Scale bars, 50 μm; DAPI in blue.

4.3.4 HtauE14 in LC of 14–16-month-old rats: 5–7 months post-infusion

To compare the potential differential effects of early onset vs. late onset tau-pathology originating in the LC, we conducted an experiment in rats infused with AAV at an older age (14–16 months old; Figure 4.5a). Six months post- infusion, htauE14 rats demonstrated more severe behavioral deficiency than rats infused at a young age (2–3 months old) had exhibited after a similar post-infusion interval. The older infused htauE14 rats were impaired in learning the first simple, dissimilar odor discrimination task (no. of blocks to reach learning criterion 7 ± 0.62, $n = 7$ in control vs. 11 ± 1.7, $n = 4$ in htauE14, $t = 2.71$, $p = 0.024$; Fig. Figure 4.5b). There was also significant LC cell loss in the older infused htauE14 rats (917 ± 57.8/ mm^2, $n = 6$) compared to their age-matched controls (1181.7 ± 55.7/mm^2, $n = 5$, $t = 3.28$, $p = 0.01$; Figure 4.5c–e).

As in the younger infused rats, NET fiber density in the piriform cortex of the older infused htauE14 rats (131.2 ± 13.7 μm/10,000 μm^2, $n = 6$) was significantly lower than in control rats (208.5 ± 22.4 μm/10,000 μm^2, $n = 6$, t = 2.94, $p = 0.015$; Figure 4.5f–h). DBH fiber density was also significantly lower in the htauE14 rats (121.7 ± 7.4 μm/10,000 μm^2, $n = 6$) compared to control rats (201.7 ± 13.0 μm/10,000 μm^2, $n = 6$, $t = 5.36$, $p = 3.21E{-}4$; Figure 4.5i–k). Additionally, there was an increased density of Iba-1^+ microglia cells in the piriform cortex in htauE14 rats (htauE14 197.3 ± 6.2/mm^2, $n = 6$ vs. control 151.7 ± 9.3/mm^2, $n = 6$, $t = 4.10$, $p = 0.002$; Figure 4.5l–n). There was no evidence of tangles as indexed by Thioflavin-S staining in the older infused htauE14 rats (Additional file 5).

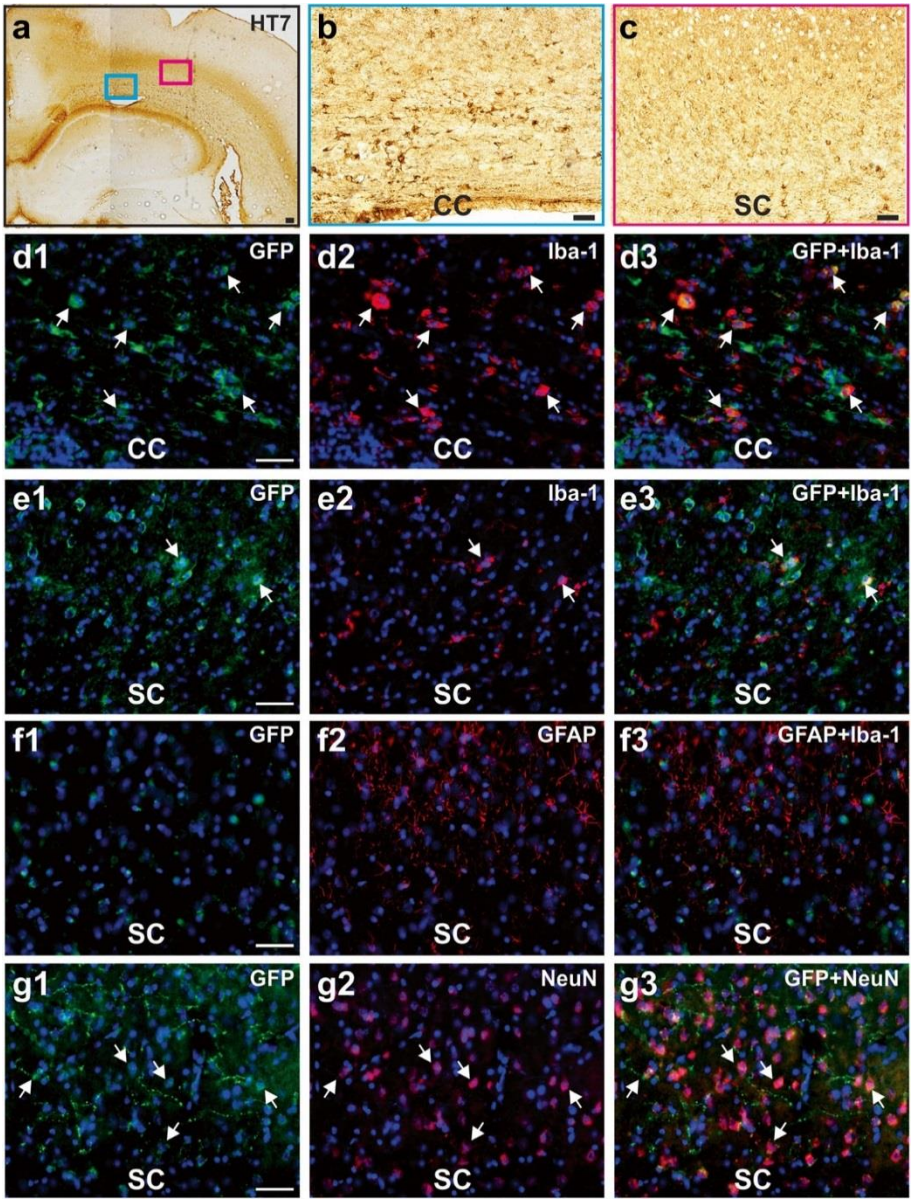

Figure 4.6 **HtauE14 release and uptake by neurons and microglia in an old AD rat**. a HT7 staining in a 21-month-old rat, 7 months post-infusion. Scale bar, 200 μm. b Enlargement of a region in the corpus callosum (CC) in A. c Enlargement of a region in the sensory cortex (SC) in A. d1–d3 GFP^+ cells in the CC and some co-localization with Iba-1^+ microglia. e1–e3 GFP^+ cells in the sensory cortex (SC) and some co-localization with Iba-1^+ microglia. f1–f3 No co-localization of GFP and $GFAP^+$ cells. g1–g3 GFP^+ cells in the SC co-localized with NeuN. Scale bars, 50 μm

Finally, in old rats, we observed neuron to microglia spread as well as transneuronal spread (Figure 4.1 e-g and Figure 4.6). $HT7^+$ cells were observed both in the genu of the corpus callosum and in the overlying sensory cortex (Figure 4.6a–c). Co-labeling with the microglia marker Iba-1 was observed in both the corpus callosum (Figure 4.6d1–d3) and sensory cortex (Figure 4.6e1–e3). Astrocyte marker GFAP showed no co-localization with GFP cells (Figure 4.6f1–f3). However, co-labeling with NeuN was also observed (Figure 4.6 g1–g3). DAPI in blue. Additional file 6 shows zoomed in images of individual cell types.

4.4 Discussion

The rats expressing hyperphosphorylated human tau in the LC in these experiments show similarities to the human pretangle stages described by Braak (Braak et al., 2011; Braak & Tredici, 2015). They exhibit abnormal tau somatodendritic mislocalization; transport of abnormal tau along LC fibers as far as the olfactory bulb by the first time point examined, 3–4 months post-infusion; and transfer of abnormal tau to the brain stem neurons, including the raphe neurons, by the same time point. Since abnormal tau is expressed in the LC neurons as early as 1 week after infusion, its influence on LC function would have been long-standing by 3–4 months post-infusion.

Despite LC pretangle tau expression, distribution, and transfer, rats 3–4 months post-infusion were not impaired on the difficult similar odor discrimination task that is sensitive to attenuation of LC input to piriform (Shakhawat et al., 2015). This parallels the human

condition, since pretangle LC stages appear in people between 10 and 30 years of age, including transfer to the subcortical nuclei, most consistently, the raphe nuclei, with further extension along the LC axons to the terminal regions from 30 to 50 years of age. During this time frame, there is little evidence of olfactory dysfunction (Doty et al., 1984).

Congruent with our hypothesis that early olfactory deficits in rats, as in humans, are predictive of pretangle progression toward AD, we find that 7–8 months post- infusion, there are two changes in rats expressing abnormal LC tau. First, LC htauE14 rats are now impaired in difficult olfactory discrimination, though they acquire the simple odor discrimination normally. The impairment in difficult odor learning is not due to the inability to detect a difference in the odor mixtures that were used, as rats showed normal detection in the habituation/dishabituation task with the same odor pair. This is also consistent with a requirement for pattern separation-dependent associative memory to solve the difficult odor discrimination task. While pattern separation itself implies the ability to remember a distinct input among other similar inputs, in the brain, we have previously shown that only associative learning of pattern separation using similar odors is indexed by increased distinctiveness of neuronal ensembles representing the two odors in the rat piriform cortex (Shakhawat et al., 2014).

Second, there is a significant reduction of LC fiber density in the piriform cortex as measured by NET or DBH fiber density. There is also upregulation of β_1-ARs in the piriform cortex. This compensatory increase of β-AR density with LC fiber loss is well known (Minneman, Dibner, Wolfe, & Molinoff, 1979). The increase in β-ARs may be compensatory but may also lead to deleterious effects. For example, CA3 hyperexcitability,

a brain aging change associated with cognitive impairment in rodents and humans (Haberman, Branch, & Gallagher, 2017; Huijbers et al., 2019), could be linked to increases in β- AR activation (Jurgens et al., 2005).

We suggest the difficult olfactory discrimination impairment is driven by the reduction in LC fibers, since a pharmacological cocktail blocking LC input to rat piriform prevents acquisition of a difficult, but not simple, odor discrimination (Shakhawat et al., 2015). While it has been thought that olfactory identification deficits with aging are likely related to the sensory changes seen generally in peripheral tissue, e.g., olfactory epithelium, Devanand has suggested that these changes are early indicators of pretangle stage progression (Devanand, 2016). In a study examining olfactory, visual, and auditory aging changes related to cognitive decline, only the olfactory identification deficit predicted decline (MacDonald et al., 2018). Our data also suggest that refinement of olfactory identification tasks, for example, by increasing odorant similarity during associative learning may lead to improved detection of preclinical Alzheimer's disease as proposed by Hsieh et al. (Hsieh, Keller, Wong, Jiang, & Vosshall, 2017).

The reduction in LC fiber input here is consistent with the reports that norepinephrine (NE), the primary LC neurotransmitter, is reduced in AD (Palmer et al., 1987). In AD, measures of LC fiber density using DBH also demonstrate reduced NE fiber density (Powers et al., 1988). Since tau facilitates axonal transport, it is not surprising that sustained production of abnormal tau eventually leads to reduced axonal support and results in axonal degeneration.

Similar to our findings here, a transgenic rat AD amyloid model in which hyperphosphorylated tau is also generated early in LC neurons exhibits a reduction in NE fiber density, in this case, in the allocortex and medial prefrontal cortex (Rorabaugh et al., 2017). In the transgenic model, as in the present model, there was no change in LC neuron number with the reduction in LC fiber density. As here, this is congruent with the preclinical human data. LC neurons are not lost in AD until Braak's stage III, when memory problems appear (Kelly et al., 2017; Weinshenker, 2018). In the transgenic rat model, rats showed deficits in spatial reversal learning. An exciting feature of the transgenic rat study was the ability of chemogenetic LC activation to eliminate the cognitive impairment thought to be associated with LC pretangles. Thus, LC activation, even in the presence of hyperphosphorylated tau, has the ability to contribute positively to learning and memory and may provide a key target for therapeutic intervention as proposed earlier (Mather, Clewett, Sakaki, & Harley, 2016). It would be of interest to examine the effects of LC activation in the present paradigm.

While consistent with the present results, the transgenic model cannot rule out a contribution of amyloid, since it is the fundamental feature of these transgenic rats and is produced in concert with the observed LC hyperphosphorylated tau. However, the present study underscores the ability of abnormal LC tau alone to drive pathology and cognition in preclinical AD as proposed by Braak.

The availability of PET markers for quantifying NET fiber density in the human brain means LC fiber density could be assessed in imaging studies (Ding et al., 2010; Moriguchi et al., 2017; Rami-Mark et al., 2015; Takano et al., 2008). An aging- related decline in LC NET

(Ding et al., 2010) consistent with LC volume loss with age in humans (Theofilas et al., 2017) has been observed. This methodology would permit a test of the prediction from the LC hyperphosphorylated tau rat models that pretangle LC tau eventually induces regression of LC axonal innervation in some, or all, cortical structures. The rat models suggest this change may be one of the earliest biomarkers of pretangle progression to AD.

In the last experiment, we showed the time course of deleterious pretangle effects is influenced by the age of the rat at initiation. The ability to manipulate the initiation of pretangle stages longitudinally is a strength of the model. Braak's human data suggest there is a long time window associated with pretangle progression. When rats were infused with the htauE14 gene at 14–16 months, their olfactory learning impairment 6 months later is more dramatic than that seen in young adult infused rats. They are impaired in acquiring, even, a simple odor discrimination. The importance for odor in a rat's life suggests difficulty in simple odor memory acquisition may index the beginning of impairments in daily living activities from a rodent point of view or may correspond to the beginning of mild cognitive impairment for these animals. This would parallel Braak stages III–IV when LC cell loss begins to be seen in humans. However, the limitation of this study is that our model does not mimic the tangle formation occurring in the human Braak stages.

Consistent with the relationship between mild cognitive impairment and LC cell loss in humans, LC cell loss was seen in the rats infused at 14–16 months when simple odor acquisition became difficult. There was also an increase in piriform microglial density. Increases in microglia density have been reported with AD (Marlatt et al., 2014; Perez et al.,

2017). Thus, age significantly modulates the progression and expression of pathology associated with LC pretangles. In our model, older rats exhibit cognitive deficits, despite the absence of tangles. This supports the suggestion that soluble hyperphosphorylated tau may be the more toxic species and be driving deleterious AD changes (Cowan & Mudher, 2013). The deleterious effects of pretangles only occurred in aged rats, however, congruent with the observation that AD is an aging disorder.

Another important observation in the older rats is the uptake of htauE14 by microglia in the corpus callosum and overlying cortex and the transfer of htauE14 to the cortical neurons. Uptake of hyperphosphorylated tau by microglia has been reported in AD (Bolos et al., 2016). The concentration of microglia containing htauE14 in the corpus callosum may relate to the white matter changes reported in AD (Mayo, Mazerolle, Ritchie, Fisk, & Gawryluk, 2017; Paola et al., 2010; Paola et al., 2015; Woodward, Dwyer, et al., 2017). Microglia could play a role in the spread of hyperphosphorylated soluble tau (Hopp et al., 2018; Leyns & Holtzman, 2017). In both young and older rat brains, hyperphosphorylated soluble tau spreads to neurons. This is likely to relate to the extra- cellular release of tau and may, or may not, involve exosomes (Schultz et al., 2018). The early transfer to the raphe neurons appears pathway specific in humans and in our rat model. Later transfer may become increasingly diffuse since ultimately most of the forebrain expresses neuronal hyperphosphorylated tau and tangles in late AD.

The present observations suggest that the LC supplies abnormal tau for both neuronal and microglial uptake. Similar transfer has been observed in another recent rodent hyperphosphorylated tau model (Schultz et al., 2018). While these observations do not rule

out prion-like transfer, they suggest that such spread is likely to co-occur with spread originating from the initial source of abnormal tau, and in our model and in humans, that is the LC.

Strengths of the htauE14 model

The htauE14 model provides control of selective expression of a functionally persistent phosphorylated human tau in LC neurons. The distribution of htauE14 corresponds to the distribution of pretangles described in Braak's study (Braak et al., 2011) of human brains from 1 to 100 years of age including its early transneuronal spread to the raphe neurons.

Age strongly modulates the htauE14 pathophysiology with more serious effects of htauE14 expression in older rats. There is no learning deficit or loss of LC neurons in young adult rats, similar to the lack of either a behavioral or pathological signature in young adult humans. In the equivalent of rat late middle age, an impairment in difficult olfactory discrimination learning appears concomitant with LC axonal regression in the olfactory piriform cortex. Difficulty with simple olfactory discrimination learning only appears with htauE14 expression in older rats and with LC neuron loss, providing functional and pathological parallels to symptomatic AD.

The htauE14 model provides a testbed for therapeutic strategies to increase the health of LC neurons and/or to prevent or slow the pathological and functional sequelae of pretangle spread from LC. Importantly, the spread of htauE14 to other neurons and microglial cells means this model can be used to elucidate the mechanisms underlying the selective spread of pathology in preclinical AD. Predictions based on the htauE14 model can be tested in

humans using PET-NET imaging. A prediction of the present dataset is the reduction of LC axonal innervation in olfactory areas indexed by NET when deficits in olfactory discriminative memory appear. If validated, this may provide the earliest biomarker of LC pretangle-associated brain changes.

Limitations of the htauE14 model

While the data suggest that deficiencies in associative olfactory memory are an early indicator of a declining LC functional support due to NE axonal retraction in the piriform cortex, deficits in olfactory identification memory are not specific for AD. In particular, similar deficits in olfactory identification are also seen in individuals who go on to develop Parkinson's disease (Benarroch, 2010; Bowman, 2017; Doty, Deems, & Stellar, 1988), athough other forms of palsy are not associated with olfactory identification deficits (Doty et al., 1993). Thus, testing olfactory identification deficits, while possibly useful in differentiating AD from other causes of later memory decline, does not provide a selective signature of preclinical AD.

Nonetheless, it appears that there is a link between the two neurodegenerative conditions that relates to failure in LC function (Ding et al., 2010; Liddell & White, 2018; Peterson & Li, 2018; Post, Lieberman, & Mosharov, 2018; Vermeiren & Deyn, 2017). Abnormal α-synuclein accumulation in the LC is one of the earliest features of Parkinson's disease, and the accumulation of this protein in LC neurons precedes its appearance in dopamine neurons (Vermeiren & Deyn, 2017). Both preclinical AD and Parkinson's disease may be associated with olfactory discrimination impairments for the same reason: the vulnerability of LC

axonal support to abnormal protein accumulation.

Individuals with olfactory discrimination impairments are not aware of their dysfunction (Bahar-Fuchs, Moss, Rowe, & Savage, 2011), yet it predicts later more problematic neurodegenerative-related decline. Olfactory discrimination impairments are also variable in their manifestation with repeated testing (Markopoulou et al., 2016) suggesting a general associative olfactory memory decline rather than a specific sensory deficit. The common olfactory identification deficits associated with preclinical Alzheimer's and Parkinson's disease argue that an early intervention that would promote LC axonal health, see, for example, the work of Nakamura's group (Kitayama et al., 1994), could be beneficial in the amelioration of both conditions.

A second limitation of the htauE14 model is related to the use of pseudophosphorylated tau as a stand-in for naturally occurring pretangle persistently phosphorylated tau in humans. Pretangle tau is normally indexed by immunohistochemistry using phosphorylation-specific antibodies post-mortem such as the AT8 antibody. These phosphorylation site-specific antibodies typically do not recognize sites that are pseudophosphorylated (Eidenmuller et al., 2000). We saw no evidence of AT8 reactivity in our tissue, although we could demonstrate that pseudophosphorylated human tau was being expressed. The lack of post-mortem reactivity to antibodies for tau phosphorylation in the present model also argues that the six rat tau isoforms were not altered by exposure to the abnormal human tau construct to become abnormally phosphorylated. While there is evidence that pseudophosphorylated htauE14 is functionally similar to biologically phosphorylated tau (Hoover et al., 2010), mechanistically, it may not behave in the same way (Prokopovich, Whittaker, Muthee, Ahmed,

& Larini, 2017). Additionally, the interactions when there are multiple pseudophosphorylated sites appear complex (Kiris et al., 2011).

The complete early pattern of persistent tau phosphorylation in pretangles in not known, but as reviewed, proline-directed sites are implicated. In the htauE14 model here, there is as yet no evidence that pseudophosphorylated tau becomes aggregated similar to other reports for multi-site pseudophosphorylated tau (Gilley et al., 2016; Hundelt et al., 2011). Consistent with our observation, pseudophosphorylation at site S422 (one of the E14 sites) may protect against aggregation (Guillozet-Bongaarts et al., 2006). However, multiple pseudophosphorylation site effects on tau aggregation cannot be predicted from single-site properties (Cao et al., 2018). Soluble tau is proposed to be more deleterious than tangle aggregates (Kopeikina, Hyman, & Spires-Jones, 2012), however, and pretangle soluble tau is produced throughout the course of AD (Bancher et al., 1989). While htauE14 interferes with synaptic function in the same way as biologically phosphorylated mutant fronto-temporal dementia tau (Hoover et al., 2010), mutant fronto-temporal dementia tau does not normally occur in the LC (Yang & Schmitt, 2001) and, thus, is a poor model of pretangle AD tau. Other attempts to model LC pretangle tau have failed. In mice, the fibrils of AD tau placed adjacent to the LC induced tau hyperphosphorylation in the LC neurons, but the spread of that hyperphosphorylated tau did not show the patterns seen in humans (Iba et al., 2015). It will be important to characterize the nature of the present LC pretangles in terms of whether and/or when oligomers form, whether or not insoluble tangles appear, and whether β-amyloid modulates htauE14 spread and functional outcomes. We also do not know if there is overexpression of total tau with the

addition of htauE14. In other models, overexpression of LC wild- type protein alone induces pathology (Henrich et al., 2018).

4.5 Conclusion

Our animal model suggests, for the first time, that Braak's hypothesis that human AD originates from the LC pretangle tau stages is plausible. Our results provide evidence that pretangle spread can occur through abnormal LC tau production, itself, rather than only through prion-like propagation. LC pretangle progression here generates both preclinical AD pathological changes and cognitive decline in the absence of amyloid. The odor discrimination deficits are similar to human odor deficits seen with aging and preclinical AD. When initiated in aged rats, pre- tangle stages progress rapidly and cause LC cell loss. These age-related outcomes are associated with more severe learning impairment consistent with memory decline in Braak stages III–IV when LC neurons are also lost.

4.6 Additional files

4.6.1 Additional file 1

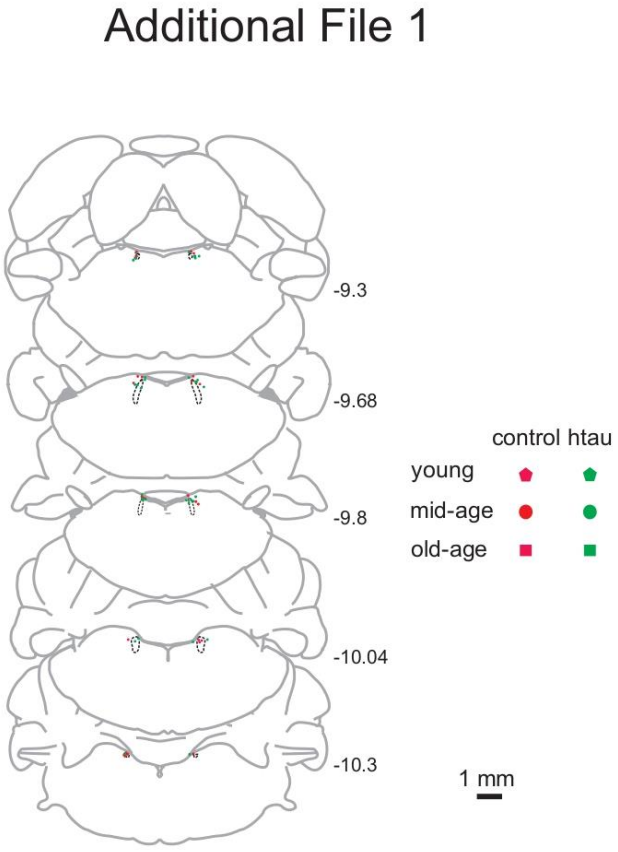

Locus coeruleus (LC) targeting reconstruction

Targeting success of 59 infusion sites from 30 rats are presented across 5 coronal planes along the rostro-caudal axis of the LC. For each hemisphere, infusion site was marked as the midpoint of maximum concentration of beads and represented in the corresponding plane in the cartoon. Black dashed outlines indicate LC. Coordinates are based on the atlas of Paxinos and Watson (4th edition).

4.6.2 Additional file 2

Additional File 2

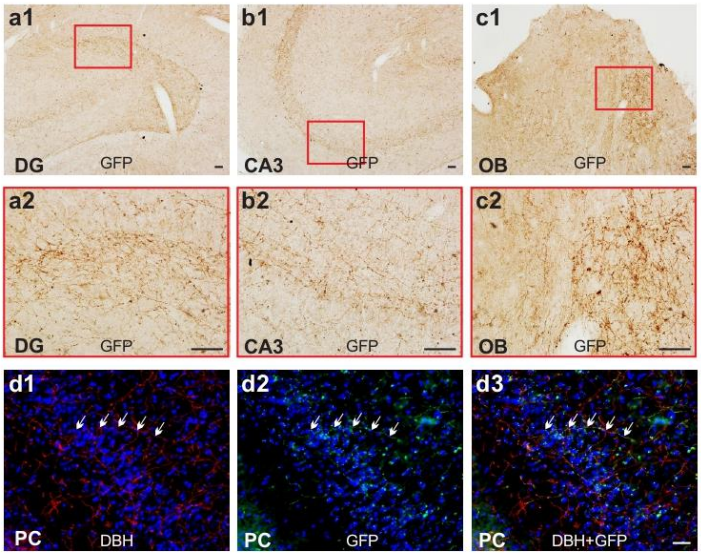

Locus coeruleus htauE14-GFP axonal projections 3 months post-infusion
GFP fibers were observed in the dentate gyrus (DG; **a1-a2**), hippocampal CA3 (**b1-b2**), olfactory bulb (OB; **c1-c2**), and piriform cortex (PC; **d1-d3** showing co-labeling of DBH fiber (d1&d3, red) and GFP fiber (d2&d3, green), indicated by arrows). Scale bars, 50 µm.

4.6.3 Additional file 3

Additional File 3

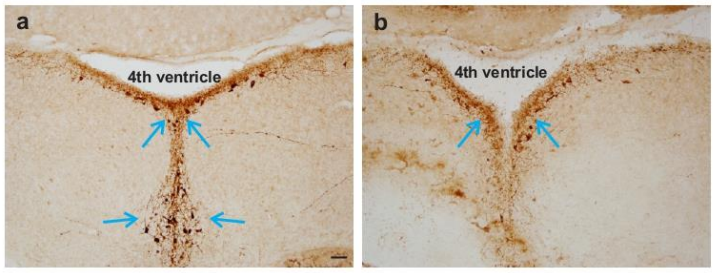

Tryptophan hydrolase (TPH) expression in the brain stem

a-b. Examples of TPH staining of raphe neurons at the level of the 4th ventricle. Arrows indicate areas of TPH^{+} cells. Scale bar, 50 µm.

4.6.4 Additional file 4

Additional File 4

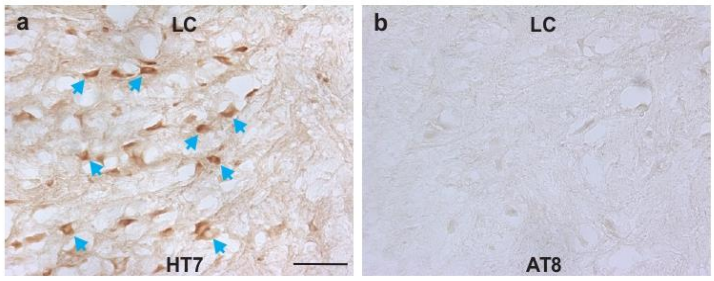

AT8 antibody failed in htauE14 pseudophosphorylated tau tissue despite human tau expression indexed by HT7

a. An example of HT7 staining in the locus coeruleus (LC) of a TH-CRE rat 3-weeks following htauE14-AAV infusion. Arrows indicate $HT7^{+}$ cells. **b.** An adjacent LC slice showing no AT8 staining. Scale bar, 50 μm.

4.6.5 Additional file 5

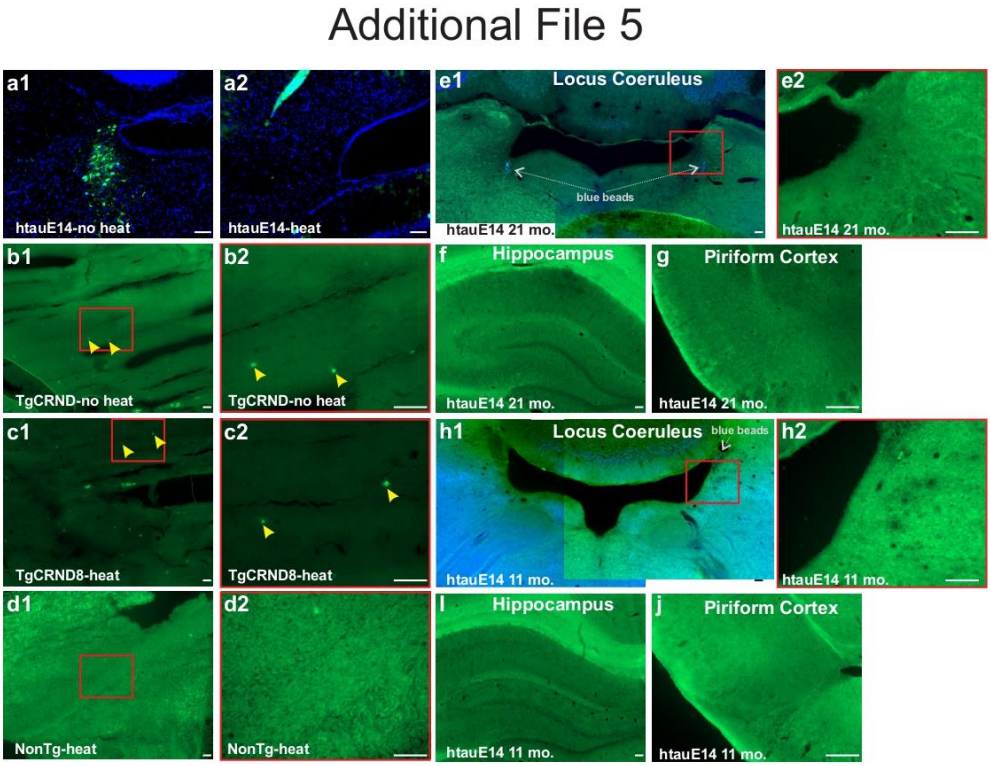

No tangle formation is apparent in htauE14 brains
a1-a2. Ten min 90°C heat treatment quenches GFP signal in a htauE14-EGFP brain. **a1** shows GFP$^+$ locus coeruleus cells without heat treatment and **a2** shows GFP quenching with heat in another section of the same brain. **b-c.** Thioflavin staining of neurofibrillary tangles in a TgCRND8[1] mouse (gift from Dr Bennett at University of Ottawa) section without heat treatment (**b1-b2**) and with heat treatment (**c1-c2**). Heat treatment does not prevent the detection of thioflavin positive tangles. Arrows indicate stained tangles. b2 and c2 are enlargements from the red square areas in b1 and c1 correspondingly. **d.** Thioflavin staining in a nonTg control mouse tissue showing no tangle formation. **e-g.** No tangle formation in a 21 month-old htauE14 rat 7 months post-infusion. **e1-e2**, Locus coeruleus; **f**, hippocampus; **g**, piriform cortex. **h-j.** No tangle formation in a 11 month-old htauE14 rat 8 months post-infusion. **h1-h2**, Locus coeruleus; **i**, hippocampus; **j**, piriform cortex. All tissue in panel **e-j** were treated with heat before thioflavin staining. Scale bars, 100 µm.

[1]Granger et al. A TgCRND8 mouse model of Alzheimer's disease exhibits sexual dimorphisms in behavioral indices of cognitive reserve. J Alzheimers Dis. 2016, 53(1), 757-73.

4.6.6 Additional file 6

Additional File 6

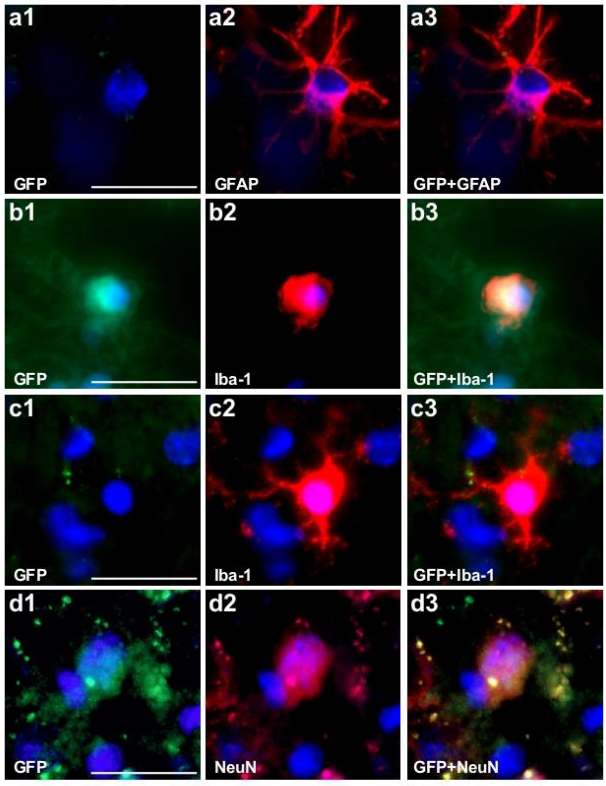

Neurons and microglia, but not astrocytes, show uptake of htauE14
a1-a3. An example of GFAP labeling in the old rat brain as in Figure 6. **b1-b3.** A GFP and Iba-1 double labeled cell. **c1-c3.** An example of an Iba-1 stained microglia in a young htauE14 rat in the same region as in **b**. Note retracted morphology of Iba-1 cell in **b** compared to **c**. **d1-d3.** A GFP and NeuN double labeled cell in the old rat brain. Scale bars, 25 μm.

5 Chapter 5: Discussion

5.1 Summary of major findings and impacts

In summary, my results suggest that β-AR modulates calcium influx through LTCC in a PKA dependent manner. This modulation is important in PC for neonatal odor preference learning and can define the associated critical period. I also showed that phasic photoactivation of LC can facilitate difficult odor discrimination learning in adult rats. This happens due to the preferential activation of TH+ neurons in the VTA and activation of the D1/D5R in the PC. Another subset of my results shows that phasic and tonic photoactivation of LC can carry opposite intrinsic valences, exerted by the activation of different ensembles in the BLA. Lastly, I established a novel rat model of Alzhemer's disease, solely based on the expression of hyperphosphorylated human tau in the rat LC. This work provides a validation of Braak's pretangle staging system. It also identifies early histopathological feature (noradrenergic axon degeneration) and behavioral marker (difficult odor discrimination learning) at the prodromal stage of the disease.

5.1.1 Mechanisms of noradrenergic modulation in learning

5.1.1.1 Noradrenergic support of the plasticity machinery

My results agree with several aspects of the existing literature and add further evidence about noradrenergic facilitation of plasticity machinery. The β-AR mediated neuronal plasticity mechanism has been widely investigated. Major downstream events include inhibition of protein phosphatase, facilitation of NMDAR and AMPAR function and ERK mediated upregulation of translation process (O'Dell et al., 2015). All these processes are either critically dependent or

importantly related to calcium signaling. β-AR is critical in a protein synthesis dependent late phase LTP induced by high frequency stimulation of afferent fibers from cortex and thalamus to lateral amygdala (Huang, Martin, & Kandel, 2000). Excitatory effect of NE on amygdalar pyramidal neuron can be attributed to a reduction in AHP immediately following action potential trains (Faber & Sah, 2005). Facilitatory role of NE on LTP in thalamo-amygdalar connection is exerted through a reduction in the frequency of GABAergic IPSC (Tully & Bolshakov, 2010). Besides pro-excitatory functions, facilitation of inhibition can also be achieved by NE. Several lines of evidence suggest that α_2-AR activation reduces excitatory neurotransmission in BLA (Ferry & McGaugh, 2008) and inhibits LTP in amygdala (DeBock et al., 2003).

In hippocampus, noradrenergic modulation varies with the region. CA1 LTP is facilitated moderately by α_1-AR agonists. But in CA3, a presynaptic inhibition of glutamate release is carried out by these receptors (Scanziani, Gahwiler, & Thompson, 1993). Interestingly CA1 depotentiation is also dependent on these receptors (Katsuki, Izumi, & Zorumski, 1997). β-AR is required for dentate gyrus LTP following high frequency stimulation (Munro, Walling, Evans, & Harley, 2001). Similar findings are evident in CA3 as well (Nguyen & Connor, 2019). Presynaptic increase in excitatory neurotransmission is a likely cause of the phenomena. CA1, however, has a different set of results regarding β-AR's role in plasticity. LTP following high frequency stimulation is not β-AR dependent; but low frequency stimulation dependent depression of synaptic strength can switch to a potentiating one when β-AR agonist is co-applied, presumably owing to PKA activation and ERK signaling(Gelinas & Nguyen, 2005; Thomas et al., 1996). Additionally, β-AR mediated mTOR signaling can also facilitate the stability of LTP in CA1(Gelinas et al., 2007). β_2-AR

activation can phosphorylate GluA1 containing AMPAR and enhance LTP (Qian et al., 2012).

My results underscore the importance of β-AR mediated modulation of LTCC in neonatal olfactory learning. I showed that blocking PKA prevents learning as well as LTCC facilitation by β-AR agonist. Direct blockade of LTCC achieves similar results in odor preference learning (Mukherjee & Yuan, 2016b). Thus, blockade of LTCC and its noradrenergic modulation seem to affect translation-machinery and possibly jeopardizes synthesis of critical proteins that can maintain late phase potentiation in already potentiated (also known as tagged) synapses through learning experience.

5.1.1.2 Norepinephrine's role in pattern separation

Pattern separation is a process by which brain differentiates two similar inputs into two orthogonalized (non-overlapping) representations (Lecei & van Winkel, 2020). Functional importance of pattern separation includes accurately identifying cues related to predators or resources critical for survival. Multiple brain areas have been identified to be engaged in pattern separation, for example, hippocampus, olfactory bulb, and piriform cortex. Hippocampus is most widely studied among these areas. Among the hippocampal subregions, dentate gyrus has critical role in pattern separation of spatial inputs. Lesion studies show DG is critical for separating two similar environments(Chen & Knierim, 2018). Further, NR1 (a subunit of the NMDAR) has been implicated in DG dependent pattern separation (McHugh et al., 2007). On the other hand, CA3 is more important for pattern completion although it may serve some role in pattern separation as well

(Yassa & Stark, 2011). The amygdala has been implicated in a reward-value based pattern separation (Gilbert & Kesner, 2002) in a hippocampus-independent manner. Interestingly norepinephrine has been proposed to facilitate pattern separation in object picture identification task (Segal, Stark, Kattan, Stark, & Yassa, 2012).

For olfactory learning, OB and PC are important for pattern separation. Previous work has shown bidirectional plasticity of pattern recognition. Pattern separation and pattern completion can occur in the piriform cortex following differential olfactory training (Chapuis & Wilson, 2012). After successful discrimination learning, pattern separation becomes more distinct in piriform cortex and representation engram of rewarded odor is stabilized (Shakhawat et al., 2014). AR blockade at OB affects similar odor discrimination (Doucette et al., 2007) and impairs pattern separation in PC (Shakhawat et al., 2015) AR blockade in PC prevents pattern separation based similar odor discrimination learning (Shakhawat et al., 2015). Thus, NE seems to have an obligatory role in PC for similar odor discrimination learning. I utilized this concept in the context of Alzheimer's disease.

Interestingly, neurocognitive aging is associated with loss of pattern separation ability (Yassa & Stark, 2011). Alzheimer's patients show an association of neurogenesis related deficit and CSF amyloid-β-42 (a fibrillogenic type of amyloid-β peptide commonly present in brain deposits) levels with reduced pattern separation ability (Wesnes, Annas, Basun, Edgar, & Blennow, 2014). These evidences are in line with my experimental result. My result shows that following htau expression in LC, difficult, but not simple, odor pairs discrimination deficit in a motivation-based adult olfactory learning paradigm. In parallel, there is degeneration of noradrenergic axons in the PC, as

evident from DBH and NET immunohistochemistry in these rats. It indicates that PC noradrenergic deficit following htau expression in LC could be causal to the pattern separation deficit in AD. This further underscores the association of noradrenergic deficit and subtle cognitive dysfunctions in the long prodromal stages of AD.

5.1.1.3 Variable norepinephrine-release and locus coeruleus spiking pattern difference influencing learning

How does NE release vary with LC spiking patterns? Is it responsible for differential learning effects of different LC-spiking patterns? A tempting explanation is that the phasic release of NE is higher than tonic, leading to higher concentration of NE in target sites, thus enhancing plasticity. This school of thought has received some support that at higher NE concentrations β-ARs are preferentially engaged, favoring cAMP-PKA-CREB pathway (Mather et al., 2016). Although higher phasic frequency imparts higher NE concentration (Florin-Lechner, Druhan, Aston-Jones, & Valentino, 1996), this cannot account for our differential effects between 10 Hz tonic and 10 Hz phasic stimulation patterns, as frequency remains unaltered between the two patterns. How the pause associated with phasic spiking critically changes NE-release dynamics, will be an interesting question to address in the future. It is possible that differential engagement of AR subtypes on the target cells underlies the phasic-tonic difference in learning paradigm. Behavioral and electrophysiological experiments with pharmacological and optogenetic interventions should be able to address this puzzle.

Sensory-input locked LC phasic spiking has been examined extensively in the field for decades. A long-standing view (Aston-Jones & Cohen, 2005) in the field suggested that time-locked LC-phasic spiking enhances memory. Here we showed that a non-time-locked continuous phasic photostimulaiton of LC could also enhance memory. This is aligned with other results in the field, where continuous LC-phasic stimulation promoted learning (Kempadoo et al., 2016; Takeuchi et al., 2016). It is important to note here that phasic pattern-mediated facilitation of learning is uniquely related to direct or indirect dopaminergic neurotransmission. Previous works established a direct release of DA from LC axons in dorsal hippocampus (Smith & Greene, 2012) and paraventricular nucleus of the thalamus (Beas et al., 2018). More work showed that photostimulation at the axon terminals in hippocampus or direct LC photostimulation, both were able to enhance learning through a dopaminergic mechanism (Kempadoo et al., 2016; Takeuchi et al., 2016). Pharmacological interventions in physiological experiments and biochemical tests confirmed DA from LC axons to be responsible for learning enhancement following phasic stimulation. In contrast, our current research discovered a VTA-mediated effect underlying LC-phasic pattern related facilitation. This difference can arise from motivation-state of the subjects as they were food-deprived in our paradigm. Alternatively, it is also possible that differentiating similar sensory inputs via pattern-separation is uniquely dependent on the VTA circuitry. Previous research did not explore the role of LC-phasic spiking in differentiating highly similar sensory inputs.

Despite having widespread axons all through the brain, it is an open question how LC spiking pattern promotes goal-directed specific functions instead of just a generalised arousal. ARs and transporters at the projection sites are expected to shape the NE release and effect on the neurons in

the vicinity – thus, perhaps, rendering the specificity of the function. It is important to note that newer interactive models describe glutamate control of NE-release as a key factor to selection specificity of salient inputs for learning (Mather et al., 2016). This echoes well with the idea of site-specific unique modulation (Berridge & Waterhouse, 2003). In parallel, an idea of modular LC is getting more support. Variable projection patterns of subgroups of LC neurons that has functional specificity (Uematsu, Tan, & Johansen, 2015), unsynchronised spiking across multiple pairs of LC neurons, and non-topographic distribution of ensembles within LC that are co-characterized by similar projection targets (Totah et al., 2019). These are all indicative of distinct sub-LC ensembles and their unique projection-patterns being responsible for functional specificity. In our experiments we exogenously photostimulated LC neurons. Thus, our current results support site-specific modulation of NE-function by ARs or glutamate over a modular activation of LC.

5.1.2 Locus coeruleus-norepinephrine system in Alzheimer's disease

5.1.2.1 Establishment of a pretangle tau model

Through the current results, we have established a pretangle Tau model, primary expression being in LC. These results provide, for the first time, an experimental validation of Braak's hypothesis that AD may originate from LC-pretangle tau. Our results broadly follow the early stages of Braak's staging (a-c, 1a). In this model we observe progressive neurodegeneration of the LC-NE system- noradrenergic axonal fiber loss in mid-age group but unaffected in younger group, and LC neuron loss in older age group. This is in agreement with the human data showing that LC neurons are not lost until quite late (Braak stages III-VI) in the disease (Kelly et al., 2017). Besides LC neuronal loss, the progressive degeneration of noradrenergic axon is also evident from human AD

data (Gulyás et al., 2010; Palmer et al., 1987; Powers et al., 1988). Besides the noradrenergic component of pathophysiology, our results also show an important feature of microglia recruitment which is also evident in AD literature (Marlatt et al., 2014). This becomes important in the context of microglial uptake of hyperphosphorylated tau (Bolos et al., 2016), which has been shown by our model as well. This echoes well with the possibility of microglial contribution in spreading of tau (Hopp et al., 2018).

5.1.2.2 Advantages and limitations of the model

The current model has several strengths. We have drawn many parallels with human AD solely basing on LC- tau. Pathological feature-wise, our model follows Braak's early stages. Somatodendritic mislocalization of abnormal tau is also relevant in humans. Critical para-midline brain stem structures, like raphe neurons, receive htau spreading from LC early in the disease. Although these pathological features appear early in the disease process, our model shows a long prodromal period before cognitive deficit takes place, similar to human AD. Olfactory deficits are an early symptom in AD. Seven months post infusion, our model also shows an olfactory deficit in the form of an inability to discriminate similar odors in a motivation based learning paradigm. The progressive degeneration of noradrenergic system bears similarity with human counterparts. It is important to note that all these features have been recapitulated in this model in absence of a tangle, underscoring the importance of the pathogenicity of soluble abnormal tau. Unlike many others, this model is not based on a transgenic model exploiting common genetic mutations associated with human AD. Thus, it is devoid of β-amyloid pathology and precisely addresses tau-related

pathophysiology only.

One major limitation of sensory discrimination related symptoms is the non-specificity to a single disease. Early stage olfactory deficit is common in other diseases, especially in Parkinson's disease (Bowman, 2017) . Thus, a confirmatory diagnosis of AD, based only on olfactory dysfunction is not feasible. Similar argument holds true for noradrenergic deficit in Parkinson's disease (Braak & Tredici, 2017). Antemortem (through imaging) or postmortem (through immunohistochemistry) quantification of noradrenergic fibers may not yield a disease-specific confirmatory diagnosis. Another limitation of our model is the lack of AT8 staining for hTauE14. AT8 and other phosphorylation targeted antibodies do not recognize pseudophosphorylation sites (Eidenmuller et al., 2000). But it is important to note that despite the lack of a phosphorylation-positive staining, we were able to demonstrate human tau expression in hTauE14 tissue. Finally, a discrepancy between the behaviors of biologically phosphorylated tau and pseudophosphorylated hTauE14 should be acknowledged in this context (Prokopovich et al., 2017).

5.1.2.3 Therapeutic implications

Our model predicts that noradrenergic fiber density could be an early brain change in AD. This can be tested by NET-PET imaging in humans, both in cross-sectional and longitudinal studies. If proven correct, NET-PET imaging can serve as an early diagnostic tool in the prodromal window. Similarly, our model emphasizes that a subtle discrimination deficit of similar odor pairs may be present as a 'sign', rather than a 'symptom', in otherwise asymptomatic potential AD/MCI patients in their long prodromal window. Developing and validating appropriate olfactory tests for humans

utilizing this principle could be beneficial in shaping another early diagnostic tool long before the symptoms appear. Furthermore, due to the long window in our model before the deficit becomes apparent (7 months post infusion), this can be used for testing efficacy of different drugs and therapies aimed at the prodromal window of the disease. In a following subsection I elaborate some future directions utilizing this scope.

5.2 Future directions

5.2.1 Mechanistic studies underlying differential effects of locus coeruleus spiking patterns

BLA is an important site for segregation of positive and negative valence. Previous work suggested NAc projecting BLA neurons register positive valence whereas CeA projecting BLA neurons are critical for negative valence (Beyeler et al., 2016; Namburi et al., 2015). Another study showed that tonic LC stimulation preferentially engages CeA projecting BLA neurons (McCall et al., 2017). Our current result supports this evidence too. Besides, we have also shown LC-phasic stimulation is capable of generating positive valence through activating NAc projecting BLA neurons.

What gives rise to the differential population activation in the BLA by two different LC photostimulation patterns? Modular organisation of LC cannot be responsible as external photostimulation widely activates LC neurons irrespective of modularity. One attractive candidate is the differential AR expression in the targeted subpopulation. McCall et al (McCall et al., 2017) has shown a role of BLA β-AR in the aversive learning promoted by LC-tonic photostimulation. Several others have shown role of amygdalar α-AR in aversive learning as well (Ferry & McGaugh,

2008; Holmes et al., 2017). One possible candidate could be β_3-AR as their activation in BLA postsynaptically enhances inhibitory postsynaptic current on the BLA neurons generated from lateral paracapsular GABAergic synapses (Silberman et al., 2010). Future behavioral and slice electrophysiological experiments with appropriate pharmacological intervention and quantitative immunohistochemistry with AR subtype-specific antibodies may be able to delineate the underlying mechanism of valence-related diversity of LC photostimulation patterns.

5.2.2 Role of locus coeruleus spiking patterns in Alzheimer's disease progression

With the current set of results and previous work done in the field, a picture emerges where LC is a critical determiner of AD pathology. LC effect can be multifold on the AD pathophysiology, including transneuronal spread of abnormal tau, reduction in noradrenergic innervation, and microglia recruitment. It is important to understand that LC neurons spike spontaneously and their spiking pattern can be critical for NE release which, in turn, can have influence on the course of the pathophysiology. It is interesting to note that stress, which is related to high tonic spiking, also worsens AD progression (Justice, 2018). On the other hand, environmental enrichment is partially related to novel stimulus presentation. It can be loosely correlated to LC-phasic spiking, has beneficial roles in slowing down AD (Lima et al., 2018) as well as in general improvement of synaptic plasticity and memory (Hullinger, O'Riordan, & Burger, 2015). This provides a conceivable basis of the idea that chronic LC stimulation in two different patterns can yield two different outcomes of AD pathophysiology. Finally, chemogenetic activation of LC in a rodent model of AD successfully rescues memory deficit and improves noradrenergic innervation

(Rorabaugh et al., 2017) - thus indicating that LC activation in an AD model can be feasible.

We hypothesize that chronic phasic stimulation in LC-htauE14 model will ameliorate cognitive deficit while chronic tonic stimulation will aggravate the disease. It is an open question what will happen to LC axon density, microglia recruitment and transneuronal spread of htau following chronic stimulation in two different patterns. Double AAV viral vector-mediated delivery of hTauE14 and ChR2 at LC of TH-cre rats, followed by LC-optical fiber implantation 3-4 months post infusion, chronically stimulating LC in respective patterns for 6 weeks and then testing them 3 months later will address this hypothesis.

5.2.3 Using the pretangle tau model to study intervention and epigenetic mechanism of Alzheimer's disease

As discussed before, stress and enrichment may have differential effects on AD progression. But does the time course of stress or enrichment have any particular significance? Early life stress (such as maternal separation) (Hui, Feng, Zheng, Jin, & Jia, 2017; Martisova, Aisa, Guereñu, & Javier Ramirez, 2013; Sotiropoulos et al., 2011) and enrichment (Canete, Blazquez, Tobena, Gimenez-Llort, & Fernandez-Teruel, 2015; Lesuis, van Hoek, Lucassen, & Krugers, 2017) may have differential effects on AD pathology. Research suggests late life stress and enrichment may also have different effects on AD pathology (Carroll et al., 2011; Lima et al., 2018). Braak's pretangle-tau staging suggests a long prodromal window and our LC-tau model recapitulates it well. Thus, our model can be aptly used to test differential effects of early and late life stress and enrichment paradigms on progression of tau-pathology. For a mechanistic counterpart, early life events are

known to cause epigenomic changes in AD profile (Lesuis et al., 2018; McEwen, Eiland, Hunter, & Miller, 2012; Roth & Sweatt, 2011). Studying DNA methylome changes along with histone modification profiling in our LC-tau model, can address fundamental aspects of environmental factors interaction with tau-pathology from an epigenetic perspective.

6 References

Abraham, P. A., Xing, G., Zhang, L., Eric, Z. Y., Post, R., Gamble, E. H., & Li, H. (2008). β_1-and β2-adrenoceptor induced synaptic facilitation in rat basolateral amygdala. *Brain research, 1209*, 65-73.

Ambroggi, F., Ishikawa, A., Fields, H. L., & Nicola, S. M. (2008). Basolateral amygdala neurons facilitate reward-seeking behavior by exciting nucleus accumbens neurons. *Neuron, 59*(4), 648-661. doi:10.1016/j.neuron.2008.07.004

Andres-Benito, P., Fernandez-Duenas, V., Carmona, M., Escobar, L. A., Torrejon-Escribano, B., Aso, E., . . . Ferrer, I. (2017). Locus coeruleus at asymptomatic early and middle braak stages of neurofibrillary tangle pathology. *Neuropathol Appl Neurobiol, 43*(5), 373-392. doi:10.1111/nan.12386

Andrews, G. D., & Lavin, A. (2006). Methylphenidate increases cortical excitability via activation of alpha-2 noradrenergic receptors. *Neuropsychopharmacology, 31*(3), 594-601. doi:10.1038/sj.npp.1300818

Aransay, A., Rodriguez-Lopez, C., Garcia-Amado, M., Clasca, F., & Prensa, L. (2015). Long-range projection neurons of the mouse ventral tegmental area: A single-cell axon tracing analysis. *Front Neuroanat, 9*, 59. doi:10.3389/fnana.2015.00059

Arriagada, P. V., Growdon, J. H., Hedley-Whyte, E. T., & Hyman, B. T. (1992). Neurofibrillary tangles but not senile plaques parallel duration and severity of alzheimer's disease. *Neurology, 42*(3), 631-631.

Aston-Jones, & Bloom. (1981). Nonrepinephrine-containing locus coeruleus neurons in behaving rats exhibit pronounced responses to non-noxious environmental stimuli. *Journal of Neuroscience, 1*(8), 887-900.

Aston-Jones, G., & Cohen, J. D. (2005). An integrative theory of locus coeruleus-norepinephrine function: Adaptive gain and optimal performance. *Annu Rev Neurosci, 28*, 403-450. doi:10.1146/annurev.neuro.28.061604.135709

Aston-Jones, G., & Waterhouse, B. (2016). Locus coeruleus: From global projection system to adaptive regulation of behavior. *Brain Res, 1645*, 75-78. doi:10.1016/j.brainres.2016.03.001

Badhwar, A., Tam, A., Dansereau, C., Orban, P., Hoffstaedter, F., & Bellec, P. (2017). Resting-state network dysfunction in alzheimer's disease: A systematic review and meta-analysis. *Alzheimers Dement (Amst), 8*, 73-85. doi:10.1016/j.dadm.2017.03.007

Bading, H., Ginty, D. D., & Greenberg, M. E. (1993). Regulation of gene expression in hippocampal neurons by distinct calcium signaling pathways. *Science, 260*(5105), 181-186. doi:10.1126/science.8097060

Bahar-Fuchs, A., Moss, S., Rowe, C., & Savage, G. (2011). Awareness of olfactory deficits in healthy aging, amnestic mild cognitive impairment and alzheimer's disease. *Int Psychogeriatr, 23*(7), 1097-1106. doi:10.1017/S1041610210002371

Bajic, D., & Proudfit, H. K. (1999). Projections of neurons in the periaqueductal gray to pontine and medullary catecholamine cell groups involved in the modulation of nociception. *Journal of comparative neurology, 405*(3), 359-379.

Bancher, C., Brunner, C., Lassmann, H., Budka, H., Jellinger, K., Wiche, G., . . . Wisniewski, H. M. (1989). Accumulation of abnormally phosphorylated τ precedes the formation of

neurofibrillary tangles in alzheimer's disease. *Brain research, 477*(1-2), 90-99. doi:10.1016/0006-8993(89)91396-6

Banko, J. L., Poulin, F., Hou, L. F., DeMaria, C. T., Sonenberg, N., & Klann, E. (2005). The translation repressor 4e-bp2 is critical for eif4f complex formation, synaptic plasticity, and memory in the hippocampus. *Journal of Neuroscience, 25*(42), 9581-9590. doi:10.1523/Jneurosci.2423-05.2005

Bari, B. A., Chokshi, V., & Schmidt, K. (2020). Locus coeruleus-norepinephrine: Basic functions and insights into parkinson's disease. *Neural Regeneration Research, 15*(6), 1006.

Barkai, E. (2005). Dynamics of learning-induced cellular modifications in the cortex. *Biol Cybern, 92*(6), 360-366. doi:10.1007/s00422-005-0564-0

Bathini, P., Brai, E., & Auber, L. A. (2019). Olfactory dysfunction in the pathophysiological continuum of dementia. *Ageing Res Rev, 55*, 100956. doi:10.1016/j.arr.2019.100956

Bathini, P., Mottas, A., Jaquet, M., Brai, E., & Alberi, L. (2019). Progressive signaling changes in the olfactory nerve of patients with alzheimer's disease. *Neurobiol Aging, 76*, 80-95. doi:10.1016/j.neurobiolaging.2018.12.006

Beas, B. S., Wright, B. J., Skirzewski, M., Leng, Y., Hyun, J. H., Koita, O., . . . Penzo, M. A. (2018). The locus coeruleus drives disinhibition in the midline thalamus via a dopaminergic mechanism. *Nat Neurosci, 21*(7), 963-973. doi:10.1038/s41593-018-0167-4

Beckstead, R. M., Domesick, V. B., & Nauta, W. J. (1979). Efferent connections of the substantia nigra and ventral tegmental area in the rat. *Brain Res, 175*(2), 191-217. doi:10.1016/0006-8993(79)91001-1

Benarroch, E. E. (2010). Olfactory system: Functional organization and involvement in neurodegenerative disease. *Neurology, 75*(12), 1104-1109. doi:10.1212/WNL.0b013e3181f3db84

Berger-Sweeney, J., Libbey, M., Arters, J., Junagadhwalla, M., & Hohmann, C. F. (1998). Neonatal monoaminergic depletion in mice (mus musculus) improves performance of a novel odor discrimination task. *Behav Neurosci, 112*(6), 1318-1326.

Berlau, D. J., & McGaugh, J. L. (2006). Enhancement of extinction memory consolidation: The role of the noradrenergic and gabaergic systems within the basolateral amygdala. *Neurobiology of Learning and Memory, 86*(2), 123-132. doi:10.1016/j.nlm.2005.12.008

Berridge, C. W. (2008). Noradrenergic modulation of arousal. *Brain Res Rev, 58*(1), 1-17. doi:10.1016/j.brainresrev.2007.10.013

Berridge, C. W., & Waterhouse, B. D. (2003). The locus coeruleus–noradrenergic system: Modulation of behavioral state and state-dependent cognitive processes. *Brain Research Reviews, 42*(1), 33-84.

Beyeler, A., Namburi, P., Glober, G. F., Simonnet, C., Calhoon, G. G., Conyers, G. F., . . . Tye, K. M. (2016). Divergent routing of positive and negative information from the amygdala during memory retrieval. *Neuron, 90*(2), 348-361. doi:10.1016/j.neuron.2016.03.004

Blake, T.-J., Tillery, C. E., & Reynolds, G. P. (1998). Antipsychotic drug affinities at α2-adrenoceptor subtypes in post-mortem human brain. *Journal of Psychopharmacology, 12*(2), 151-154.

Bolos, M., Llorens-Martin, M., Jurado-Arjona, J., Hernandez, F., Rabano, A., & Avila, J. (2016). Direct evidence of internalization of tau by microglia in vitro and in vivo. *J Alzheimers Dis, 50*(1), 77-87. doi:10.3233/JAD-150704

Bouret, S., & Richmond, B. J. (2015). Sensitivity of locus ceruleus neurons to reward value for goal-directed actions. *J Neurosci, 35*(9), 4005-4014. doi:10.1523/JNEUROSCI.4553-14.2015

Bouret, S., & Sara, S. J. (2002). Locus coeruleus activation modulates firing rate and temporal organization of odour-induced single-cell responses in rat piriform cortex. *Eur J Neurosci, 16*(12), 2371-2382. doi:10.1046/j.1460-9568.2002.02413.x

Bowman, G. L. (2017). Biomarkers for early detection of parkinson disease: A scent of consistency with olfactory dysfunction. *Neurology, 89*(14), 1432-1434. doi:10.1212/WNL.0000000000004383

Braak, H., & Braak, E. (1991). Alzheimer's disease affects limbic nuclei of the thalamus. *Acta Neuropathol, 81*(3), 261-268. doi:10.1007/BF00305867

Braak, H., & Del Tredici, K. (2011). The pathological process underlying alzheimer's disease in individuals under thirty. *Acta Neuropathol, 121*(2), 171-181. doi:10.1007/s00401-010-0789-4

Braak, H., & Del Tredici, K. (2017). Neuropathological staging of brain pathology in sporadic parkinson's disease: Separating the wheat from the chaff. *Journal of Parkinson's disease, 7*(s1), S71-S85.

Braak, H., Thal, D. R., Ghebremedhin, E., & Del Tredici, K. (2011). Stages of the pathologic process in alzheimer disease: Age categories from 1 to 100 years. *J Neuropathol Exp Neurol, 70*(11), 960-969. doi:10.1097/NEN.0b013e318232a379

Braak, H., & Tredici, K. (2015). In H. W. Korf, F. Clascá, B. Singh, & J. P. Timmermans (Eds.), *Neuroanatomy and pathology of sporadic alzheimer's disease*. Switzerland: Springer International Publishing.

Braga, M. F., Aroniadou-Anderjaska, V., Xie, J., & Li, H. (2003). Bidirectional modulation of gaba release by presynaptic glutamate receptor 5 kainate receptors in the basolateral amygdala. *J Neurosci, 23*(2), 442-452.

Bray, J. G., & Mynlieff, M. (2011). Involvement of protein kinase c and protein kinase a in the enhancement of l-type calcium current by gabab receptor activation in neonatal hippocampus. *Neuroscience, 179*, 62-72. doi:10.1016/j.neuroscience.2011.01.054

Brosh, I., Rosenblum, K., & Barkai, E. (2006). Learning-induced reversal of the effect of noradrenalin on the postburst ahp. *J Neurophysiol, 96*(4), 1728-1733. doi:10.1152/jn.00376.2006

Bullido, M. J., Ramos, M. C., Ruiz-Gómez, A., Tutor, A. S., Sastre, I., Frank, A., . . . Valdivieso, F. (2004). Polymorphism in genes involved in adrenergic signaling associated with alzheimer's. *Neurobiology of aging, 25*(7), 853-859.

Bush, D. E., Caparosa, E. M., Gekker, A., & LeDoux, J. (2010). Beta-adrenergic receptors in the lateral nucleus of the amygdala contribute to the acquisition but not the consolidation of auditory fear conditioning. *Frontiers in behavioral neuroscience, 4*, 154.

Cain, C. K., Blouin, A. M., & Barad, M. (2004). Adrenergic transmission facilitates extinction of conditional fear in mice. *Learn Mem, 11*(2), 179-187. doi:10.1101/lm.71504

Camp, L. L., & Rudy, J. W. (1988). Changes in the categorization of appetitive and aversive events during postnatal development of the rat. *Dev Psychobiol, 21*(1), 25-42. doi:10.1002/dev.420210103

Canete, T., Blazquez, G., Tobena, A., Gimenez-Llort, L., & Fernandez-Teruel, A. (2015). Cognitive and emotional alterations in young alzheimer's disease (3xtgad) mice: Effects of neonatal handling stimulation and sexual dimorphism. *Behavioural Brain Research, 281*, 156-171. doi:10.1016/j.bbr.2014.11.004

Cao, L., Liang, Y., Liu, Y., Xu, Y., Wan, W., & Zhu, C. (2018). Pseudo-phosphorylation at at8 epitopes regulates the tau truncation at aspartate 421. *Exp Cell Res, 370*(1), 103-115. doi:10.1016/j.yexcr.2018.06.010

Carew, S. J., Mukherjee, B., MacIntyre, I. T. K., Ghosh, A., Li, S., Kirouac, G. J., . . . Yuan, Q. (2018). Pheromone-induced odor associative fear learning in rats. *Sci Rep, 8*(1), 17701. doi:10.1038/s41598-018-36023-w

Carroll, J. C., Iba, M., Bangasser, D. A., Valentino, R. J., James, M. J., Brunden, K. R., . . . Trojanowski, J. Q. (2011). Chronic stress exacerbates tau pathology, neurodegeneration, and cognitive performance through a corticotropin-releasing factor receptor-dependent mechanism in a transgenic mouse model of tauopathy. *Journal of Neuroscience, 31*(40), 14436-14449. doi:10.1523/Jneurosci.3836-11.2011

Carter, M. E., Yizhar, O., Chikahisa, S., Nguyen, H., Adamantidis, A., Nishino, S., . . . de Lecea, L. (2010). Tuning arousal with optogenetic modulation of locus coeruleus neurons. *Nat Neurosci, 13*(12), 1526-1533. doi:10.1038/nn.2682

Cedarbaum, J. M., & Aghajanian, G. K. (1978). Afferent projections to the rat locus coeruleus as determined by a retrograde tracing technique. *Journal of comparative neurology, 178*(1), 1-15.

Cerf-Ducastel, B., & Murphy, C. (2003). Fmri brain activation in response to odors is reduced in primary olfactory areas of elderly subjects. *Brain research, 986*(1-2), 39-53. doi:10.1016/S0006-8993(03)03168-8

Cesetti, T., Hernandez-Guijo, J., Baldelli, P., Carabelli, V., & Carbone, E. (2003). Opposite action of β1-and β2-adrenergic receptors on cav1 l-channel current in rat adrenal chromaffin cells. *Journal of Neuroscience, 23*(1), 73-83.

Chai, N., Liu, J. F., Xue, Y. X., Yang, C., Yan, W., Wang, H. M., . . . Lu, L. (2014). Delayed noradrenergic activation in the dorsal hippocampus promotes the long-term persistence of extinguished fear. *Neuropsychopharmacology, 39*(8), 1933-1945. doi:10.1038/npp.2014.42

Chandler, D. J., Gao, W. J., & Waterhouse, B. D. (2014). Heterogeneous organization of the locus coeruleus projections to prefrontal and motor cortices. *Proc Natl Acad Sci U S A, 111*(18), 6816-6821. doi:10.1073/pnas.1320827111

Chandler, D. J., Jensen, P., McCall, J. G., Pickering, A. E., Schwarz, L. A., & Totah, N. K. (2019). Redefining noradrenergic neuromodulation of behavior: Impacts of a modular locus coeruleus architecture. *J Neurosci, 39*(42), 8239-8249. doi:10.1523/JNEUROSCI.1164-19.2019

Chang, C. Y., Gardner, M. P. H., Conroy, J. C., Whitaker, L. R., & Schoenbaum, G. (2018). Brief, but not prolonged, pauses in the firing of midbrain dopamine neurons are sufficient to produce a conditioned inhibitor. *J Neurosci, 38*(41), 8822-8830. doi:10.1523/JNEUROSCI.0144-18.2018

Chapuis, J., & Wilson, D. A. (2012). Bidirectional plasticity of cortical pattern recognition and behavioral sensory acuity. *Nature neuroscience, 15*(1), 155-U194. doi:10.1038/nn.2966

Chay, A., Zamparo, I., Koschinski, A., Zaccolo, M., & Blackwell, K. T. (2016). Control of β-AR-and n-methyl-d-aspartate (nmda) receptor-dependent camp dynamics in hippocampal neurons. *PLoS computational biology, 12*(2), e1004735.

Chen, X., & Knierim, J. J. (2018). It's about time: Temporal dynamics of dentate gyrus pattern separation. *Neuron, 98*(4), 681-683.

Chen, Y., Peng, Y., Che, P., Gannon, M., Liu, Y., Li, L., . . . Wang, Q. (2014). A2a adrenergic receptor promotes amyloidogenesis through disrupting app-sorla interaction. *Proceedings of the National Academy of Sciences, 111*(48), 17296-17301.

Clark, N. C., Nagano, N., Kuenzi, F. M., Jarolimek, W., Huber, I., Walter, D., . . . Seabrook, G. R. (2003). Neurological phenotype and synaptic function in mice lacking the cav1.3 alpha

subunit of neuronal l-type voltage-dependent ca2+ channels. *Neuroscience, 120*(2), 435-442. doi:10.1016/s0306-4522(03)00329-4

Cole, B. J., & Robbins, T. W. (1987). Dissociable effects of lesions to the dorsal or ventral noradrenergic bundle on the acquisition, performance, and extinction of aversive conditioning. *Behav Neurosci, 101*(4), 476-488. doi:10.1037//0735-7044.101.4.476

Collier, T. J., Greene, J. G., Felten, D. L., Stevens, S. Y., & Collier, K. S. (2004). Reduced cortical noradrenergic neurotransmission is associated with increased neophobia and impaired spatial memory in aged rats. *Neurobiology of aging, 25*(2), 209-221. doi:10.1016/S0197-4580(03)00042-3

Combarros, O., Warden, D. R., Hammond, N., Cortina-Borja, M., Belbin, O., Lehmann, M. G., . . . Barber, R. (2010). The dopamine β-hydroxylase-1021c/t polymorphism is associated with the risk of alzheimer's disease in the epistasis project. *BMC medical genetics, 11*(1), 162.

Conti, M. Z., Vicini-Chilovi, B., Riva, M., Zanetti, M., Liberini, P., Padovani, A., & Rozzini, L. (2013). Odor identification deficit predicts clinical conversion from mild cognitive impairment to dementia due to alzheimer's disease. *Arch Clin Neuropsychol, 28*(5), 391-399. doi:10.1093/arclin/act032

Cowan, C. M., & Mudher, A. (2013). Are tau aggregates toxic or protective in tauopathies? *Front Neurol, 4*, 114. doi:10.3389/fneur.2013.00114

Crosby, E. C., & Humphrey, T. (1941). Studies of the vertebrate telencephalon. Ii. The nuclear pattern of the anterior olfactory nucleus, tuberculum olfactorium and the amygdaloid complex in adult man. *The Journal of Comparative Neurology, 74*(2), 309-352. doi:10.1002/cne.900740209

Cui, W., Smith, A., Darby-King, A., Harley, C. W., & McLean, J. H. (2007). A temporal-specific and transient camp increase characterizes odorant classical conditioning. *Learn Mem, 14*(3), 126-133. doi:10.1101/lm.496007

Curtis, A. L., Leiser, S. C., Snyder, K., & Valentino, R. J. (2012). Predator stress engages corticotropin-releasing factor and opioid systems to alter the operating mode of locus coeruleus norepinephrine neurons. *Neuropharmacology, 62*(4), 1737-1745. doi:10.1016/j.neuropharm.2011.11.020

Dahlström, A., & Fuxe, K. (1964). Localization of monoamines in the lower brain stem. *Experientia, 20*(7), 398-399.

Date, Y., Ueta, Y., Yamashita, H., Yamaguchi, H., Matsukura, S., Kangawa, K., . . . Nakazato, M. (1999). Orexins, orexigenic hypothalamic peptides, interact with autonomic, neuroendocrine and neuroregulatory systems. *Proc Natl Acad Sci U S A, 96*(2), 748-753. doi:10.1073/pnas.96.2.748

Datiche, F., & Cattarelli, M. (1996). Catecholamine innervation of the piriform cortex: A tracing and immunohistochemical study in the rat. *Brain Res, 710*(1-2), 69-78. doi:10.1016/0006-8993(95)01279-6

Davare, M. A., Avdonin, V., Hall, D. D., Peden, E. M., Burette, A., Weinberg, R. J., . . . Hell, J. W. (2001). A β2 adrenergic receptor signaling complex assembled with the ca2+ channel cav1. 2. *Science, 293*(5527), 98-101. doi:10.1126/science.293.5527.98

Davies, D., Brooks, J., & Lewis, D. (1993). Axonal loss from the olfactory tracts in alzheimer's disease. *Neurobiology of aging, 14*(4), 353-357. doi:10.1016/0197-4580(93)90121-q

Davies, M. F., Tsui, J., Flannery, J. A., Li, X., DeLorey, T. M., & Hoffman, B. B. (2004). Activation of α 2 adrenergic receptors suppresses fear conditioning: Expression of c-fos and phosphorylated creb in mouse amygdala. *Neuropsychopharmacology, 29*(2), 229-239. doi:10.1038/sj.npp.1300324

Davis, S. E., & Bauer, E. P. (2012). L-type voltage-gated calcium channels in the basolateral amygdala are necessary for fear extinction. *The Journal of Neuroscience, 32*(39), 13582-13586. doi:10.1523/jneurosci.0809-12.2012

Day, H. E., Campeau, S., Watson Jr, S. J., & Akil, H. (1997). Distribution of α1a-, α1b-and α1d-adrenergic receptor mrna in the rat brain and spinal cord. *Journal of chemical neuroanatomy, 13*(2), 115-139. doi:10.1016/s0891-0618(97)00042-2

Dayan, P., & Yu, A. J. (2006). Phasic norepinephrine: A neural interrupt signal for unexpected events. *Network: Computation in Neural Systems, 17*(4), 335-350. doi:10.1080/09548980601004024

de Almeida, L., Reiner, S. J., Ennis, M., & Linster, C. (2015). Computational modeling suggests distinct, location-specific function of norepinephrine in olfactory bulb and piriform cortex. *Front Comput Neurosci, 9*, 73. doi:10.3389/fncom.2015.00073

De Jongh, K. S., Murphy, B. J., Colvin, A. A., Hell, J. W., Takahashi, M., & Catterall, W. A. (1996). Specific phosphorylation of a site in the full-length form of the α1 subunit of the cardiac l-type calcium channel by adenosine 3 ‘, 5 ‘-cyclic monophosphate-dependent protein kinase. *Biochemistry, 35*(32), 10392-10402.

Debiec, J., & LeDoux, J. E. (2004). Disruption of reconsolidation but not consolidation of auditory fear conditioning by noradrenergic blockade in the amygdala. *Neuroscience, 129*.

DeBock, F., Kurz, J., Azad, S., Parsons, C., Hapfelmeier, G., Zieglgänsberger, W., & Rammes, G. (2003). A2-adrenoreceptor activation inhibits ltp and ltd in the basolateral amygdala: Involvement of gi/o-protein-mediated modulation of ca2+-channels and inwardly rectifying k+-channels in ltd. *European Journal of Neuroscience, 17*(7), 1411-1424.

Deisseroth, K., Heist, E. K., & Tsien, R. W. (1998). Translocation of calmodulin to the nucleus supports creb phosphorylation in hippocampal neurons. *Nature, 392*(6672), 198. doi:10.1038/32448

Del Cid-Pellitero, E. Garzon m (2011a) hypocretin1/orexina-containing axons innervate locus coeruleus neurons that project to the rat medial prefrontal cortex. Implication in the sleep-wakefulness cycle and cortical activation. *Synapse, 65*, 843-857.

Deutch, A. Y., Goldstein, M., & Roth, R. H. (1986). Activation of the locus coeruleus induced by selective stimulation of the ventral tegmental area. *Brain research, 363*(2), 307-314. doi:10.1016/0006-8993(86)91016-4

Devanand, D., Michaels-Marston, K. S., Liu, X., Pelton, G. H., Padilla, M., Marder, K., . . . Mayeux, R. (2000). Olfactory deficits in patients with mild cognitive impairment predict alzheimer’s disease at follow-up. *American Journal of Psychiatry, 157*(9), 1399-1405.

Devanand, D. P. (2016). Olfactory identification deficits, cognitive decline, and dementia in older adults. *Am J Geriatr Psychiatry, 24*(12), 1151-1157. doi:10.1016/j.jagp.2016.08.010

Devanand, D. P., Lee, S., Manly, J., Andrews, H., Schupf, N., & Doty, R. L. (2015). Olfactory deficits predict cognitive decline and alzheimer dementia in an urban community. *Neurology., 84*(2), 182-189. doi:10.1212/WNL.0000000000001132

Devanand, D. P., Liu, X., Tabert, M. H., Pradhaban, G., Cuasay, K., Bell, K., . . . Pelton, G. H. (2008). Combining early markers strongly predicts conversion from mild cognitive impairment to alzheimer's disease. *Biological psychiatry, 64*(10), 871-879. doi:10.1016/j.biopsych.2008.06.020

Devauges, V., & Sara, S. J. (1991). Memory retrieval enhancement by locus coeruleus stimulation: Evidence for mediation by β-receptors. *Behavioural Brain Research, 43*(1), 93-97. doi:10.1016/s0166-4328(05)80056-7

Devore, S., Lee, J., & Linster, C. (2013). Odor preferences shape discrimination learning in rats. *Behavioral neuroscience, 127*(4), 498. doi:10.1037/a0033329

Díaz-Mataix, L., Piper, W. T., Schiff, H. C., Roberts, C. H., Campese, V. D., Sears, R. M., & LeDoux, J. E. (2017). Characterization of the amplificatory effect of norepinephrine in the acquisition of pavlovian threat associations. *Learning & memory, 24*(9), 432-439.

Ding, Y. S., Singhal, T., Planeta-Wilson, B., Gallezot, J. D., Nabulsi, N., & Labaree, D. (2010). Pet imaging of the effects of age and cocaine on the norepinephrine transporter in the human brain using (s,s)-[(11) c]o-methylreboxetine and hrrt. *Synapse., 64*(1), 30-38. doi:10.1002/syn.20696

Dittmer, P. J., Dell'Acqua, M. L., & Sather, W. A. (2014). Ca(2+)/calcineurin-dependent inactivation of neuronal l-type ca(2+) channels requires priming by akap-anchored protein kinase a. *Cell reports, 7*(5), 1410-1416. doi:10.1016/j.celrep.2014.04.039

Djordjevic, J., Jones-Gotman, M., De Sousa, K., & Chertkow, H. (2008). Olfaction in patients with mild cognitive impairment and alzheimer's disease. *Neurobiology of aging, 29*(5), 693-706. doi:10.1016/j.neurobiolaging.2006.11.014

Dolmetsch, R. E., Pajvani, U., Fife, K., Spotts, J. M., & Greenberg, M. E. (2001). Signaling to the nucleus by an l-type calcium channel-calmodulin complex through the map kinase pathway. *Science, 294*(5541), 333-339. doi:DOI 10.1126/science.1063395

Domyancic, A. V., & Morilak, D. A. (1997). Distribution of α1a adrenergic receptor m rna in the rat brain visualized by in situ hybridization. *Journal of comparative neurology, 386*(3), 358-378.

Dong, X., Li, S., & Kirouac, G. J. (2017). Collateralization of projections from the paraventricular nucleus of the thalamus to the nucleus accumbens, bed nucleus of the stria terminalis, and central nucleus of the amygdala. *Brain Struct Funct, 222*(9), 3927-3943. doi:10.1007/s00429-017-1445-8

Doty, R. L., Deems, D. A., & Stellar, S. (1988). Olfactory dysfunction in parkinsonism: A general deficit unrelated to neurologic signs, disease stage, or disease duration. *Neurology., 38*(8), 1237-1244. doi:10.1212/WNL.38.8.1237

Doty, R. L., Ferguson-Segall, M., Lucki, I., & Kreider, M. (1988). Effects of intrabulbar injections of 6-hydroxydopamine on ethyl acetate odor detection in castrate and non-castrate male rats. *Brain research, 444*(1), 95-103. doi:10.1016/0006-8993(88)90917-1

Doty, R. L., Golbe, L. I., McKeown, D. A., Stern, M. B., Lehrach, C. M., & Crawford, D. (1993). Olfactory testing differentiates between progressive supranuclear palsy and idiopathic parkinson's disease. *Neurology., 43*(5), 962-965. doi:10.1212/WNL.43.5.962

Doty, R. L., Shaman, P., Applebaum, S. L., Giberson, R., Siksorski, L., & Rosenberg, L. (1984). Smell identification ability: Changes with age. *Science., 226*(4681), 1441-1443. doi:10.1126/science.6505700

Doucette, W., Milder, J., & Restrepo, D. (2007). Adrenergic modulation of olfactory bulb circuitry affects odor discrimination. *Learning & memory, 14*(8), 539-547. doi:10.1101/lm.606407

Drolet, G., Van Bockstaele, E. J., & Aston-Jones, G. (1992). Robust enkephalin innervation of the locus coeruleus from the rostral medulla. *Journal of Neuroscience, 12*(8), 3162-3174.

Egan, T., & North, R. (1985). Acetylcholine acts on m2-muscarinic receptors to excite rat locus coeruleus neurones. *British journal of pharmacology, 85*(4), 733-735. doi:10.1111/j.1476-5381.1985.tb11070.x

Ehrenberg, A. J., Nguy, A. K., Theofilas, P., Dunlop, S., Suemoto, C. K., Di Lorenzo Alho, A. T., . . . Grinberg, L. T. (2017). Quantifying the accretion of hyperphosphorylated tau in the locus

coeruleus and dorsal raphe nucleus: The pathological building blocks of early alzheimer's disease. *Neuropathology and Applied Neurobiology, 43*(5), 393-408. doi:10.1111/nan.12387
Eidenmuller, J., Fath, T., Hellwig, A., Reed, J., Sontag, E., & Brandt, R. (2000). Structural and functional implications of tau hyperphosphorylation: Information from phosphorylation-mimicking mutated tau proteins. *Biochemistry., 39*(43), 13166-13175. doi:10.1021/bi001290z
Elobeid, A., Soininen, H., & Alafuzoff, I. (2012). Hyperphosphorylated tau in young and middle-aged subjects. *Acta Neuropathol, 123*(1), 97-104. doi:10.1007/s00401-011-0906-z
Ennis, M., & Aston-Jones, G. (1986). A potent excitatory input to the nucleus locus coeruleus from the ventrolateral medulla. *Neuroscience letters, 71*(3), 299-305. doi:10.1016/0304-3940(86)90637-3
Ennis, M., & Aston-Jones, G. (1988). Activation of locus coeruleus from nucleus paragigantocellularis: A new excitatory amino acid pathway in brain. *Journal of Neuroscience, 8*(10), 3644-3657.
Ennis, M., & Aston-Jones, G. (1989a). Gaba-mediated inhibition of locus coeruleus from the dorsomedial rostral medulla. *Journal of Neuroscience, 9*(8), 2973-2981.
Ennis, M., & Aston-Jones, G. (1989b). Potent inhibitory input to locus coeruleus from the nucleus prepositus hypoglossi. *Brain research bulletin, 22*(5), 793-803. doi:10.1016/0361-9230(89)90022-1
Escanilla, O., Alperin, S., Youssef, M., Ennis, M., & Linster, C. (2012). Noradrenergic but not cholinergic modulation of olfactory bulb during processing of near threshold concentration stimuli. *Behavioral neuroscience, 126*(5), 720.
Escanilla, O., Arrellanos, A., Karnow, A., Ennis, M., & Linster, C. (2010). Noradrenergic modulation of behavioral odor detection and discrimination thresholds in the olfactory bulb. *Eur J Neurosci, 32*(3), 458-468. doi:10.1111/j.1460-9568.2010.07297.x
España, R. A., & Berridge, C. W. (2006). Organization of noradrenergic efferents to arousal-related basal forebrain structures. *Journal of comparative neurology, 496*(5), 668-683.
España, R. A., Reis, K. M., Valentino, R. J., & Berridge, C. W. (2005). Organization of hypocretin/orexin efferents to locus coeruleus and basal forebrain arousal-related structures. *Journal of comparative neurology, 481*(2), 160-178.
Faber, E. L., & Sah, P. (2005). Independent roles of calcium and voltage-dependent potassium currents in controlling spike frequency adaptation in lateral amygdala pyramidal neurons. *European Journal of Neuroscience, 22*(7), 1627-1635. doi:10.1111/j.1460-9568.2005.04357.x
Farb, C., Chang, W., & LeDoux, J. (2010). Ultrastructural characterization of noradrenergic axons and beta-adrenergic receptors in the lateral nucleus of the amygdala. *Frontiers in behavioral neuroscience, 4*, 162. doi:10.3389/fnbeh.2010.00162
Farrell, S. R., Rankin, D. R., Brecha, N. C., & Barnes, S. (2014). Somatostatin receptor subtype 4 modulates l-type calcium channels via gβγ and pkc signaling in rat retinal ganglion cells. *Channels, 8*(6), 519-527.
Farrell, S. R., Raymond, I. D., Foote, M., Brecha, N. C., & Barnes, S. (2010). Modulation of voltage-gated ion channels in rat retinal ganglion cells mediated by somatostatin receptor subtype 4. *Journal of Neurophysiology, 104*(3), 1347-1354. doi:10.1152/jn.00098.2010
Ferry, B., & McGaugh, J. L. (2008). Involvement of basolateral amygdala α2-adrenoceptors in modulating consolidation of inhibitory avoidance memory. *Learning & memory, 15*(4), 238-243.

Fitzgerald, P. J., Giustino, T. F., Seemann, J. R., & Maren, S. (2015). Noradrenergic blockade stabilizes prefrontal activity and enables fear extinction under stress. *Proceedings of the National Academy of Sciences, 112*(28), E3729-E3737. doi:10.1073/pnas.1500682112

Flicker, C., & Geyer, M. A. (1982). Behavior during hippocampal microinfusions. I. Norepinephrine and diversive exploration. *Brain Res, 257*(1), 79-103.

Florin-Lechner, S. M., Druhan, J. P., Aston-Jones, G., & Valentino, R. J. (1996). Enhanced norepinephrine release in prefrontal cortex with burst stimulation of the locus coeruleus. *Brain research, 742*(1-2), 89-97. doi:10.1016/s0006-8993(96)00967-5

Fontaine, C. J., Harley, C. W., & Yuan, Q. (2013). Lateralized odor preference training in rat pups reveals an enhanced network response in anterior piriform cortex to olfactory input that parallels extended memory. *Journal of Neuroscience, 33*(38), 15126-15131. doi:10.1523/Jneurosci.2503-13.2013

Foote, S., Aston-Jones, G., & Bloom, F. (1980). Impulse activity of locus coeruleus neurons in awake rats and monkeys is a function of sensory stimulation and arousal. *Proceedings of the National Academy of Sciences, 77*(5), 3033-3037. doi:DOI 10.1073/pnas.77.5.3033

Förster, S., Vaitl, A., Teipel, S. J., Yakushev, I., Mustafa, M., la Fougère, C., . . . Hampel, H. (2010). Functional representation of olfactory impairment in early alzheimer's disease. *Journal of Alzheimer's Disease, 22*(2), 581-591. doi:10.3233/Jad-2010-091549

Förstl, H., Levy, R., Burns, A., Luthert, P., & Cairns, N. (1994). Disproportionate loss of noradrenergic and cholinergic neurons as cause of depression in alzheimer's disease-a hypothesis. *Pharmacopsychiatry, 27*(01), 11-15.

Francis, B. M., Yang, J., Hajderi, E., Brown, M. E., Michalski, B., McLaurin, J., . . . Mount, H. T. (2012). Reduced tissue levels of noradrenaline are associated with behavioral phenotypes of the tgcrnd8 mouse model of alzheimer's disease. *Neuropsychopharmacology, 37*(8), 1934-1944. doi:10.1038/npp.2012.40

Franks, K. M., & Isaacson, J. S. (2005). Synapse-specific downregulation of nmda receptors by early experience: A critical period for plasticity of sensory input to olfactory cortex. *Neuron, 47*(1), 101-114. doi:10.1016/j.neuron.2005.05.024

Fuller, M. D., Emrick, M. A., Sadilek, M., Scheuer, T., & Catterall, W. A. (2010). Molecular mechanism of calcium channel regulation in the fight-or-flight response. *Science signaling, 3*(141), ra70-ra70. doi:10.1126/scisignal.2001152

Gallvez, R., Mesches, M., & McGaugh, J. L. (1996). Norepinephrine release in the amygdala in response to footshock stimulation. *Neurobiol Learn Mem, 66*.

Gamache, K., Pitman, R. K., & Nader, K. (2012). Preclinical evaluation of reconsolidation blockade by clonidine as a potential novel treatment for posttraumatic stress disorder. *Neuropsychopharmacology, 37*(13), 2789-2796. doi:10.1038/npp.2012.145

Gannon, M., Che, P., Chen, Y., Jiao, K., Roberson, E. D., & Wang, Q. (2015). Noradrenergic dysfunction in alzheimer's disease. *Frontiers in neuroscience, 9*, 220. doi:10.3389/fnins.2015.00220

Gao, T., Puri, T. S., Gerhardstein, B. L., Chien, A. J., Green, R. D., & Hosey, M. M. (1997). Identification and subcellular localization of the subunits of l-type calcium channels and adenylyl cyclase in cardiac myocytes. *Journal of Biological Chemistry, 272*(31), 19401-19407. doi:DOI 10.1074/jbc.272.31.19401

Gao, V., Suzuki, A., Magistretti, P. J., Lengacher, S., Pollonini, G., Steinman, M. Q., & Alberini, C. M. (2016). Astrocytic β2-adrenergic receptors mediate hippocampal long-term memory consolidation. *Proceedings of the National Academy of Sciences, 113*(30), 8526-8531.

Garcia-Cabezas, M. A., John, Y. J., Barbas, H., & Zikopoulos, B. (2016). Distinction of neurons, glia and endothelial cells in the cerebral cortex: An algorithm based on cytological features. *Front Neuroanat, 10*, 107. doi:10.3389/fnana.2016.00107

Gatter, K., & Powell, T. (1977). The projection of the locus coeruleus upon the neocortex in the macaque monkey. *Neuroscience, 2*(3), 441-445.

Gazarini, L., Stern, C. A., Piornedo, R. R., Takahashi, R. N., & Bertoglio, L. J. (2015). Ptsd-like memory generated through enhanced noradrenergic activity is mitigated by a dual step pharmacological intervention targeting its reconsolidation. *International Journal of Neuropsychopharmacology, 18*(1). doi:10.1093/ijnp/pyu026

Gazarini, L., Stern, C. A. J., Carobrez, A. P., & Bertoglio, L. J. (2013). Enhanced noradrenergic activity potentiates fear memory consolidation and reconsolidation by differentially recruiting α1-and β-adrenergic receptors. *Learning & memory, 20*(4), 210-219.

Gean, P.-W., Huang, C.-C., Lin, J.-H., & Tsai, J.-J. (1992). Sustained enhancement of nmda receptor-mediated synaptic potential by isoproterenol in rat amygdalar slices. *Brain research, 594*(2), 331-334. doi:Doi 10.1016/0006-8993(92)91146-6

Gelinas, J. N., Banko, J. L., Hou, L., Sonenberg, N., Weeber, E. J., Klann, E., & Nguyen, P. V. (2007). Erk and mtor signaling couple β-adrenergic receptors to translation initiation machinery to gate induction of protein synthesis-dependent long-term potentiation. *Journal of Biological Chemistry, 282*(37), 27527-27535. doi:10.1074/jbc.M701077200

Gelinas, J. N., & Nguyen, P. V. (2005). B-adrenergic receptor activation facilitates induction of a protein synthesis-dependent late phase of long-term potentiation. *Journal of Neuroscience, 25*(13), 3294-3303. doi:10.1523/JNEUROSCI.4175-04.2005

Geyer, M. A., & Masten, V. L. (1989). Increases in diversive exploration in rats during hippocampal microinfusions of isoproterenol but not methoxamine. *Physiol Behav, 45*(1), 213-217.

Ghiasvand, M., Rezayof, A., Ahmadi, S., & Zarrindast, M.-R. (2011). B1-noradrenergic system of the central amygdala is involved in state-dependent memory induced by a cannabinoid agonist, win55, 212-2, in rat. *Behavioural Brain Research, 225*(1), 1-6.

Ghosh, A., Carew, S. J., Chen, X., & Yuan, Q. (2017). The role of l-type calcium channels in olfactory learning and its modulation by norepinephrine. *Frontiers in cellular neuroscience, 11*, 394. doi:10.3389/fncel.2017.00394

Ghosh, A., Purchase, N. C., Chen, X., & Yuan, Q. (2015). Norepinephrine modulates pyramidal cell synaptic properties in the anterior piriform cortex of mice: Age-dependent effects of β-adrenoceptors. *Frontiers in cellular neuroscience, 9*, 450. doi:10.3389/fncel.2015.00450

Giannakopoulos, P., Gold, G., von Gunten, A., Hof, P. R., & Bouras, C. (2009). Pathological substrates of cognitive decline in alzheimer's disease *Dementia in clinical practice* (Vol. 24, pp. 20-29): Karger Publishers.

Gilbert, P. E., & Kesner, R. P. (2002). The amygdala but not the hippocampus is involved in pattern separation based on reward value. *Neurobiology of Learning and Memory, 77*(3), 338-353.

Gilley, J., Ando, K., Seereeram, A., Rodriguez-Martin, T., Pooler, A. M., & Sturdee, L. (2016). Mislocalization of neuronal tau in the absence of tangle pathology in phosphomutant tau knockin mice. *Neurobiol Aging, 39*, 1-18. doi:10.1016/j.neurobiolaging.2015.11.028

Giustino, T. F., & Maren, S. (2018). Noradrenergic modulation of fear conditioning and extinction. *Frontiers in behavioral neuroscience, 12*, 43. doi:10.3389/fnbeh.2018.00043

Giustino, T. F., Seemann, J. R., Acca, G. M., Goode, T. D., Fitzgerald, P. J., & Maren, S. (2017). B-adrenoceptor blockade in the basolateral amygdala, but not the medial prefrontal cortex, rescues the immediate extinction deficit. *Neuropsychopharmacology, 42*(13), 2537-2544.

Glennon, E., Carcea, I., Martins, A. R. O., Multani, J., Shehu, I., Svirsky, M. A., & Froemke, R. C. (2019). Locus coeruleus activation accelerates perceptual learning. *Brain Research, 1709*, 39-49. doi:10.1016/j.brainres.2018.05.048

Goedert, M. (1993). Tau protein and the neurofibrillary pathology of alzheimer's disease. *Trends Neurosci, 16*(11), 460-465. doi:10.1016/0166-2236(93)90078-Z

Gordon, B. A., McCullough, A., Mishra, S., Blazey, T. M., Su, Y., Christensen, J., . . . Morris, J. C. (2018). Cross-sectional and longitudinal atrophy is preferentially associated with tau rather than amyloid β positron emission tomography pathology. *Alzheimer's & Dementia: Diagnosis, Assessment & Disease Monitoring, 10*, 245-252.

Gottfried, J. A., Deichmann, R., Winston, J. S., & Dolan, R. J. (2002). Functional heterogeneity in human olfactory cortex: An event-related functional magnetic resonance imaging study. *Journal of Neuroscience, 22*(24), 10819-10828.

Gottfried, J. A., & Zald, D. H. (2005). On the scent of human olfactory orbitofrontal cortex: Meta-analysis and comparison to non-human primates. *Brain Research Reviews, 50*(2), 287-304. doi:10.1016/j.brainresrev.2005.08.004

Goudsmit, J. (2016). The incubation period of alzheimer's disease and the timing of tau versus amyloid misfolding and spreading within the brain. *Eur J Epidemiol, 31*(2), 99-105. doi:10.1007/s10654-016-0144-8

Goveas, J. S., Xie, C., Chen, G., Li, W., Ward, B. D., Franczak, M. B., . . . Li, S.-J. (2013). Functional network endophenotypes unravel the effects of apolipoprotein e epsilon 4 in middle-aged adults. *PLoS One, 8*(2), e55902. doi:10.1371/journal.pone.0055902

Gray, C. M., Freeman, W. J., & Skinner, J. E. (1986). Chemical dependencies of learning in the rabbit olfactory bulb: Acquisition of the transient spatial pattern change depends on norepinephrine. *Behavioral neuroscience, 100*(4), 585. doi:10.1037//0735-7044.100.4.585

Gray, R., & Johnston, D. (1987). Noradrenaline and β-adrenoceptor agonists increase activity of voltage-dependent calcium channels in hippocampal neurons. *Nature, 327*(6123), 620-622. doi:10.1038/327620a0

Grimes, M. T., Harley, C. W., Darby-King, A., & McLean, J. H. (2012). Pka increases in the olfactory bulb act as unconditioned stimuli and provide evidence for parallel memory systems: Pairing odor with increased pka creates intermediate-and long-term, but not short-term, memories. *Learning & memory, 19*(3), 107-115.

Grover, L. M., & Teyler, T. J. (1990). Two components of long-term potentiation induced by different patterns of afferent activation. *Nature, 347*(6292), 477-479. doi:10.1038/347477a0

Grzanna, R., & Molliver, M. (1980). The locus coeruleus in the rat: An immunohistochemical delineation. *Neuroscience, 5*(1), 21-40. doi:10.1016/0306-4522(80)90068-8

Guerin, D., Peace, S. T., Didier, A., Linster, C., & Cleland, T. A. (2008). Noradrenergic neuromodulation in the olfactory bulb modulates odor habituation and spontaneous discrimination. *Behavioral neuroscience, 122*(4), 816. doi:10.1037/a0012522

Guérin, D., Sacquet, J., Mandairon, N., Jourdan, F., & Didier, A. (2009). Early locus coeruleus degeneration and olfactory dysfunctions in tg2576 mice. *Neurobiology of aging, 30*(2), 272-283. doi:10.1016/j.neurobiolaging.2007.05.020

Guillozet-Bongaarts, A. L., Cahill, M. E., Cryns, V. L., Reynolds, M. R., Berry, R. W., & Binder, L. I. (2006). Pseudophosphorylation of tau at serine 422 inhibits caspase cleavage: In vitro evidence and implications for tangle formation in vivo. *J Neurochem, 97*(4), 1005-1014. doi:10.1111/j.1471-4159.2006.03784.x

Gulyás, B., Brockschnieder, D., Nag, S., Pavlova, E., Kása, P., Beliczai, Z., . . . Dyrks, T. (2010). The norepinephrine transporter (net) radioligand (s, s)-[18f] fmener-d2 shows significant

decreases in net density in the human brain in alzheimer's disease: A post-mortem autoradiographic study. *Neurochemistry international, 56*(6-7), 789-798.
Haberman, R. P., Branch, A., & Gallagher, M. (2017). Targeting neural hyperactivity as a treatment to stem progression of late-onset alzheimer's disease. *Neurotherapeutics., 14*(3), 662-676. doi:10.1007/s13311-017-0541-z
Hall, D. D., Davare, M. A., Shi, M., Allen, M. L., Weisenhaus, M., McKnight, G. S., & Hell, J. W. (2007). Critical role of camp-dependent protein kinase anchoring to the l-type calcium channel cav1. 2 via a-kinase anchor protein 150 in neurons. *Biochemistry, 46*(6), 1635-1646. doi:10.1021/bi062217x
Hammerschmidt, T., Kummer, M. P., Terwel, D., Martinez, A., Gorji, A., Pape, H.-C., . . . Schultze, J. (2013). Selective loss of noradrenaline exacerbates early cognitive dysfunction and synaptic deficits in app/ps1 mice. *Biological psychiatry, 73*(5), 454-463. doi:10.1016/j.biopsych.2012.06.013
Hansen, N., & Manahan-Vaughan, D. (2015). Hippocampal long-term potentiation that is elicited by perforant path stimulation or that occurs in conjunction with spatial learning is tightly controlled by beta-adrenoreceptors and the locus coeruleus. *Hippocampus, 25*(11), 1285-1298.
Harley, C. W. (1987). A role for norepinephrine in arousal, emotion and learning?: Limbic modulation by norepinephrine and the kety hypothesis. *Progress in Neuro-Psychopharmacology and Biological Psychiatry, 11*(4), 419-458. doi:10.1016/0278-5846(87)90015-7
Harley, C. W., Darby-King, A., McCann, J., & McLean, J. H. (2006). B1-adrenoceptor or α1-adrenoceptor activation initiates early odor preference learning in rat pups: Support for the mitral cell/camp model of odor preference learning. *Learning & memory, 13*(1), 8-13.
Hasselmo, M. E., Linster, C., Patil, M., Ma, D., & Cekic, M. (1997). Noradrenergic suppression of synaptic transmission may influence cortical signal-to-noise ratio. *Journal of Neurophysiology, 77*(6), 3326-3339.
Hayar, A., Heyward, P. M., Heinbockel, T., Shipley, M. T., & Ennis, M. (2001). Direct excitation of mitral cells via activation of α1-noradrenergic receptors in rat olfactory bulb slices. *Journal of Neurophysiology, 86*(5), 2173-2182.
Hell, J. W., Westenbroek, R. E., Warner, C., Ahlijanian, M. K., Prystay, W., Gilbert, M. M., . . . Catterall, W. A. (1993). Identification and differential subcellular localization of the neuronal class c and class d l-type calcium channel alpha 1 subunits. *The Journal of cell biology, 123*(4), 949-962. doi:DOI 10.1083/jcb.123.4.949
Heneka, M. T., Nadrigny, F., Regen, T., Martinez-Hernandez, A., Dumitrescu-Ozimek, L., Terwel, D., . . . Hanisch, U.-K. (2010). Locus ceruleus controls alzheimer's disease pathology by modulating microglial functions through norepinephrine. *Proceedings of the National Academy of Sciences, 107*(13), 6058-6063. doi:10.1073/pnas.0909586107
Henrich, M. T., Geibl, F. F., Lee, B., Chiu, W. H., Koprich, J. B., & Brotchie, J. M. (2018). A53t-alpha-synuclein overexpression in murine locus coeruleus induces parkinson's disease-like pathology in neurons and glia. *Acta Neuropathol Commun, 6*(1), 39. doi:10.1186/s40478-018-0541-1
Hess, P., Lansman, J., Nilius, B., & Tsien, R. (1986). Calcium channel types in cardiac myocytes: Modulation by dihydropyridines and β-adrenergic stimulation. *Journal of Cardiovascular Pharmacology, 8*, S11-21.
Hirschberg, S., Li, Y., Randall, A., Kremer, E. J., & Pickering, A. E. (2017). Functional dichotomy in spinal- vs prefrontal-projecting locus coeruleus modules splits descending noradrenergic

analgesia from ascending aversion and anxiety in rats. *Elife (Cambridge), 6*. doi:10.7554/eLife.29808

Hobson, J. A., McCarley, R. W., & Wyzinski, P. W. (1975). Sleep cycle oscillation: Reciprocal discharge by two brainstem neuronal groups. *Science, 189*(4196), 55-58. doi:10.1126/science.1094539

Hoddah, H., Marcantoni, A., Comunanza, V., Carabelli, V., & Carbone, E. (2009). L-type channel inhibition by cb1 cannabinoid receptors is mediated by ptx-sensitive g proteins and camp/pka in gt1-7 hypothalamic neurons. *Cell calcium, 46*(5-6), 303-312. doi:10.1016/j.ceca.2009.08.007

Holmes, N., Crane, J., Tang, M., Fam, J., Westbrook, R., & Delaney, A. (2017). A 2-adrenoceptor-mediated inhibition in the central amygdala blocks fear-conditioning. *Scientific reports, 7*(1), 1-10. doi:ARTN 11712

10.1038/s41598-017-12115-x

Hoogendijk, W. J., Feenstra, M. G., Botterblom, M. H., Gilhuis, J., Sommer, I. E., Kamphorst, W., . . . Swaab, D. F. (1999). Increased activity of surviving locus ceruleus neurons in alzheimer's disease. *Annals of Neurology: Official Journal of the American Neurological Association and the Child Neurology Society, 45*(1), 82-91. doi:10.1002/1531-8249(199901)45:1<82::aid-art14>3.0.co;2-t

Hoogland, T. M., & Saggau, P. (2004). Facilitation of l-type ca²⁺ channels in dendritic spines by activation of β₂ adrenergic receptors. *The Journal of Neuroscience, 24*(39), 8416-8427. doi:10.1523/jneurosci.1677-04.2004

Hoover, B. R., Reed, M. N., Su, J., Penrod, R. D., Kotilinek, L. A., & Grant, M. K. (2010). Tau mislocalization to dendritic spines mediates synaptic dysfunction independently of neurodegeneration. *Neuron., 68*(6), 1067-1081. doi:10.1016/j.neuron.2010.11.030

Hopp, S. C., Lin, Y., Oakley, D., Roe, A. D., DeVos, S. L., & Hanlon, D. (2018). The role of microglia in processing and spreading of bioactive tau seeds in alzheimer's disease. *J Neuroinflammation, 15*(1), 269. doi:10.1186/s12974-018-1309-z

Hsieh, J. W., Keller, A., Wong, M., Jiang, R. S., & Vosshall, L. B. (2017). Smell-s and smell-r: Olfactory tests not influenced by odor-specific insensitivity or prior olfactory experience. *Proc Natl Acad Sci U S A, 114*(43), 11275-11284. doi:10.1073/pnas.1711415114

Huang, Y.-Y., & Kandel, E. R. (1996). Modulation of both the early and the late phase of mossy fiber ltp by the activation of β-adrenergic receptors. *Neuron, 16*(3), 611-617.

Huang, Y.-Y., Levine, A., Kandel, D. B., Yin, D., Colnaghi, L., Drisaldi, B., & Kandel, E. R. (2014). D1/d5 receptors and histone deacetylation mediate the gateway effect of ltp in hippocampal dentate gyrus. *Learning & memory, 21*(3), 153-160. doi:10.1101/lm.032292.113

Huang, Y.-Y., Martin, K. C., & Kandel, E. R. (2000). Both protein kinase a and mitogen-activated protein kinase are required in the amygdala for the macromolecular synthesis-dependent late phase of long-term potentiation. *Journal of Neuroscience, 20*(17), 6317-6325. doi:Doi 10.1523/Jneurosci.20-17-06317.2000

Hui, J., Feng, G., Zheng, C., Jin, H., & Jia, N. (2017). Maternal separation exacerbates alzheimer's disease-like behavioral and pathological changes in adult appswe/ps1de9 mice. *Behavioural Brain Research, 318*, 18-23.

Huijbers, W., Schultz, A. P., Papp, K. V., LaPoint, M. R., Hanseeuw, B., Chhatwal, J. P., . . . Sperling, R. A. (2019). Tau accumulation in clinically normal older adults is associated with

hippocampal hyperactivity. *Journal of Neuroscience, 39*(3), 548-556. doi:10.1523/Jneurosci.1397-18.2018

Hullinger, R., O'Riordan, K., & Burger, C. (2015). Environmental enrichment improves learning and memory and long-term potentiation in young adult rats through a mechanism requiring mglur5 signaling and sustained activation of p70s6k. *Neurobiology of Learning and Memory, 125*, 126-134. doi:10.1016/j.nlm.2015.08.006

Hundelt, M., Fath, T., Selle, K., Oesterwind, K., Jordan, J., & Schultz, C. (2011). Altered phosphorylation but no neurodegeneration in a mouse model of tau hyperphosphorylation. *Neurobiol Aging, 32*(6), 991-1006. doi:10.1016/j.neurobiolaging.2009.06.007

Hyman, B. T., Van Hoesen, G. W., Damasio, A. R., & Barnes, C. L. (1984). Alzheimer's disease: Cell-specific pathology isolates the hippocampal formation. *Science, 225*(4667), 1168-1170. doi:10.1126/science.6474172

Iba, M., McBride, J. D., Guo, J. L., Zhang, B., Trojanowski, J. Q., & Lee, V. M. Y. (2015). Tau pathology spread in ps19 tau transgenic mice following locus coeruleus (lc) injections of synthetic tau fibrils is determined by the lc's afferent and efferent connections. *Acta Neuropathol, 130*(3), 349-362. doi:10.1007/s00401-015-1458-4

Impey, S., Mark, M., Villacres, E. C., Poser, S., Chavkin, C., & Storm, D. R. (1996). Induction of cre-mediated gene expression by stimuli that generate long-lasting ltp in area ca1 of the hippocampus. *Neuron, 16*(5), 973-982. doi:Doi 10.1016/S0896-6273(00)80120-8

Ishikawa, M., Shimada, S., & Tanaka, C. (1975). Histochemical mapping of catecholamine neurons and fiber pathways in the pontine tegmentum of the dog. *Brain research, 86*(1), 1-16. doi:10.1016/0006-8993(75)90633-2

Iversen, L., Rossor, M., Reynolds, G., Hills, R., Roth, M., Mountjoy, C., . . . Bloom, F. (1983). Loss of pigmented dopamine-β-hydroxylase positive cells from locus coeruleus in senile dementia of alzheimer's type. *Neuroscience letters, 39*(1), 95-100.

Jacobs, H. I., Wiese, S., van de Ven, V., Gronenschild, E. H., Verhey, F. R., & Matthews, P. M. (2015). Relevance of parahippocampal-locus coeruleus connectivity to memory in early dementia. *Neurobiology of aging, 36*(2), 618-626. doi:10.1016/j.neurobiolaging.2014.10.041

Jedema, H. P., & Grace, A. A. (2004). Corticotropin-releasing hormone directly activates noradrenergic neurons of the locus ceruleus recorded in vitro. *Journal of Neuroscience, 24*(43), 9703-9713. doi:10.1523/JNEUROSCI.2830-04.2004

Jerome, D., Hou, Q., & Yuan, Q. (2012). Interaction of nmda receptors and l-type calcium channels during early odor preference learning in rats. *European Journal of Neuroscience, 36*(8), 3134-3141. doi:10.1111/j.1460-9568.2012.08210.x

Johanson, I. B., & Hall, W. (1979). Appetitive learning in 1-day-old rat pups. *Science, 205*(4404), 419-421. doi:10.1126/science.451612

Johanson, I. B., & Teicher, M. H. (1980). Classical conditioning of an odor preference in 3-day-old rats. *Behavioral and neural biology, 29*(1), 132-136. doi:10.1016/s0163-1047(80)92596-0

Jones, B. E. (1990). Immunohistochemical study of choline acetyltransferase-immunoreactive processes and cells innervating the pontomedullary reticular formation in the rat. *Journal of comparative neurology, 295*(3), 485-514. doi:10.1002/cne.902950311

Jones, B. E., & Yang, T. Z. (1985). The efferent projections from the reticular formation and the locus coeruleus studied by anterograde and retrograde axonal transport in the rat. *Journal of comparative neurology, 242*(1), 56-92. doi:DOI 10.1002/cne.902420105

Josefsson, M., Larsson, M., Nordin, S., Adolfsson, R., & Olofsson, J. (2017). Apoe-varepsilon4 effects on longitudinal decline in olfactory and non-olfactory cognitive abilities in middle-aged and old adults. *Sci Rep, 7*(1), 1286. doi:10.1038/s41598-017-01508-7

Jurgens, C. W., Boese, S. J., King, J. D., Pyle, S. J., Porter, J. E., & Doze, V. A. (2005). Adrenergic receptor modulation of hippocampal ca3 network activity. *Epilepsy Res, 66*(1-3), 117-128. doi:10.1016/j.eplepsyres.2005.07.007

Justice, N. J. (2018). The relationship between stress and alzheimer's disease. *Neurobiology of stress, 8*, 127-133. doi:10.1016/j.ynstr.2018.04.002

Kalaria, R., Andorn, A., Tabaton, M., Whitehouse, P., Harik, S., & Unnerstall, J. (1989). Adrenergic receptors in aging and alzheimer's disease: Increased β2-receptors in prefrontal cortex and hippocampus. *Journal of neurochemistry, 53*(6), 1772-1781. doi:10.1111/j.1471-4159.1989.tb09242.x

Kalaria, R. N. (1989). Characterization of [125i] heat binding to α1-receptors in human brain: Assessment in aging and alzheimer's disease. *Brain research, 501*(2), 287-294.

Kalinin, S., Gavrilyuk, V., Polak, P. E., Vasser, R., Zhao, J., Heneka, M. T., & Feinstein, D. L. (2007). Noradrenaline deficiency in brain increases β-amyloid plaque burden in an animal model of alzheimer's disease. *Neurobiology of aging, 28*(8), 1206-1214. doi:10.1016/j.neurobiolaging.2006.06.003

Kapur, A., Yeckel, M. F., Gray, R., & Johnston, D. (1998). L-type calcium channels are required for one form of hippocampal mossy fiber ltp. *Journal of Neurophysiology, 79*(4), 2181-2190. doi:10.1152/jn.1998.79.4.2181

Kareken, D. A., Doty, R. L., Moberg, P. J., Mosnik, D., Chen, S. H., Farlow, M. R., & Hutchins, G. D. (2001). Olfactory-evoked regional cerebral blood flow in alzheimer's disease. *Neuropsychology, 15*(1), 18. doi:10.1037//0894-4105.15.1.18

Karls, A., & Mynlieff, M. (2015). Gabab receptors couple to gαq to mediate increases in voltage-dependent calcium current during development. *Journal of neurochemistry, 135*(1), 88-100.

Katsuki, H., Izumi, Y., & Zorumski, C. F. (1997). Noradrenergic regulation of synaptic plasticity in the hippocampal ca1 region. *Journal of Neurophysiology, 77*(6), 3013-3020. doi:10.1152/jn.1997.77.6.3013

Kaur, S., Saxena, R., & Mallick, B. N. (2001). Gabaergic neurons in prepositus hypoglossi regulate rem sleep by its action on locus coeruleus in freely moving rats. *Synapse, 42*(3), 141-150. doi:DOI 10.1002/syn.1109

Kavalali, E. T., Hwang, K. S., & Plummer, M. R. (1997). Camp-dependent enhancement of dihydropyridine-sensitive calcium channel availability in hippocampal neurons. *Journal of Neuroscience, 17*(14), 5334-5348.

Kawagoe, T., Tamura, R., Uwano, T., Asahi, T., Nishijo, H., Eifuku, S., & Ono, T. (2007). Neural correlates of stimulus–reward association in the rat mediodorsal thalamus. *Neuroreport, 18*(7), 683-688.

Kelly, S. C., He, B., Perez, S. E., Ginsberg, S. D., Mufson, E. J., & Counts, S. E. (2017). Locus coeruleus cellular and molecular pathology during the progression of alzheimer's disease. *Acta Neuropathol Commun, 5*(1), 8. doi:10.1186/s40478-017-0411-2

Kempadoo, K. A., Mosharov, E. V., Choi, S. J., Sulzer, D., & Kandel, E. R. (2016). Dopamine release from the locus coeruleus to the dorsal hippocampus promotes spatial learning and memory. *Proceedings of the National Academy of Sciences, 113*(51), 14835-14840. doi:10.1073/pnas.1616515114

Kety, S. (1970). The biogenic amines in the central nervous system: Their possible roles in arousal, emotion and learning. *The neurosciences: Second study program*.

Kim, J., Pignatelli, M., Xu, S., Itohara, S., & Tonegawa, S. (2016). Antagonistic negative and positive neurons of the basolateral amygdala. *Nature Neuroscience, 19*(12), 1636-1646. doi:10.1038/nn.4414

Kim, M.-A., Lee, H. S., Lee, B. Y., & Waterhouse, B. D. (2004). Reciprocal connections between subdivisions of the dorsal raphe and the nuclear core of the locus coeruleus in the rat. *Brain research, 1026*(1), 56-67. doi:10.1016/j.brainres.2004.08.022

Kiris, E., Ventimiglia, D., Sargin, M. E., Gaylord, M. R., Altinok, A., & Rose, K. (2011). Combinatorial tau pseudophosphorylation: Markedly different regulatory effects on microtubule assembly and dynamic instability than the sum of the individual parts. *J Biol Chem, 286*(16), 14257-14270. doi:10.1074/jbc.M111.219311

Kitayama, I., Nakamura, S., Yaga, T., Murase, S., Nomura, J., & Kayahara, T. (1994). Degeneration of locus coeruleus axons in stress-induced depression model. *Brain Res Bull, 35*(5-6), 573-580. doi:10.1016/0361-9230(94)90171-6

Kjelvik, G., Saltvedt, I., White, L. R., Stenumgård, P., Sletvold, O., Engedal, K., . . . Håberg, A. K. (2014). The brain structural and cognitive basis of odor identification deficits in mild cognitive impairment and alzheimer's disease. *BMC neurology, 14*(1), 168. doi:10.1186/s12883-014-0168-1

Klann, E., Antion, M. D., Banko, J. L., & Hou, L. (2004). Synaptic plasticity and translation initiation. *Learning & memory, 11*(4), 365-372. doi:10.1101/lm.79004

Komatsu, M., Shibata, N., Ohnuma, T., Kuerban, B., Tomson, K., Toda, A., . . . Arai, H. (2014). Polymorphisms in the aldehyde dehydrogenase 2 and dopamine β hydroxylase genes are not associated with alzheimer's disease. *Journal of neural transmission, 121*(4), 427-432.

Kopeikina, K. J., Hyman, B. T., & Spires-Jones, T. L. (2012). Soluble forms of tau are toxic in alzheimer's disease. *Transl Neurosci, 3*(3), 223-233. doi:10.2478/s13380-012-0032-y

Korotkova, T. M., Sergeeva, O. A., Ponomarenko, A. A., & Haas, H. L. (2005). Histamine excites noradrenergic neurons in locus coeruleus in rats. *Neuropharmacology, 49*(1), 129-134. doi:10.1016/j.neuropharm.2005.03.001

Kovacs, T., Cairns, N. J., & Lantos, P. L. (2001). Olfactory centres in alzheimer's disease: Olfactory bulb is involved in early braak's stages. *Neuroreport., 12*(2), 285-288. doi:10.1097/00001756-200102120-00021

Lafaille-Magnan, M. E., Poirier, J., Etienne, P., Tremblay-Mercier, J., Frenette, J., & Rosa-Neto, P. (2017). Odor identification as a biomarker of preclinical ad in older adults at risk. *Neurology., 89*(4), 327-335. doi:10.1212/WNL.0000000000004159

LaLumiere, R. T., Buen, T.-V., & McGaugh, J. L. (2003). Post-training intra-basolateral amygdala infusions of norepinephrine enhance consolidation of memory for contextual fear conditioning. *Journal of Neuroscience, 23*(17), 6754-6758.

Larsson, M., Semb, H., Winblad, B., Amberla, K., Wahlund, L.-O., & Bäckman, L. (1999). Odor identification in normal aging and early alzheimer's disease: Effects of retrieval support. *Neuropsychology, 13*(1), 47. doi:10.1037//0894-4105.13.1.47

Lashgari, R., Motamedi, F., Asl, S. Z., Shahidi, S., & Komaki, A. (2006). Behavioral and electrophysiological studies of chronic oral administration of l-type calcium channel blocker verapamil on learning and memory in rats. *Behavioural Brain Research, 171*(2), 324-328. doi:10.1016/j.bbr.2006.04.013

Lazzaro, S. C., Hou, M., Cunha, C., LeDoux, J. E., & Cain, C. K. (2010). Antagonism of lateral amygdala alpha1-adrenergic receptors facilitates fear conditioning and long-term potentiation. *Learning & memory, 17*(10), 489-493. doi:10.1101/lm.1918210

Lecei, A., & van Winkel, R. (2020). Hippocampal pattern separation of emotional information determining risk or resilience in individuals exposed to childhood trauma: Linking exposure to neurodevelopmental alterations and threat anticipation. *Neuroscience & Biobehavioral Reviews, 108*, 160-170. doi:10.1016/j.neubiorev.2019.11.010

Lee, H. J., Berger, S. Y., Stiedl, O., Spiess, J., & Kim, J. J. (2001). Post-training injections of catecholaminergic drugs do not modulate fear conditioning in rats and mice. *Neuroscience letters, 303*(2), 123-126.

Lee, H. S., Lee, B. Y., & Waterhouse, B. D. (2005). Retrograde study of projections from the tuberomammillary nucleus to the dorsal raphe and the locus coeruleus in the rat. *Brain research, 1043*(1-2), 65-75. doi:10.1016/j.brainres.2005.02.050

Lemmer, B., Langer, L., Ohm, T., & Bohl, J. (1993). Beta-adrenoceptor density and subtype distribution in cerebellum and hippocampus from patients with alzheimer's disease. *Naunyn-Schmiedeberg's archives of pharmacology, 347*(2), 214-219.

Lemon, N., Aydin-Abidin, S., Funke, K., & Manahan-Vaughan, D. (2009). Locus coeruleus activation facilitates memory encoding and induces hippocampal ltd that depends on β-adrenergic receptor activation. *Cerebral Cortex, 19*(12), 2827-2837.

Lesuis, S. L., Hoeijmakers, L., Korosi, A., de Rooij, S. R., Swaab, D. F., Kessels, H. W., . . . Krugers, H. J. (2018). Vulnerability and resilience to alzheimer's disease: Early life conditions modulate neuropathology and determine cognitive reserve. *Alzheimer's Research & Therapy, 10*(1), 1-20.

Lesuis, S. L., van Hoek, B. A., Lucassen, P. J., & Krugers, H. J. (2017). Early postnatal handling reduces hippocampal amyloid plaque formation and enhances cognitive performance in appswe/ps1de9 mice at middle age. *Neurobiology of Learning and Memory, 144*, 27-35. doi:10.1016/j.nlm.2017.05.016

Lethbridge, R., Hou, Q., Harley, C. W., & Yuan, Q. (2012). Olfactory bulb glomerular nmda receptors mediate olfactory nerve potentiation and odor preference learning in the neonate rat. *PLoS One, 7*(4), e35024. doi:10.1371/journal.pone.0035024

Leyns, C. E. G., & Holtzman, D. M. (2017). Glial contributions to neurodegeneration in tauopathies. *Mol Neurodegener, 12*(1), 50. doi:10.1186/s13024-017-0192-x

Li, W., Howard, J. D., & Gottfried, J. A. (2010). Disruption of odour quality coding in piriform cortex mediates olfactory deficits in alzheimer's disease. *Brain., 133*(9), 2714-2726. doi:10.1093/brain/awq209

Liang, X., Ding, D., Zhao, Q., Guo, Q., Luo, J., & Hong, Z. (2016). Association between olfactory identification and cognitive function in community-dwelling elderly: The shanghai aging study. *BMC Neurol, 16*. doi:10.1186/s12883-016-0725-x

Liddell, J. R., & White, A. R. (2018). Nexus between mitochondrial function, iron, copper and glutathione in parkinson's disease. *Neurochem Int, 117*, 126-138. doi:10.1016/j.neuint.2017.05.016

Lima, M. G. P., Schimidt, H. L., Garcia, A., Daré, L. R., Carpes, F. P., Izquierdo, I., & Mello-Carpes, P. B. (2018). Environmental enrichment and exercise are better than social enrichment to reduce memory deficits in amyloid beta neurotoxicity. *Proceedings of the National Academy of Sciences, 115*(10), E2403-E2409. doi:10.1073/pnas.1718435115

Linster, C. (2019). Cellular and network processes of noradrenergic modulation in the olfactory system. *Brain research, 1709*, 28-32. doi:10.1016/j.brainres.2018.03.008

Linster, C., & Escanilla, O. (2019). Noradrenergic effects on olfactory perception and learning. *Brain research, 1709*, 33-38. doi:10.1016/j.brainres.2018.03.021

Linster, C., Nai, Q., & Ennis, M. (2011). Nonlinear effects of noradrenergic modulation of olfactory bulb function in adult rodents. *Journal of Neurophysiology, 105*(4), 1432-1443. doi:10.1152/jn.00960.2010

Liu, F., Weng, S.-J., Yang, X.-L., & Zhong, Y.-M. (2015). Orexin-a potentiates l-type calcium/barium currents in rat retinal ganglion cells. *Neuroscience, 305*, 225-237. doi:10.1016/j.neuroscience.2015.08.008

Llorca-Torralba, M., Suarez-Pereira, I., Bravo, L., Camarena-Delgado, C., Garcia-Partida, J. A., Mico, J. A., & Berrocoso, E. (2019). Chemogenetic silencing of the locus coeruleus-basolateral amygdala pathway abolishes pain-induced anxiety and enhanced aversive learning in rats. *Biol Psychiatry, 85*(12), 1021-1035. doi:10.1016/j.biopsych.2019.02.018

Lojkowska, W., Sawicka, B., Gugala, M., Sienkiewicz-Jarosz, H., Bochynska, A., Scinska, A., . . . Ryglewicz, D. (2011). Follow-up study of olfactory deficits, cognitive functions, and volume loss of medial temporal lobe structures in patients with mild cognitive impairment. *Current Alzheimer Research, 8*(6), 689-698. doi:10.2174/156720511796717212

Loughlin, S., Foote, S., & Grzanna, R. (1986). Efferent projections of nucleus locus coeruleus: Morphologic subpopulations have different efferent targets. *Neuroscience, 18*(2), 307-319.

Lu, J., Jhou, T. C., & Saper, C. B. (2006). Identification of wake-active dopaminergic neurons in the ventral periaqueductal gray matter. *Journal of Neuroscience, 26*(1), 193-202. doi:10.1523/JNEUROSCI.2244-05.2006

Lv, J., Zhan, S.-Y., Li, G.-X., Wang, D., Li, Y.-S., & Jin, Q.-H. (2016). A1-adrenoceptors in the hippocampal dentate gyrus involved in learning-dependent long-term potentiation during active-avoidance learning in rats. *Neuroreport, 27*(16), 1211-1216.

MacDonald, S. W. S., Keller, C. J. C., Brewster, P. W. H., & Dixon, R. A. (2018). Contrasting olfaction, vision, and audition as predictors of cognitive change and impairment in non-demented older adults. *Neuropsychology., 32*(4), 450-460. doi:10.1037/neu0000439

Magistretti, J., Brevi, S., & De Curtis, M. (1999). Biophysical and pharmacological diversity of high-voltage-activated calcium currents in layer ii neurones of guinea-pig piriform cortex. *The Journal of Physiology, 518*(3), 705-720.

Mandairon, N., Peace, S., Karnow, A., Kim, J., Ennis, M., & Linster, C. (2008). Noradrenergic modulation in the olfactory bulb influences spontaneous and reward-motivated discrimination, but not the formation of habituation memory. *European Journal of Neuroscience, 27*(5), 1210-1219. doi:10.1111/j.1460-9568.2008.06101.x

Manella, L. C., Alperin, S., & Linster, C. (2013). Stressors impair odor recognition memory via an olfactory bulb-dependent noradrenergic mechanism. *Frontiers in integrative neuroscience, 7*, 97. doi:10.3389/fnint.2013.00097

Mann, D., Lincoln, J., Yates, P., Stamp, J., & Toper, S. (1980). Changes in the monoamine containing neurones of the human cns in senile dementia. *The British Journal of Psychiatry, 136*(6), 533-541. doi:10.1192/bjp.136.6.533

Manns, I. D., Alonso, A., & Jones, B. E. (2000a). Discharge profiles of juxtacellularly labeled and immunohistochemically identified gabaergic basal forebrain neurons recorded in association with the electroencephalogram in anesthetized rats. *Journal of Neuroscience, 20*(24), 9252-9263.

Manns, I. D., Alonso, A., & Jones, B. E. (2000b). Discharge properties of juxtacellularly labeled and immunohistochemically identified cholinergic basal forebrain neurons recorded in association with the electroencephalogram in anesthetized rats. *Journal of Neuroscience, 20*(4), 1505-1518.

Manns, I. D., Lee, M. G., Modirrousta, M., Hou, Y. P., & Jones, B. E. (2003). Alpha 2 adrenergic receptors on gabaergic, putative sleep-promoting basal forebrain neurons. *European Journal of Neuroscience, 18*(3), 723-727. doi:10.1046/j.1460-9568.2003.02788.x

Markopoulou, K., Chase, B. A., Robowski, P., Strongosky, A., Narozanska, E., & Sitek, E. J. (2016). Assessment of olfactory function in mapt-associated neurodegenerative disease reveals odor-identification irreproducibility as a non-disease-specific, general characteristic of olfactory dysfunction. *PLoS One, 11*(11), e0165112. doi:10.1371/journal.pone.0165112

Marlatt, M. W., Bauer, J., Aronica, E., Haastert, E. S., Hoozemans, J. J., & Joels, M. (2014). Proliferation in the alzheimer hippocampus is due to microglia, not astroglia, and occurs at sites of amyloid deposition. *Neural Plasticity, 2014*, 1-12. doi:10.1155/2014/693851

Marowsky, A., Yanagawa, Y., Obata, K., & Vogt, K. E. (2005). A specialized subclass of interneurons mediates dopaminergic facilitation of amygdala function. *Neuron, 48*(6), 1025-1037. doi:10.1016/j.neuron.2005.10.029

Martignoni, E., Blandini, F., Petraglia, F., Pacchetti, C., Bono, G., & Nappi, G. (1992). Cerebrospinal fluid norepinephrine, 3-methoxy-4-hydroxyphenylglycol and neuropeptide y levels in parkinson's disease, multiple system atrophy and dementia of the alzheimer type. *Journal of neural transmission-Parkinson's disease and dementia section, 4*(3), 191-205. doi:10.1007/BF02260903

Martins, A. R., & Froemke, R. C. (2015). Coordinated forms of noradrenergic plasticity in the locus coeruleus and primary auditory cortex. *Nature Neuroscience, 18*(10), 1483-1492. doi:10.1038/nn.4090

Martisova, E., Aisa, B., Guereñu, G., & Javier Ramirez, M. (2013). Effects of early maternal separation on biobehavioral and neuropathological markers of alzheimer's disease in adult male rats. *Current Alzheimer Research, 10*(4), 420-432. doi:10.2174/1567205011310040007

Mason, S. T., & Fibiger, H. C. (1979). Noradrenaline and avoidance learning in the rat. *Brain research, 161*(2), 321-333. doi:10.1016/0006-8993(79)90073-8

Mather, M., Clewett, D., Sakaki, M., & Harley, C. W. (2016). Norepinephrine ignites local hotspots of neuronal excitation: How arousal amplifies selectivity in perception and memory. *Behavioral and Brain Sciences, 39*. doi:ARTN e200

10.1017/S0140525X15000667

Matthews, K. L., Chen, C. P.-H., Esiri, M. M., Keene, J., Minger, S. L., & Francis, P. T. (2002). Noradrenergic changes, aggressive behavior, and cognition in patients with dementia. *Biological psychiatry, 51*(5), 407-416. doi:10.1016/s0006-3223(01)01235-5

Mayo, C. D., Mazerolle, E. L., Ritchie, L., Fisk, J. D., & Gawryluk, J. R. (2017). Alzheimer's disease neuroimaging i. Longitudinal changes in microstructural white matter metrics in alzheimer's disease. *Neuroimage Clin, 13*, 330-338. doi:10.1016/j.nicl.2016.12.012

McBurney-Lin, J., Lu, J., Zuo, Y., & Yang, H. (2019). Locus coeruleus-norepinephrine modulation of sensory processing and perception: A focused review. *Neuroscience & Biobehavioral Reviews, 105*, 190-199. doi:10.1016/j.neubiorev.2019.06.009

McCall, J. G., Al-Hasani, R., Siuda, E. R., Hong, D. Y., Norris, A. J., Ford, C. P., & Bruchas, M. R. (2015). Crh engagement of the locus coeruleus noradrenergic system mediates stress-induced anxiety. *Neuron, 87*(3), 605-620. doi:10.1016/j.neuron.2015.07.002

McCall, J. G., Siuda, E. R., Bhatti, D. L., Lawson, L. A., McElligott, Z. A., Stuber, G. D., & Bruchas, M. R. (2017). Locus coeruleus to basolateral amygdala noradrenergic projections promote anxiety-like behavior. *Elife, 6*, e18247. doi:10.7554/eLife.18247

McCormick, D., Pape, H.-C., & Williamson, A. (1991). Actions of norepinephrine in the cerebral cortex and thalamus: Implications for function of the central noradrenergic system *Progress in brain research* (Vol. 88, pp. 293-305): Elsevier.

McEwen, B. S., Eiland, L., Hunter, R. G., & Miller, M. M. (2012). Stress and anxiety: Structural plasticity and epigenetic regulation as a consequence of stress. *Neuropharmacology, 62*(1), 3-12. doi:10.1016/j.neuropharm.2011.07.014

McHugh, T. J., Jones, M. W., Quinn, J. J., Balthasar, N., Coppari, R., Elmquist, J. K., . . . Tonegawa, S. (2007). Dentate gyrus nmda receptors mediate rapid pattern separation in the hippocampal network. *Science, 317*(5834), 94-99. doi:10.1126/science.1140263

McLean, J., Darby-King, A., & Harley, C. (2005). Potentiation and prolongation of long-term odor memory in neonate rats using a phosphodiesterase inhibitor. *Neuroscience, 135*(2), 329-334. doi:10.1016/j.neuroscience.2005.06.029

McLean, J. H., Darby-King, A., Sullivan, R. M., & King, S. R. (1993). Serotonergic influence on olfactory learning in the neonate rat. *Behavioral and neural biology, 60*(2), 152-162. doi:10.1016/0163-1047(93)90257-i

McLean, J. H., Harley, C. W., Darby-King, A., & Yuan, Q. (1999). Pcreb in the neonate rat olfactory bulb is selectively and transiently increased by odor preference–conditioned training. *Learning & memory, 6*(6), 608-618.

Minneman, K. P., Dibner, M. D., Wolfe, B. B., & Molinoff, P. B. (1979). Beta1- and beta2-adrenergic receptors in rat cerebral cortex are independently regulated. *Science., 204*(4395), 866-868. doi:10.1126/science.35829

Mintz, I. M., Adams, M. E., & Bean, B. P. (1992). P-type calcium channels in rat central and peripheral neurons. *Neuron, 9*(1), 85-95. doi:Doi 10.1016/0896-6273(92)90223-Z

Moore, C. L., & Power, K. L. (1992). Variation in maternal care and individual differences in play, exploration, and grooming of juvenile norway rat offspring. *Developmental Psychobiology: The Journal of the International Society for Developmental Psychobiology, 25*(3), 165-182. doi:10.1002/dev.420250303

Moosmang, S., Haider, N., Klugbauer, N., Adelsberger, H., Langwieser, N., Müller, J., . . . Lacinova, L. (2005). Role of hippocampal cav1. 2 ca2+ channels in nmda receptor-independent synaptic plasticity and spatial memory. *Journal of Neuroscience, 25*(43), 9883-9892.

Moreno, M. M., Bath, K., Kuczewski, N., Sacquet, J., Didier, A., & Mandairon, N. (2012). Action of the noradrenergic system on adult-born cells is required for olfactory learning in mice. *Journal of Neuroscience, 32*(11), 3748-3758. doi:10.1523/Jneurosci.6335-11.2012

Moreno, M. M., Linster, C., Escanilla, O., Sacquet, J., Didier, A., & Mandairon, N. (2009). Olfactory perceptual learning requires adult neurogenesis. *Proceedings of the National Academy of Sciences, 106*(42), 17980-17985. doi:10.1073/pnas.0907063106

Moriceau, S., & Sullivan, R. M. (2004). Unique neural circuitry for neonatal olfactory learning. *Journal of Neuroscience, 24*(5), 1182-1189. doi:10.1523/JNEUROSCI.4578-03.2004

Moriguchi, S., Kimura, Y., Ichise, M., Arakawa, R., Takano, H., & Seki, C. (2017). Pet quantification of the norepinephrine transporter in human brain with (s,s)-(18) f-fmener-d2. *J Nucl Med, 58*(7), 1140-1145. doi:10.2967/jnumed.116.178913

Morrison, G. L., Fontaine, C. J., Harley, C. W., & Yuan, Q. (2013). A role for the anterior piriform cortex in early odor preference learning: Evidence for multiple olfactory learning structures in the rat pup. *Journal of Neurophysiology, 110*(1), 141-152. doi:10.1152/jn.00072.2013

Mouly, A.-M., Elaagouby, A., & Ravel, N. (1995). A study of the effects of noradrenaline in the rat olfactory bulb using evoked field potential response. *Brain research, 681*(1-2), 47-57. doi:Doi 10.1016/0006-8993(95)00280-4

Mukherjee, B., & Yuan, Q. (2016a). Nmda receptors in mouse anterior piriform cortex initialize early odor preference learning and l-type calcium channels engage for long-term memory. *Sci Rep, 6*, 35256. doi:10.1038/srep35256

https://www.nature.com/articles/srep35256#supplementary-information

Mukherjee, B., & Yuan, Q. (2016b). Nmda receptors in mouse anterior piriform cortex initialize early odor preference learning and l-type calcium channels engage for long-term memory. *Scientific reports, 6*, 35256. doi:10.1038/srep35256

Mundinano, I.-C., Caballero, M.-C., Ordóñez, C., Hernandez, M., DiCaudo, C., Marcilla, I., . . . Luquin, M.-R. (2011). Increased dopaminergic cells and protein aggregates in the olfactory bulb of patients with neurodegenerative disorders. *Acta neuropathologica, 122*(1), 61. doi:10.1007/s00401-011-0830-2

Munro, C. A., Walling, S. G., Evans, J. H., & Harley, C. W. (2001). B-adrenergic blockade in the dentate gyrus in vivo prevents high frequency-induced long-term potentiation of epsp slope, but not long-term potentiation of population spike amplitude. *Hippocampus, 11*(3), 322-328.

Murphy, C., Jernigan, T. L., & Fennema-Notestine, C. (2003). Left hippocampal volume loss in alzheimer's disease is reflected in performance on odor identification: A structural mri study. *Journal of the International Neuropsychological Society, 9*(3), 459-471.

Murphy, G. J., Darcy, D. P., & Isaacson, J. S. (2005). Intraglomerular inhibition: Signaling mechanisms of an olfactory microcircuit. *Nature neuroscience, 8*(3), 354-364. doi:http://dx.doi.org/10.1038/nn1403

Murphy, J. G., Sanderson, J. L., Gorski, J. A., Scott, J. D., Catterall, W. A., Sather, W. A., & Dell'Acqua, M. L. (2014). Akap-anchored pka maintains neuronal l-type calcium channel activity and nfat transcriptional signaling. *Cell reports, 7*(5), 1577-1588. doi:10.1016/j.celrep.2014.04.027

Nai, Q., Dong, H.-W., Hayar, A., Linster, C., & Ennis, M. (2009). Noradrenergic regulation of gabaergic inhibition of main olfactory bulb mitral cells varies as a function of concentration and receptor subtype. *Journal of Neurophysiology, 101*(5), 2472-2484. doi:10.1152/jn.91187.2008

Nai, Q., Dong, H.-W., Linster, C., & Ennis, M. (2010). Activation of α1 and α2 noradrenergic receptors exert opposing effects on excitability of main olfactory bulb granule cells. *Neuroscience, 169*(2), 882-892.

Nakamura, S., Kimura, F., & Sakaguchi, T. (1987). Postnatal development of electrical activity in the locus ceruleus. *Journal of Neurophysiology, 58*(3), 510-524. doi:10.1152/jn.1987.58.3.510

Namburi, P., Al-Hasani, R., Calhoon, G. G., Bruchas, M. R., & Tye, K. M. (2016). Architectural representation of valence in the limbic system. *Neuropsychopharmacology, 41*(7), 1697-1715. doi:10.1038/npp.2015.358

Namburi, P., Beyeler, A., Yorozu, S., Calhoon, G. G., Halbert, S. A., Wichmann, R., . . . Tye, K. M. (2015). A circuit mechanism for differentiating positive and negative associations. *Nature, 520*(7549), 675-678. doi:10.1038/nature14366

Nazarali, A. J., & Reynolds, G. P. (1992). Monoamine neurotransmitters and their metabolites in brain regions in alzheimer's disease: A postmortem study. *Cellular and molecular neurobiology, 12*(6), 581-587.

Nelson, L., Guo, T., Lu, J., Saper, C., Franks, N., & Maze, M. (2002). The sedative component of anesthesia is mediated by gaba a receptors in an endogenous sleep pathway. *Nature neuroscience, 5*(10), 979-984. doi:10.1038/nn913

Nguyen, P. V., & Connor, S. A. (2019). Noradrenergic regulation of hippocampus-dependent memory. *Central Nervous System Agents in Medicinal Chemistry (Formerly Current Medicinal Chemistry-Central Nervous System Agents), 19*(3), 187-196. doi:10.2174/1871524919666190719163632

Niepel, G., Bibani, R. H., Vilisaar, J., Langley, R. W., Bradshaw, C. M., Szabadi, E., & Constantinescu, C. S. (2013). Association of a deficit of arousal with fatigue in multiple sclerosis: Effect of modafinil. *Neuropharmacology, 64*, 380-388. doi:10.1016/j.neuropharm.2012.06.036

Nieuwenhuys, R. (1985). Chemoarchitecture of the brain. 1985: Springer-Verlag, Berlin.

Nunes, E. J., Bitner, L., Hughley, S. M., Small, K. M., Walton, S. N., Rupprecht, L. E., & Addy, N. A. (2019). Cholinergic receptor blockade in the vta attenuates cue-induced cocaine-seeking and reverses the anxiogenic effects of forced abstinence. *Neuroscience, 413*, 252-263. doi:10.1016/j.neuroscience.2019.06.028

O'Dell, T. J., Connor, S. A., Guglietta, R., & Nguyen, P. V. (2015). B-adrenergic receptor signaling and modulation of long-term potentiation in the mammalian hippocampus. *Learning & memory, 22*(9), 461-471. doi:10.1101/lm.031088.113

O'Neill, P. K., Gore, F., & Salzman, C. D. (2018). Basolateral amygdala circuitry in positive and negative valence. *Current Opinion in Neurobiology, 49*, 175-183. doi:10.1016/j.conb.2018.02.012

Oliveira-Pinto, A. V., Santos, R. M., Coutinho, R. A., Oliveira, L. M., Santos, G. B., Alho, A. T., . . . Grinberg, L. T. (2014). Sexual dimorphism in the human olfactory bulb: Females have more neurons and glial cells than males. *PLoS One, 9*(11), e111733. doi:ARTN e111733

10.1371/journal.pone.0111733

Ornstein, K., Milon, H., McRae-Degueurce, A., Alvarez, C., Berger, B., & Würzner, H. (1987). Biochemical and radioautographic evidence for dopaminergic afferents of the locus coeruleus originating in the ventral tegmental area. *Journal of neural transmission, 70*(3-4), 183-191.

Palmer, A. M., Francis, P. T., Bowen, D. M., Benton, J. S., Neary, D., & Mann, D. M. (1987). Catecholaminergic neurones assessed ante-mortem in alzheimer's disease. *Brain Res, 414*(2), 365-375. doi:10.1016/0006-8993(87)90018-7

Palta, P., Chen, H., Deal, J. A., Sharrett, A. R., Gross, A., & Knopman, D. (2018). Olfactory function and neurocognitive outcomes in old age: The atherosclerosis risk in communities neurocognitive study. *Alzheimers Dement, 14*(8), 1015-1021. doi:10.1016/j.jalz.2018.02.019

Pandipati, S., & Schoppa, N. E. (2012). Age-dependent adrenergic actions in the main olfactory bulb that could underlie an olfactory-sensitive period. *Journal of Neurophysiology, 108*(7), 1999-2007.

Paola, M., Iulio, F., Cherubini, A., Blundo, C., Casini, A. R., & Sancesario, G. (2010). When, where, and how the corpus callosum changes in mci and ad: A multimodal mri study. *Neurology., 74*(14), 1136-1142. doi:10.1212/WNL.0b013e3181d7d8cb

Paola, M., Phillips, O., Orfei, M. D., Piras, F., Cacciari, C., & Caltagirone, C. (2015). Corpus callosum structure is topographically correlated with the early course of cognition and depression in alzheimer's disease. *J Alzheimers Dis, 45*(4), 1097-1108. doi:10.3233/JAD-142895

Papay, R., Gaivin, R., Jha, A., Mccune, D. F., Mcgrath, J. C., Rodrigo, M. C., . . . Perez, D. M. (2006). Localization of the mouse α1a-adrenergic receptor (ar) in the brain: A1aar is expressed in neurons, gabaergic interneurons, and ng2 oligodendrocyte progenitors. *Journal of comparative neurology, 497*(2), 209-222.

Paschalis, A., Churchill, L., Marina, N., Kasymov, V., Gourine, A., & Ackland, G. (2009). B1-adrenoceptor distribution in the rat brain: An immunohistochemical study. *Neuroscience letters, 458*(2), 84-88.

Paskavitz, J. F., Lippa, C. F., Hamos, J. E., Pulaski-Salo, D., & Drachman, D. A. (1995). Role of the dorsomedial nucleus of the thalamus in alzheimer's disease. *Journal of geriatric psychiatry and neurology, 8*(1), 32-37.

Pedersen, H., Morishima, H. O., Finster, M., Arthur, G. R., & Covino, B. G. (1982). Pharmacokinetics of etidocaine in fetal and neonatal lambs and adult sheep. *Anesthesia and analgesia, 61*(2), 104-108.

Perez, S. E., Nadeem, M., He, B., Miguel, J. C., Malek-Ahmadi, M. H., & Chen, K. (2017). Neocortical and hippocampal trem2 protein levels during the progression of alzheimer's disease. *Neurobiol Aging, 54*, 133-143. doi:10.1016/j.neurobiolaging.2017.02.012

Peterson, A. C., & Li, C. R. (2018). Noradrenergic dysfunction in alzheimer's and parkinson's diseases-an overview of imaging studies. *Front Aging Neurosci, 10*, 127. doi:10.3389/fnagi.2018.00127

Petrella, J., Sheldon, F., Prince, S., Calhoun, V. D., & Doraiswamy, P. (2011). Default mode network connectivity in stable vs progressive mild cognitive impairment. *Neurology, 76*(6), 511-517. doi:10.1212/WNL.0b013e31820af94e

Pitman, R. K., Milad, M. R., Igoe, S. A., Vangel, M. G., Orr, S. P., Tsareva, A., . . . Nader, K. (2011). Systemic mifepristone blocks reconsolidation of cue-conditioned fear; propranolol prevents this effect. *Behavioral neuroscience, 125*(4), 632. doi:10.1037/a0024364

Poitras, D., & Parent, A. (1978). Atlas of the distribution of monoamine-containing nerve cell bodies in the brain stem of the cat. *Journal of comparative neurology, 179*(4), 699-717. doi:10.1002/cne.901790402

Poo, C., & Isaacson, J. S. (2011). A major role for intracortical circuits in the strength and tuning of odor-evoked excitation in olfactory cortex. *Neuron, 72*(1), 41-48. doi:10.1016/j.neuron.2011.08.015

Post, M. R., Lieberman, O. J., & Mosharov, E. V. (2018). Can interactions between alpha-synuclein, dopamine and calcium explain selective neurodegeneration in parkinson's disease? *Front Neurosci, 12*. doi:10.3389/fnins.2018.00161

Pottier, C., Hannequin, D., Coutant, S., Rovelet-Lecrux, A., Wallon, D., Rousseau, S., . . . Pariente, J. (2012). High frequency of potentially pathogenic sorl1 mutations in autosomal dominant early-onset alzheimer disease. *Molecular psychiatry, 17*(9), 875-879. doi:10.1038/mp.2012.15

Poulin, S. P., Dautoff, R., Morris, J. C., Barrett, L. F., Dickerson, B. C., & Initiative, A. s. D. N. (2011). Amygdala atrophy is prominent in early alzheimer's disease and relates to symptom severity. *Psychiatry Research: Neuroimaging, 194*(1), 7-13. doi:10.1016/j.pscychresns.2011.06.014

Powers, R. E., Struble, R. G., Casanova, M. F., O'Connor, D. T., Kitt, C. A., & Price, D. L. (1988). Innervation of human hippocampus by noradrenergic systems: Normal anatomy and structural abnormalities in aging and in alzheimer's disease. *Neuroscience., 25*(2), 401-417. doi:10.1016/0306-4522(88)90248-5

Price, J. L. (1990). *Olfactory system. The human nervous system*. New York: Academic Press.

Price, J. L., Davis, P. B., Morris, J. C., & White, D. L. (1991). The distribution of tangles, plaques and related immunohistochemical markers in healthy aging and alzheimer's disease. *Neurobiol Aging, 12*(4), 295-312. doi:10.1016/0197-4580(91)90006-6

Prokopovich, D. V., Whittaker, J. W., Muthee, M. M., Ahmed, A., & Larini, L. (2017). Impact of phosphorylation and pseudophosphorylation on the early stages of aggregation of the microtubule-associated protein tau. *J Phys Chem B, 121*(9), 2095-2103. doi:10.1021/acs.jpcb.7b00194

Przybyslawski, J., Roullet, P., & Sara, S. J. (1999). Attenuation of emotional and nonemotional memories after their reactivation: Role of beta adrenergic receptors. *Neurosci, 19*(15), 6623-6628.

Pu, Z., Krugers, H. J., & Joëls, M. (2009). B-adrenergic facilitation of synaptic plasticity in the rat basolateral amygdala in vitro is gradually reversed by corticosterone. *Learning & memory, 16*(2), 155-160.

Pugh, P. L., Vidgeon-Hart, M. P., Ashmeade, T., Culbert, A. A., Seymour, Z., Perren, M. J., . . . Virley, D. J. (2007). Repeated administration of the noradrenergic neurotoxin n-(2-chloroethyl)-n-ethyl-2-bromobenzylamine (dsp-4) modulates neuroinflammation and amyloid plaque load in mice bearing amyloid precursor protein and presenilin-1 mutant transgenes. *Journal of neuroinflammation, 4*(1), 8.

Qian, H., Matt, L., Zhang, M., Nguyen, M., Patriarchi, T., Koval, O. M., . . . Hell, J. W. (2012). B2-adrenergic receptor supports prolonged theta tetanus-induced ltp. *Journal of Neurophysiology, 107*(10), 2703-2712.

Qian, H., Patriarchi, T., Price, J. L., Matt, L., Lee, B., Nieves-Cintrón, M., . . . Nystoriak, M. A. (2017). Phosphorylation of ser1928 mediates the enhanced activity of the l-type ca2+ channel cav1. 2 by the β2-adrenergic receptor in neurons. *Science signaling, 10*(463).

Qu, L. L., Guo, N. N., & Li, B. M. (2008). B1-and β2-adrenoceptors in basolateral nucleus of amygdala and their roles in consolidation of fear memory in rats. *Hippocampus, 18*(11), 1131-1139.

Quarmley, M., Moberg, P. J., Mechanic-Hamilton, D., Kabadi, S., Arnold, S. E., & Wolk, D. A. (2017). Odor identification screening improves diagnostic classification in incipient alzheimer's disease. *J Alzheimers Dis., 55*(4), 1497-1507. doi:10.3233/JAD-160842

Quinlan, M. A. L., Strong, V. M., Skinner, D. M., Martin, G. M., Harley, C. W., & Walling, S. G. (2018). Locus coeruleus optogenetic light activation induces long-term potentiation of perforant path population spike amplitude in rat dentate gyrus. *Front Syst Neurosci, 12*, 67. doi:10.3389/fnsys.2018.00067

Quirarte, G. L., Galvez, R., Roozendaal, B., & McGaugh, J. L. (1998). Norepinephrine release in the amygdala in response to footshock and opioid peptidergic drugs. *Brain research, 808*(2), 134-140. doi:10.1016/s0006-8993(98)00795-1

Quiroz, Y. T., Schultz, A. P., Chen, K., Protas, H. D., Brickhouse, M., Fleisher, A. S., . . . Shah, A. R. (2015). Brain imaging and blood biomarker abnormalities in children with autosomal dominant alzheimer disease: A cross-sectional study. *JAMA neurology, 72*(8), 912-919. doi:10.1001/jamaneurol.2015.1099

Rahayel, S., Frasnelli, J., & Joubert, S. (2012). The effect of alzheimer's disease and parkinson's disease on olfaction: A meta-analysis. *Behavioural Brain Research, 231*(1), 60-74. doi:10.1016/j.bbr.2012.02.047

Rami-Mark, C., Berroteran-Infante, N., Philippe, C., Foltin, S., Vraka, C., & Hoepping, A. (2015). Radiosynthesis and first preclinical evaluation of the novel norepinephrine transporter pet-ligand [(11) c]me@hapthi. *EJNMMI Res, 5*(1), 113. doi:10.1186/s13550-015-0113-3

Ramos, B. P., & Arnsten, A. F. (2007). Adrenergic pharmacology and cognition: Focus on the prefrontal cortex. *Pharmacology & therapeutics, 113*(3), 523-536. doi:10.1016/j.pharmthera.2006.11.006

Rankovic, V., Landgraf, P., Kanyshkova, T., Ehling, P., Meuth, S. G., Kreutz, M. R., . . . Munsch, T. (2011). Modulation of calcium-dependent inactivation of l-type ca 2+ channels via β-adrenergic signaling in thalamocortical relay neurons. *PLoS One, 6*(12), e27474.

Reinikainen, K. J., Paljärvi, L., Huuskonen, M., Soininen, H., Laakso, M., & Riekkinen, P. J. (1988). A post-mortem study of noradrenergic, serotonergic and gabaergic neurons in alzheimer's disease. *Journal of the neurological sciences, 84*(1), 101-116. doi:10.1016/0022-510x(88)90179-7

Reuter, H. (1983). Calcium channel modulation by neurotransmitters, enzymes and drugs. *Nature, 301*(5901), 569-574. doi:10.1038/301569a0

Rey, N. L., Jardanhazi-Kurutz, D., Terwel, D., Kummer, M. P., Jourdan, F., Didier, A., & Heneka, M. T. (2012). Locus coeruleus degeneration exacerbates olfactory deficits in app/ps1 transgenic mice. *Neurobiology of aging, 33*(2), 426. e421-426. e411. doi:ARTN 426.e1

10.1016/j.neurobiolaging.2010.10.009

Risacher, S. L., Tallman, E. F., West, J. D., Yoder, K. K., Hutchins, G. D., & Fletcher, J. W. (2017). Olfactory identification in subjective cognitive decline and mild cognitive impairment: Association with tau but not amyloid positron emission tomography. *Alzheimers Dement (Amst), 9*.

Ritter, S., & Stein, L. (1973). Self-stimulation of noradrenergic cell group (a6) in locus coeruleus of rats. *J Comp Physiol Psychol, 85*(3), 443-452. doi:10.1037/h0035289

Roalf, D. R., Moberg, M. J., Turetsky, B. I., Brennan, L., Kabadi, S., & Wolk, D. A. (2017). A quantitative meta-analysis of olfactory dysfunction in mild cognitive impairment. *J Neurol Neurosurg Psychiatry, 88*(3), 226-232. doi:10.1136/jnnp-2016-314638

Roberts, R. O., Christianson, T. J., Kremers, W. K., Mielke, M. M., Machulda, M. M., & Vassilaki, M. (2016). Association between olfactory dysfunction and amnestic mild cognitive impairment and alzheimer disease dementia. *JAMA Neurol, 73*(1), 93-101. doi:10.1001/jamaneurol.2015.2952

Rodenkirch, C., Liu, Y., Schriver, B. J., & Wang, Q. (2019). Locus coeruleus activation enhances thalamic feature selectivity via norepinephrine regulation of intrathalamic circuit dynamics. *Nat Neurosci, 22*(1), 120-133. doi:10.1038/s41593-018-0283-1

Rodriguez-Manzo, G., & Canseco-Alba, A. (2017). A new role for gabaergic transmission in the control of male rat sexual behavior expression. *Behavioural Brain Research, 320*, 21-29. doi:10.1016/j.bbr.2016.11.041

Roozendaal, B., Hahn, E. L., Nathan, S. V., Dominique, J.-F., & McGaugh, J. L. (2004). Glucocorticoid effects on memory retrieval require concurrent noradrenergic activity in the hippocampus and basolateral amygdala. *Journal of Neuroscience, 24*(37), 8161-8169. doi:10.1523/JNEUROSCI.2574-04.2004

Rorabaugh, J. M., Chalermpalanupap, T., Botz-Zapp, C. A., Fu, V. M., Lembeck, N. A., Cohen, R. M., & Weinshenker, D. (2017). Chemogenetic locus coeruleus activation restores reversal learning in a rat model of alzheimer's disease. *Brain, 140*(11), 3023-3038. doi:10.1093/brain/awx232

Roth, T. L., & Sullivan, R. M. (2001). Endogenous opioids and their role in odor preference acquisition and consolidation following odor–shock conditioning in infant rats.

Developmental Psychobiology: The Journal of the International Society for Developmental Psychobiology, 39(3), 188-198.
Roth, T. L., & Sullivan, R. M. (2003). Consolidation and expression of a shock-induced odor preference in rat pups is facilitated by opioids. *Physiology & behavior, 78*(1), 135-142. doi:Pii S0031-9384(02)00961-7

Doi 10.1016/S0031-9384(02)00961-7
Roth, T. L., & Sweatt, J. D. (2011). Annual research review: Epigenetic mechanisms and environmental shaping of the brain during sensitive periods of development. *J Child Psychol Psychiatry, 52*(4), 398-408. doi:10.1111/j.1469-7610.2010.02282.x
Saar, D., & Barkai, E. (2009). Long-lasting maintenance of learning-induced enhanced neuronal excitability: Mechanisms and functional significance. *Molecular neurobiology, 39*(3), 171-177. doi:10.1007/s12035-009-8060-5
Saiz-Sanchez, D., De la Rosa-Prieto, C., Ubeda-Banon, I., & Martinez-Marcos, A. (2015). Interneurons, tau and amyloid-β in the piriform cortex in alzheimer's disease. *Brain Structure and Function, 220*(4), 2011-2025.
Sanchez-Padilla, J., Guzman, J. N., Ilijic, E., Kondapalli, J., Galtieri, D. J., Yang, B., . . . Schumacker, P. T. (2014). Mitochondrial oxidant stress in locus coeruleus is regulated by activity and nitric oxide synthase. *Nature neuroscience, 17*(6), 832-840. doi:10.1038/nn.3717
Sara, S. J., & Devauges, V. (1988). Priming stimulation of locus coeruleus facilitates memory retrieval in the rat. *Brain research, 438*(1-2), 299-303. doi:10.1016/0006-8993(88)91351-0
Sarvey, J. M., Burgard, E. C., & Decker, G. (1989). Long-term potentiation: Studies in the hippocampal slice. *Journal of neuroscience methods, 28*(1-2), 109-124. doi:10.1016/0165-0270(89)90016-2
Scanziani, M., Gahwiler, B., & Thompson, S. M. (1993). Presynaptic inhibition of excitatory synaptic transmission mediated by alpha adrenergic receptors in area ca3 of the rat hippocampus in vitro. *Journal of Neuroscience, 13*(12), 5393-5401.
Scheiderer, C. L., Dobrunz, L. E., & McMahon, L. L. (2004). Novel form of long-term synaptic depression in rat hippocampus induced by activation of α1 adrenergic receptors. *Journal of Neurophysiology, 91*(2), 1071-1077. doi:10.1152/jn.00420.2003
Scheinin, M., Lomasney, J. W., Hayden-Hixson, D. M., Schambra, U. B., Caron, M. G., Lefkowitz, R. J., & Fremeau Jr, R. T. (1994). Distribution of α2-adrenergic receptor subtype gene expression in rat brain. *Molecular Brain Research, 21*(1-2), 133-149. doi:10.1016/0169-328x(94)90386-7
Scherzer, C. R., Offe, K., Gearing, M., Rees, H. D., Fang, G., Heilman, C. J., . . . Lah, J. J. (2004). Loss of apolipoprotein e receptor lr11 in alzheimer disease. *Archives of neurology, 61*(8), 1200-1205. doi:10.1001/archneur.61.8.1200
Schneider, A. M., Simson, P. E., Daimon, C. M., Mrozewski, J., Vogt, N. M., Keefe, J., & Kirby, L. G. (2014). Stress-dependent opioid and adrenergic modulation of newly retrieved fear memory. *Neurobiology of Learning and Memory, 109*, 1-6. doi:10.1016/j.nlm.2013.11.013
Schofield, S., & Everitt, B. J. (1981). The organisation of catecholamine-containing neurons in the brain of the rhesus monkey (macaca mulatta). *Journal of Anatomy, 132*(Pt 3), 391.
Schultz, M. K., Gentzel, R., Usenovic, M., Gretzula, C., Ware, C., & Parmentier-Batteur, S. (2018). Pharmacogenetic neuronal stimulation increases human tau pathology and trans-synaptic spread of tau to distal brain regions in mice. *Neurobiol Dis, 118*, 161-176. doi:10.1016/j.nbd.2018.07.003

Schulz, B., Fendt, M., & Schnitzler, H. U. (2002). Clonidine injections into the lateral nucleus of the amygdala block acquisition and expression of fear-potentiated startle. *Eur J Neurosci, 15*(1), 151-157. doi:DOI 10.1046/j.0953-816x.2001.01831.x

Schwarz, L. A., & Luo, L. (2015). Organization of the locus coeruleus-norepinephrine system. *Current Biology, 25*(21), R1051-R1056. doi:10.1016/j.cub.2015.09.039

Schwarz, L. A., Miyamichi, K., Gao, X. J., Beier, K. T., Weissbourd, B., DeLoach, K. E., . . . Luo, L. (2015). Viral-genetic tracing of the input-output organization of a central noradrenaline circuit. *Nature, 524*(7563), 88-92. doi:10.1038/nature14600

Scullion, G., Kendall, D., Marsden, C., Sunter, D., & Pardon, M.-C. (2011). Chronic treatment with the α2-adrenoceptor antagonist fluparoxan prevents age-related deficits in spatial working memory in app× ps1 transgenic mice without altering β-amyloid plaque load or astrocytosis. *Neuropharmacology, 60*(2-3), 223-234.

Segal, S. K., Stark, S. M., Kattan, D., Stark, C. E., & Yassa, M. A. (2012). Norepinephrine-mediated emotional arousal facilitates subsequent pattern separation. *Neurobiology of Learning and Memory, 97*(4), 465-469. doi:10.1016/j.nlm.2012.03.010

Selden, N., Everitt, B., & Robbins, T. (1991). Telencephalic but not diencephalic noradrenaline depletion enhances behavioural but not endocrine measures of fear conditioning to contextual stimuli. *Behavioural Brain Research, 43*(2), 139-154.

Selden, N., Robbins, T. W., & Everitt, B. (1990). Enhanced behavioral conditioning to context and impaired behavioral and neuroendocrine responses to conditioned stimuli following ceruleocortical noradrenergic lesions: Support for an attentional hypothesis of central noradrenergic function. *Journal of Neuroscience, 10*(2), 531-539.

Serby, M., Larson, P., & Kalkstein, D. S. (1991). The nature and course of olfactory deficits in alzheimer's disease. *The American journal of psychiatry, 148*(3), 357-360. doi:10.1176/ajp.148.3.357

Seseña, E., Vega, R., & Soto, E. (2014). Activation of μ-opioid receptors inhibits calcium-currents in the vestibular afferent neurons of the rat through a camp dependent mechanism. *Frontiers in cellular neuroscience, 8*, 90.

Shakhawat, A. M., Gheidi, A., MacIntyre, I. T., Walsh, M. L., Harley, C. W., & Yuan, Q. (2015). Arc-expressing neuronal ensembles supporting pattern separation require adrenergic activity in anterior piriform cortex: An exploration of neural constraints on learning. *Journal of Neuroscience, 35*(41), 14070-14075. doi:10.1523/JNEUROSCI.2690-15.2015

Shakhawat, A. M., Harley, C. W., & Yuan, Q. (2014). Arc visualization of odor objects reveals experience-dependent ensemble sharpening, separation, and merging in anterior piriform cortex in adult rat. *Journal of Neuroscience, 34*(31), 10206-10210. doi:10.1523/JNEUROSCI.1942-14.2014

Shea, S. D., Katz, L. C., & Mooney, R. (2008). Noradrenergic induction of odor-specific neural habituation and olfactory memories. *The Journal of neuroscience: the official journal of the Society for Neuroscience, 28*(42), 10711. doi:10.1523/JNEUROSCI.3853-08.2008

Shibata, E., Sasaki, M., Tohyama, K., Kanbara, Y., Otsuka, K., Ehara, S., & Sakai, A. (2006). Age-related changes in locus ceruleus on neuromelanin magnetic resonance imaging at 3 tesla. *Magnetic Resonance in Medical Sciences, 5*(4), 197-200.

Shimohama, S., Taniguchi, T., Fujiwara, M., & Kameyama, M. (1986). Biochemical characterization of α-adrenergic receptors in human brain and changes in alzheimer-type dementia. *Journal of neurochemistry, 47*(4), 1294-1301.

Shin, R. W., Kitamoto, T., & Tateishi, J. (1991). Modified tau is present in younger nondemented persons: A study of subcortical nuclei in alzheimer's disease and progressive supranuclear palsy. *Acta Neuropathol, 81*(5), 517-523. doi:10.1007/BF00310132

Silberman, Y., Ariwodola, O. J., Chappell, A. M., Yorgason, J. T., & Weiner, J. L. (2010). Lateral paracapsular gabaergic synapses in the basolateral amygdala contribute to the anxiolytic effects of β 3 adrenoceptor activation. *Neuropsychopharmacology, 35*(9), 1886-1896. doi:10.1038/npp.2010.59

Silberman, Y., Ariwodola, O. J., & Weiner, J. L. (2012). B1-adrenoceptor activation is required for ethanol enhancement of lateral paracapsular gabaergic synapses in the rat basolateral amygdala. *Journal of Pharmacology and Experimental Therapeutics, 343*(2), 451-459.

Singewald, N., Salchner, P., & Sharp, T. (2003). Induction of c-fos expression in specific areas of the fear circuitry in rat forebrain by anxiogenic drugs. *Biol Psychiatry, 53*(4), 275-283. doi:10.1016/s0006-3223(02)01574-3

Sirviö, J., & MacDonald, E. (1999). Central α1-adrenoceptors: Their role in the modulation of attention and memory formation. *Pharmacology & therapeutics, 83*(1), 49-65.

Skelly, M. J., Ariwodola, O. J., & Weiner, J. L. (2017). Fear conditioning selectively disrupts noradrenergic facilitation of gabaergic inhibition in the basolateral amygdala. *Neuropharmacology, 113*(Pt A), 231-240. doi:10.1016/j.neuropharm.2016.10.003

Skelly, M. J., Snyder, A. E., & Silberman, Y. (2020). Noradrenergic regulation of the basolateral amygdala *Handbook of behavioral neuroscience* (Vol. 26, pp. 213-226): Elsevier.

Smith, C. C., & Greene, R. W. (2012). Cns dopamine transmission mediated by noradrenergic innervation. *J Neurosci, 32*(18), 6072-6080. doi:10.1523/JNEUROSCI.6486-11.2012

Sotiropoulos, I., Catania, C., Pinto, L. G., Silva, R., Pollerberg, G. E., Takashima, A., . . . Almeida, O. F. (2011). Stress acts cumulatively to precipitate alzheimer's disease-like tau pathology and cognitive deficits. *J Neurosci, 31*(21), 7840-7847. doi:10.1523/JNEUROSCI.0730-11.2011

Stanton, P. K., & Sarvey, J. M. (1985). Depletion of norepinephrine, but not serotonin, reduces long-term potentiation in the dentate gyrus of rat hippocampal slices. *Journal of Neuroscience, 5*(8), 2169-2176.

Steininger, T. L., Gong, H., Mcginty, D., & Szymusiak, R. (2001). Subregional organization of preoptic area/anterior hypothalamic projections to arousal-related monoaminergic cell groups. *Journal of comparative neurology, 429*(4), 638-653.

Stranahan, A. M., & Mattson, M. P. (2010). Selective vulnerability of neurons in layer ii of the entorhinal cortex during aging and alzheimer's disease. *Neural Plasticity, 2010*, 108190. doi:10.1155/2010/108190

Stratmann, K., Heinsen, H., Korf, H. W., Turco, D., Ghebremedhin, E., & Seidel, K. (2016). Precortical phase of alzheimer's disease (ad)-related tau cytoskeletal pathology. *Brain Pathol, 26*(3), 371-386. doi:10.1111/bpa.12289

Sullivan, R., Stackenwalt, G., Nasr, F., Lemon, C., & Wilson, D. (2000). Association of an odor with an activation of olfactory bulb noradrenergic β-receptors or locus coeruleus stimulation is sufficient to produce learned approach responses to that odor in neonatal rats. *Behavioral neuroscience, 114*(5), 957. doi:10.1037/0735-7044.114.5.957

Sullivan, R. M., & Leon, M. (1986). Early olfactory learning induces an enhanced olfactory bulb response in young rats. *Developmental Brain Research, 27*(1), 278-282. doi:10.1016/0165-3806(86)90256-7

Sullivan, R. M., Zyzak, D., Skierkowski, P., & Wilson, D. A. (1992). The role of olfactory bulb norepinephrine in early olfactory learning. *Brain Res Dev Brain Res, 70*(2), 279-282. doi:10.1016/0165-3806(92)90207-d

Suzuki, N., & Bekkers, J. M. (2006). Neural coding by two classes of principal cells in the mouse piriform cortex. *Journal of Neuroscience, 26*(46), 11938-11947. doi:10.1523/JNEUROSCI.3473-06.2006

Swanson, L. (1976). The locus coeruleus: A cytoarchitectonic, golgi and immunohistochemical study in the albino rat *Brain research* (Vol. 110, pp. 39-56).

Szabadi, E. (2013). Functional neuroanatomy of the central noradrenergic system *Journal of Psychopharmacology* (Vol. 27, pp. 659-693).

Szot, P., White, S. S., Greenup, J. L., Leverenz, J. B., Peskind, E. R., & Raskind, M. A. (2006). Compensatory changes in the noradrenergic nervous system in the locus ceruleus and hippocampus of postmortem subjects with alzheimer's disease and dementia with lewy bodies. *Journal of Neuroscience, 26*(2), 467-478. doi:10.1523/JNEUROSCI.4265-05.2006

Szot, P., White, S. S., Greenup, J. L., Leverenz, J. B., Peskind, E. R., & Raskind, M. A. (2007). Changes in adrenoreceptors in the prefrontal cortex of subjects with dementia: Evidence of compensatory changes. *Neuroscience, 146*(1), 471-480. doi:10.1016/j.neuroscience.2007.01.031

Takahashi, J., Shibata, T., Sasaki, M., Kudo, M., Yanezawa, H., Obara, S., . . . Terayama, Y. (2015). Detection of changes in the locus coeruleus in patients with mild cognitive impairment and a lzheimer's disease: High-resolution fast spin-echo t 1-weighted imaging. *Geriatrics & gerontology international, 15*(3), 334-340.

Takano, A., Varrone, A., Gulyas, B., Karlsson, P., Tauscher, J., & Halldin, C. (2008). Mapping of the norepinephrine transporter in the human brain using pet with (s,s)-[18f]fmener-d2. *Neuroimage., 42*(2), 474-482. doi:10.1016/j.neuroimage.2008.05.040

Takeuchi, T., Duszkiewicz, A. J., Sonneborn, A., Spooner, P. A., Yamasaki, M., Watanabe, M., . . . Greene, R. W. (2016). Locus coeruleus and dopaminergic consolidation of everyday memory. *Nature, 537*(7620), 357-362. doi:10.1038/nature19325

Tejani-Butt, S. M., Yang, J., & Zaffar, H. (1993). Norepinephrine transporter sites are decreased in the locus coeruleus in alzheimer's disease. *Brain research, 631*(1), 147-150. doi:10.1016/0006-8993(93)91201-3

Theofilas, P., Ehrenberg, A. J., Dunlop, S., Lorenzo Alho, A. T., Nguy, A., & Leite, R. E. (2017). Locus coeruleus volume and cell population changes during alzheimer's disease progression: A stereological study in human postmortem brains with potential implication for early-stage biomarker discovery. *Alzheimers Dement, 13*(3), 236-246. doi:10.1016/j.jalz.2016.06.2362

Thomas, M. J., Moody, T. D., Makhinson, M., & O'Dell, T. J. (1996). Activity-dependent β-adrenergic modulation of low frequency stimulation induced ltp in the hippocampal ca1 region. *Neuron, 17*(3), 475-482. doi:10.1016/s0896-6273(00)80179-8

Tohgi, H., Ueno, M., Abe, T., Takahashi, S., & Nozaki, Y. (1992). Concentration of monoamines and their metabolites in the cerebrospinal fluid from patients with senile dementia of the alzheimer type and vascular dementia of the binswanger type. *Journal of neural transmission-Parkinson's disease and dementia section, 4*(1), 69-77. doi:Doi 10.1007/Bf02257623

Topolnik, L., Chamberland, S., Pelletier, J.-G., Ran, I., & Lacaille, J.-C. (2009). Activity-dependent compartmentalized regulation of dendritic ca2+ signaling in hippocampal interneurons. *Journal of Neuroscience, 29*(14), 4658-4663. doi:10.1523/Jneurosci.0493-09.2009

Totah, N. K., Logothetis, N. K., & Eschenko, O. (2019). Noradrenergic ensemble-based modulation of cognition over multiple timescales. *Brain research, 1709*, 50-66. doi:10.1016/j.brainres.2018.12.031

Trombley, P. Q., & Shepherd, G. M. (1992). Noradrenergic inhibition of synaptic transmission between mitral and granule cells in mammalian olfactory bulb cultures. *Journal of Neuroscience, 12*(10), 3985-3991.

Tsaltas, E., Gray, J., & Fillenz, M. (1984). Alleviation of response suppression to conditioned aversive stimuli by lesions of the dorsal noradrenergic bundle. *Behavioural Brain Research, 13*(2), 115-127. doi:10.1016/0166-4328(84)90142-6

Tully, K., & Bolshakov, V. Y. (2010). Emotional enhancement of memory: How norepinephrine enables synaptic plasticity. *Molecular brain, 3*(1), 15. doi:Artn 15

10.1186/1756-6606-3-15

Tully, K., Li, Y., Tsvetkov, E., & Bolshakov, V. Y. (2007). Norepinephrine enables the induction of associative long-term potentiation at thalamo-amygdala synapses. *Proceedings of the National Academy of Sciences, 104*(35), 14146-14150. doi:10.1073/pnas.0704621104

Uematsu, A., Tan, B. Z., & Johansen, J. P. (2015). Projection specificity in heterogeneous locus coeruleus cell populations: Implications for learning and memory. *Learn Mem, 22*(9), 444-451. doi:10.1101/lm.037283.114

Uematsu, A., Tan, B. Z., Ycu, E. A., Cuevas, J. S., Koivumaa, J., Junyent, F., . . . Johansen, J. P. (2017). Modular organization of the brainstem noradrenaline system coordinates opposing learning states. *Nature neuroscience, 20*(11), 1602. doi:10.1038/nn.4642

Uschakov, A., Grivel, J., Cvetkovic-Lopes, V., Bayer, L., Bernheim, L., Jones, B. E., . . . Serafin, M. (2011). Sleep-deprivation regulates α-2 adrenergic responses of rat hypocretin/orexin neurons. *PLoS One, 6*(2), e16672.

Van Bockstaele, E., & Aston-Jones, G. (1995). Integration in the ventral medulla and coordination of sympathetic, pain and arousal functions. *Clinical and Experimental Hypertension, 17*(1-2), 153-165. doi:10.3109/10641969509087062

Van Bockstaele, E. J., Pieribone, V. A., & Aston-Jones, G. (1989). Diverse afferents converge on the nucleus paragigantocellularis in the rat ventrolateral medulla: Retrograde and anterograde tracing studies. *Journal of comparative neurology, 290*(4), 561-584.

Van Hoesen, G. W., Parvizi, J., & Chu, C.-C. (2000). Orbitofrontal cortex pathology in alzheimer's disease. *Cerebral Cortex, 10*(3), 243-251.

Varazzani, C., San-Galli, A., Gilardeau, S., & Bouret, S. (2015). Noradrenaline and dopamine neurons in the reward/effort trade-off: A direct electrophysiological comparison in behaving monkeys. *Journal of Neuroscience, 35*(20), 7866-7877. doi:10.1523/JNEUROSCI.0454-15.2015

Vasavada, M. M., Martinez, B., Wang, J., Eslinger, P. J., Gill, D. J., Sun, X., . . . Yang, Q. X. (2017). Central olfactory dysfunction in alzheimer's disease and mild cognitive impairment: A functional mri study. *Journal of Alzheimer's Disease, 59*(1), 359-368.

Vassilaki, M., Christianson, T. J., Mielke, M. M., Geda, Y. E., Kremers, W. K., & Machulda, M. M. (2017). Neuroimaging biomarkers and impaired olfaction in cognitively normal individuals. *Ann Neurol, 81*(6), 871-882. doi:10.1002/ana.24960

Vazey, E. M., Moorman, D. E., & Aston-Jones, G. (2018). Phasic locus coeruleus activity regulates cortical encoding of salience information. *Proc Natl Acad Sci U S A, 115*(40), E9439-E9448. doi:10.1073/pnas.1803716115

Vermeiren, Y., & Deyn, P. P. (2017). Targeting the norepinephrinergic system in parkinson's disease and related disorders: The locus coeruleus story. *Neurochem Int, 102*, 22-32. doi:10.1016/j.neuint.2016.11.009

Veyrac, A., Nguyen, V., Marien, M., Didier, A., & Jourdan, F. (2007). Noradrenergic control of odor recognition in a nonassociative olfactory learning task in the mouse. *Learning & memory, 14*(12), 847-854. doi:10.1101/lm.708807

Wagatsuma, A., Okuyama, T., Sun, C., Smith, L. M., Abe, K., & Tonegawa, S. (2018). Locus coeruleus input to hippocampal ca3 drives single-trial learning of a novel context. *Proceedings of the National Academy of Sciences, 115*(2), E310-E316. doi:10.1073/pnas.1714082115

Wanaka, A., Kiyama, H., Murakami, T., Matsumoto, M., Kamada, T., Malbon, C., & Tohyama, M. (1989). Immunocytochemical localization of β-adrenergic receptors in the rat brain. *Brain research, 485*(1), 125-140. doi:10.1016/0006-8993(89)90674-4

Wang, J., Eslinger, P. J., Doty, R. L., Zimmerman, E. K., Grunfeld, R., Sun, X., . . . Smith, M. B. (2010). Olfactory deficit detected by fmri in early alzheimer's disease. *Brain research, 1357*, 184-194. doi:10.1016/j.brainres.2010.08.018

Weinshenker, D. (2018). Long road to ruin: Noradrenergic dysfunction in neurodegenerative disease. *Trends Neurosci, 41*(4), 211-223. doi:10.1016/j.tins.2018.01.010

Weiss, S., & Dascal, N. (2015). Molecular aspects of modulation of l-type calcium channels by protein kinase c. *Current molecular pharmacology, 8*(1), 43-53. doi:10.2174/1874467208666150507094733

Weisskopf, M. G., Bauer, E. P., & LeDoux, J. E. (1999). L-type voltage-gated calcium channels mediate nmda-independent associative long-term potentiation at thalamic input synapses to the amygdala. *Journal of Neuroscience, 19*(23), 10512-10519.

Wesnes, K. A., Annas, P., Basun, H., Edgar, C., & Blennow, K. (2014). Performance on a pattern separation task by alzheimer's patients shows possible links between disrupted dentate gyrus activity and apolipoprotein e∈ 4 status and cerebrospinal fluid amyloid-β42 levels. *Alzheimer's Research & Therapy, 6*(2), 20.

Williams, A. M., Nguyen, M. L. D., & Morilak, D. A. (1997). Co-localization of α1d adrenergic receptor mrna withmineralocorticoid and glucocorticoid receptormrna in rat hippocampus. *Journal of neuroendocrinology, 9*(2), 113-119.

Williams, J., North, R., Shefner, S., Nishi, S., & Egan, T. (1984). Membrane properties of rat locus coeruleus neurones. *Neuroscience, 13*(1), 137-156. doi:10.1016/0306-4522(84)90265-3

Wilson, D. A., Xu, W., Sadrian, B., Courtiol, E., Cohen, Y., & Barnes, D. C. (2014). Cortical odor processing in health and disease *Progress in brain research* (Vol. 208, pp. 275-305): Elsevier.

Wilson, R. S., Arnold, S. E., Schneider, J. A., Boyle, P. A., Buchman, A. S., & Bennett, D. A. (2009). Olfactory impairment in presymptomatic alzheimer's disease. *Ann N Y Acad Sci, 1170*, 730-735. doi:10.1111/j.1749-6632.2009.04013.x

Wilson, R. S., Arnold, S. E., Schneider, J. A., Tang, Y., & Bennett, D. A. (2007). The relationship between cerebral alzheimer's disease pathology and odour identification in old age. *J Neurol Neurosurg Psychiatry, 78*(1), 30-35. doi:10.1136/jnnp.2006.099721

Wise, R. A. (1978). Catecholamine theories of reward: A critical review. *Brain Research, 152*(2), 215-247. doi:10.1016/0006-8993(78)90253-6

Woodward, M. R., Amrutkar, C. V., Shah, H. C., Benedict, R. H., Rajakrishnan, S., & Doody, R. S. (2017). Validation of olfactory deficit as a biomarker of alzheimer disease. *Neurol Clin Pract, 7*(1), 5-14. doi:10.1212/CPJ.0000000000000293

Woodward, M. R., Dwyer, M. G., Bergsland, N., Hagemeier, J., Zivadinov, R., & Benedict, R. H. (2017). Olfactory identification deficit predicts white matter tract impairment in alzheimer's disease. *Psychiatry Res Neuroimaging, 266*, 90-95. doi:10.1016/j.pscychresns.2017.06.004

Xia, J., Fan, S., Yan, J., Chen, F., Li, Y., Yu, Z., & Hu, Z. (2009). Orexin a-induced extracellular calcium influx in prefrontal cortex neurons involves l-type calcium channels. *Journal of physiology and biochemistry, 65*(2), 125-136. doi:10.1007/BF03179063

Yamanaka, A., Muraki, Y., Tsujino, N., Goto, K., & Sakurai, T. (2003). Regulation of orexin neurons by the monoaminergic and cholinergic systems. *Biochemical and biophysical research communications, 303*(1), 120-129. doi:10.1016/s0006-291x(03)00299-7

YANG, S.-N., YU, J., MAYR, G. W., HOFMANN, F., LARSSON, O., & BERGGREN, P.-O. (2001). Inositol hexakisphosphate increases l-type ca2+ channel activity by stimulation of adenylyl cyclase. *The FASEB Journal, 15*(10), 1753-1763. doi:10.1096/fj.00-0799com

Yang, Y., & Schmitt, H. P. (2001). Frontotemporal dementia: Evidence for impairment of ascending serotoninergic but not noradrenergic innervation. Immunocytochemical and quantitative study using a graph method. *Acta Neuropathol, 101*.

Yassa, M. A., & Stark, C. E. (2011). Pattern separation in the hippocampus. *Trends in neurosciences, 34*(10), 515-525. doi:10.1016/j.tins.2011.06.006

Yi, H.-A., Möller, C., Dieleman, N., Bouwman, F. H., Barkhof, F., Scheltens, P., . . . Vrenken, H. (2016). Relation between subcortical grey matter atrophy and conversion from mild cognitive impairment to alzheimer's disease. *Journal of Neurology, Neurosurgery & Psychiatry, 87*(4), 425-432. doi:10.1136/jnnp-2014-309105

Young, C., Huang, Y.-C., Lin, C.-H., Shen, Y.-Z., & Gean, P.-W. (2001). Selective enhancement of l-type calcium currents by corticotropin in acutely isolated rat amygdala neurons. *Molecular Pharmacology, 59*(3), 604-611. doi:10.1124/mol.59.3.604

Yu, J.-T., Tan, L., Ou, J.-R., Zhu, J.-X., Liu, K., Song, J.-H., & Sun, Y.-P. (2008). Polymorphisms at the β2-adrenergic receptor gene influence alzheimer's disease susceptibility. *Brain research, 1210*, 216-222.

Yuan, Q. (2009). Theta bursts in the olfactory nerve paired with β-adrenoceptor activation induce calcium elevation in mitral cells: A mechanism for odor preference learning in the neonate rat. *Learning & memory, 16*(11), 676-681. doi:10.1101/lm.1569309

Yuan, Q., Harley, C. W., Darby-King, A., Neve, R. L., & McLean, J. H. (2003). Early odor preference learning in the rat: Bidirectional effects of camp response element-binding protein (creb) and mutant creb support a causal role for phosphorylated creb. *Journal of Neuroscience, 23*(11), 4760-4765.

Yuan, Q., Shakhawat, A., & Harley, C. W. (2014). Mechanisms underlying early odor preference learning in rats. *Prog Brain Res, 208*, 115-156. doi:10.1016/B978-0-444-63350-7.00005-X

Yue, D. T., Herzig, S., & Marban, E. (1990). Beta-adrenergic stimulation of calcium channels occurs by potentiation of high-activity gating modes. *Proceedings of the National Academy of Sciences, 87*(2), 753-757. doi:10.1073/pnas.87.2.753

Yun, I. A., Wakabayashi, K. T., Fields, H. L., & Nicola, S. M. (2004). The ventral tegmental area is required for the behavioral and nucleus accumbens neuronal firing responses to incentive cues. *Journal of Neuroscience, 24*(12), 2923-2933. doi:10.1523/JNEUROSCI.5282-03.2004

Zanatta, L., Goulart, P. B., Gonçalves, R., Pierozan, P., Winkelmann-Duarte, E. C., Woehl, V. M., . . . Zamoner, A. (2012). 1α,25-dihydroxyvitamin d3 mechanism of action: Modulation of l-type calcium channels leading to calcium uptake and intermediate filament phosphorylation in cerebral cortex of young rats. *Biochimica et Biophysica Acta (BBA) - Molecular Cell Research, 1823*(10), 1708-1719. doi:http://dx.doi.org/10.1016/j.bbamcr.2012.06.023

Zarow, C., Lyness, S. A., Mortimer, J. A., & Chui, H. C. (2003). Neuronal loss is greater in the locus coeruleus than nucleus basalis and substantia nigra in alzheimer and parkinson diseases. *Archives of neurology, 60*(3), 337-341. doi:DOI 10.1001/archneur.60.3.337

Zelano, C., Mohanty, A., & Gottfried, J. A. (2011). Olfactory predictive codes and stimulus templates in piriform cortex. *Neuron, 72*(1), 178-187. doi:10.1016/j.neuron.2011.08.010

Zhang, C., Guo, Y.-Q., Qiao, J.-T., & Dafny, N. (1998). Locus coeruleus modulates thalamic nociceptive responses via adrenoceptors. *Brain research, 784*(1-2), 116-122. doi:10.1016/s0006-8993(97)01197-9

Zhang, J., Okutani, F., Huang, G., Taniguchi, M., Murata, Y., & Kaba, H. (2010). Common properties between synaptic plasticity in the main olfactory bulb and olfactory learning in young rats. *Neuroscience, 170*(1), 259-267. doi:10.1016/j.neuroscience.2010.06.002

Zhao, S., Rangaprakash, D., Venkataraman, A., Liang, P., & Deshpande, G. (2017). Investigating focal connectivity deficits in alzheimer's disease using directional brain networks derived from resting-state fmri. *Frontiers in aging neuroscience, 9*, 211. doi:ARTN 211

10.3389/fnagi.2017.00211

Zou, Y.-m., Da Lu, L.-p. L., Zhang, H.-h., & Zhou, Y.-y. (2016). Olfactory dysfunction in alzheimer’s disease. *Neuropsychiatric disease and treatment, 12*, 869.

7 Appendices

7.1 Ethics Approval

MEMORIAL UNIVERSITY
Animal Care Committee (ACC)
St. John's, NL, Canada A1C 5S7
Tel: 709 777-6620 acs@mun.ca
https://www.mun.ca/research/about/acs/acc/

Dear: Dr. Qi Yuan, Associate Professor/Faculty of Medicine\Division of BioMedical Sciences

Researcher Portal File No.: 20181846
Animal Care File: 18-01-QY
Entitled: (18-01-QY) Locus coeruleus norepinephrine modulation in learning and Alzheimer's Disease
Status: Active
Related Awards:

Awards File No	Title	Status	
20131039	The engram of odor learning in the piriform cortex of the rat	Active	1. Research Grant and Contract Services (RGCS) – St. John's and Grenfell Campuses
20160955	Memory: Modifiable odor representations, adaptive behavior and Alzheimer's disease	Active	1. Research Grant and Contract Services (RGCS) – St. John's and Grenfell Campuses
20170409	A rat model of tauopathy testing the locus coeruleus origin hypothesis of Alzheimer's Disease	Active	1. Research Grant and Contract Services (RGCS) – St. John's and Grenfell Campuses

Approval Date: May 1, 2018

Annual Report Due: May 01, 2019
Ethics Clearance Expires: May 01, 2021

Your Animal Use Protocol has been renewed for a three-year term. This file replaces previous File ID [[20151497]] and Animal Care ID [[15-08-QY]] as the active ethics clearance associated with this project. Please note the new file ID and Animal Care ID when referring to this protocol.

This ethics clearance includes the following Team Members:
Dr. Qi Yuan (Principal Investigator)
Dr. Carolyn Harley (Co-Investigator)
Dr. Gerard Martin (Co-Investigator) Dr. Susan Walling (Co-Investigator) Dr. Xihua Chen (Co-Investigator) Ella Chirinos (Student)
Mihiran Upekdha (Student)
Mr. Bandhan Mukherjee (Student)
Abhinaba Ghosh (Student)
Sarah Torraville (Student)

This ethics clearance includes the following related awards:

Awards File No	Title	Status	
20131039	The engram of odor learning in the piriform cortex of the rat	Active	1. Research Grant and Contract Services (RGCS) – St. John's and Grenfell Campuses
20160955	Memory: Modifiable odor representations, adaptive behavior and Alzheimer's disease	Active	1. Research Grant and Contract Services (RGCS) – St. John's and Grenfell Campuses
20170409	A rat model of tauopathy testing the locus coeruleus origin hypothesis of Alzheimer's Disease	Active	1. Research Grant and Contract Services (RGCS) – St. John's and Grenfell Campuses

An Event [Annual Report] will be required following each year of protocol activity.

Should you encounter an unexpected incident that negatively affects animal welfare or the research project relating to animal use, please submit an Event [Incident Report].

Any alterations to the protocol requires prior submission and approval of an Event [Amendment].

Sincerely,

ANULIKA MBAKWE | IACC COORDINATOR
Department of Animal Care Services
Memorial University of Newfoundland
Health Sciences Centre | Room H1848
P: 709-777-6621
E-Mail: ambakwe@mun.ca
www.mun.ca/acs